Bundesforschungsanstalt für Landwirtschaft

Aus dem Institut für Technologie und Biosystemtechnik

Ulf Prüße
Klaus-Dieter Vorlop (Eds.)

Practical aspects of encapsulation technologies

Manuskript, zu finden in www.fal.de

Published as: Landbauforschung Völkenrode Sonderheft 241

Braunschweig
Bundesforschungsanstalt für Landwirtschaft (FAL)
2002

Sonderheft 241
Special Issue

FAL
Bundesforschungsanstalt für Landwirtschaft

Landbauforschung
Völkenrode
FAL Agricultural Research

Practical Aspects of Encapsulation Technologies

edited by
Ulf Prüße and Klaus-Dieter Vorlop

Content

Foreword

In November 1998 the COST 840 action "Bioencapsulation – Innovation and Technologies" funded by the European Community started its five-year work. COST 840 is devoted "to develop the bioencapsulation methods in view of their transfer and development in agricultural and industrial applications". Thus, the extension of the knowledge in bioencapsulation by input from people with different scientific backgrounds and the broadening of application fields for existing encapsulation technologies are major items of this work.

Due to this interdisciplinary approach Cost 840 is divided into five working groups with different focuses. This special issue of the "Landbauforschung Völkenrode" is the outcome of the workshop "Practical Aspects of Encapsulation Technologies" held on 12.-14.10.2001 in the Institute of Technology and Biosystems Engineering of the Federal Agricultural Research Centre (FAL) in Braunschweig, Germany, which has been organised by the working group 3 within COST 840, a working group with the focus on the evaluation of encapsulation methods and technologies for large scale applications.

The workshop has been attended by nearly 50 persons, about 2/3 from academia and 1/3 from industry, and has been divided into oral and poster presentations. Every author also submitted a full manuscript of his contribution which is now printed in this special issue after it has been reviewed by known experts in the field of encapsulation.

The content of this special issue covers the whole range from fundamentals to industrial-scale applications of different encapsulation methods and technologies. It contains a more fundamental insight of the different technologies for the production of beads and their applicability to be scaled-up to industrial dimension, new encapsulation methodologies with a high potential to be used in industry within the next years and existing industrial scale applications both of encapsulation methods and technologies.

The application fields of the presented contributions range from agriculture and food industry over biotechnology and medicine to chemistry. Thus, this special issue gives a comprehensive summary of up to date possibilities of encapsulation technologies and applications.

Braunschweig, October 2002

Ulf Prüße and Klaus-Dieter Vorlop

Bead production with JetCutting and rotating disc/nozzle technologies

Ulf Prüße[1], Ulrich Jahnz[2], Peter Wittlich[2], Jürgen Breford[1], and Klaus-Dieter Vorlop[1]

Abstract

Different technologies for the production of solid beads from liquids via a single droplet state are compared. The mentioned technologies include simple dropping, electrostatic-enhanced dropping, vibration, rotating disc, rotating nozzle and especially the JetCutter, which is discussed more in detail. The JetCutter is a simple and efficient technology for the production of monodisperse spherical beads from solutions, melts and dispersions. Currently, it is the only technology which is also able to satisfactorily process fluids with a viscosity up to several thousands mPa·s. The cutting process and the reduction of the losses are presented in detail. New developments in JetCutter technology like a pre-gelation line, a heating device and a two-fluid nozzle for simultaneous coating are discussed. Finally, manifold applications in various industrial fields are presented.

Keywords: JetCutter, rotating disc, rotating nozzle, beads, spherical particles, encapsulation

1 Introduction

Solid particles (pellets, beads) in the size range between µm and mm play an important role in various industries like agriculture, biotechnology, chemical, pharmaceuticals and the food industry. Thus, plenty of particle production technologies exist and their further development is of major interest both from an economic and scientific point of view.

Generally, single and discrete solid particles may be produced with three different approaches:

1. from larger solid entities by grinding,
2. from smaller solid entities by agglomeration, granulation, pressing or tabletting - small fluid entities may also be used if in-situ drying is applied -, or
3. from fluid entities in the same size range with an immediate physical or chemical solidification step.

Although it is necessary to produce solid particles in industrial quantities, in recent years, solid particles are required more and more to have an ideal spherical shape. Such beads are much easier to dose, and pose less danger to humans and equipment during manufacturing (less respirable abrasion and lower explosion risk). Last but not least, they look much nicer from an aesthetic point of view, which is very important if the beads are part of a final product.

From the three different approaches named above, the third is, in principle, best suited for the production of ideal spherical beads. Only with this approach can the solid bead be a more or less equally sized liquid droplet – which is perfectly round due to the surface tension – directly prior to its solidification. Correspondingly, numerous different techniques exist which use the principle of generating a droplet which immediately afterwards is solidified to a spherical bead by physical means, e.g. cooling or heating, or chemical means, e.g. gelation, precipitation or polymerisation. This paper will give a short overview of these techniques with the focus on high-throughput techniques, like the rotating nozzle and rotating disc technique and particularly the JetCutter.

2 Technologies for bead production

2.1 Dropping technologies

Three different methodologies are considered dropping technologies: simple dropping, electrostatic enhanced dropping and vibrational jet-breakup. In this order the technologies become more and more complicated but also more sophisticated. A scheme of these technologies is shown in Figure 1, the literature about these technologies is summarised by Kuncová 2002, Nedović 2002 and Lacík 2002.

Bead production by simple dropping (Figure 1, left) is by far the easiest method. When a liquid flows out of a nozzle or a cannula, a droplet begins to form at the end of the nozzle. The “growing droplet” first adheres to the nozzle. When the gravity force of the growing droplet exceeds the adhesion force at the nozzle, the droplet will be pulled off the nozzle and will fall down. During falling the droplet will assume a spherical shape due to the surface tension of the liquid. Afterwards the generated single droplets may be collected, e.g., in a gelation bath.

The bead size depends mainly on the viscosity of the liquid and the diameter of the nozzle. Generally, only large beads (Ø > 2 mm) are accessible by simple

[1] Ulf Prüße, Jürgen Breford and Klaus-Dieter Vorlop, Institute of Technology and Biosystems Engineering, Federal Agricultural Research Centre (FAL), Bundesallee 50, 38116 Braunschweig, Germany

[2] Ulrich Jahnz and Peter Wittlich, geniaLab Biotechnologie GmbH, Bundesallee 50, 38116 Braunschweig, Germany

dropping, smaller beads will only be generated if an additional annular air flow around the nozzle is applied. This air flow often leads to a significant broadening of the size distribution, which otherwise is usually very narrow. Other disadvantages are the low throughput of this technology, which limits its applications to the lab-scale, and the fact that only low-viscous fluids can be processed without problems (usually below 200 mPa·s).

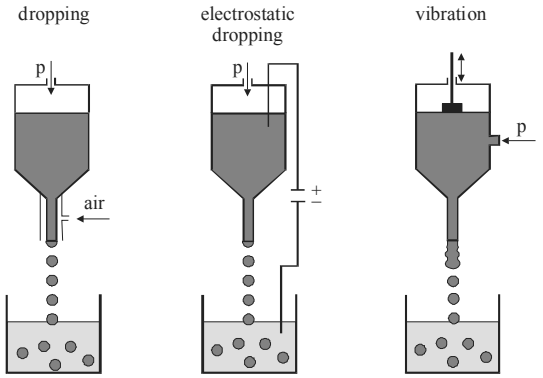

Figure 1:
Scheme of different dropping technologies for bead production

The electrostatic enhanced dropping (Figure 1, middle) is a quite similar technique. In this case, a growing bead will be pulled off the nozzle, if the sum of the gravity force and the electrostatic force exceeds the adhesion at the nozzle. This technique allows the production of very narrowly distributed beads in a broad accessible size range (approx. 0.3-5 mm). Nevertheless, the limitations concerning the low viscosity of processible fluids and the low throughput are still present, so that this technique is restricted to lab-scale. Further details about this technique can be found in this issue (Nedović et al. 2002).

The vibrational jet-breakup, or simply vibration technique (Figure 1, right), is the most sophisticated dropping technique. Bead production is achieved by superposing a oscillation on a fluid jet coming out of a nozzle. This vibration leads to a definite constriction of the jet which finally disintegrates into discrete beads which can be collected afterwards. The vibration technique also enables the production of very narrowly distributed beads in a broadly accessible size range (approx. 0.3-5 mm), but again, the low viscosity of the processible fluids limits its applications. A scale-up of this technology by multi-nozzle systems has already been done, so that this technology might also be used on a technical scale. Detailed information about this technology can also be found in this issue (Heinzen et al. 2002).

2.2 Rotating disc and rotating nozzle atomizer

Quite different from the dropping technologies are the rotating disc and nozzle technologies (Figure 2, for a literature overview see Prüße and Vorlop 2002a). In these cases, the bead generation is achieved by a spinning device which is either a disc (Figure 3) or a multi-nozzle device (Figure 4) not too different from a drum screen or the drum inside a washing machine. The fluid is either fed onto the spinning disc or into the spinning nozzle system and will flow over the perimeter of the disc or through the nozzles. If the disc/nozzle rotates, the flowing fluid disintegrates, driven by the centrifugal force and its own inertia. Depending on the rotation speed, three different disintegration regimes might be distinguished:

1. slow rotation: single beads are formed directly at the disc perimeter or the nozzle
2. medium rotation: ligaments are formed at the disc perimeter or the nozzle which disintegrate after a certain ligament length
3. fast rotation: a fluid film is formed which disintegrates in a irreproducible manner

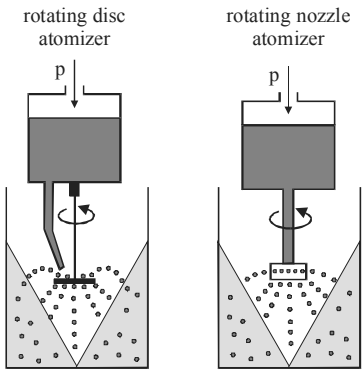

Figure 2:
Scheme of the rotating disc and nozzle technology for bead production

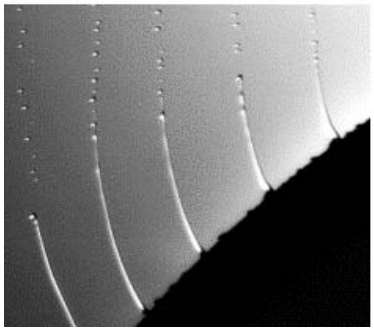

Figure 3:
Photo of bead formation (ligament regime) by a rotating disc device (Koch and Walzel 2001)

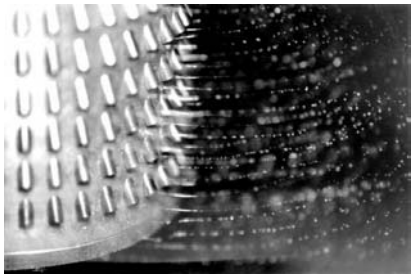

Figure 4:
Photo of bead formation by a rotating nozzle device (Walzel 2001)

The bead size accessible with these technologies ranges from between a few hundred microns up to several millimetres. The size is mainly influenced by the viscosity of the fluid and the rotation speed of the disc/nozzles. The throughput has to be adjusted to the spinning speed in order to be within the desired disintegration regime.

In any case, the bead formation with these technologies is not as well defined as for the dropping technologies, so that generally the particles are quite broadly distributed. Another, very severe problem is the occurrence of satellite beads (Champagne et al. 2000). Satellite beads are beads which are significantly smaller than the beads which were produced. They are generated by a non-ideal disintegration of the ligaments. Although satellite beads might also be generated by dropping technologies if the device is not run correctly, they can almost entirely be eliminated for the dropping technologies. In contrast, for the two rotating technologies, the avoidance of satellite beads is more the exception than the rule. Another disadvantage is again a severe limitation in the fluid's viscosity, which usually has to be below a value of approximately 200 mPa·s. Nevertheless, as these two classical technologies possess a very high throughput, they both are widely used for industrial processes.

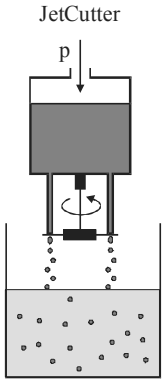

Figure 5:
Scheme of the JetCutter technology for bead production

2.3 JetCutter

The JetCutter technology is based on a completely different principle from bead generation and is achieved by a mechanical cut of a solid liquid jet (Figure 5). The JetCutter is described in detail in the next chapter. For a literature overview see Prüße and Vorlop 2002b.

3 The JetCutter

3.1 Principle and device

In bead production by the JetCutter, the fluid is pressed with a high velocity out of a nozzle as a solid jet. Directly underneath the nozzle the jet is cut into cylindrical segments by a rotating cutting tool made of small wires fixed in a holder. Driven by the surface tension, the cut cylindrical segments form spherical beads while falling further down to an area where they finally can be gathered.

Bead generation with JetCutting is based on the mechanical impact of the cutting wire on the liquid jet. This impact leads to the cut together with a cutting loss, which in a first approach can be regarded as a cylindrical segment with the height of the diameter of the cutting wire. This segment is pushed out of the jet and slung aside where it can be gathered and recycled (Figure 6). As only a mechanical cut and the subsequent bead shaping driven by the surface tension are responsible for bead generation, the viscosity of the fluid has no direct influence on the bead formation itself. Thus, the JetCutter technology is capable of processing fluids with viscosities up to several thousand mPa·s.

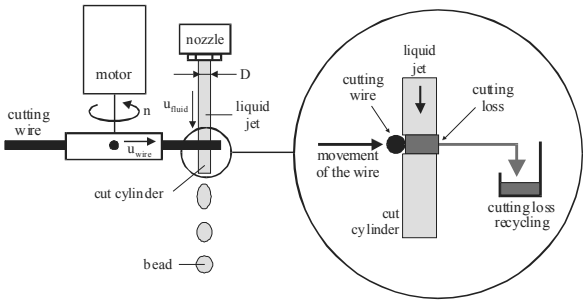

Figure 6:
Scheme of the cutting process, simplified model

The size of the beads can be adjusted within a range of between approx. 200 µm up to several millimetres. The main parameters are the nozzle diameter, the flow rate through the nozzle, the number of cutting wires and the rotation speed of the cutting tool. In order to get narrowly distributed beads one has to maintain a steady flow through the nozzle which may

achieved with a pressure vessel or a pulsation-free pump and a uniform rotation speed of the cutting tool.

The cutting tool itself also has to fulfil one major requirement. In order to produce beads of the same size, the wires have to have equal distances. This is best achieved by a circular stabilisation of the wires on the outer perimeter as is shown in Figure 7.

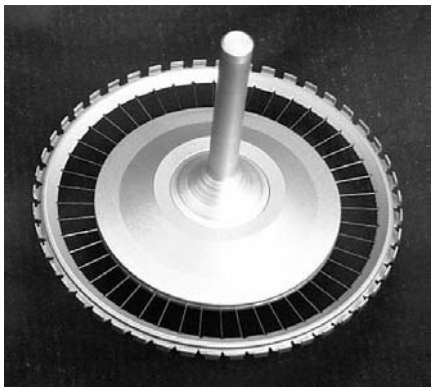

Figure 7:
Photo of a cutting tool with 48 stainless steel wires (Ø = 50 µm) and circular stabilisation

This circular stabilisation is essential even if the wire diameter is reduced in order to decrease the cutting losses (see also Figure 6). The diameter of the cutting wire may be decreased down to 30 µm. Usually, stainless steel wires are used, but the application of polymer fibres is also practicable.

Another requirement for the JetCutter is that a solid jet is formed. Therefore, special solid jet nozzles have to be applied. Even with these solid jet nozzles the liquid jet disintegrates after a certain length. This length depends on the viscosity and velocity of the fluid. In order to ensure a perfectly shaped jet at the point where it is cut by the wires, the cutting tool should not be too far away from the nozzle outlet, e.g. only a few millimetres (Figure 8).

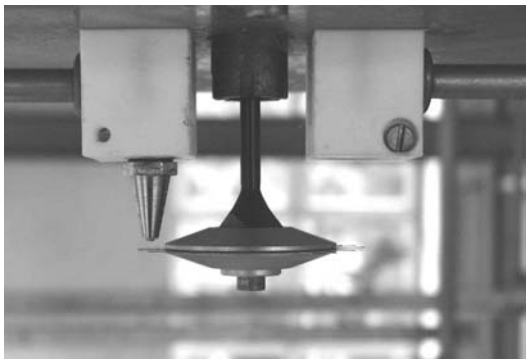

Figure 8:
Arrangement of nozzle (left, in the white holder) and cutting tool

3.2 Detailed description of the cutting process

At first glance, the principle of the JetCutter is very simple. Nevertheless, at second glance, it is much more complicated. The cutting process as shown in Figure 6 is idealised and only holds true if the velocity of the cutting wire is much higher than the velocity of the liquid jet. Actually, these two velocities are in the same range so that the progressive movement of the liquid jet has to be taken into account for a proper description of the cutting process (Figure 9, see also Prüße, Bruske et al. 1998 and Prüße, Fox et al. 1998a).

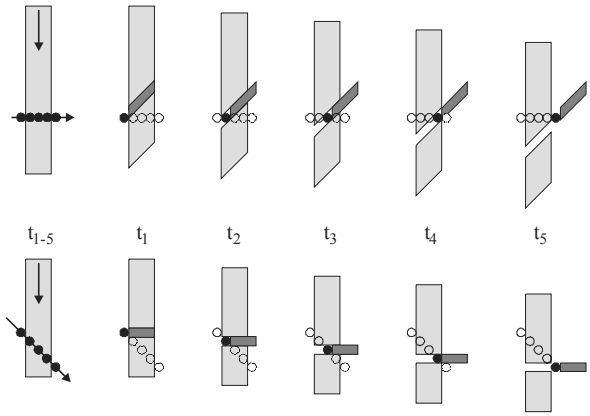

Figure 9:
Locally and temporally resolved schematic representation of the cutting process for a horizontal cutting plane (top) and an inclined cutting plane (bottom), actual position of the cutting wire: black circles, former and future positions of the cutting wires: blank circles, cutting loss: dark grey, liquid jet: bright grey, t = time

Figure 9 shows both a locally and temporally resolved scheme of the cutting process. On the very left hand side, the liquid jet and the positions of the cutting wires at the different times t_1 to t_5 (cutting plane) in relation to the liquid jet are shown. Further to the right, the progressive movement of the jet is shown at each time (t_1 - t_5) as well as the actual position of the cutting wire at that time (black circle). Prior and subsequent positions of the wire are indicated by blank circles. The cutting loss which is pushed out of the jet is also displayed.

In the case of a vertical nozzle and a horizontal cutting plane (Figure 9, top) it can be seen that the progressive movement of the liquid jet during the cutting process leads to a diagonal cut through the liquid jet. Accordingly, a proper inclination of the cutting tool should lead to a straight cut through the jet (Figure 9, bottom).

Figure 9 displayed that the progressive movement of the jet during cutting leads to a diagonal cut through the liquid jet. Thus, the cutting loss has a

somewhat ellipsoidal shape – and is therefore larger than it is in the idealised model in Figure 6 – and the cut cylinders are distorted (Figure 10). Further, it is conceivable that the ends of the distorted cylinders might be torn off from the rest of the cylinder and form additional spraying losses. In that case the overall losses generated by the mechanical cut through the liquid jet would be quite high. Nevertheless, it is also shown that a proper inclination either of the cutting tool (Figure 10, middle) or the nozzle (Figure 10, bottom) lead to straight cut through the jet with the "normal" cutting loss and no additional spraying losses.

On the basis of this more sophisticated geometrical model a set of equations displayed in Table 1 has been derived which is capable of describing the cutting process both for a perpendicular arrangement of nozzle and cutting plane (horizontal cutting plane) as well as for an inclined arrangement (inclined cutting plane). Table 2 shows the check-up of the model. Here, the experimental values of the overall losses during the production of PVA beads in dependence on the diameter of the cutting wires used are displayed. Two sets of experiments are shown, one with a horizontal cutting plane (cutting losses and additional spraying losses) and one with a properly inclined cutting plane (only cutting losses). For comparison, the theoretical values are also given. Table 2 offers three important pieces of information:

1. The losses decrease if a proper inclination is applied.
2. Experimental and theoretical values are in good agreement, so that the model is suited to describe the cutting process.
3. By using small cutting wires and an inclined cutting plane, the losses can be decreased down to less than 2 %. Such low losses are tolerable, no loss recycling has to be applied.

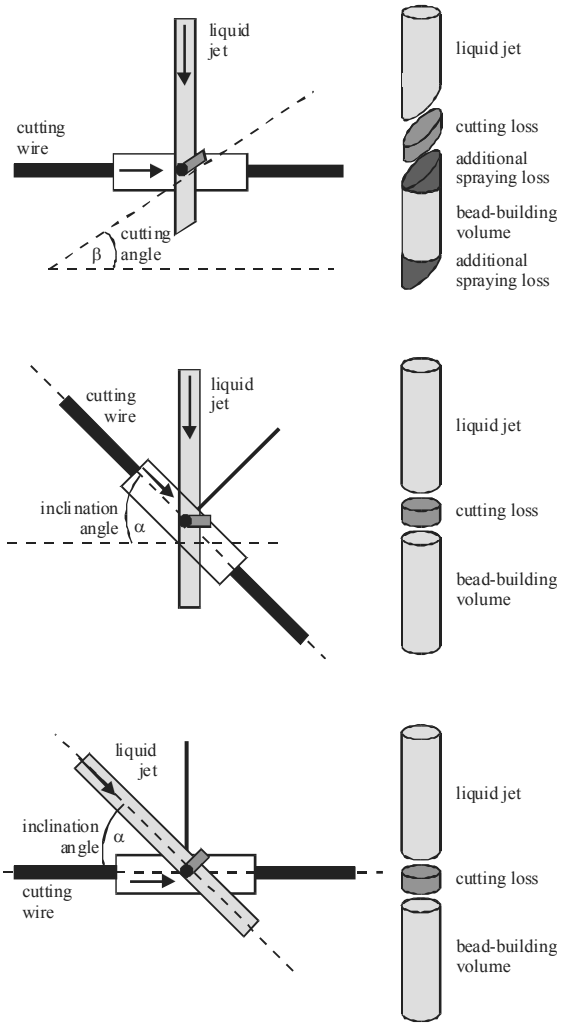

Figure 10:
Possible arrangements of nozzle and cutting tool and resulting losses, from top to bottom: perpendicular arrangement, inclined cutting tool, inclined nozzle

Table 1:
Mathematical model of the JetCutter

parameter	horizontal cutting plane	inclined cutting plane
angle	$\beta = \arctan\left(\frac{u_{fluid}}{u_{wire}}\right)$	$\alpha = \arcsin\left(\frac{u_{fluid}}{u_{wire}}\right)$
cutting loss	$V_{loss} = \frac{\pi \cdot D^2}{4} \cdot \frac{d_{wire}}{\cos\beta}$	$V_{loss} = \frac{\pi \cdot D^2}{4} \cdot d_{wire}$
overall loss	$V^*_{loss} = \frac{\pi \cdot D^2}{4} \cdot \left[\frac{u_{fluid}}{n \cdot z} \cdot \frac{(d_{wire} + D \cdot \sin\beta)}{\cos\beta}\right]$	$V^*_{loss} = \frac{\pi \cdot D^2}{4} \cdot d_{wire}$
bead diameter	$d_{bead} = \sqrt[3]{\frac{3}{2} \cdot D^2 \cdot \left[\frac{u_{fluid}}{n \cdot z} \cdot \frac{(d_{wire} + D \cdot \sin\beta)}{\cos\beta}\right]}$	$d_{bead} = \sqrt[3]{\frac{3}{2} \cdot D^2 \cdot \left[\frac{u_{fluid}}{n \cdot z} - d_{wire}\right]}$

Table 2:
Overall losses for horizontal (horiz.) and inclined (incl.) cutting plane in dependence on the diameter of the cutting wire, exp: experimental, calc: calculation

Wire diameter, mm	Overall losses, %			
	horiz. cutting plane		incl. cutting plane	
	exp	calc	exp	calc
0.1	8.8	7.9	2.4	2.0
0.2	10.4	10.1	4.0	3.9
0.3	10.2	12.5	6.6	5.8

But, although the model is able to describe the process in terms of losses and also the resulting bead diameter, it is still a model. Thus, it is not really surprising that the reality still looks different (Figure 11).

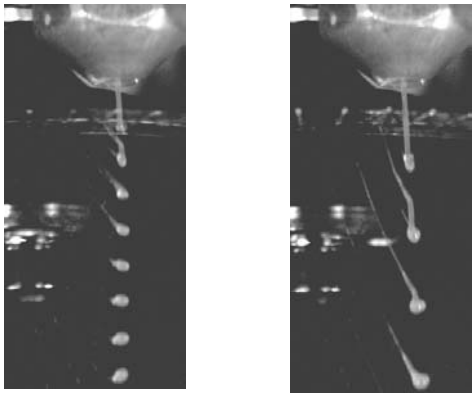

Figure 11:
High speed images of the cutting process during the production of alginate beads, left: high wire velocity and low fluid velocity = small beads, right: low wire velocity and high fluid velocity = large beads

In Figure 11, two photos of the cutting process taken with a high speed camera are shown. In both cases a horizontal cutting plane has been applied. It is obvious that the cut segments do not really have a cylindrical shape. Nevertheless, these segments are able to form spherical beads after a short period (Figure 11, left). With regard to losses, a bent end of the cut segment is on top, but it remains almost in contact with the cutting wire, which pulls it from the cut segment as if it were molten cheese (Figure 11, right). But in this case beads are still formed after a short period of time. The photos clearly indicate that there is still a lot of work to do in order to fully understand the process of bead formation by JetCutting.

3.3 Throughput and scale-up

A necessary requirement for bead production in JetCutting is that a really solid jet be pressed out of the nozzle and that this solid jet be maintained until it is cut by the wires. This can be achieved with a combination of special solid jet nozzles and a high fluid velocity (up to 30 m/s), the latter with corresponding high flow rates. Due to the solid jet requirement, the flow rate per nozzle is considerably higher for the JetCutter than for any other bead production technology. Nevertheless, since the two rotating techniques both contain multi nozzles or multi bead generation sites, the bead production rate from the rotating disc in each device is higher for these two technologies as compared with a single nozzle JetCutter. For the JetCutter technology two methods of scaling-up are possible.

First, a multi-nozzle JetCutting device can be applied, in which the nozzles are staggered near the perimeter of the cutting tool. In this case, special attention has to be paid to avoid additional spraying losses. If a horizontal cutting tool is used with vertically arranged nozzles, considerable additional spraying losses will be occur, which, of course, is undesirable. The application of an inclined cutting tool, although perfectly suited for a single-nozzle system, is not much better since the additional spraying losses can only be avoided at one single site on the circuit, whereas on the opposite side of the circuit these losses would be even higher than usual. The problem can be solved only if properly inclined nozzles are used together with a horizontal cutting tool. With this arrangement, the additional spraying losses can be avoided at any site on the cutting tool‘s circuit (Figure 12).

The second possibility for a JetCutter scale-up is the increase of the cutting frequency. The cutting frequency determines how often the jet is cut in a definite time period and, thus, how many beads are generated in that time. The cutting frequency is given by the number of cutting wires in the cutting tool and its rotation speed. Usually, the JetCutter is used with cutting frequencies between 5000 and 10000 Hertz (Hz) (maximum 14400 Hz), which means that from 5000 to 10000 beads per second are generated. A further enhancement of the cutting frequency will be achieved when a motor drive with a higher rotation speed and a cutting tool with more wires are applied. With this approach, for special applications cutting frequencies of up to 25000 Hz might be realised.

The production rates of a single nozzle JetCutter device for three common cutting frequencies are shown in Table 3. The rates are given in terms of L/(h·nozzle). Table 3 indicates that – depending on the desired particle size – even with the single nozzle JetCutter device and common cutting frequencies, the production rate per day can range between one kilogram and several tons of beads.

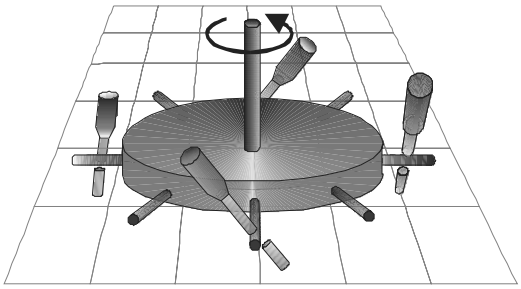

Figure 12:
Scheme of a multi nozzle JetCutter operating without additional spraying losses

Table 3:
Theoretical throughput of the JetCutter in L/(h·nozzle) for different bead diameters and a cutting frequency of 5000, 7500 and 10000 Hertz (Hz), respectively

Bead diameter, mm	Theoretical throughput, L/(h·nozzle)		
	5000 Hz	7500 Hz	10000 Hz
0.2	0.08	0.11	0.15
0.4	0.60	0.91	1.2
0.6	2.1	3.1	4.1
0.8	4.8	7.2	9.7
1.0	9.4	14.1	18.8
1.5	31.8	47.7	63.6
2.0	75.4	113	151
2.5	147	221	295
3.0	254	382	509
4.0	603	905	1206
5.0	1178	1767	2356

3.4 New developments

Currently, three major developments concerning the JetCutter are in process:

1. spraying tunnel for larger beads
2. heating device for melt processing
3. 2-fluid nozzle for simultaneous coating

The high fluid, and therefore bead, velocity is one of the advantages of the JetCutter, as high throughputs are easily realised. Nevertheless, this high droplet velocity is a problem for the collection of beads with a spherical shape, especially for larger beads. If the droplets were collected in a collection bath, e.g. a $CaCl_2$ bath for alginate beads, the droplets may be deformed at the liquid surface when entering the bath. For small droplets, the problems are minor even at speeds of up to 30 m/s. However, larger droplets which have such high speeds will be deformed at the collection bath surface due to their higher weight.

In order to overcome this problem, the droplets have to be pre-gelled prior to entering the collection bath. This pre-gelation is achieved by letting the droplets fall through a tunnel (5 m length) equipped with several spraying nozzles (Figure 13). The collection bath is permanently pumped through the spraying nozzles, which generate a fine mist (aerosol) from the collection bath inside the tunnel. While falling, the spherical droplets are covered with the mist and, thus, are pre-gelled, maintaining their spherical shape. The pre-gelation hardens the droplets – in fact they are not droplets anymore but capsules – so that they maintain their spherical shape when they enter the collection bath.

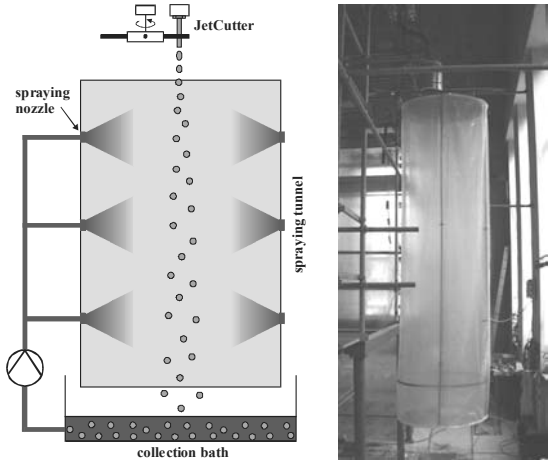

Figure 13:
Scheme (left) and photo (right) of the 5 m spraying tunnel for pre-gelation

The second new development covers the processing of all kinds of hot material, which might be melts, e.g. waxes, or hot solutions, e.g. gelatin solutions. In order to process such materials both the nozzle and the cutting tool have to be heated to avoid clogging. Therefore, the JetCutter has to be surrounded by a heating chamber (Figure 14).

Figure 14:
Heating chamber surrounding the JetCutter sitting on top of the 5 m tunnel

The heated JetCutter sits on top of the 5 m tunnel, which in this case acts as cooling line. This cooling line is sufficient to harden small beads, which have high velocities. In order to harden larger beads as well, the top of tunnel might be additionally equipped with a device to distribute cold gas in the tunnel.

The third new development is devoted to the simultaneous coating of beads by a 2-fluid nozzle (Figure 15). For details about this procedure see Prüße et al. 2000.

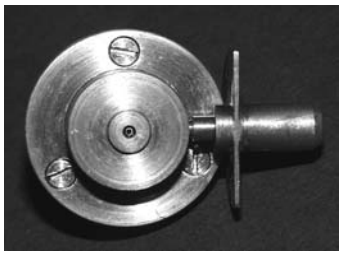

Figure 15:
2-fluid nozzle for the JetCutter

3.5 Applications

Since spherical beads are intermediates or products in different industrial sectors, e.g. agriculture, biotechnology, pharmaceutical, chemical or food industry, many applications exist for the JetCutter technology. Generally, each application field has its own requirements and restrictions concerning the materials to be encapsulated, the type and viscosity of the fluid, the desired particle size or the medium in which the beads should be gathered. In this connection it is advantageous that the JetCutter is capable of processing all kinds of liquid material covering

- solutions,
- melts and
- dispersions.

A tabular summary – not necessarily complete – of fluids tested so far or assumed to work with the JetCutter, as well as substances and materials to be encapsulated is given in Table 4.

Table 4:
Summary of fluids and materials applicable for bead production/encapsulation with the JetCutter

Fluids	Materials
• Alginate	• Pharmaceuticals, pesticides
• Pectinate	• Vitamins, amino acids
• Chitosan	• Fragrances
• Gelatin	• Bacteria, fungi, enzymes
• Cellulose derivatives	• Dyes
• Waxes	• Pigments
• Polymer melts	• Magnetite
• Inorganic sols	• Metal catalysts

Many of these substances can be connected to life sciences. Indeed, life sciences is the application field with the most diverse and challenging tasks for the JetCutter technology. For example, formulations of active agents or fragrances, controlled release systems or functional foods (e.g. vitamins, amino acids, probiotics) are generally made by encapsulation in spheri-

Figure 16:
Photos of different types of beads prepared by Jet Cutting (not in true scale). From top left to bottom right: Ca-alginate (Ø = 0.6 mm), Ca-alginate, freeze-dried (Ø = 0.3 mm), Ca-pectinate (Ø = 0.53 mm), chitosan (Ø = 0.5 mm), gelatin (Ø = 0.8 mm), wax (Ø = 0.7 mm)

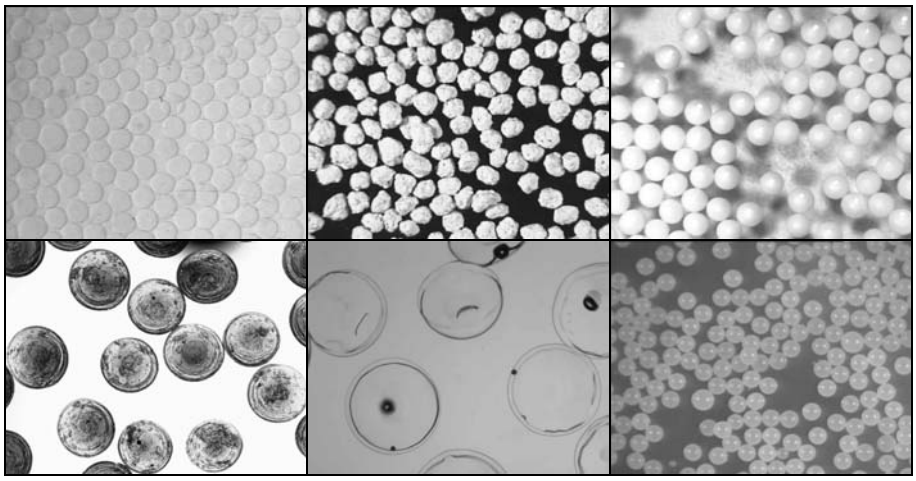

cal beads. In these fields, special legal requirements may exist which affect the encapsulation materials or special substances, for example sensitive biological matter, may need to be treated in a special manner.

The common polymers applied as an encapsulation matrix in the life sciences (e.g. alginate, pectinate, gelatin, cellulose derivatives, waxes) have already been used for bead production by the JetCutter. Some examples of these beads are displayed in Fig. 16.

As already mentioned, one of the major advantages of the JetCutter is that the viscosity of the fluid does not limit bead generation. That means that not only the formulation recipes used at the moment can be applied to bead production by JetCutting, but also those whose transformation into products failed due to a too high viscosity. For the same reason biological matter can be treated at lower temperatures, i.e. more carefully, with the JetCutter since heating for viscosity reduction is not needed.

In biotechnology the JetCutter was used for the preparation of immobilised/encapsulated biocatalysts, i.e., enzymes, bacteria or fungi (Muscat et al. 1996, Prüße, Fox et al. 1998b, Leidig et al. 1999, Jahnz et al. 2001). In this field, the independence of the fluid viscosity also was proven to be advantageous since encapsulation matrices with high polymer contents and corresponding high viscosities can be used (e.g. polyvinyl alcohol) to form mechanically very stable, abrasion-free beads. Such beads were also used for the encapsulation of metal catalysts (Prüße, Morawsky et al. 1998).

As far as dispersions are concerned, sols, suspensions and emulsions may be processed with the JetCutter. Two examples of processed suspensions are shown in the Figures 17 and 18.

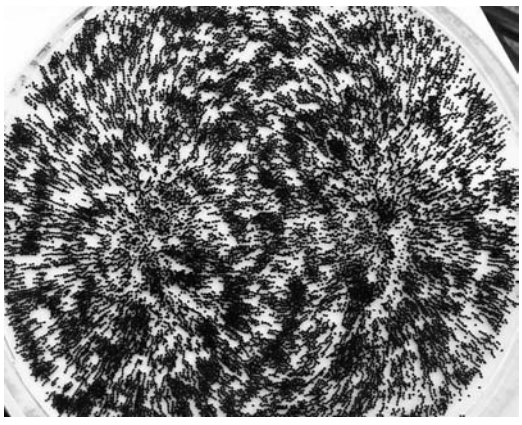

Figure 17:
20 % magnetite (in initial suspension) encapsulated in chitosan beads (Ø = 0.8 mm)

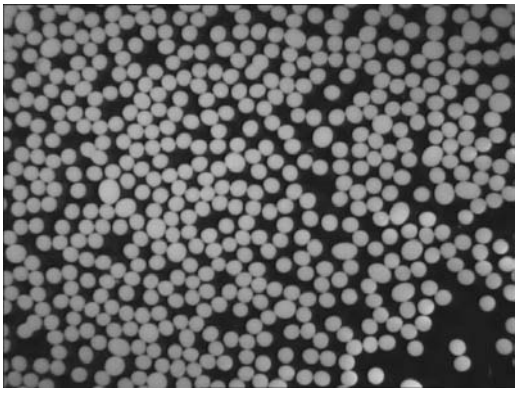

Figure 18:
40 % TiO_2 (in initial suspension) encapsulated in alginate beads (Ø = 1.3 mm)

4 Summary and prospect

Different bead production technologies based on the generation of droplets prior to their solidification were compared. Simple dropping and electrostatic-enhanced dropping are well suited for lab-scale applications. Vibrational bead production is further used in technical scale applications. The rotating disc and rotating nozzle technology suffer from the broad particle size distribution. But as real high throughput technologies they are widely used in industry. All these technologies are limited due to the viscosity of the fluids to be processed.

So far, the JetCutter is the only technology for which bead generation is not limited by the fluid viscosity. Thus, highly viscous fluids also can be transformed into beads. Furthermore, the JetCutter is a simple and efficient technology for the production of spherical beads. Monodisperse beads in the particle size ranging from approximately 200 µm up to several millimetres can be prepared with high production rates. In addition, scaling-up the JetCutter will be easily achievable. Losses can be regarded as negligible. None of the other technologies for beads production shows this combination of advantages. Further, the JetCutter may also be used to produce coated beads in a one-step process.

The JetCutter technology can be applied in different industrial sectors and for various applications such as solutions, melts and dispersions are processible. In the life sciences it might be used for the encapsulation of active agents or fragrances, as well as for the production of some functional foods (e.g. encapsulated vitamins or probiotics). In the chemical industry, applications such as the production of catalysts supports, packages for chromatographic columns or polymer pellets are possible. Many other applications are also imaginable.

The JetCutter is a very promising technology for the production of spherical beads with manifold application possibilities. According to the sum of its advantages, the JetCutter can be regarded as a superior technology for bead production. Accordingly, the first technical scale application of bead production with the JetCutter technology (capacity of about 1.2 tons/day for 1 mm beads with a density of 1 kg/L) started in summer 2002.

Symbols and abbreviations

calc	calculation
d_{wire}	diameter of the cutting wire
d_{bead}	bead diameter
D	nozzle diameter
exp	experimental
h	hour
horiz.	horizontal
Hz	Hertz
incl.	inclined
L	litre
m	meter, milli
mm	millimetre
n	number of rotations
p	pressure
Pa	Pascal
s	second
t	time
u_{fluid}	velocity of the liquid jet
u_{wire}	velocity of the cutting wire
V_{loss}	volume of the cutting loss
V^*_{loss}	volume of the overall loss
z	number of cutting wires
α	inclination angle
β	cutting angle
µm	micrometer
Ø	diameter

References

Champagne C, Blahuta N, Brion F, Gagnon C (2000) A vortex-bowl disk atomizer system for the production of alginate beads in a 1500-liter fermenter. Biotechnol Bioeng 68(6):681-688

Heinzen C, Marison I, Berger A, von Stockar U (2002) Use of vibration technology for jet break-up for encapsulation of cells, microbes and liquids in monodisperse microcapsules. Landbauforsch Völkenrode SH 241:19-25

Jahnz U, Wittlich P, Prüße U, Vorlop K-D (2001) New matrices and bioencapsulation processes. Focus on biotechnology 4:293-307

Koch M, Walzel P (2001) New findings on catalyst encapsulation in a pilot plant. 3rd European Congress on Chemical Engineering [CD-ROM] Dechema e.V. Frankfurt/Main

Kuncová G (2002) Web-based literature database "Encapsulation Technologies": Dropping. <http://www.genialab.de/WG3/>

Lacík I (2002) Web-based literature database "Encapsulation Technologies": Vibration. <http://www.genialab.de/WG3/>

Leidig E, Prüße U, Vorlop K-D, Winter J (1999) Biotransformation of Poly R-478 by continuous cultures of PVAL-encapsulated Trametes versicolor under non-sterile conditions. Bioprocess Eng 21(1):5-12

Muscat A, Prüße U, Vorlop K-D (1996) Stable support materials for the immobilization of viable cells. In: Wijffels RH, Buitelaar RM, Bucke C (eds) Immobilized cells: basics and applications, Elsevier, Amsterdam, pp 55-61

Nedović V (2002) Web-based literature database "Encapsulation Technologies": Electorstatic-enhanced dropping. <http://www.genialab.de/WG3/>

Nedović VA, Obradović B, Poncelet D, Goosen MFA, Leskošek-Čukalović I, Bugarski B (2002) Cell immobilisation by electrostatic droplet generation. Landbauforsch Völkenrode SH 241:11-17

Prüße U, Bruske F, Breford J, Vorlop K-D (1998) Improvement of the Jet Cutting Method for the Preparation of Spherical Particles from Viscous Polymer Solutions. Chem Eng Technol 21(2):153-157

Prüße U, Dalluhn J, Breford J, Vorlop K-D (2000) Production of spherical beads by JetCutting. Chem Eng Technol 23(12): 1105-1110

Prüße U, Fox B, Kirchhoff M, Bruske F, Breford J, Vorlop K-D (1998) New Process (Jet Cutting Method) for the Production of Spherical Beads from Highly Viscous Polymer Solutions. Chem Eng Technol 21 (1):29-33

Prüße U, Fox B, Kirchhoff M, Bruske F, Breford J, Vorlop K-D (1998) The Jet Cutting Method as a new Immobilization Technique. Biotechnology Techniques 12 (2):105-108

Prüße U, Morawsky V, Dietrich A, Dierich A, Vaccaro A, Vorlop K-D (1998) Encapsulation of Microscopic Catalysts in Polyvinyl Alcohol Hydrogel Beads. Stud Surf Sci Catal 118:137-146

Prüße U, Vorlop K-D (2002a) Web-based literature database "Encapsulation Technologies": Rotating disc, rotating nozzle. <http://www.genialab.de/WG3/>

Prüße U, Vorlop K-D (2002b) Web-based literature database "Encapsulation Technologies": JetCutter. <http://www.genialab.de/WG3/>

Walzel P (2001) <http://www.chemietechnik.uni-dortmund.de/mv/>

Cell immobilisation by electrostatic droplet generation

Viktor A. Nedović[1], Bojana Obradović[2], Denis Poncelet[3], Mattheus F.A. Goosen[4], Ida Leskošek-Čukalović[1], and Branko Bugarski[2]

Abstract

This paper reviews the feasibility of electrostatic droplet generation for the production of uniform hydrogel microbeads and applications of this technique for cell immobilization. This is a novel extrusion technique that uses electrostatic forces to disrupt a liquid surface at the capillary/needle tip and form a charged stream of small droplets. Experimental parameters which are critical for production of polymer microbeads (in the range of 0.1 to 1 mm in diameter), as well as mechanisms of alginate droplet formation are presented here. It was shown that microbead size was a function of applied potential, polymer surface tension, needle size and electrode geometry. In addition, this technique was applied for immobilization of several cell types (yeast, mammalian and plant cells). There was no detectable loss in viability of these cell cultures after exposure to high electrostatic potentials. Cultivation studies of cells immobilized by electrostatic droplet generation showed good maintenance of cell viability and activity, indicating broad potential of this technique for the immobilization of a variety of cell types for applications in different fields of biotechnology, pharamceuticals and medicine.

Keywords: Electrostatic droplet generation, cell immobilization, alginate carrier, microbead

1 Introduction

Hydrogel-immobilized cell systems are attractive for a variety of applications in biotechnology and medicine. Natural polysaccharides (e.g. agar, alginates, κ-carrageenan), gel-forming proteins (e.g. gelatin) and synthetic polymers (e.g. polyacrylamide) have gained a leading role as cell carriers in entrapment and encapsulation technology (Jen et al. 1996; Murano 2000). Among these, spherical beads based on Ca-alginate gels are the most-used supports for the immobilization of living cells (Strand et al. 2000).

For many bioprocesses, there is a distinctive demand for the utilization of very small hydrogel beads (< 1 mm in diameter) with immobilized cells to avoid diffusional limitations of nutrients and metabolic products within the beads (Ogbona et al. 1991; Bugarski et al. 1994a; Nedovic et al. 2001). In recent years, several techniques were developed and established for the production of such microbeads on laboratory and industrial scales. These include an atomisation method, emulsion technology, resonance method, jet cutting method and electrostatic droplet generation (Ogbona et al. 1991; Bugarski et al. 1994a; Brandenberger and Widmer 1997; Jahnz et al. 2001; Poncelet et al. 2001).

This paper reviews the feasibility of electrostatic droplet generation for the production of uniform hydrogel microbeads and applications of this technique for cell immobilization.

2 Formation of hydrogel microbeads by electrostatic droplet generation

The electrostatic droplet generation technique is based on the use of electrostatic forces to disrupt a liquid surface at the capillary/needle tip and form a charged stream of small droplets (Bugarski et al. 1994a). Electrostatic potential is applied between the droplet formation device and the collecting solution, inducing a charge at the surface of the polymer solution, and resulting in a decrease in surface tension. In this way, a significant reduction of droplet size may be realized as compared to the simple dropping method.

The basic experimental set-up for this technique is shown in Figure 1. Spherical droplets were formed by the extrusion of a polymer or polymer/cell suspension through a blunt stainless steel needle using a syringe pump. As the polymer solution was forced out of the tip of the needle by the syringe pump, the droplets were pulled off by the action of gravitational and electrostatic forces. Droplets were collected in a hard-

[1] Viktor A. Nedović and Ida Leskošek-Čukalović, Department of Food Technology and Biochemistry, Faculty of Agriculture, University of Belgrade, Nemanjina 6, 11081 Belgrade-Zemun, Yugoslavia

[2] Bojana Obradović and Branko Bugarski, Department of Chemical Engineering, Faculty of Technology and Metallurgy, University of Belgrade, Karnegijeva 4, 11000 Belgrade, Yugoslavia

[3] Denis Poncelet, ENITIAA, Rue de la Géraudiere, BP 82 225, Nantes, 44322, France

[4] Mattheus F.A. Goosen, Department of Bioresource and Agricultural Engineering, College of Agriculture, Sultan Qaboos University, Al-Khod 123, Muscat, Sultanate of Oman

ening solution where the ion exchange took place, providing gellation and the formation of microbeads.

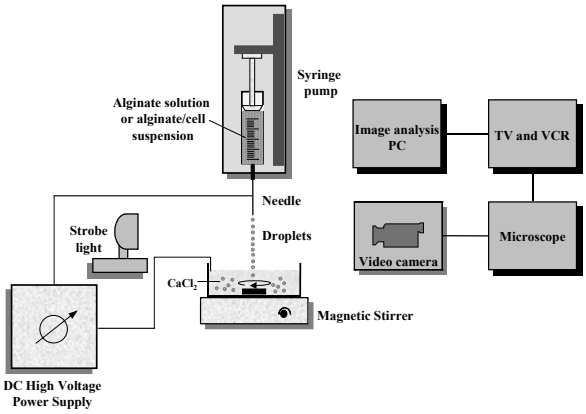

Figure 1:
Experimental set-up for electrostatic droplet generation

Investigated polymers were low viscosity alginate at concentrations in the range 0.8 - 4 % and κ-carrageenan at a concentration of 4 % alone or in a mixture with 0.25 % locust been gum (Keshavarz et al. 1992; Bugarski et al. 1994a; Goosen et al. 1997). Hardening solutions were $CaCl_2$ in concentrations of 1,5 or 2 % in the case of alginate and a mixture of 1.125 % KCl and 0.5 % $CaCl_2$ in the case of κ-carrageenan. The potential difference was controlled with a voltage power supply with voltages from 0 to 30 kV.

In addition, distance between the needle tip and hardening solution, flow rate of polymer solution and needle diameter were varied in the ranges 2 to 10 cm, 4 to 45 ml/h, and 19 to 27 gauge, respectively, as process parameters (Keshavarz et al. 1992; Bugarski et al. 1994a; Goosen et al. 1997).

Video image analysis of the alginate extrusion process revealed the influences of the electrostatic field on mechanisms of droplet formation (Bugarski et al. 1993;1994a).

In the absence of an electrostatic field with gravitational force acting alone, each alginate drop grew at the tip of the needle until its weight overcame the net vertical component of the surface tension force (Figure 2A). After a voltage was applied, the liquid meniscus at the needle tip was distorted from a spherical shape into an inverted cone-like shape (Figure 2B). A charge at the tip of the inverted cone reduced the surface tension of the alginate solution resulting in formation of a neck-like filament (Figure 2C&D). When this filament broke away, producing small droplets (Figure 2E), the meniscus relaxed back to a spherical shape until flow of the polymer caused the process to start again (Bugarski et al. 1994a). In this way, under appropriate process parameters, a 6 to 10-fold reduction in bead diameter as compared to the simple dropping method was obtained.

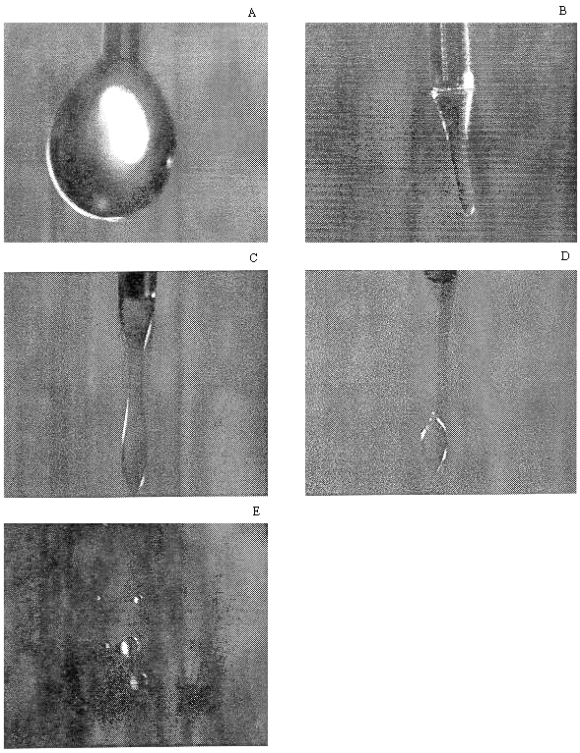

Figure 2:
Droplet formation of a 1.5 % sodium alginate solution at a needle tip: A) no electrostatic potential applied; B) meniscus formation when applied potential was between 4 and 5 kV; C) neck formation; D) stretching of the liquid filament; E) brake-up of the liquid filament

Three electrode geometries were considered (Bugarski et al. 1994a&b; Poncelet et al. 1994):

- a parallel plate arrangement in which the positive charge was applied to a plate held parallel to the collecting solution and through the center of which the needle protruded (Figure 3A). This system was employed to produce a uniform electric field in the same direction as that of gravity. The grounded plate with the collecting solution had the same dimensions as the upper charged plate;
- a positive charge applied directly to the collecting solution and a grounded needle (Figure 3B);
- a positively charged needle and a grounded collecting solution (Figure 3C).

In the case of alginate bead formation, the most effective electrode and charge arrangement for producing small droplets was shown to be the third set-up, i.e., a positively charged needle and a grounded collecting solution (Bugarski et al. 1994a&b; Poncelet et

al. 1999a). In this arrangement, a significantly smaller area is available for charge distribution (needle tip), resulting in higher overall surface charge and smaller droplets as compared to the parallel plate set-up. In addition, the positively charged needle induced the concentration of positively charged small Na^+-ions at the droplet surface (Figure 4A). When the polarity of the electrodes is permuted as in the second set-up i.e. a positively charged collecting solution and a grounded needle, the negatively charged functional groups of alginate tend to be adsorbed at the droplet surface (Figure 4B). As the alginate ions are much larger than the Na^+-ions and have lower diffusion mobility, the surface charge is lower. Consequently, the resulting droplets in this electrode arrangement are larger as compared to those obtained in the positively charged needle set-up (Figure 5).

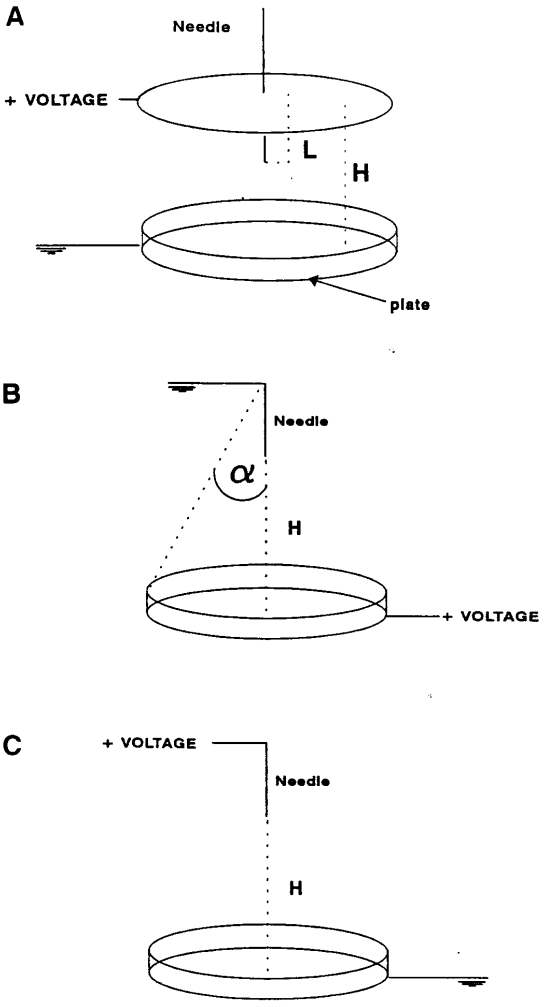

Figure 3:
Electrode geometry and charge arrangements: A) parallel plate set-up with positively charged plate and grounded collecting solution; B) grounded needle and positively charged collecting solution; C) positively charged needle and grounded collecting solution

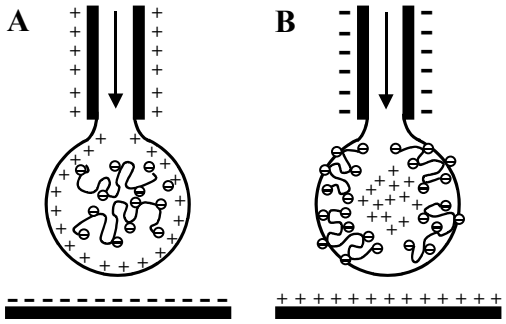

Figure 4:
Schematic illustration of disposition of counter-ions (Na^+) and macro-ions (alginate) for two opposite charge arrangements. A) Positively charged needle causes the adsorption of positively charged counter-ions at the droplet surface; B) Positively charged collecting solution causes the adsorption of negatively charged macro-ions at the droplet surface

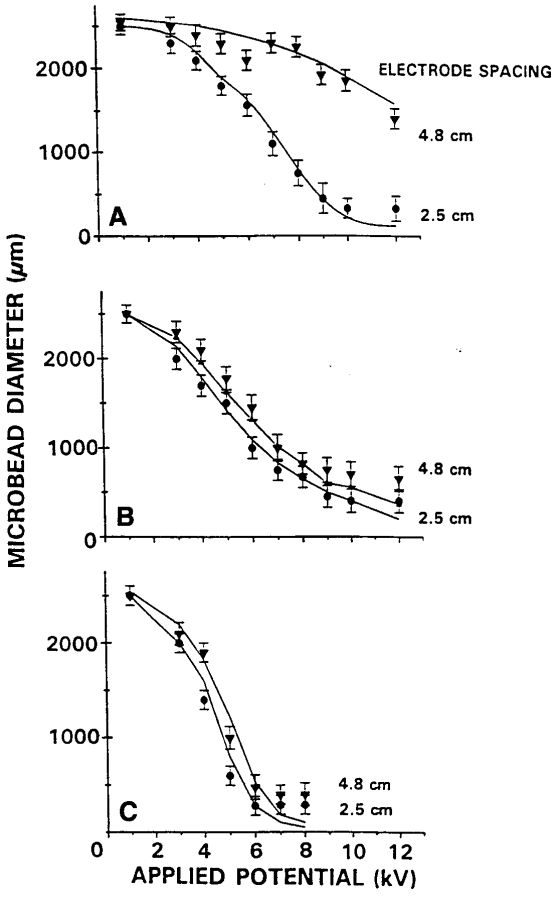

Figure 5:
Effect of applied potential on microbead size for two electrode distances (2.5 and 4.8 cm) and for the 22-gauge needle and alginate concentration of 1.5 %. (A) Parallel plate set-up; (B) Positively charged collecting solution; (C) Positively charged needle

For the parallel plate arrangement the critical potential (U_{cr}) was mainly a function of the distance between the electrodes (h) in the form:

$$U_{cr} = \sqrt{\frac{h\gamma_o}{k\varepsilon_o}} \quad (1)$$

where γ_o is the surface tension of the polymer solution at zero voltage (in case of alginate solutions γ_o is approximated by the surface tension of water), ε_o is the permittivity of vacuum and k is a fitting parameter accounting for geometrical and kinetic approximations.

For the positively charged needle set-up, the critical potential was a function of the capillary diameter (d_c) in a similar fashion:

$$U_{cr} = \sqrt{\frac{d_c\gamma_o}{k\varepsilon_o}} \quad (2)$$

Droplet diameter (d) was then correlated to the applied potential (U) in the form:

$$d = d_o\left[1-\left(\frac{U}{U_{cr}}\right)^2\right]^{1/3} \quad (3)$$

where d_o is droplet diameter at U = 0.

As can be deduced from the above equations, droplet diameter is mainly a function of the applied potential, polymer surface tension and distance between electrodes or capillary diameter depending on the electrode arrangement. In the parallel plate set-up, a decrease in electrode distance resulted in a significant decrease in critical potential and microbead diameter (Figure 5A). Similarly, in the positively charged needle set-up as the capillary diameter was decreased, the critical potential was decreased and microbead diameter reduced (Figure 6B&C). The other investigated parameters had little effect on droplet diameter, such that two alginate concentrations of 0.8 and 1.5 % and three electrode distances (2.5, 3.4, and 4.8 cm) resulted in microbeads with comparable diameters (Figure 6A,B&C). The above model was shown to fit well the experimental data for the positively charged needle set-up and for the parallel plate arrangement at electrode distances significantly larger than the capillary diameter ($h >> d_c$) (Poncelet et al. 1999a).

Electrostatic droplet generation with positively charged needle set-up and the applied potential of 6 kV, 26-gauge needle and 2.5 cm electrode distance provided production of alginate microbeads with diameters down to 170 mm at narrow size distribution (Bugarski et al. 1994a).

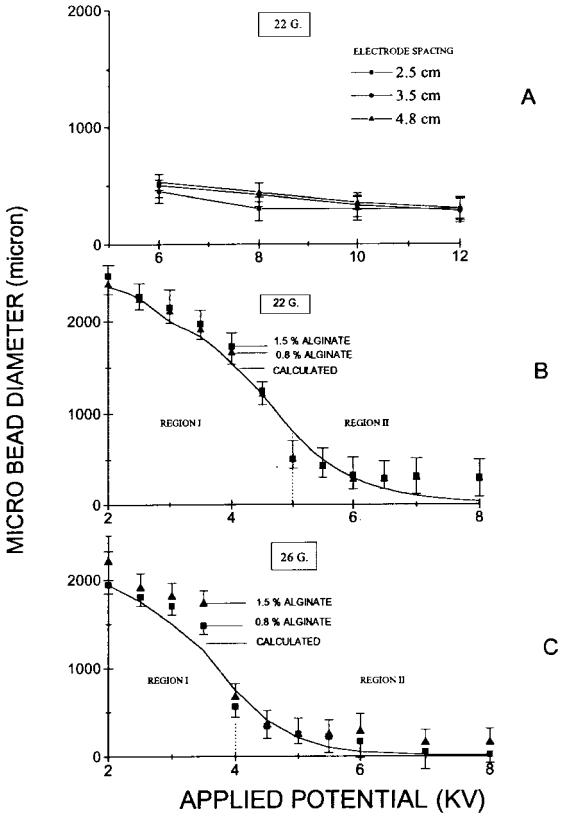

Figure 6:
Positively charged needle set-up: Microbead size as a function of electrode distance (A), alginate concentration (B,C), and needle size (B,C)

3 Cell immobilization studies

The main objectives for cell immobilization are the preservation of cell viability and activity. Major concerns in the use of electrostatic droplet generation for this purpose are possible negative effects of electrostatic field on cells. These effects and cell immobilization using this technique were investigated for different cell types such as insect, fungi, bacteria, yeast, mammalian, and plant cells.

The effects of electrostatic potentials were investigated for insect cells (*Spodoptera frugiperda*), which are attractive as hosts for baculoviruses, used for genetic engineering (Goosen 1996). Suspension of these insect cells at the initial cell density of 4 x 10^5 cells/ml was extruded using an electrostatic droplet generator with positively charged needle set-up at the applied potentials of 6 and 8 kV. The cell concentration immediately after the extrusion remained essentially unchanged at 3.85 x 10^5 and 3.8 x 10^5 cell/ml, respectively, while the prolonged cultivation of these

cells did not show any loss of cell density or viability (Goosen 1996).

In a similar study, the effects of electrostatic potentials were investigated for fungi (spores of *Penicillium chrysogenum*), bacteria (*Pseudomonas putida*) and yeast (*Saccharomyces cerevisiae*) (Keshavarz et al. 1992). Suspensions of these cells were extruded through an electrostatic droplet generator with positively charged needle set-up at the applied potential of 5 kV. As compared to the non-treated control cultures, there were no detectable differences in the germination and growth for the spores, and growth of the bacteria and yeast cell cultures.

Brewing yeast cells (*Saccharomyces uvarum*) were immobilized in alginate microbeads by electrostatic droplet generation and cultivated in growth medium for 6 days (Nedovic et al. 2001).

Microbeads were produced by extrusion of cell suspensions in 2 % sodium alginate through an electrostatic droplet generator with positively charged needle set-up at applied potentials in the range 0 - 8 kV. Initial cell concentration, needle size and electrode distance were varied in the ranges 10^6 to 10^9 cell/ml, 20 to 27-gauge and 2 to 8 cm, respectively (Nedovic et al. 2001).

Diameter of microbeads loaded with yeast cells was a function of the applied potential and needle diameter (Figure 7) in a similar fashion as it was previously shown for pure alginate solutions (Figure 5C, Bugarski et al. 1994b). However, critical potentials for cell suspensions in alginate were significantly higher than those for pure alginate solutions at approximately the same other process parameters. Consequently, the obtained microbeads loaded with yeast cells were larger than those without cells (see Figs 5C, 6B&C and 7). The possible explanation lies in the mechanism of droplet formation. The investigated yeast concentrations were sufficiently high to influence the surface tension of the droplet due to the negative cell surface charge. In the case of the positively charged needle set-up used in this study, the presence of negatively charged cells would decrease the positive charge of the droplet surface and increase the surface tension as compared to the pure alginate.

Effects of yeast immobilization by electrostatic droplet generation were investigated over 6 days of cultivation of the obtained microbeads in growth medium in well mixed flasks (Nedovic et al. 2001). Growth of the yeast cells in these microbeads of three different sizes was compared to the growth of yeast cells immobilized in alginate microbeads using extrusion under coaxial air jet (Figure 8). There were no notable differences in growth curves and specific growth rates of the immobilized yeast cells among the experimental groups.

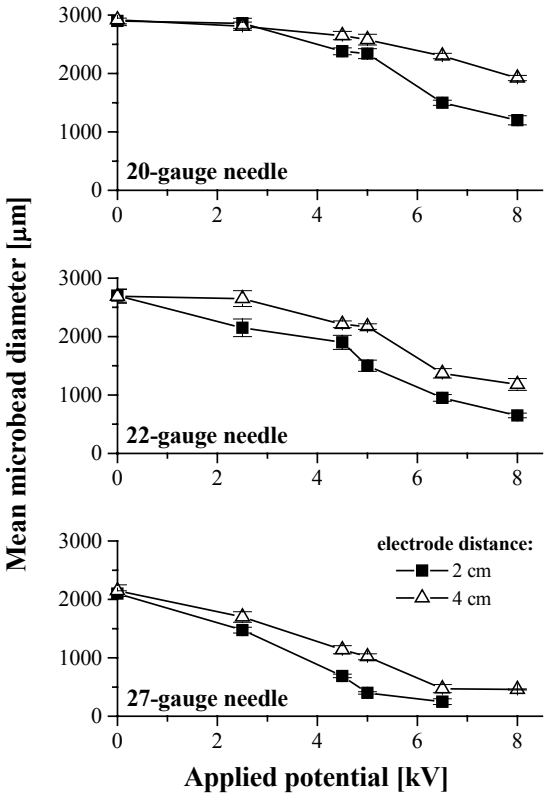

Figure 7:
Effects of applied potential and needle diameter on the size of alginate microbeads loaded with brewing yeast at high concentrations (~10^9 cells/ml of gel) for two electrode distances

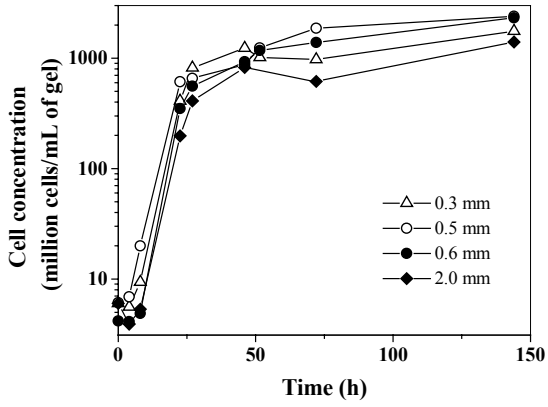

Figure 8:
Growth of immobilized yeast cells in alginate microbeads obtained by electrostatic droplet generation (0.3, 0.5 and 2 mm bead diameters) and by extrusion under coaxial air jet (0.6 mm bead diameter)

Islets of Langerhans were investigated for immobilization in alginate-based microcapsules by electrostatic droplet generation for potential application in diabetes therapy (Bugarski et al. 1997; Gåserød 1998). Extrusion of a suspension of islets of neonatal

rat pancreas using electrostatic droplet generator has shown preservation of cell viability (Bugarski et al. 1997). The islet cells were then, in a separate study, microencapsulated in alginate/poly-L-ornithine (PLO) microcapsules using electrostatic droplet generation and cultivated in tissue culture medium for 15 days (Bugarski et al. 1997). Spherical capsules of 150-200 μm in diameter, each containing 1 islet, were subsequently produced using a positively charged needle set-up at applied voltage of 5 kV. Over the cultivation time there was no significant loss in cell viability: 94 and 89 % after 9 and 15 days of cultivation, respectively. The microencapsulated islets retained their morphology and activity over the cultivation period.

In a similar study, mouse islets were encapsulated in alginate/poly-L-lyzine (PLL) microcapsules using electrostatic droplet generation and cultivated in a tissue culture medium for 2 days (Gåserød 1998). The cells encapsulated by this technique showed similar insulin release as those encapsulated using extrusion under coaxial air jet.

Callus cells from carnation leaves were immobilized in alginate microbeads using an electrostatic droplet generator with a positively charged needle set-up at the applied potential of 5.7 kV and cultivated for 2 months in growth medium (Goosen et al. 1997). Initial cell concentration was 20 % v/v in 2 % sodium alginate. Over the cultivation time, the immobilized callus cells retained viability and showed some growth through cell division and cell enlargement without clear differentiation. It was supposed that cell differentiation was inhibited by high alginate concentration (Goosen et al. 1997).

4 Scale-up

The parallel plate arrangement (Figure 2A) is suitable for the scale-up of this technique in which multiple needles are protruded through the plate (Bugarski et al. 1994a&b). Two multi-needle set-ups were constructed (Bugarski et al. 1994a; Gåserød 1998).

The first set-up consisted of a 1.5 l cylindrical reservoir (15 cm height by 10 cm diameter) containing 20 stainless steel needles (22-gauge) positioned 1.2 cm radially apart and connected to a high potential unit (Bugarski et al. 1994a). The liquid flow rate was kept constant by adjusting the air pressure head above the polymer solution. A ground collecting plate was placed 2,5 cm below the needles. This set-up resulted in production of alginate microbeads 950 ± 100 mm and 400 ± 150 mm in diameter at the applied potentials of 7 and 12 kV, respectively (Figure 9). The processing capacity was 0,7 l/h (36 ml/h per needle).

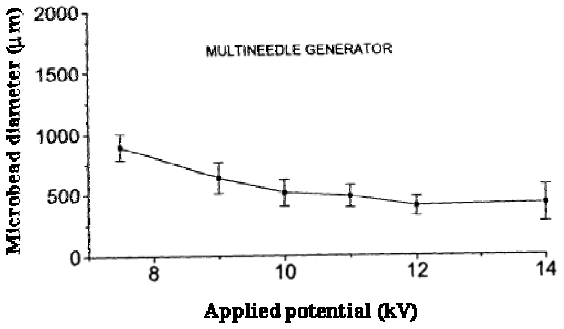

Figure 9:
20-needle set-up: Effect of applied potential on the size of alginate microbeads

The second set-up consisted of a grounded plate with 10 needles with outer diameters of 200 and 400 mm and a collecting solution connected to a power supply of 0 - 10 kV (Gåserød 1998). This set-up produced around 250,000 beads/min with diameters in the range of 160 to 1000 mm at narrow size distribution (SD ± 3 -5 %).

5 Conclusions

Electrostatic droplet generation was shown to be a suitable system for production of hydrogel microbeads at uniform size distributions. The microbead size was shown to depend on the applied potential, polymer surface tension, and needle size or electrode distance depending on the electrode geometry. In the case of alginate bead formation, the most effective electrode and charge arrangement for producing small droplets was shown to be a positively charged needle and a grounded collecting solution. This set-up and the applied potential of 6 kV, 26-gauge needle and 2.5 cm electrode distance provided production of alginate microbeads with diameters down to 170 mm at narrow size distribution.

Different cell types such as insect, fungi, bacteria, yeast, mammalian, and plant cells were shown to be insensitive to exposure to electrostatic fields. In addition, cultivation studies of cells immobilized by electrostatic droplet generation showed preservation of cell viability and activity.

Further development of large scale production devices will make this technique potentially attractive for variety of applications in cell immobilization technology.

References

Brandenberger H, Widmer F (1998) A new multinozzle encapsulation/immobilization system to produce uniform beads of alginate. J Biotechnol 63:73-80

Bugarski B, Smith J, Wu J, Goosen MFA (1993) Methods for animal cell immobilization using electrostatic droplet generation. Biotechnol Tech 7:677-682

Bugarski B, Li Q, Goosen MFA, Poncelet D, Neufeld RJ, Vunjak G (1994a) Electrostatic droplet generation: mechanism of polymer droplet formation. AIChE J 40:1026-1031

Bugarski B, Amsden B, Neufeld RJ, Poncelet D, Goosen MFA (1994b) Effect of electrode geometry and charge on the production of polymer microbeads by electrostatics. Canad J Chem Engineer 72:517-521

Bugarski B, Sajc L, Plavsic M, Goosen M, Jovanovic G (1997) Semipermeable alginate – PLO microcapsules as a bioartifical pancreas. In: Funatsu K, Shirai Y, Matsushita T (eds) Animal Cell Technology: Basic & Applied Aspects, Vol. 8. Kluwer Academic Publishers, Dordrecht, pp. 479-486

Gåserød O (1998) Microcapsules of alginate-chitosan: A study of capsule formation and functional properties. PhD Thesis, NTNU, Trondheim, Norway

Goosen MFA (1996) Microencapsulation of living cells. In: Willaert RG, Baron GV and De Backer L (eds.) Immobilized Living Cell Systems: Modelling and Experimental Methods. John Wiley & Sons Ltd., Chichester, pp. 295-322

Goosen MFA, Al-Ghafri AS, El Mardi O, Al-Belushi MIJ, Al-Hajri HA, Mahmoud ESE, Consolacion EC (1997b) Electrostatic droplet generation for encapsulation of somatic tissue: Assessment of high-voltage power supply. Biotechnol Prog 13:497-502

Jahnz U, Wittlich P, Prüβe U, Vorlop K-D (2001) New matrices and bioencapsulation processes. In: Thonart Ph, Hofman M (eds) Focus on Biotechnology Series, Volume 4: Engineering and Manufacturing for Biotechnology. Kluwer Academic Publishers, Dordrecht, pp. 293-307

Jen AC, Wake MC, Mikos AG (1996) Review: Hydrogels for cell immobilization. Biotechnol Bioeng 50:357-364

Keshavarz T, Ramsden G, Phillips P, Mussenden P, Bucke C (1992) Application of electric field for production of immobilized biocatalysts. Biotechnol Tech 6(5):445-450

Murano E (2000) Natural gelling polysaccharides: indispensable partners in bioencapsulation technology. Minerva Biotec 12(4):213-222

Nedovic V, Obradovic B, Leskosek-Culakovic I, Trifunovic O, Pesic R, Bugarski B (2001) Electrostatic generation of alginate microbeads loaded with brewing yeast. Proc Biochem 37(1):17-22

Ogbona JC, Matsumara M, Kataoka H (1991) Effective oxigenation of immobilized cells through reduction in bead diameters: A review. Proc Biochem 26:109-121

Poncelet D, Bugarski B. Amsden BG, Zhu J, Neufeld R, Goosen MFA (1994) A parallel plate electrostatic droplet generator: parameters affecting microbead size. Appl Microbiol Biotechnol 42:251-255

Poncelet D, Babak VG, Neufeld RJ, Goosen MFA, Bugarski B (1999a) Theory of electrostatic dispersion of polymer solutions in the production of microgel beads containing biocatalyst. Adv Colloid Interface Sci 79:213-228

Poncelet D, Neufeld RJ, Goosen MFA, Bugarski B, Babak V. (1999b) Formation of microgel beads by electrostatic dispersion of polymer solutions. AIChE J 45(9):2018-2023

Poncelet D, Desobry S, Jahnz U, Vorlop K-D (2001) Immobilization at large scale by dispersion. In: Wijffels R (ed) Immobilized cells. Springer Lab Manual, Heidelberg, Chapter 13, pp. 139-149

Strand BL, Mørch YA, Skjåk-Bræk G (2000) Alginate as immobilization matrix for cells. Minerva Biotec 12(4):223-233

Use of vibration technology for jet break-up for encapsulation of cells, microbes and liquids in monodisperse microcapsules

Christoph Heinzen[1], Ian Marison[2], Andreas Berger[1], and Urs von Stockar[2]

Abstract

Adding a vibration on a laminar jet for controlled break-up into monodisperse microcapsules is one among different extrusion technologies for encapsulation of cells, microbes, yeast, enzymes and liquids (Poncelet, 1997).

The vibration technology is based on the principle that a laminar liquid jet breaks up into equally sized droplets by a superimposed vibration. In the late 19th century, Lord Rayleigh theoretically analysed the instability of liquid jets (Rayleigh, 1878). He showed that the frequency for maximum instability is related to the velocity of the jet and the nozzle diameter.

The optimal vibration parameters are easily and quickly determined in the light of a stroboscope. Once determined, the parameters can be reset in the future, making the process highly reproducible.

In this presentation we will show optimal production parameters for beads and capsules including monodispersity parameter for narrow size distributions, we will provide examples of encapsulation of animal cells and organic liquids in microcapsules and analyse the prerequisites for scale-up strategies of the vibration jet break-up technology.

Keywords: vibrating, monodispersity, jet break-up, immobilization, encapsulation

1 Introduction

Microcapsules are defined as particles, spherical or irregular, in the size range of about 1 mm to 2 mm, and composed of an excipient polymer matrix (shell or wall) and an incipient core substance (Gutcho, 1979). Depending on material, manufacturing technique and application, microcapsules are divided into four main classes. Solid particles are dispersed in a matrix, while droplets are encapsulated either in mono- or polynuclear form. A second wall layer can be coated around the capsules to modify its permeability and stability.

Microcapsules have been prepared by a variety of different methods, that are often combined or overlap to a certain extent. For the sake of simplicity, the main microencapsulation techniques are categorized as mechanical (see below), physico-chemical (simple and complex coacervation, phase separation) or chemical operations (in-situ polymerisation, interfacial polycondensation).

Mechanical microencapsulation operations result rather from mechanical procedures than from a well defined physical or chemical phenomenon. Various coating and spray drying methods are routinely used in industry. Extrusion of polymer solutions through nozzles to produce either beads or capsules is mainly used on laboratory scale, where often simple devices such as syringes are applied. If the droplet formation occurs in a well controlled way (contrary to spraying) the technique is known as prilling. This is preferably done by pulsation of the jet or vibration of the nozzle (Kegel, 1988; Heinzen, 1995). The use of coaxial air flow (Lee and Palsson, 1993) or an electrostatic field (Poncelet, 1994) are other common techniques to form droplets. Mass production of beads can either be achieved by multi-nozzle systems (Brandenberger, 1998), rotating disc atomizers (Goodwin, 1974) or by the recently developed jet-cutting technique (Prüsse, 1998a). Centrifugal systems using either a multi-nozzle system or a rotating disk have also been developed for the mass production of microcapsules (Somerville, 1980).

1.1 Why are cells and other ingredients encapsulated

The encapsulation of human, animal and plant cells, microbes, enzymes and drugs or other ingredients into microbeads has different purposes: the encapsulated item must be protected from environmental influences, e.g. immune system of a patient, or it has to resist share forces in a bioreactor or must be protected against oxidation. Following these demands, the encapsulation technology has its use in many different applications. A selection of known applications is presented below:

- Cell transplantation for the treatment of cancer, diabetes or liver diseases
- Test systems for screening experiments for new drugs
- Starter cultures in food production

[1] Christoph Heinzen and Andreas Berger, Inotech Encapsulation AG, Kirchstrasse 1, 5605 Dottikon, Switzerland

[2] Ian Marison and Urs von Stockar, Laboratory of Chemical and Biochemical Engineering, Swiss Federal Institute of Technology (EPFL), 1015 Lausanne, Switzerland

- Production of pharmaceutical drugs with encapsulated cell cultures
- Production of cosmetic products with encapsulated flavours or fragrances

By encapsulating cells or other ingredients, it is important that the beads:

- have a small diameter, preferentially less than 0.7 mm in order to prevent diffusion limitations and necrotic areas in the centre of the beads. Cells must be provided with nutrients, otherwise cells in the centre of such beads will die and they will send necrotic messages to living cells.
- have a narrow size distribution of the diameters. By using a suboptimal production technique, large droplets will be produced and they will create diffusion limitations and send necrotic messages to the living cells (see above)
- must be produced in a short production time. If the production time - formation of droplets and their solidification - exceeds a certain length, the viability of the cells will decrease dramatically.

1.2 Example of medical applications of encapsulation

Many diseases are caused by the inability of the body to produce the necessary amount of a needed molecule, such as a hormone, factor, or enzyme. Cell therapy offers enormous potential for the treatment of such diseases. Encapsulated cell systems consist of living cells that are immobilized and protected inside micro- or macrocapsules. Such capsules are implanted into a patient, where the cells produce the therapeutic substances that the body cannot produce itself. Figure 1 depicts the most important diseases that lend themselves to such treatment with encapsulated cells (Kühtreiber, 1999).

2 Technical background

As mentioned above, this article focuses on the production of beads and capsules by using the vibration technology.

Five different mechanisms of droplet formation occur at the nozzle outlet as a function of the jet outflow velocity (Figure 2). They arise through the interaction of gravity, impulse, surface tension and friction forces (Müller, 1985).

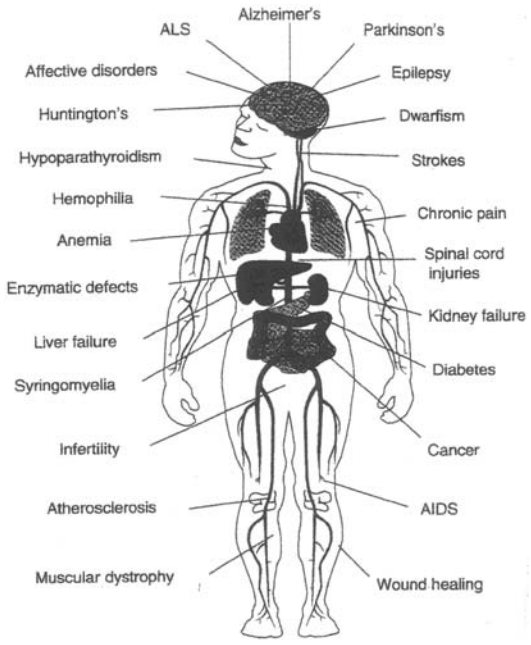

Figure 1:
Important diseases to be treated with encapsulated cells

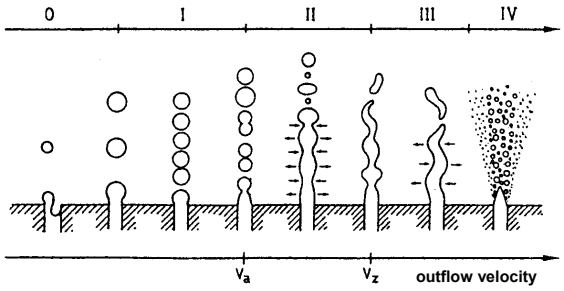

Figure 2:
Different mechanisms of droplet formation (Müller, 1985)

At a low outflow velocity, single droplets are directly formed at the orifice outlet (mechanisms 0 and I, mechanism I is referred to as "Abtropfen" in German). The droplet diameter d_D is calculated in equation 1 from the equilibrium of the main forces present, gravity and surface tension:

$$d_D = \sqrt[3]{\frac{6 d_N \sigma}{g \Delta \rho}} \qquad (1)$$

Increasing kinetic force causes the uninterrupted outflow of the jet, which breaks up afterwards by axial symmetrical vibrations and the surface tension (mechanism II, referred to as "Zertropfen"). A further increase of the jet velocity leads to statistical distribution of the droplet size, that are caused either by spiral symmetrical vibrations (mechanisms III, referred as "Zerwellen") or by the high friction forces that are present when the jet is sprayed (mechanism IV).

The controlled formation of monodisperse droplets is only possible via mechanisms I and II. However, only the latter is of industrial importance. By introducing an additional sinusoidal force on the droplet formation mechanism II, the laminar jet breaks up in droplets, the size of which can be freely chosen in a certain range depending on the applied frequency. This is in contrast to the droplet formation without pulsation described in equation 1, where the droplet diameter of a certain liquid depends only on the nozzle diameter. The sinusoidal force can be applied to the prilling system by either pulsating the feed or by vibrating the nozzle.

The technology is based on the principle that a laminar liquid jet is broken into equally sized droplets by a superimposed vibration. In the late 19th century, Lord Rayleigh theoretically analysed the instability of liquid jets. He showed that the frequency for maximum instability is related to the velocity of the jet and the nozzle diameter (Equations (2) - (4), Figure 3). The optimal vibration parameters have to be determined in the light of the incorporated stroboscope. Once determined, the parameters can be reset in the future, making the process highly reproducible. The bead diameter can be set between 0.1 - 1.5 mm.

$$\lambda = \frac{v_J}{f} \tag{2}$$

$$\lambda_{opt} = \pi\sqrt{2}\, d_N \sqrt{1+\frac{3\eta}{\sqrt{\rho\sigma d_N}}} \tag{3}$$

$$d_D = \sqrt[3]{1.5\, d_N^2\, \lambda_{opt}} \tag{4}$$

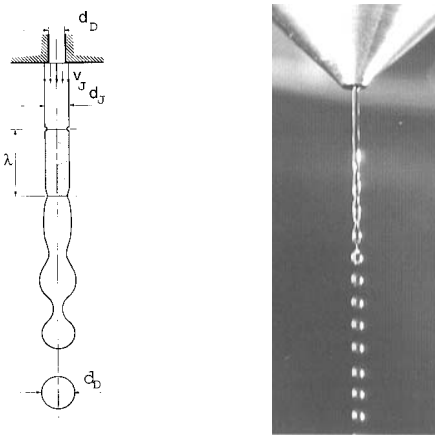

Figure 3:
Droplet formation parameters and photo of the droplet formation

Figure 4 shows the dependence of the flow rate to the jet velocity and the nozzle diameter as calculated by equation 2 & 4. The working range of the jet velocity will normally lay between 1.5 and 2.5 m/s, depending on the liquid viscosity and the nozzle diameter.

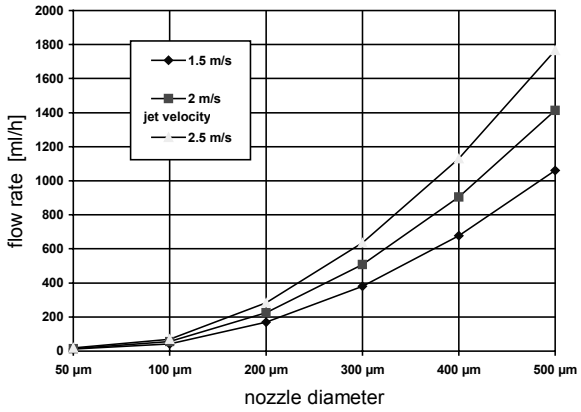

Figure 4:
Influence of the liquid jet velocity and the nozzle diameter on the flow rate, as calculated by equation 2 & 4

Figure 5 shows the correlation between the vibration frequency and the bead diameter for five different flow rates as calculated by equation 2 & 4. Lower flow rates corresponding to lower pumping rates produce smaller beads. Higher vibration frequencies produce smaller beads too.

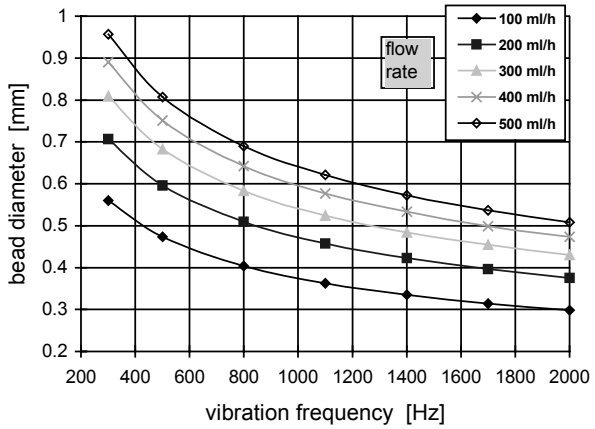

Figure 5:
Influence of the vibration frequency and the flow rate on the bead diameter

The production of uniform beads or capsules is a key factor in encapsulation processes. To avoid large size distributions due to coalescence effects during the flight and the hitting phase at the surface of the hardening solution the use of the dispersion unit with the electrostatic generator is essential (Figure 6). Droplet formation without an applied potential of the electrostatic generator shows several particles of double or triple size caused by coalescence (Brandenberger, 1999).

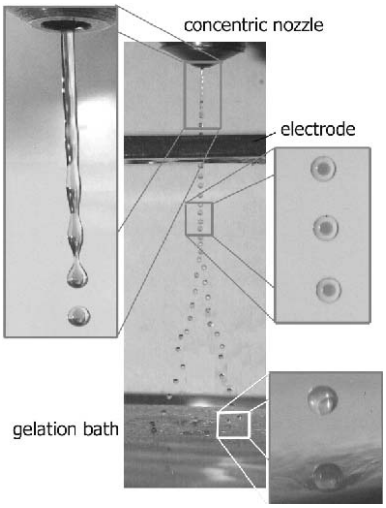

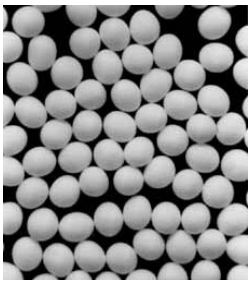

Beads produced WITH the use of the electrostatic dispersion unit: Monodisperse & spherical beads

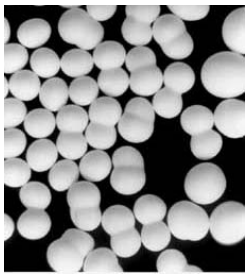

Beads produced WITHOUT the use of the electrostatic dispersion unit: Non-spherical beads Jumbo beads

Figure 6:
Prevention of coalescence with use of Inotech's electrostatic dispersion unit

3 Materials and methods

The main parts of the concentric nozzle encapsulator research are shown in Figure 7. All parts of the instrument which are in direct contact with the capsules can be sterilized by autoclaving. The product to be encapsulated (hydrophobic or hydrophilic liquid) is put into the syringe (1) or the product delivery bottle (2). The shell material (polymer) is put into the syringe (3) or the product delivery bottle (4). Both liquids are forced to the concentric nozzle by either a syringe pump (S) or by air pressure (P). The liquids then pass through a precisely drilled concentric-sapphire-nozzle (7) and separate to into concentric, equal sized droplets on exiting the nozzle. These droplets pass an electrical field between the concentric nozzle (7) and the electrode (8) resulting in a surface charge. Electrostatic repulsion forces disperse the capsules as they drop to the hardening solution.

Capsule size is controlled by several parameters including the vibration frequency, nozzle size, flow rate, and physical properties of the polymer-product mixture. Optimal parameters for capsule formation are indicated by visualization of real-time droplet formation in the light of a stroboscope lamp (15). When optimal parameters are reached, a standing chain of droplets is clearly visible.

Once established, the optimal parameters can be preset for subsequent capsule production runs with the same encapsulating polymer-product mixture. Poorly formed capsules, which occur at the beginning and end of production runs, are intercepted by the bypass-collection-cup (10).

Depending on several variables, 50 – 4000 capsules per second are generated and collected in a hardening solution within the reaction vessel (9).

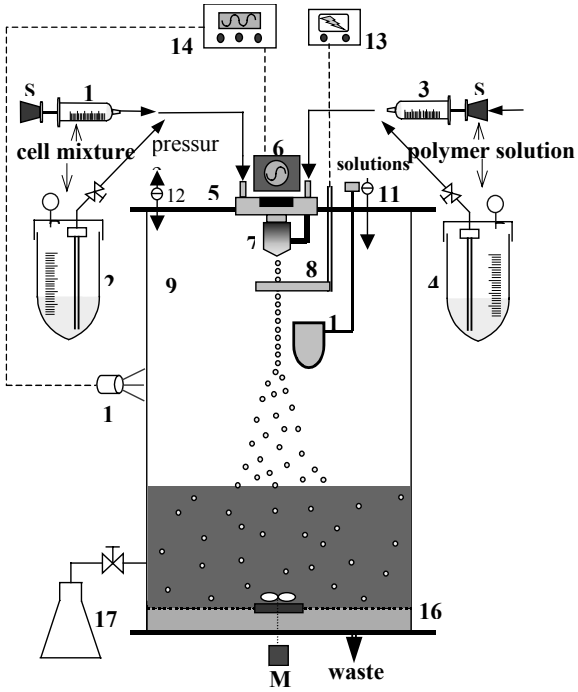

Figure 7:
Schematic representation of the concentric nozzle encapsulator research system. 1: Syringe (core), 2: Product delivery bottle (core), 3: Syringe (shell), 4: Product delivery bottle (shell), 5: Pulsation chamber, 6: Vibration system, 7: Concentric nozzle, 8: Dispersion system, 9: Reaction vessel, 10: Bypass cup, 11: Liquid filter, 12: Air filter, 13: Electrostatic charge generator, 14: Frequency generator, 15: Stroboscope, 16: Filtration grid, 17: Bead collection flask, M: Magnetic stirrer, P: Pressure control system, S: Syringe pump

Solutions in the reaction vessel are continuously mixed by a magnetic stir bar (M) to prevent capsule

clumping. At the conclusion of the production run, the hardening solution is drained off (waste port), while the capsules are retained by a filtration grid (16). Washing solutions, or other reaction solutions, are added aseptically through a sterile membrane filter (11). The capsules can be further processed into microcapsules, or transferred to the capsules collection flask (17).

Figure 8:
Photo of Inotech Encapsulator Research IER-20 for monodisperse production of beads and capsules under sterile and reproducible production conditions

In general, all experiments were performed with 1.5 % Na-alginate (IE-1010, Inotech Encapsulation AG, Switzerland). The hardening bath was a 0.1 M solution of $CaCl_2$ (IE-1020, Inotech Encapsulation AG, Switzerland). Size distribution of the capsules were measured using a coulter counter (Coulter Electronics GmbH, Germany). Detailed encapsulation protocols are described elsewhere for CHO cells (Pernetti, 2001) and for liquid core capsules (Heinzen, 2001).

4 Results

Using the vibration technology for jet break-up performed with the Inotech Encapsulators (but also with other devices using the vibration technology), we and other scientists were able to encapsulate a large variety of ingredients:

- islets, hepatocytes and other human and mammalian cells for cell implantation
- genetically engineered cell lines, e.g. CHO cells for medical application
- microbes and yeast, e.g., bioconversion applications
- fragrances and flavours for food and cosmetic applications

A detailed analysis of different applications of the vibration technology for medical, food, agrochemistry, environment, cell storage, catalysed chemical reactions and other application are presented in Marison et al., 2000. Below two applications are described in more detail, the encapsulation of CHO cells and the production of liquid core capsules.

4.1 Encapsulation of CHO cells

Animal cells can be used as biocatalysts to produce pharmaceutical proteins, including monoclonal antibodies, hormones, cytokines and viral vaccines (Shuler et al., 1992). An interesting technique to protect cells from shear stresses and toxic metabolites and to attain high cell density is immobilization in microcapsules with a liquid core and a resistant membrane. In this example, poly-L-lysine (PLL) was employed to form membranes composed of polyelectrolytic and covalent interactions (Pernetti, 2001).

The encapsulated CHO cells were seeded into a spinner flask and grown in repeated fed-batch mode for 30 days. Fresh medium was added when the glucose concentration fell below 4 mM, in order to avoid glucose limitation. Figure 9 shows that the cells colonized the core to a great extent. The cells continued to grow for more than 30 days retaining an efficient metabolism, thus showing that they were neither affected by the encapsulation protocol nor were there any strong diffusion limitations.

4.2 Liquid core capsules

Recently, the availability of capsules having a liquid core show a merging of interests from biotechnology, food and cosmetic industry, e.g.

- hydrogel capsules with an organic core can be used as controlled release tool for flavours and fragrances
- liquid core capsules enable in-situ extraction of organic compounds in a fermentation process

Figure 10 display sunflower oil-alginate capsules after gelation in a hardening solution. Diameter of the core bead vary between 400 and 800 mm, diameter of the capsule vary between 550 and 1000 mm. The relative standard deviation of the capsules vary for the different samples between 2.8 and 4.9 % and demonstrate therefore very narrow size distribution. All

samples were produced by using the electrostatic dispersion unit (Heinzen, 2001).

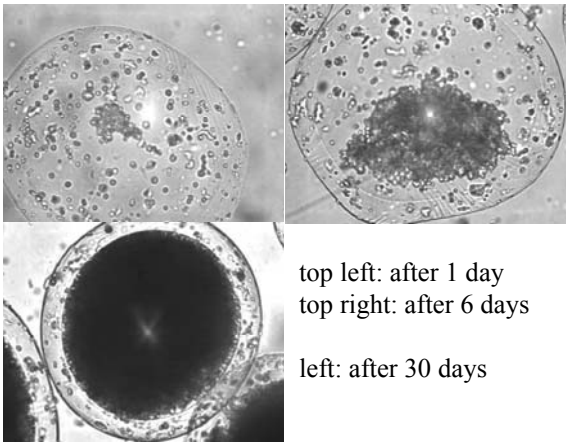

top left: after 1 day
top right: after 6 days

left: after 30 days

Figure 9:
Microscope photographs during the repetitive fed-batch culture of encapsulated CHO cells (Pernetti, 2001)

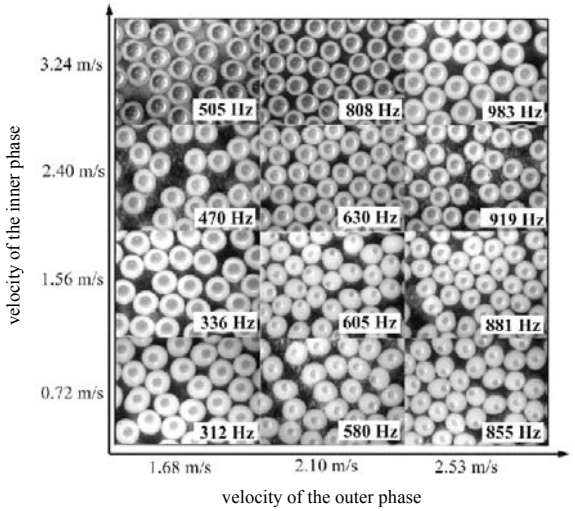

Figure 10:
Liquid core capsules made of sunflower oil (core) and 1.5 % alginate (shell)

5 Conclusions

With the vibration technology and the specific know-how of INOTECH ENCAPSULATION one is able:

- to reproducibly produce beads with equal diameters
- to produce beads with a spherical shape
- to work under sterile and reproducible working conditions (complying to GMP)
- to set diameters between 0.1 up to 1.5 mm
- to scale up the process to flow rates up to 200 l/h (see fig. 11)
- to encapsulate without viability loss: Islets, human T-cells, fibroblasts, hepatocytes, CHO and many other cells!

Figure 11:
Scale-up of vibration technology: Multinozzle head of Inotech pilot plant (5 l/h)

Advantages of vibration technology:

- Exact determination of droplet diameter
- Narrow size distribution
- Easy to scale-up: multiplication of 1 to x nozzles

Limits of vibration technology:

- Viscosity: the liquid should show Newton‘s fluid dynamic
- Flow rate / nozzle: laminar flow jet limits a maximum flow rate per nozzle

In this presentation, the identification of production parameters for the vibration technology was described and the use of the Inotech Encapsulator Research with a concentric nozzle for the production of liquid core capsules has been presented. Different systems of core and shell material were tested and the capsules show under reproducible production conditions very narrow size distributions. Geometry of the concentric nozzle was optimised and the use of the dispersion unit is a very powerful tool for reproducible production conditions. Tests with a pilot scale multinozzle system (production rate 5 l / h) enabled identical results. The possibility of encapsulation of cells in a liquid core lead to better cultivation conditions. The easy and reproducible production of monodisperse liquid core capsules with an organic liquid offer a broad range of new applications in food and cosmetic industry.

Symbols and abbreviations

d_D	droplet diameter
d_N	nozzle diameter
f	frequency
σ	surface tension
Δ_ρ	density difference
v_J	jet velocity
λ_{opt}	optimal wavelength
η	dynamic viscosity
ρ	density

References

Berger A, Marison I, Stark D, von Stockar U, Widmer F, Heinzen Ch (2001) Production and characterization parameters of liquid core capsules for biological and non-biological applications. Proceedings of IX international BRG workshop, Warsaw, pp. III-3

Brandenberger H and Widmer F (1998) A new multinozzle encapsulation / immobilization system to produce uniform beads of alginate. J Biotechnol 63:73-80

Brandenberger H, Nussli D, Piech V, Widmer F (1999) Monodisperse particle production: a method to prevent drop coalescence using electrostatic forces. J. Electrostatics 45:227-238

Goodwin JT and Somerville GR (1974) Microencapsulation by physical methods. Chemtech 4:623-626

Gutcho MH (1979) Microcapsules and other capsules. Noyes Data Corporation, New Jersey

Heinzen Ch (1995) Herstellung von monodispersen Mikrokugeln durch Hydroprillen. Thesis, Swiss Federal Institute of Technology, Zurich

Kegel BHR (1988) Mikroverkapselung durch Hydroprillierung. Thesis, Swiss Federal Institute of Technology, Zurich

Kühtreiber WM, Lanza RP and Chick WL (eds) (1999) Cell encapsulation technology and therapeutics. Birkhäuser, Boston, p. X

Lee GM and Palsson BO (1993) Stability of antibody productivity is improved when hybridoma cells are entrapped in calcium alginate beads. Biotechnol Bioeng 42:1131-1135

Serp D, Cantana E, Heinzen C, von Stockar U, Marison IW (2000) Characterization of an encapsulation device for the production of monodisperse alginate beads for cell immobilization. Biotech and Bioeng 70:41-53

Müller C (1995) Bildung einheitlicher Feststoffpartikel aus Schmelzen in einer inerten Kühlflüssigkeit (Hydroprilling). Thesis, Swiss Federal Institute of Technology, Zurich

Pernetti M, Rugerli R, Marison I, von Stockar U (2001) Animal cell encapsulation within polyelectrolyte and covalent membranes. Proceedings of IX international BRG workshop, Warsaw, pp. VI-3

Poncelet D (1997) Fundamentals of dispersion in encapsulation technology, Proceedings of BRG Meeting 1997 in Barcelona

Poncelet D (1994) A parallel-plate electrostatic droplet generator: parameters affecting microbead size. Appl Microbiol Biotechnol 42:251-255

Prüsse U, Bruske F, Breford J, Vorlop K-D (1998) Improvements to the jet cutting process for manufacturing spherical-particles from viscous polymer solutions. Chem Ing Tech 70:556-560

Rayleigh (1878) On the stability of jets. Proc London Math Soc 10:4-13

Shuler ML, Kargi F (1992) Bioprocess Engineering. Prentice Hall. Englewood cliffs, New Jersey

Somerville GR and Goodwin JT (1980) Microencapsulation using physical methods. In: Kydonieus AF (ed): Controlled release technologies: methods, theory and applications. CRC press, Boca Raton, pp. 155-164

Weber C (1931) Zum Zerfall eines Flüssigkeitsstrahles. Zeitschrift für angewandte Mathematik und Mechanik 11:136-154

Emulsification and microencapsulation: State of art

Denis Poncelet, Ernest Teunou, Anne Desrumaux, and Dominique Della Valle[1]

Abstract

Encapsulation processes generally involve dispersing a liquid and solidifying the droplet. The contribution describes the different microencapsulation methods based on emulsification. It looks to provide some information on the advantages and limitations of the emulsification for encapsulating biological or biochemical material.

Keywords: emulsion, static mixer, gelation

1 Introduction

Encapsulation was proposed more than 50 years ago to immobilize, protect, release and functionalize diverse types of materials. The process could generally be divided in two steps: liquid core dispersion and encapsulation it-self of the dispersed material (called solidification below). During solidification, the dispersed phase is gelified or a membrane is formed around the droplets of particles. The dispersion could be done in the air (spray, extrusion, grinding) but also inside a non-miscible phase (mainly emulsification). Both methods have advantages and disadvantages. Obviously, emulsification is required when an interfacial reaction between two non-miscible liquids is involved or when encapsulation proceed by coacervation (precipitation of polymers at the droplet surface). Emulsification allows very large production (up to tons per hour) even for very small microcapsules (down to a few micrometers). However, there are some drawbacks with the emulsification methods. The size dispersion is always large. In most cases of bioencapsulation (aqueous core), the continuous phase is generally an oil phase. Washing of the capsules may be a tedious problem and may cost as much as the capsules it-self. The present contribution will try to give an overview of the different encapsulation technologies linked to the emulsification and give some rules along when and how to use them.

2 Dispersion methods

2.1 Batch systems

Emulsification is generally done in a batch reactor equipped with impeller or a rotor-stator system. The most usual system at laboratory and pilot scale is the Rushton's turbine reactor (Figure 1). Such a system optimizes the shear and then the drop breakage. Without baffles, the turbine entrains the liquid and the mixing/dispersion effect is reduced. On the other hand, baffles prevent vortex and foam formation.

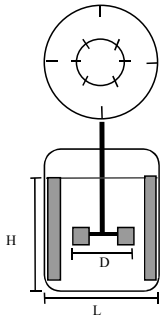

Figure 1:
Rushton type reactor. Reactor description: Cylindrical reactor equipped, D: turbine diameter, L: reactor diameter (D*2), H: liquid height (D*2); Turbine: 6 vertical blades located at H/2, Size D/4*D/4; Baffles: 4 located at distance D/10 of the reactor wall, Width = D /5

At industrial scale, the type of impeller is often different, looking more like a marine impeller. Suppliers generally provide their equipment with characteristic numbers to define the mixing regime.

In bioencapsulation, the continuous phase is generally vegetable or mineral oil. The viscosity ranges from 30 to 60 mPa·s and the interfacial tension with aqueous dispersed phase is quite important ($45 \cdot 10^{-3}$ N/m). A lipophilic emulsifier such as Span 80 (1 %) is often added to the mixture to reduce the interfacial tension and get lower size distribution. For one defined system (reactor, phase composition), the size distribution is mainly determined by the rotational speed of the impeller. Figure 2 presents some data showing the influence of the viscosity of the dispersed phase on the mean size.

The size distribution is generally defined by a log-normal distribution. An interesting parameter to define the size dispersion is the span corresponding to equation 1.

$$span = \frac{d_{90} - d_{10}}{d_{50}} \qquad (1)$$

[1] Denis Poncelet, Ernest Teunou, Anne Desrumaux, and Dominique Della Valle, ENITIAA, BP 82225, 44322 Nantes cedex 3, France

where d_{90}, d_{50} and d_{10} are the diameter corresponding to 90, 50 and 10 % of the cumulative size fraction (generally given as volumetric fraction). Span takes into account a large part of the particles and is not sensible to the extremes (very small and very large particles). It is quite reproducible between samples. It could be related to usual (but confusing) standard deviation by dividing it by 2.67.

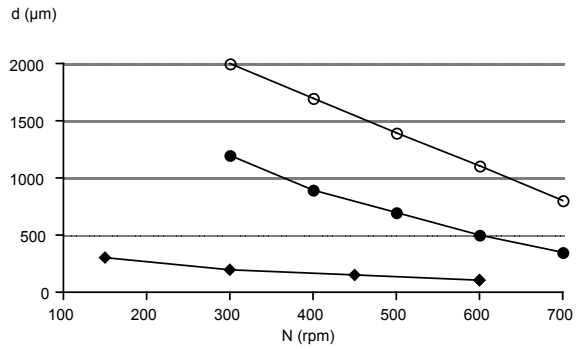

Figure 2:
Mean size of nylon microcapsules (diamond) and κ-carrageenan beads (2 % filled circles, 3 % open circles) from Poncelet et al. 1990a and Audet et al. 1989

The span may range from 67 % to 160 % of the mean (Figure 3). Kolmogoroff's theory (see below) predicts a value of 80 %. The size dispersion is lower while reducing the mean size. It is also improved if the two liquids have more similar physical properties (density, viscosity). Interfacial tension has little influence on the size distribution.

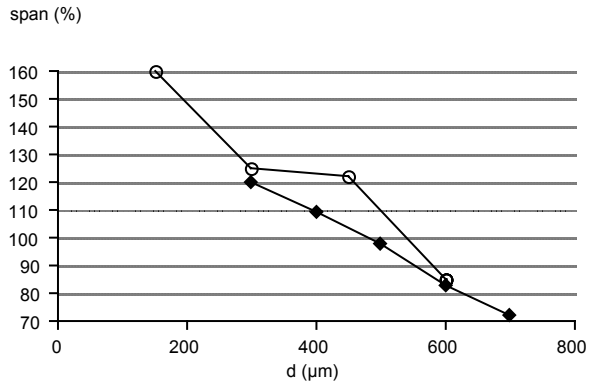

Figure 3:
Standard deviation of nylon microcapsules (open circles) and κ-carrageenan beads (diamonds) in function of the size

2.2 Continuous systems (static mixer)

Several disadvantages of the batch system are:

- Cleaning and filling reactor: these tasks reduce the productivity
- Limitation for scale-up: it is difficult to expect reactors larger than 1 cubic meter.
- Emulsifying viscous liquid in turbine reactor requires 5 to 15 minutes of mixing.
- Good emulsification is linked to high shear that may damage biological cells

Poncelet et al. (1993) then proposed to realize the emulsification using continuous systems based on static mixers (Figure 4). The static mixers consist of a series of stationary elements placed transversely in a tube. These elements form crossed channels that promote division and longitudinal recombination of the liquid flowing through the static mixer. While applied to a two-phase system, emulsion is formed. Figure 4a shows an example of installation using a static mixer. Figure 4b demonstrates the power of the static mixer for emulsification. Passing through 10 elements Kenics mixer (series of single elements), the flow is divided 128 times longitudinally and 128 times transversally. Sulzer mixers (Figure 4 c) are formed by several stationary elements and are even more efficient.

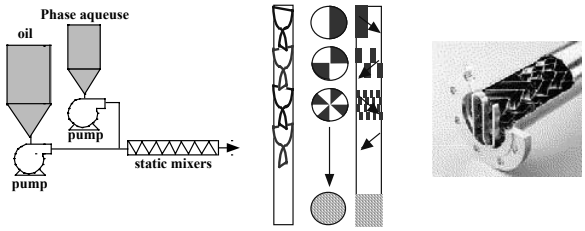

Figure 4:
Static mixers: a) installation, b) emulsification, c) Sulzer mixers

The system could be run continuously, scale-up was realized by simply increasing the tube diameter, even for viscous system, residence or emulsification times could be as low as 0.2 seconds while shear stress was quite low (Poncelet et al, 1993).

With Sulzer mixers, 5 to 10 elements are needed to get fine emulsion. Due to the higher dispersion power of static mixers in regard to turbine mixers, similar mean size could be reached without the use of emulsifier. This constitutes an unexpected advantage of the static mixers.

2.3 Size distribution prediction

Because of the variety of designs, one may be confused by the number of different correlations proposed to describe the dispersion in mixing devices. However, most equations are based on Kolmogorov's theory. The droplet sizes are deduced from the size of

the eddies formed by the agitation. This assumes that the mixing regime is turbulent. The mean size is then given by equation 2.

$$\frac{d_{32}}{D} = A\ W^{-0.6} \qquad (2)$$

where d_{32} is the mean Sauter diameter , D is the reactor diameter, A is a constant function of the system, We the Weber number. The mean Sauter diameter, d_{32}, is defined by equation 3.

$$d_{32} = \frac{\sum_i n_i\ d_i^3}{\sum_i n_i\ d_i^2} \qquad (3)$$

where n_i is the number of droplets having the diameter d_i. The mean Sauter diameter, d_{32}, is equal to the inverse of the specific surface or the surface per unit volume of dispersed phase. The Weber number, We, defines the ratio between inertial force and interfacial surface force and is given by equation 4.

$$We = \frac{\rho_c\ u^2\ D}{2\ \sigma} \qquad (4)$$

where ρ_c is the density of the continuous phase, u the linear liquid-to-blade velocity and σ is the interfacial tension between the two liquids. For turbine, linear liquid-to-blade velocity is given by (π D N), where N is the rotational speed of the impeller. For static mixer, it will be given as the ratio of the flow rate divided by the mixer section.

In fact, one may observe that equation 2 assumes that most of the dispersion energy is linked to increase interfacial surface. However, encapsulation generally involves a viscous liquid (especially for internal phase) and the mixing regime could be laminar or transitional. The viscosity of the continuous phase and the dispersed phase may influence the size distribution. Equation 2 may be rewritten (equation 5), based on both mechanistic analyses and empirical correlations (Hass 1987).

$$\frac{d_{32}}{D} = A\ We^{-0.6}\ \mathrm{Re}^{-0.2} \left(\frac{\mu_d}{\mu_c}\right)^{0.5} \qquad (5)$$

where μ_c and μ_d are the viscosities of the continuous and dispersed phase. The Reynold number, Re, is representative of the ratio between the inertial forces and viscosity forces (equation 6).

$$\mathrm{Re} = \frac{\rho\ u\ D}{\mu_c} \qquad (6)$$

Equation 1 (or 5) described above are valid to calculate the mean diameter for turbine reactor and static mixers. The value of constant A is function of the design of both the impeller, reactor and/or static mixers. For Kenics mixer, one could use 1.2 (Haas 1987) and for SMV Sulzer mixer 0.2 (Streiff 1977). Lower sizes could then obtained with Sulzer mixer. For a more complete review, we advise readers to read the series of papers from Calabrese et al. (1986) for turbines and Legrand et al. (2001) for static mixers.

Referring to the Kolmogoroff's theory, the size distribution of eddies in the reactor determine the size distribution droplets formed by liquid breakage in turbulent system. This leads to a distribution following a lognormal law. The frequency is then defined by equation 7.

$$f(z) = \frac{1}{\sqrt{2\pi}\ \sigma_z} e^{-\frac{(z-\bar{z})^2}{\sigma_z^2}} \qquad (7)$$

where z = log(d) and σ_z is the standard deviation of z. The span corresponds to 80 % of the mean.

3 Encapsulation methods

3.1 Interfacial polymerization and polymer cross-linking

Interfacial polymerization consists of dispersing a solution of one monomer in an immiscible solvent and adding a second monomer soluble in the continuous phase. A typical example is the reaction of a diamine (water-soluble) with a diacid chloride (oil soluble) (Wittbecker 1959). The reaction generally requires a solvent of high polarity (chloroform) and high pH value (> 11). It was then necessary to improve the method to apply it to biocatalyst encapsulation.

Three laboratories was involved in this research: TMS Kondo (Wakamatsu, 1974) in Japan, MC Levy (Guerin 1983) in France and R. Neufeld (Groboillot 1993) in Canada. Their results were quite similar. To avoid drastic conditions, the process must involve low pKa amine (like amino acid) and polyamine (like proteins, polyethyleneimine) (Poncelet 1990b).

The process which then corresponds more to a polymer cross-linking, could be performed at pH as low as 8 and with a solvent like vegetal oil. The weak point remains the use of a strong cross-linker such as diacid chloride, which could react with the encapsulated material near to the surface. Moreover, diacid

chloride frees acid chloride by reaction with water and the polyamine. The pH then drops quickly inside the capsule (Hyndman 1993). Use of thiocyanate as a cross-linker allows avoiding pH drop but capsules are not as strong. Preliminary studies show that diacid anhydride could be a good candidate to replace diacid chloride. At this stage, interfacial polymer cross-linking has been proved successful for enzyme encapsulation (Monshipouri 1992) but still limited for cell encapsulation (Hyndman 1993).

Interfacial polymerization may also be used to form oil loaded microcapsules by dispersing the hydrophobic monomer solution in an aqueous solution and then adding a water soluble monomer. This could be useful for encapsulation of some enzymatic systems (such as lipase for ester synthesis). Another use may be as a carrier of hydrophobic component. Silicone loaded microcapsules have been proved very efficient for transferring oxygen in bioreactor (Poncelet, 1993).

3.2 Coacervation

Coacervation relates to polymer precipitation. In the frame of bioencapsulation, two processes have been mainly developed. Prof. TMS Chang has developed a method (Chang 1966) consisting of dispersing an aqueous phase in an ether solution of cellulose nitrate to yield to a water-in-oil emulsion. The cellulose nitrate is precipitated by addition of a non-solvent (n-butyl benzoate). As only one polymer is involved, this is called simple coacervation. The process is not easy to control. The size distribution is a function of the mixing conditions but also the physico-chemical properties during coacervation (Poncelet 1989). The toxicity of the solvent involved in the process restricts its use to enzyme and biochemical encapsulation.

Complex coacervation involves the precipitation of two or more polymers together. The most well known example is the emulsification of oil in water phase containing arabic gum and gelatin. By dropping the pH, the charge of the gelatin becomes positive and a complex is formed with the negative arabic gum (Madam 1972). This method was extensively used in industry for carbonless copy paper and aroma encapsulation. It could be of interest for enzyme release in consumer products.

3.3 Thermal gelation

Thermal gelation is probably the most usual and simple method of encapsulation by emulsification. A κ-carrageenan, agar or agarose solution is dispersed in oil at 45°C and the temperature is dropped to cause gelification (Scheirer 1984, Tosa 1979). Suppliers now provide low temperature (28-30°C) gelling material which allows encapsulation of even fragile animal or plant cells.

Dropping the hot gelling solution in cold water forms thermal gel beads but emulsification in oil allows larger scale (Audet 1989). The use of static mixers even opens production to a very large scale (Descamp 2002).

3.4 Ionic gelation

Since its introduction (Kierstan, 1977), alginate beads remains the favorite system for cell entrapment. The dropping technologies have been strongly improved and allow now relatively large production. However, for very large scale (cubic meters), especially for small microcapsules (down to 25 μm), an emulsification method is still beneficial. The key point is that alginate gelifies in the presence of calcium ions. The question remains of how to transfer calcium through an oil phase.

Paul Heng (Chan 1990) proposed to add a calcium chloride solution to an alginate solution-in-oil emulsion. However, the transfer of the calcium is critical. The bead size is very inhomogeneous and the shape of the capsules is not spherical. A better alternative is to introduce an insoluble calcium source ($CaCO_3$) into the alginate solution before dispersing it in the oil. By addition of a small volume of acetic acid (soluble both in oil and water), the calcium is released provoking gelation of the dispersed alginate droplets (Poncelet, 1992). The calcium vector must be well selected and in the form of a very fine powder (2 μm). It is possible then to provoke gelation in a very small pH range (dropping from 7.5 to 6).

4 Transfer and washing of capsules

In many applications, traces of organic solvent, even vegetable oil, will be a source of problems. As for example in beer production, even a small amount of hydrophobic liquid could alter the taste and influence foam formation. At lab scale, the transfer and washing of the microcapsules from an organic solvent could be performed using three main methods:

- Removing as much as solvent as possible, transferring the microcapsules to a high concentrate water soluble emulsifier (Tween 20 at 50 %), dilution with water, filtration and resuspension in water
- Transferring the bead-in-oil suspension in a baker containing some water and gently mixing the interface between the phase with a flexible

tube to allow a settling of capsules to the lower aqueous phase.
- Filtrating the bead-in-oil suspension on nylon mesh (40 µm) under vacuum, washing of microcapsules by spraying water on the filter.

The selection of the method depends on the type of microcapsules and solvent. However, while scaling-up the production, the transfer and washing may become a critical point. The volume of water needed to get clean capsules could be important (200 ml for 20 g of capsules) and the cost associated with this step as high as the microcapsule cost it-self. If some data exists at the industrial or pilot scale, they don't seem to have been published.

5 Conclusions

This review is not expected to be complete but to give a good introduction of the potential and limitation of the microencapsulation using emulsification as dispersing techniques. When to use emulsification methods? If one of the extrusion or dropping methods could fit your needs, don't use emulsification. It will allow narrower size dispersion and it will reduce the washing problem. However, extrusion methods don't allow reaching as large scale as emulsification.

On the other hand, sometimes, emulsification set-up may be simpler than extrusion (for example during thermal gel bead preparation). Very strong capsules may be obtained by interfacial polymerization. Emulsification is the first method useful for oil-loaded capsules.

References

Audet P, Lacroix C (1989) Two-Phase Dispersion Process for the Production of Biopolymer Gel Beads: Effect of Various Parameters on Bead Size and their Distribution. Proc Biochem 24(12):217-225

Calabrese RV, Wang CY, Bryner NP (1986) Drop Breakup in Turbulent Stirred-Tank Contactors Part 1-3. AIChE J 32(4):654-681

Chan LW, Heng PWS, Wan LSC (1990) Development of alginate microcapsules by emulsification. Nus-JSPS Seminar, 23-26 October 1990, CHIBA

Chang TMS, MacIntosh FC, Mason SG (1966) Semipermeable Aqueous Microcapsules. I. Preparation and Properties. Can J Physiol Pharmacol 44:115-128

Groboillot A, Champagne CP, Darling GD, Poncelet D, Neufeld RJ (1993) Membrane Formation by Interfacial Cross-linking of Chitosan for Microencapsulation of lactococcus lactis. Biotechnology and Bioengineering 42:1157-1163

Descamps C, Norton S, Poncelet D, Neufeld RJ (2002) New emulsion process using static mixer for the production of κ-carrageenan gel beads. AIChE J, submited

Guerin, D, Rambourg P, Levy MC, Gayot A, Traisnel M (1983) Microencapsulation. VIII: Microcapsules de Charbon Actif à Parois de Sérum-Albumine Humaine Réticulée. Innov Tech Biol Med 4(1):24-32

Haas PA (1987) Turbulent Dispersion of Aqueous Drops in Organic Liquids. AIChE J 33(6):987-995

Hyndman CL, Groboillot A, Poncelet D, Champagne C, Neufeld RJ (1993) Microencapsulation of Lactococcus lactis within Cross-linked Gelatin Membranes. Journal of Chemical Technology and Biotechnology 56:259-263

Kierstan M, Bucke C (1977). The Immobilization of Microbial Cells, Subcellular Organelles, and Enzymes in Calcium Alginate Gels. Biotechnol Bioeng 19:387-397

Legrand J, Morançais G, Carnelle G (2001) Liquid-liquid dispersion in a SMX-sulzer static mixer. International Symposium on Mixing in Industrial Processes. May 14-16, Toulouse, France

Madan PL, Luzzi LA, Price JC (1972) Factors Influencing Microencapsulation of a Waxy Solid by Complex Coacervation. J Pharm Sci 61(10):1586-1588

Monshipouri M, Neufeld RJ (1992) Kinetics and activity distribution of urease coencapsulated with hemoglobin within polyamide membranes. Appl Biochem Biotechnol 32:111-126

Poncelet D, Smet B, Poncelet D, Neufeld RJ (1989) Control of Mean Diameter and Size Distribution during Formulation of Microcapsules with Cellulose Nitrate Membranes. Enzyme Microb Technol 11(1):29-37

Poncelet B, Poncelet D, Neufeld RJ (1990a) Preparation of hemolysate-filled hexamethylene sebacamide microcapsules with controlled diameter. Can J Chem Eng 68(3):443-448

Poncelet, D, Smet B, Beaulieu C, Neufeld RJ (1993) Scale-up of Gel Bead and Microcapsule Production in Cell Immobilization. In: Goosen MFA (ed) Fundamentals of Animal Cell Encapsulation and Immobilization. Boca Raton, Florida, USA, CRC Press, pp. 113-142

Poncelet D, Smet B, Neufeld RJ (1990b) Nylon Membrane Formation in Biocatalyst Microencapsulation: Physicochemical Modelling. Journal of Membrane Science 50:249-267

Poncelet D, Lencki R, Beaulieu C, Hallé JP, Neufeld RJ, Fournier A (1992) Alginate Beads by Emulsification/Internal Gelation: I Methodology. Applied Microbiology and Biotechnology 38:39-45

Poncelet D, Leung R, Centomo L, Neufeld RJ (1993). Microencapsulation of silicone oils within polyamide-polyethylene membranes as oxygen carriers for bioreactor oxygenation. Journal of Chemical Technology and Biotechnology 57:253-263

Poncelet D, Smet B, Beaulieu C, Huguet ML, Fournier A, Neufeld RJ (1995) Production of alginate Beads by Emulsification/Internal Gelation II: physicochemistry. Appl Microbiol Biotechnol 42:644-650

Scheirer, W, Nilsson K, Merten OW, Katinger HWD, Mosbach K (1984) Entrapment of Animal Cells for the Production of Biomolecules such as monoclonal Antibodies. Dev Bio Stand 55:155-161

Streiff F (1977) In line dispersion and mass transfer using static mixers. Revue Technique Sulzer 3:108-113

Tosa T, Sato T, Mori T, Yamamoto K, Takata I, Nishida Y, Chibata I (1979) Immobilization of Enzymes and Microbial Cells Using Carrageenan as Matrix. Biotechnol Bioeng 21:1697-1709

Wakamatsu Y, Koishi M, Kondo T (1974) Studies on Microcapsules. XVII.Effect of Chemical Structure of Acid Dichlorides and Bisphenols on the Formation of Polyphenyl Ester Microcapsules. Chem Pharm Bull 22(6):1319-1325

Wittbecker EL, Morgan PW (1959) Interfacial Polycondensation. Journal of Polymer Science XL:289-297

Optimization of the pelletization processes – A review

Evdokia S. Korakianiti and Dimitrios M. Rekkas[1]

Abstract

Pelletization is a process of converting fine powders of drugs and/or excipients into small (0.5 - 1.5 μm) free-flowing spherical units, which are called pellets. There are several techniques and types of equipment for their preparation. Thus a series of process and formulation factors affect their quality characteristics. The formulator should be aware of the fact that the above mentioned parameters do not equally contribute to the desired pellets' specifications.

For this reason it is necessary to use the appropriate tools for the identification of the factors affecting the process, their relative importance and possible interactions (Process characterisation). The result of such an approach is the reduction of variability, which is inversely proportional to quality. Furthermore, the selected important factors can now be used to optimise the process. This simply means the determination of the region that the values of these factors should fall in order to have the best possible response (Process optimization). Experimental design techniques such as factorial design, response surface methodology etc., provide the means of the characterisation and optimization of a process like pelletization. These methods have been widely used and during recent years their value has been recognised by scientists, because the statistical design of experiments is probably the most effective tool against variability.

Keywords: Pellets, pelletization, experimental design, optimization, response surface methodology

1 Introduction

Pellets are spherical or semi-spherical free flowing particles whose diameter varies between 200 μm and 2000 μm, but usually between 500 and 1500 μm (Ghebre-Sellasie 1989). They are filled into hard gelatine capsules, but they can also be compressed into tablets (Bechgard and Leroux 1992), (Millili and Schwartz 1990).

Oral multiple unit dosage forms have gained importance due to the technological and therapeutical advantages they offer (Ghebre-Sellasie 1989). Pellets disperse freely in the gastro-intestinal tract (GI tract) resulting in reduction of the variation in gastric emptying rates and overall transit times (Clarke et al. 1995). The uniform distribution of the multi-particulates in the GI tract results also in reduction of peak plasma fluctuations (Sandberg et al. 1998) and high local concentrations (Bodmeier 1997). The lowered risk of side effects caused by dose dumping is another major advantage. Moreover spherical particles exhibit good flow properties, they are less friable compared to other solid dosage forms and are ideal for coating because of their minimum surface to volume ratio (Ghebre-Sellasie 1989).

Most of the methods employed for the production of pellets are multi-variable processes, in which several factors affect the final characteristics of the pellets produced. Despite the fact that many formulation and development studies are conducted by varying one factor at a time, this approach is both time and energy consuming and thus expensive. Moreover, misleading conclusions can be drawn, particularly when there are interactions between the variables (Wehrle et al. 1993). For this reason the pelletization processes should be regarded as good candidates for the application of statistically designed experiments.

2 Pelletization techniques

There are many different pelletization techniques (Vervaert et al. 1995). Pellets can be produced by spraying a solution or suspension of a binder and a drug onto an inner core (solution /suspension layering) (Singh et al. 1995), spraying a melt of waxes from the top of a cold tower (spray congealing) (Thies and Kleinebudde 1999), spray drying of a solution or a suspension of the drug and formation of pellets due to the evaporation of the solvent (Ghebre-Sellasie 1989). A common method for producing pellets is extrusion spheronisation. It consists of four steps: wet granulation of the masses, shaping of the granules into cylinders (extrusion), forming the particles into spheres (spheronisation) and drying of the pellets (Law and Deasy 1997), (Krogars et al. 2000), (Baert et al. 1993). The most recent method for pellet production is pelletization by means of wet granulation in a fluid bed rotary processor (Vecchio et al. 1994), (Vertommen et al. 1997), (Vertommen and Kinget 1997), (Rashid et al. 1999), (Vertommen et al. 1996), (Kristensen et al. 2000), (Vertommen et al. 1998), (Holm et al. 1996). It is a one step method, where

[1] Evdokia S. Korakianiti and Dimitrios M. Rekkas, Division of Pharmaceutical Technology, School of Pharmacy, University of Athens, Panepistimiopolis, Zografou, Athens 157 71, Greece

pellets are produced dried and coated with the same equipment.

3 Experimental design

Regardless of the pelletization technique employed, several factors affect the production process and consequently the quality characteristics of the pellets. In general, a production process is a system with input factors and output variables. The process transforms the inputs into a finished product (output) that has several quality characteristics.

Some of the input factors are controllable and some are uncontrollable such as the environmental conditions. The identification of the significant factors that affect the process and the quality characteristics of the output from the non-significant ones (process characterization) can be achieved by the means of a designed experiment. This is an approach of systematically varying the controllable input factors in the process and determining their effect on the output product parameters. Statistically designed experiments play a crucial role in reducing the variability in the quality characteristics of the output. A major type of a designed experiment is the factorial design (Montgomery 1997).

Once the significant variables that affect the process output have been identified, then it is useful to model the relationship between the influential factors and the output quality characteristics. This enables the determination of the region that the values of these factors should fall in order to have the best possible response (Process optimization) (Wehrle and Stamm 1994), (Montgomery 1996).

4 Optimization

The aim of optimization is, as previously mentioned, to determine those values of the independent variables that maximize the objective. Two different methodologies can be applied to obtain the optimum values. With the first, one may determine the general configuration of the response to fit a second order polynomial to the data (Response surface methodology). With the other, one could proceed in finding the optimum without determining the general form of the response (Path of steepest ascent/descent). The most commonly used optimization technique is that of Response surface methodology, which is discussed in detail below.

4.1. Response Surface methodology (RSM)

Response surface methodology based on experimental designs is an economical approach aimed at collecting the maximum information with a minimum of properly designed experiments (Gonzalez 1993). Another important advantage is that the experimental field can be run sequentially until an efficient model is found to describe the process (Wehrle et al. 1996). According to Montgomery (Montgomery 1996), response surface methodology is a collection of mathematical and statistical techniques useful for modeling and analysis in applications where a response is influenced by several variables and the objective is to optimize the response.

The first step in RSM is to find a model that approximates adequately the relationship between the response (y) and the independent variables (x_i). Usually a low order polynomial is employed. If the response is adequately described by a linear function, then the first order model is used (1)

$$y = \beta_0 + \sum_{i=1}^{k} \beta_i x_i + \varepsilon \qquad (1)$$

If there is a curvature in the system, then a higher order degree is employed. Usually a second order polynomial (2) approximates adequately the experimental field under study

$$y = \beta_0 + \sum_{i=1}^{k} \beta_i x_i + \sum_{i=1}^{k} \beta_{ii} x_i^2 + \sum \sum_{i<j} \beta_{ii} x_i x_j + \varepsilon \qquad (2)$$

The method of least squares is employed for the estimation of the parameters in the polynomials and analysis of variance is performed to validate the model.

The second step in RSM is to challenge the model obtained. This is achieved by conducting further experiments under the predicted optimum conditions and by comparison between the estimated and the observed values of the responses.

Commonly used designs for fitting the first order model are the 2^k factorial and fractions of the 2^k, as well as the simplex design. For fitting the second order polynomial the central composite (CCD), the Box – Behnken, the 3^k factorial or more rarely some equiradial designs can be used.

4.2. Multiple response optimization

During optimisation, usually several responses should be optimised. Some of these response variables should be maximized and some minimized. In many cases these responses compete, meaning that improving one response may have a negative effect on another. Therefore all responses should be taken into consideration during the optimization process

(Khawala et al. 1996). To solve this problem, several approaches have been proposed like the use of constraint optimization, the superimposition of contour diagrams or the use of desirability functions. The latter offers several advantages because it permits the comparison of both qualitative and quantitative factors or of factors with different scaling, while it transforms all different responses in one measurement. The simplified form of the desirability function as it has been introduced by (Derringer and Suich 1980) has been used effectively for optimization purposes (Bodea and Leucuta 1998), (Khawala et al. 1996), (Outinen et al. 1998).

These functions take one of the following forms depending on whether the response is to be maximised (3) or minimised (4)

$$d = \begin{cases} 0 & \hat{y} < low \\ \left(\frac{\hat{y} - low}{high - low}\right)^s & low \le \hat{y} \le high \\ 1 & \hat{y} > high \end{cases} \quad (3)$$

$$d = \begin{cases} 1 & \hat{y} < low \\ \left(\frac{\hat{y} - high}{low - high}\right)^s & low \le \hat{y} \le high \\ 0 & \hat{y} > high \end{cases} \quad (4)$$

where: high and low are the maximum and minimum acceptable values of each response respectively. In the case of maximisation and for s=1 the desirability function rises linearly from 0 at the low value to 1 at the high value. For s <1 it increases quickly at the beginning and then levels off, while for s > 1 it increases slowly at first and then speeds up. When minimisation is desired, the function has a similar shape to that of maximisation, but it starts at 1 for the low value and goes to 0 for the high.

After the calculation of the individual desirability values, the overall desirability can be determined according to the following equation (5)

$$D = \{d_1\, d_2\, \ldots\, d_m\}^{1/m} \quad (5)$$

where m represents the number of responses.

5 Applications of optimization methodology in pelletization techniques

Table 1 depicts a review of the optimization techniques that can be found in the literature for optimizing pelletization processes.

6 Conclusions

The increasing use of experimental design techniques for process characterization and optimization is a clear recognition of their value, since with relatively few properly designed experiments the gained information allows the researcher to minimize the variability in products and processes.

The reduction of variability is the definition of quality improvement. This is the reason why experi-

Table 1:
Review of the optimization techniques used in optimizing pelletization processes

Ref.	Purpose of optimization	Pelletization technique used	Independent variables	Responses	Optimization technique involved
Noche et al. 1994	Optimizing the pelletization and coating process	Extrusion-spheronisation, Wurster coating	Amount of granulating liquid, Kneading time, Screen plate diameter, Batch size, Pulverization rate, Pulverization pressure, Inlet air rate, Outlet air temp.	Size, Friability, Coating efficiency, Sieving efficiency, Drug dosage, Dissolution constant	2^3 full factorial design
Vojnovic et al. 1995	Optimization of the production of theophylline pellets	High shear mixer	Impeller speed, Amount of binding solution	Porous structure, Size distribution	Doehlert and simplex matrix
Zhou F. et al. 1998	Optimization of the process for producing matrix pellets based on waxes and starch	Fluid bed rotor granulation	Impeller speed , Mixing time	Yield	3x3 orthogonal array
Bodea A. et al. 1998	Evaluation of three process parameters for the application of ethylcellulose films to obtain sustain release pellets	Coating pan	Film thickness, Lacquer concentration, Plasticizer concentration	t_{85}, Stuck pellets, Duration of process	Box-Behnken, Desirability function

continuing Table 1:

Ref.	Purpose of optimization	Pelletization technique used	Independent variables	Responses	Optimization technique involved
Singh S. K et al. 1995	Experimental latex evaluation	Drug layering	Solids content, Volume of coating, Plasticizer concentration	Cumulative dissolved in 1,6,12 h	Box-Behnken
Law et al. 1997	Optimization of a formulation for indomethacin pellets	Extrusion spheronisation	SLS, PVP, water content	Size, Roundness, Dissolution profile	3^3 factorial design, Canonical analysis
Hileman et al. 1997	Predict water requirements for extrusion spheronisation processing for drugs with known water solubility	Extrusion spheronisation	Amount of water, Wet mixing time, Spheronizing time	Yield, Roundness, Size distribution	Central Composite design
Baert et al. 1993	Determination of the influence of important parameters in pellet production	Extrusion spheronisation	Spheroniser speed, Spheroniser time, Water content	Pellet yield, Roundness	Pareto analysis
Krogars et al. 2000	Evaluation of extrusion spheronisation for preparing pH sensitive matrix pellet	Extrusion spheronisation	Amount of Eudragit, Amount of citric acid , Spheronising time	Aspect ratio, Roundness	Central Composite Design
Fekete R. et al. 1998	Evaluation of process and formulation variables on pellets´ characterisics	High shear mixer	Rotating speed, MCC content	Size, Size distribution, Sphericity	Central Composite design
Korakianiti et al. 2000	Optimization of a process and formulation variables	Fluid bed rotor granulator	Rotor speed , Amount of water, Spray pressure	Size , Size distribution	3^2 factorial design
Kennedy et al. 1996	Process optimization	Fluid bed coater	Inlet air temp., Outlet air temp., Coating agent level, Coating agent particle size	Coating thickness, Coating uniform., Loss on chamber walls, Weight post coating	Central Composite Design
Heng et al. 1996	Process optimization	Fluid bed rotor granulator	Spray rate, Amount of moistening liquid	Yield, Size, Size distribution	RSM
Ku et al. 1993	Process optimization	Extrusion Spheroniser	Amount of water, Water temp., Extruder speed, Spheroniser speed, Spheroniser dwell time	Yield	Split-plot factorial design

mental design has been considered the key to the magic kingdom of Quality (Bhote 1991).

References

Baert L, Vermeersch H, Remon JP, Smeyers-Verbeke J, Massart DL (1993) Study of parameters important in the spheronisation process. Int J Pharm 96:225 -229

Bechgard SR, Leroux JC (1992) Coated pelletized dosage form: effect of compaction on drug release. Drug Dev Ind Pharm 18:1927-1944

Bhote KR (1991) World class quality. Using design of experiments to make it happen, AMACOM, New York, p 25

Bodea A, Leucuta SE (1998) Optimization of propanolol hydrochloride sustained release pellets using Box Behnken design and desirability function. Drug Dev Ind Pharm 24(2):145-155

Bodmeier R (1997) Tabletting of coated pellets. Eur J Pharm Biopharm 43:1-8

Clarke GM, Newton JM, Short MD (1995) Comparative gastrointestinal transit of pellets systems of varying density. Int J Pharm 114:1-11

Derringer G, Suich RJ (1980) Simultaneous optimization of several response variables. J Quality Technol 12:214-219

Fekete R, Zelko R, Marton, Racz (1998) Effect of the formulation parameters on characteristics of pellets. Drug Dev Ind Pharm 24(11):1073-1076

Ghebre-Shellasie I (1989) Pellets: A general overview. In: Ghebre-Shellasie I. Pharmaceutical Pelletization Technology. Marcel Dekker, New York, pp. 6-7

Gonzalez AG (1993) Optimization of pharmaceutical formulations based on response surface experimental designs. Int J Pharm 97:149-159

Heng PWS, Wan LSC, Tan YTF (1996) Optimization of spheroid production by centrifugal processing. Int J Pharm 143:107-112

Holm P, Bonde M, Wigmore T (1996) Pelletization by granulation in a roto-processor RP-2. Part I: Effects of process and product variables on granule growth. Pharm Tech Eur 228:22-36

Kennedy JP, Niebergall PJ (1996) Development and optimization of a solid dispersion hot melt fluid bed coating method. Pharm Dev Tech 1(1):51-62

Khawala AI, Garcia Contreras L, Robert LD (1996) Preparation and Evaluation of Zidovudine-Loaded Sustained Release Microspheres. 2. Optimization of Multiple Response Variables. J Pharm Sci 85(6):572-576

Korakianiti ES, Rekkas DM, Dallas PP, Choulis NH (2000) Optimization of the pelletization process in a fluid bed rotor granulator using experimental design. Pharm Sci Tech 1(4), nr 35

Krinstensen J, Schaefer T, Kleinebudde P (2000) Direct pelletization in a rotary processor controlled by torque measurements. I. Influence of process variables. Pharm Dev Tech 5(2):247-256

Krogars K, Heinamaki J, Vesalaht J, Marvola M, Antikainen O, Yliruusi J (2000) Extrusion spheronisation of pH- sensitive polymeric matrix pellets for possible colonic drug delivery. Int J Pharm199:187-194

Ku CC, Joshi YM, Bergum JS, Jain NM (1993) Bead manufacture by extrusion / spheronization a statistical design for process optimization. Drug Dev Ind Pharm 19(13):1505-1519

Law M, Deasy PB (1997) Use of a cononical and other analyses for the optimization of an extrusion-spheronization process for indomethacin. Int J Pharm 146:1-9

Millili GP, Schwartz JB (1990) The strength of microcrystalline cellulose pellets: The effect of granulating with water/ethanol mixtures. Drug Dev Ind Pharm 16:1411-1426

Montgomery DC (1996) Design and Analysis of experiments, 4th edition, John Wiley, New York USA

Montgomery DC (1997) Quality improvement in the modern business environment. In: Montgomery DC (ed) Introduction to Statistical Quality control, 3rd edition, John Wiley, New York, pp.12-14

Noche C, Barochez BH, Brossard C, Horvard S, Cuine A (1994) Optimizing the manufacturing process for controlled release pellets. Pharm Tech Eur April:39-43

Outinen K, Haario H, Vuorela P, Nyman M, Ukkonen E, Vuorela H (1998) Optimization of selectivity in high performance liquid chromatography using desirability functions and mixture designs according to PRISMA. Eur J Pharm Sci 6:197-205

Rashid HA, Heinamaki J, Antikainen O, Yliruusi J (1999) Effects of process variables on the size, shape surface characteristics of microcrystalline cellulose beads prepared in a centrifugal granulator. Drug Dev Ind Pharm 25(5):605-611

Sandberg A, Blomqvist I, Johnson UE, Lundborg P (1998) Pharmacokinetic and pharmacodynamic properties of a new controlled release formulation of metoprolol: a comparison with conventional tablets. Eur J Clin Pharmacol 33:9-14

Singh SK, Dodge J, Durrani M, Khan MA (1995) Optimization and characterisation of controlled release pellets coated with an experimental latex: I. Anionic drug 125:243-255

Thies R, Kleinebudde P (1999) Melt pelletization of a hydroscopic drug in a high shear mixer. Part. 1. Influence of process variables. Int J Pharm 188:131-143

Vecchio C, Bruni G, Gazzaniga A (1994) Preparation of indobufen pellets by using centrifugal rotary fluidized bed equipment without starting seeds. Drug Dev Ind Pharm 20(12):1943-1956

Vertommen J, Jaucot B, Rombaut P, Kinget R (1996) Improvement of the material motion in a rotary processor, Pharm Dev Tech 1(4):365-371

Vertommen J, Kinget R, (1997) The influence of five selected processing and formulation variables on the particle size, particle size distribution and friability of pellets produced in a rotary processor. Drug Dev Ind Pharm 23(1):39-46

Vertommen J, Rombaut P, Kinget R (1997) Shape and surface smoothness of pellets made in a rotary processor. Int J Pharm 146:21-29

Vertommen J., Rombaut P, Kinget R (1998) Internal and external structure of pellets made in a rotary processor. Int J Pharm 161:225-236

Vervaet C, Baert L, Remon J (1995) Extrusion Spheronisation. A literature Review. Int J Pharm 116:131-146

Vojnovic D, Moneghini M, Masiello S (1995) Design and optimization of theophylline pellets obtained by wet spheronization in a high shear mixer. Drug Dev Ind Pharm 21(18):2129-2137

Wehrle P, Koner D, Benita S (1996) Sequential statistical optimization of a positively charged submicron emulsion of miconazole. Pharm Dev Tech 1(1):97-111

Wehrle P, Nobelis Ph, Cuine A, Stamm A (1993) Response surface methodology: An interesting statistical tool for process optimization and validation: Example of wet granulation in a high-shear mixer. Drug Dev Ind Pharm 19(13):1637-1653

Wehrle P, Stamm A (1994) Statistical tools for process control and quality improvement in the pharmaceutical industry. Drug Dev Ind Pharm 20(2):141-164

Zhou F, Vervaert C, Massart DL, Massart B, Simon J-P (1998) Optimization of matrix pellets based on the combination of waxes and starch using experimental design, Drug Dev Ind Pharm 24(4):353-358

Fluid bed filmcoating

Klaus Eichler[1]

1 Introduction

With the increasing number of pharmaceutical sustained-release products on the world market, there is also an increasing need for reliable processing equipment, warranting perfect reproducibility of the process parameters and therewith of the film morphology.

Since fluid bed technology is renowned for its optimal heat and mass exchange, it is particularly suitable for the application of filmcoating. It causes fast and effective evaporation of the liquid vehicle which transports the coating material to the surface of the substrate, irrespectivewhether the latter is a powder, a crystal, a granule, a pellet or a tablet.

The fluid bed method offers three processing options:

- top spray
- bottom spray
- tangential spray

Each method will be individually discussed as each spray method has different effect on the final film quality. The coating principle, however, is the same for each option.

Whenever a particle passes through the coating zone, small patches of coating material are applied until the entire surface has been covered. Droplet formation, contact, spreading, coalescence and evaporation occur almost simultaneously during the process. By continuous repetition of the 'patchwork,' the film thickness can be steadily increased. Actually, the drug itself maybe applied as a neutral nuclei with filmcoating, a process we would then call "layering".

Usually, air atomized spray nozzles are used for all fluid bed filmcoating options, since the atomization air allows better control of droplet size compared with airless nozzles. A common target of each option is also to minimize droplet travel distance for uniform and optimal spreadability.

2 Top spray coating

The conventional top spray method shown has been used for nearly 20 years (40 years for fluid bed drying and granulation), originally for the lipid coating of vitamin granules.

The coating material is sprayed downwards on the fluidized product. To prevent agglomeration, the particles should travel fast enough through the coating zone and the droplets should be small enough not to embrace the suspended particles, but to just deposit the coating material on the surface of the substrate. The finer the droplets the denser the final film. However, the droplets must still remain spreadable on the surface of the substrate, i. e. premature evaporation of the liquid vehicle is not desired.

Like any other fluid bed process, top spray filmcoating is a thermo-dynamic process, thus requiring moisture control, i.e., by carefully monitoring the product bed temperature and process air volume.

Since a maximum product surface is exposed to the spray mist, this is a fast process and feasible for batches up to 1500 kg. But since the fluidization pattern is random and unrestricted, a perfect control of each droplet's travel towards the substrate is not possible as in pinholes or spray-dried particles on the surface of the final film. However, for taste masking or enteric coating of non-toxic substances, this may present satisfying results.

For lipid coating (hot melt), top spraying is the system of choice. The product container of the top spray system is designed for an unrestricted particle flow, an important feature for hot melt coating. Materials with a melting point of less than 100°C can be applied to the fluidized particles by carefully controlling the liquid and atomizing air temperatures and the product bed temperature. The degree of protection offered by the coating is related to the rate at which it is applied and how slowly it congeals. Keeping the product bed temperature close to the coating's congealing temperature results in a significant increase in the viscous drag in the bed.

3 Bottom spray filmcoating

Also known as the "Wurster" system, originally designed by Prof. Dale Wurster from the University of Wisconsin for the coating of tablets - meanwhile used for the coating of all kindsof particles down to 80 micron.

The processing hardware is quite different from the top spray configuration. The coating chamber contains a cylindrical partition and a perforated bottom screen with varying free areas. The largest free

[1] Klaus Eichler, Technology Training Center, Buehlmuehle, 79589 Binzen, Germany

area is just below the central partition, thus leading the majority of the processing air through this nozzle provides a very dense spreading is at its best.

If particles are exposed in very regular time intervals to a very uniform spray mist with droplets of uniform spreadability, the film is bound to be of an uniform thickness, without the imperfections introduced by the randomness of the top spray system.

4 Tangential spray coating

This is a relatively new technology, using a fluid bed with a rotating disc in the bottom of the product container. Originally this technology had been conceived for high-density fluid bed granulation and is now frequently used to produce high-dose pellets by layering drugs on nuclei. A controlled release film may subsequently be applied.

The rotor processor consists of a cylindrically shaped product bowl and expansion chamber. The rotor disk sits at the base of the product bowl and seats along the circumference of the chamber when the rotor is not in motion. The disk is raised during processing to create a slit between the edge of the rotor disk and the conical shaped bottom of the rotor product bowl. The patented adjustable disk height allows control of air volume through the slit independent of velocity. This key feature permits very low drying rates for direct pelletization and pelletizing by powder layering. For coating applications requiring a medium to be evaporated quickly, the air volume can be significantly increased while keeping air velocity constant. This flexibility results in a single unit processor capable of granulating, pelletizing, layering and coating.

The fluidization pattern in the rotor processor can best be described as a spiraling helix. Three factors act on the product to create this flow pattern. The centrifugal force of the rotating disk causes product to flow radially towards the product bowl wall. Airflow through the slit creates a vertical force causing the product to become fluidized. Gravity soon overcomes the force of the airflow and the fluidized product falls back into the bowl towards the center.

Liquids or powdered solids can be added to the process through air atomizing nozzles located on the product bowl side wall. The nozzles spray tangentially into the processing chamber in the same direction as the fluidization pattern.

For the filmcoating application, the tangential spray systems compares equally to the bottom spray system, since the three main physical criteria are the same:

1. Concurrent spraying, with the nozzle buried inside the product. Hence: Minimal droplet travel distance
2. Uniform statistical exposure of the particles to the spray mist
3. High product density in the spraying zone

Consequently, the quality of the film produced by tangential spray coating fully measures up to the bottom spray standard.

5 Summary

The evaporative efficiency of fluidized bed equipment and the ability to apply a film to particles discretely suspended in an air stream have resulted in widespread use of this technique for coating products ranging from 100 μm particles to tablets. The three fluidized bed techniques, all of which are used commercially for film coating, offer a variety of applications.

These methods have some common features and variables, but each has unique advantages and limitations. In the development of a product with commercialization as the ultimate goal, criteria such as economics, product and process variables, and dosages form performances must be considered.

In recent years, there have been significant improvements in instrumentation and control for the many variables encountered in fluidized bed processing. Further equipment evolution may result in either the improvement of the limitations of a given technique or the development of an entirely new method.

Immobilization of biomaterials into organic-inorganic matrices

Gabriela Kuncová, Jiří Hetflejš, Janoš Szilva, and Stanislav Šabata[1]

Abstract

We compared activities and mechanical properties of two Lipolase 100 L biocatalysts that differed in the manner of their entrapment into organic-inorganic matrices. Model reactions for evaluation of the activities of the biocatalysts were esterification of stearic acid with aliphatic alcohols in hexane, toluene and acetone and the hydrolysis of canola oil. In the first process, one step sol-gel technique, the enzyme was entrapped into silica prepolymers prepared from tetramethoxysilane, methyltrimethoxysilane, propyltrimethoxysilane and

(3-aminopropyl)triethoxysilane. The two-step process was based on immobilization by sorption of enzyme on fine inorganic particles and their subsequent entrapment into a silicone based polymer. In a typical example Lipolase100 L was sorbed on the surface of poly(methylhydroxysiloxane) particles that were entrapped into poly(dimethylsiloxane) and cross-linked. The biocatalysts were shaped by molding. The one- step biocatalysts were fragile and hard. Mechanical properties of the two-step biocatalysts were changed from the hard, high abrasion resistant material, to elastic rubber. The activities of two-step biocatalysts (22.5 $mg_{protein}/g_{biocatalyst}$) were proportional to their swelling of the biocatalyst in reaction media and were to a certain extent insensitive to modifications of the elasticity and dimensions of biocatalyst particles. In the esterification of stearic acid, the activity of two-step immobilized lipases was higher than that of the commercial sol-gel lipase Fluka.

Keywords: immobilization of lipases, sol-gel, silicone rubber

1 Introduction

Immobilization of biomaterials into an organic-inorganic matrix with a sol-gel technique ensured that biocatalysts would be non-toxic, highly thermal and chemically stable. The variability of the sol-gel process makes possible a tailoring of the chemical composition and porosity of the matrix to be optimal for desired enzyme and catalytic reactions. To preserve the high activity of biomaterial, the entrapment process should be done under mild conditions, low temperature and pH near 7. Under these conditions, however, polymerisation and polycondensation of alkoxymetals are difficult to control. The low temperature treatment and inelasticity of oxide-based materials resulted in a poor abrasion resistance of biocatalysts. Uncontrolled changes in prepolymer structure have lead to difficulties in shaping biocatalysts. These drawbacks of the immobilization into organic-inorganic matrices were overcome a with a two-step process of immobilization into a silicone based matrix.

When compared to other enzymes, lipases immobilized by the sol-gel process often show higher activity than the native enzyme in both water and organic solvents (M.T. Reetz et al. 1996; I. Gill et al. 1999). The increased activity of lipases resulting from the use of a particular sol-gel procedure and the effects of precursor composition, polymerizaton procedure and drying on specific surface and porosity of biocatalysts are still to be elucidated. One reason is that porosity data reported so far were determined by BET method, using gel heated at 100-150°C *in vacuo*. Under the conditions of enzymatic catalysis the matrices are swelled, and the actual porosity is thus quite different from BET porosity. This difference is very likely responsible for unexpected relations between the BET surface and biocatalyst activity.

Lipases differ from other enzymes in that they operate on a hydrophobic-hydrophilic interface. Their characteristic feature is their activation in the presence of hydrophobic interfaces. When these interfaces are absent, lipases have some elements of secondary structure ("lid") covering their active sites and making them inaccessible to substrates (Fernandez-Lafuente R. 1998). In the presence of hydrophobic interfaces, the conformational changes take place, yielding the "open structure" of lipases. The enzyme is adsorbed on hydrophobic interfaces through hydrophobic surface. This complex mechanism of the enzyme action makes the understanding and control of the behavior of lipases in organic synthesis difficult.

Many lipases were immobilized into organic-inorganic matrices by various techniques. The obtained results can be hardly compared because in addition a to different immobilization process also a variety of enzymes and activity assays were used. In our experimental work we compared biocatalysts based on inorganic-organic carriers using esterification of carboxylic acids with alcohols under anhydrous conditions as a model reaction.

[1] Gabriela Kuncová, Jiří Hetflejš, Janoš Szilva, and Stanislav Šabata, Institute of Chemical Processes Fundamentals ASCR, 16500 Praha 6, Rozvojova 135, Czech Republic

The goal of this study was to develop a reproducible process of immobilization of lipases into organic-inorganic matrices. The process of preparation of highly active and abrasion resistant biocatalyst should be readily scaled up.

2 Experimental

2.1 Materials

Lipolase 100L was commercial product of Novo Nordisk (5 $mg_{proteine}$/ml), Lipase Sol-Gel AK (*Aspergillus niger*), tetramethoxysilane (TMOS), methyltrimethoxysilane (MTMS), (3-aminopropyl)triethoxysilane (APTS), propyltrimethoxysilane (PTMS) and the other compounds were purchased from Fluka. Solvents were dried with 4 Å sieve prior to use. Zn(2-ethylhexanoate)$_2$, Sn(2-ethylhexanoate)$_2$, poly(dimethylsiloxane)-silanol terminated (HO-PDMS, viscosity 45-85 cSt and 100 cSt) were supplied by ABCR (Karlsruhe, FRG), $NaBH_4$ and poly(methylhydrosiloxane) (PHMS, 98% Si-H bonds) were purchased from Sigma-Aldrich. Ethyl silicate 40 was from the laboratory stock, bentonite BENTOGRAN® was gift of Compo co. (Czech Rep.).

2.2 One-step immobilization

2.2.1 Entrapment of lipase into a silica prepolymer

The prepolymer was prepared by stirring a mixture of alkoxysilanes (8 g) and water for 24 h with a magnetic stirrer. Mol. ratios of the silanes were TMOS:MTMS = 3:1, 1:1 and 1:3, TMOS:PTMS = 3:1 and 1:1, HCl conc. 6.10^{-5} mol/l. The molar ratio of silanes:water was h = 0.22. The acidity of the prepolymer was adjusted to pH 6.5 by 1M-phosphate buffer (l ml) and the lipase was immediately added. The solutions gellified during the few minutes after pouring into moulds (i.d. 3 x 2 mm cylinders). Prepolymer with APTS and TMOS was prepared with the reported procedure (Kuncova et al. 1995). Gels were dried at 25°C for 5 days under laboratory conditions and for 2 days in dry air. Xerogels were crushed, sieved and 0,1-0,3 mm particles were collected.

2.3 Two-step immobilization

2.3.1 Preparation of poly(methylhydroxysiloxane) (PHOMS)

To a magnetically stirred suspension of $NaBH_4$ (1.52 g, 40 mmol) in anhydrous ethanol (40 ml), a solution of Zn(2-ethylhexanoate)$_2$ (14.08 g, 40 mmol) in anhydrous ethanol (40 ml) was added during 30 min while cooling the mixture on a water bath. Then PHMS (50 ml, 0.78 mol) was added dropwise during 80 min, the water bath was removed, the mixture warmed up to 50 °C and was maintained at this temperature for 1.5 h and at 70 °C for 2.5 h, and then set aside to cool to ambient temperature overnight. The IR showed complete solvolysis of the Si-H bonds of PHMS (the absence of the Si-H stretch band at 2168 cm^{-1}). NMR spectrum indicated that poly(ethoxymethylsiloxane) (further PEtOMS) so prepared is to about 20 % cross-linked.

The viscous mixture was diluted with ethanol-water (1:1, 350 ml), alkalized by adding 5M-NaOH (200 ml) in one portion, and the silanolate solution so formed was acidified with 5M-HCl to pH 5-6 under efficient stirring. The fine precipitate of PHOMS was separated by vacuum filtration, washed several times with water to remove NaCl (checked by the absence of Cl^- in the filtrate) and stored wet in a refrigerator.

2.3.2 Immobilization of lipase on PHOMS

PHOMS-adsorbate

In a typical example, an aqueous lipase solution (20 ml containing 100 mg lipase) was added to a stirred, wet ice-cold PHOMS (30 g, 28 wt. % solids) in 0.05M hexametaphosphate buffer (36 ml) and isopropanol (4 ml). After 15 min-stirring, ice-cold 0,25M hexametaphosphate buffer (30 ml) was added and the mixture stirred for another 2 h. Then lipase-PHOMS-adsorbate was separated by filtration with suction, washed successively with three 30 ml-portions of ice-cold 0,25 M-buffer, acetone, and pentane. The filtrate was analysed on the content of lipase (see below the chapter „Characterization of biocatalysts"), and the lipase-PHOMS-adsorbate was dried at room temperature for 2 h and then stored in a dessicator over a molecular sieve. As found by repeated experiments, the adsorption efficiency of PHOMS was 95.2 % for 20 mg lipase per 1 g PHOMS conc. and 91.6 % for 100 mg/g conc.

PHOMS-bentonite-adsorbate

The lipase-PHOMS-adsorbate containing 90 and 10 w. % bentonite resp. were prepared by the procedure described above, except that the alkaline hydrolysis of PEtOMS to the silanolate was carried out after addition of the bentonite to the stirred poly(alkoxymethylsiloxane) solution. The washed samples obtained by vacuum filtration were dried at room temperature and pulverized before activity tests.

2.4 Encapsulation of PHOMS-adsorbate (PHOMS-SR)

In a typical example, a dry PHOMS-adsorbate (3.4 g) was homogenized with HO-PDMS (4 g each of m.w. 1750 and 26.000), then ethyl silicate 40 (3.6 g) and Sn(2-ethylhexanoate)$_2$ (96 mmol) were added and the medium was stirred to achieve its homogenization. The homogeneous mixture was poured onto a Petri dish or coated on an expanded metal and cured at room temperature for 4 h. The flexible sheet (15 g, 1.5 mm thick) was cut into 1x1 mm and 2x2 mm cubes, 5x40 mm 1.2 mm thick sheets.

2.5 Characterization of biocatalysts

Specific surface areas and mean pore sizes of biocatalysts were measured after drying of xerogels (120°C, 2 hod.) by N_2 absorption (BET) with ASAP 2010 instrument. The average pore diameter (D) was calculated by BJH method. Concentrations of immobilized proteins were determined by measuring intensities of the fluorescence of tryptophane of the residual lipases in solutions after immobilization. Swelling of rubber-like biocatalyst (PHOMS-SR). The 40x5x1 mm sheets of the biocatalysts were weighed before and after 12 h-immersion in solvent at 40°C.

2.6 Model reactions

Esterification of stearic acid with alcohols. Alcohol (butanol, ethanol, and propanol - 2 mmol), solvent (acetone, benzene, decane, hexane and toluene - 10 ml), stearic acid (2 mmol) and a biocatalyst containing the lipase equivalent 4 KLU were placed in a 25 ml flask. After 48 h reaction at 25°C, the residual stearic acid was determined by potentiometric titration.

Hydrolysis: Canola oil (5 ml) and distilled water (4 ml) were placed in a 25 ml-flask. After 4 hours (shaker 300 rpm) at 40°C the biocatalyst was removed by pouring off the emulsion and the free fatty acids were determined (Kuncova et al. 1994).

Leakage of lipases from biocatalysts was determined by the measurement of stearic acid conversion (or the content of free fatty acids in the case of the hydrolysis) obtained with the lipase released into solution during the first reaction cycle.

3 Results and discussion

The lipases immobilized into a prepolymerized TMOS were not active in esterification reactions. In order to form solid hydrophobic-hydrophilic interfaces we added organosilanes (MTMS, PTMS or APTS) to precursor solutions. Increasing MTMS content did not improve the conversion of stearic acid (SAC) (Table 1). This might be explained by two opposite effects of MTMS content. The higher content of methyl groups leads to the more hydrophobic sol-gel matrices thus, increasing the activity of lipases by opening the lid. Or, the biocatalyst with MTMS or PTMS had lower specific surface. PTMS biocatalysts were very fragile and the lipase was released during the first cycle. APTS (the most frequently used compound for binding proteins on glass surfaces) is expected to improve fixation of the hydrophilic part of the enzyme. The biocatalyst with APTS showed 30 %

Table 1:
The influence of precursor composition on specific surface (BET), specific surface of mesopores (S), BJH Adsorption Average Pore Diameter (D), stearic acid conversion (SAC), and stearic acid conversion by the lipase released after first reaction cycle (SACRL)

Matrix, Precursors composition	BET, m^2/g	S, m^2/g	D, nm	SAC, %	SACRL, %
TMOS	650	380	1.6	5	0
TMOS:MTMS=3:1	350	160	2.1	35	0
TMOS:MTMS=1:1	27	3.3	2.2	32	0
TMOS:MTMS=1:3	0.03	-	-	30	0
TMOS:PTMS=3:1	71	-	-	95	95
TMOS:PTMS=1:1	0.9	-	-	95	95
TMOS+APTS	300	120	2.0	30	15
PHOMS adsorbate	36	18	10	95	13
PHOMS-SR	0	0	0	95	0
Lipase Sol-Gel AK	0.1	-	-	35	15

SAC, but lipase was partially released. In organic solvents the biocatalysts with the molar ratio TMOS/MTOS ≤ 1/1 were rigid and brittle. These materials were suitable for column reactors.

The biocatalysts with sol-gel matrices showed higher hydrolytical activities than free enzyme (see also Kuncova et al. 1995). In aqueous solutions the silica particles of the biocatalyst swelled and became very soft, the column reactors became stuffed, and in reactors with intensive mixing the biocatalysts were disintegrated.

Commercial Sol-Gel lipase Fluka showed similar activity to the biocatalysts prepared in the present work (Figure 1). The conversion of stearic acid obtained with the lipase released from the commercial lipase was 15 % (SACRL). Any leakage of lipase from the biocatalysts containing MTMOS and TMOS was not detected. In a purely inorganic matrix, which is resistant to swelling in hexane, lipase is probably closed in fine pores, which blocked enzyme release and substrate conversions. In organic-inorganic matrices, hydrophobic interactions with alkyl groups probably increased lipase activity by opening the lid. The impact of decreasing surface area on the efficiency of these biocatalysts has been masked by hyperactivation. The influence of silica matrix composition and of solvents on the esterification of stearic acid with propanol (SAC) is shown in Figure 1. Similar relations as with propanol were also observed with ethanol and butanol. The activities of lipases increased in the sequence ethanol > propanol > butanol. The entrapment of the enzyme in TMOS/MTOS matrices decreased SAC. Solvents, acetone and toluene, impaired the free enzyme activity. In the case of the immobilized enzyme, these solvents led to lesser changes in SAC compared to the free enzyme. This agrees with common finding that immobilization suppresses the action of denaturation and inhibition agents. The inhibiton of free Lipolase 100L by organophosphates was eliminated by the entrapment into sol-gel matrix and also by its immobilization on hydrophobic glass surfaces (Kuncova and Sivel 1997).

The biocatalysts prepared by the adsorption of lipase on poly(methylhydroxysiloxane) (PHOMS adsorbate) led to SAC > 90 %. The low specific surface might be an artifact caused by the condensation of hydroxy groups during drying before BET measurements (see Table 1). The effect of drying was probably stronger than in the case of sol-gel biocatalysts, because of the higher content of OH groups. The PHOMS-adsorbate encapsulated into silicone rubber (PHOMS-SR) was shaped into 1x1 mm and 2x2 mm cubes, and 1¸2 mm thick sheets, and coated on expanded metal (Figure 2).

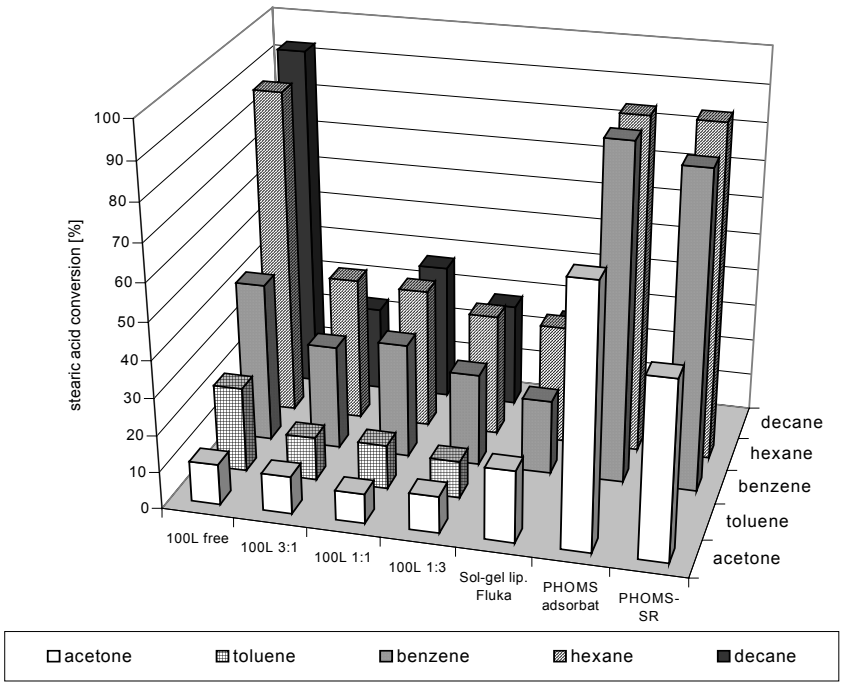

Figure 1:
Esterification of stearic acid with propanol in organic solvents catalyzed by Lipolase 100L free, and entrapped in TMOS/MTOS = 1:1, 3:1 and 1:3, Sol-gel lipase Fluka, lipase 100 L immobilized on poly(methylhydroxysiloxane) (PHOMS-adsorbate) and PHOMS-adsorbate encapsulated in a silicone rubber (PHOMS-SR)

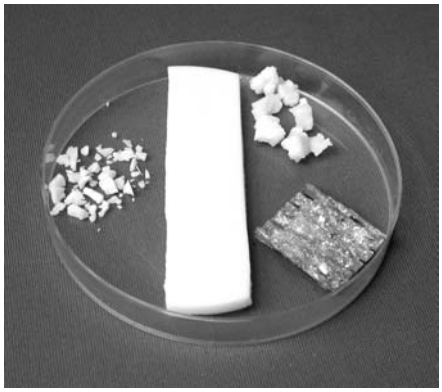

Figure 2:
The lipase adsorbed on poly(methyhydroxylsiloxane) encapsulated in a silicone rubber (PHOMS-SR) shaped in cubes, sheet and coated on an expanded metal

The shaping of biocatalyst to sheets or coating on a expanded metal enables changing of reactor design from columns to more efficient reactors, e.g., reactors with vibrating liquid. The elasticity of PHOMS-SR biocatalysts can be decreased by increasing the content of cross-linking agent - $Sn(2\text{-ethylhexanoate})_2$. The changes in the content of hardener ± 10 % modified hardness and elasticity of the biocatalyst without decreasing SAC. However, the brittle biomaterial with dense polymer network obtained with a twofold amount of hardener did not catalyze the esterification of stearic acid in hexane. Thus, the lipase immobilized on hydrofobic-hydrofilic interface might be inactive after encapsulation into polymer with an unsuitable network.

PHOMS-SR, and also PHOMSR-SR with bentonite, had zero specific surfaces, as measured by BET (Table 1). SACs in hexane and in toluene were > 90 %, but the extent of hydrolysis of oil in water was only 4 %. The activities of the rubber-like biocatalysts have been proportional to the degree of their swelling in reaction mixture (Figure 3). After 12 hours PHOMS-SR sheets adsorbed 40 % vol. of hexane, 30 % of toluene, 13 % of acetone and < 5 % of water-canola oil.

In general, the choice of optimal polymer network depends not only on the polymer mixture components but also on a given reaction performed.

The time dependencies of stearic acid conversion (SAC) presented in Figure 4 show that in hexane the reaction rate is not substantially decreased when using the biocatalyst shaped to 1-mm particles or to 40x5x1 mm sheet. In acetone and toluene, the low conversions during the first day of the reaction might be ascribed to a slow swelling of the silicone polymer into which PHOMS-adsorbate was encapsulated. The higher conversions after two days were probably caused by the penetration of the reaction components into a disrupted biocatalyst. The dispersion of PHOMS-adsorbate in silicone polymer was not perfectly homogeneous and thus in PHOMS-SR there are spots with highly different hydrophobicity. Heterogeneous penetration of the solvent and reaction components into different places disrupted the compact biocatalyst. The reaction was very probably catalyzed on the surface of newly developed cracks.

We further tried to substitute PHOMS by the less expensive carrier – bentonite preparing two samples in which 10 res. 90 % of poly(methyhydroxysiloxane) support were replaced by bentonite.

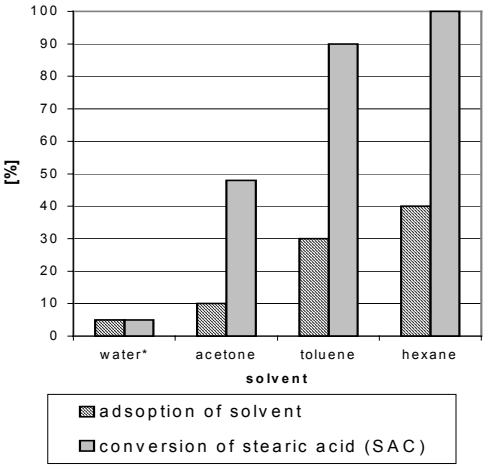

Figure 3:
The influence of solvent adsorption by PHOMS-SR biocatalyst on conversion of stearic acid in acetone, toluene and hexane. Water*- hydrolysis of canola oil; adsorption of water + canola oil emulsion

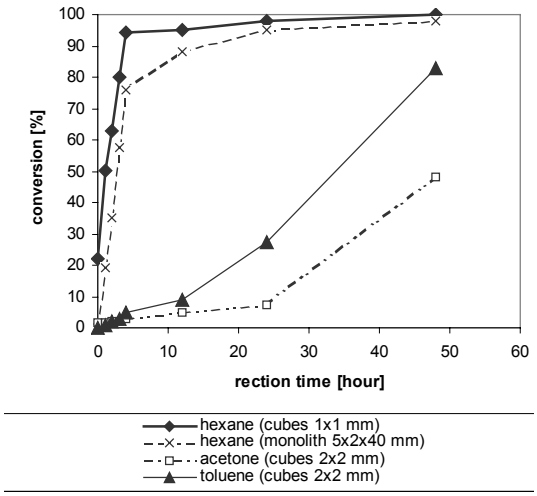

Figure 4:
Time dependence of conversion of stearic acid (SAC) catalyzed by PHOMS-SR in hexane, acetone and toluene. PHOMS-SR biocatalysts were cut into cubes 2x2 mm, 1x1 mm and monolith sheet 5x2x40mm

PHOMS-bentonite-adsorbates showed SAC higher then 80 % (48 h reaction, hexane). After encapsulation of the biocatalyst containing 10 % of bentonite, SAC decreased to 50 %, and with 90 % of bentonite it was < 10 %. Screening of cheaper carriers is under current research. After 10 recycles the decreasing of conversions of stearic acid catalyzed by PHOMS-SR biocatalysts (all prepared shapes) were < 15 %.

4 Conclusions

The two-step immobilization of lipase into silicone based polymer was first reported by Gill, 1999. In this study we report the reproducible and easily scaled-up procedure of a preparation of the biocatalyst - PHOMS-SR - which is highly active in organic solvents swelling the polymer matrix. The biocatalyst can be used as flexible several mm thick sheets without decreasing its activity as compared to a granulate. A comparison of PHOMS-adsorbate and PHOMS-SR with the biocatalyst prepared by entrapment of lipase into prepolymerized organoalkoxysilanes - one-step immobilization - showed that increasing lipase activity due to immobilization on hydrophobic surfaces can be masked by decreasing accessibility of the enzyme for reaction components.

Acknowledgements

Funding for this research was provided by the Grant Agency of the Czech Republic (grant No. 104/01/461) and by the Czech Ministry of Education Youth and PT (Programmes COST 840 and EUPRO OK368.

References

Fernandez-Lafuente R, Armisén P, Sabuquillo P, Fernandez-Lorente G and Guisan JM (1998) Immobilization of lipases by selective adsorption on hydrophobic supports. Chem Phys Lipids 93:185-197

Gill I, Pastor E, Ballesteros A (1999) Lipase-silicone biocomposites: Efficient and versatile immobilized biocatalysts. J Am Chem Soc 121(41):9487-9496

Kuncova G, Maleterova Y, Lovecka P (1994) Hydrolysis of rapeseed oil by lipase immobilized on inorganic oxide supports, Biotechnol Tech 8:535-540

Kuncova G, Guglielmi M, Dubina P and Safar B (1995) Lipase Immobilized by Sol-Gel Technique in Layers. Collec Czech Chem Commun 60(9):1573-1577

Kuncova G, Sivel M (1997) Lipase Immobilized on Organic-Inorganic Matrices. J Sol-Gel Sci Tech 8:667-671

Reetz MT, Zonta A, Simpelkamp J, Rufinska A and Tesche B (1996) Characterisation of Hydrophobic Sol-Gel Materials Containing Entrapped Lipases. J Sol-Gel Sci Tech 7:35-43

Electrostatic microencapsulation of parathyroid cells as a tool for the investigation of cell's activity after transplantation

Stefan Rosinski[1], Dorota Lewinska[1], Malgorzata Migaj[2], Bogdan Wozniewicz[2], and Andrzej Werynski[1]

Abstract

Parathyroid cells were entrapped in alginate beads using an electrostatic microcapsule generator and cultured for three weeks in a Chang medium. Microscopic analysis of cells in bead cross sections revealed that at the beginning of culturing the majority of more than 107 entrapped cells was strongly aggregated and concentrated in clusters of more than 200 cells on average. During the culture period the number of aggregates decreased and the number of small clusters increased but the total number of cells did not change significantly. Concentration of parathyroid hormone outside the beads decreased gradually from the initial value of more than 2700 ng/ml to zero during three weeks. The reasons for this behaviour and relevance of results for evaluation of the activity of transplanted parathyroid cells are currently being investigated.

Keywords: parathyroid cells, alginate beads, microencapsulation

1 Introduction

Cell microencapsulation has been done in various ways to protect transplanted cells from immune cells, antibodies and the entire immunological system of the host. In the case of postoperative parathyroid deficiency (hypoparathyroidism), considerable experience has been collected concerning the possible application of microencapsulated parathyroid tissue and cells for the medical treatment. Successful experimental rat transplantations of, e.g., parathyroid cells encapsulated in calcium alginate-poly-L-lysine-alginate capsules (Fu and Sun 1989), parathyroid tissue in barium alginate (Hasse et al. 1998), cells and tissue in multilayer polyacrylate-alginate capsules (Gaumann et al. 2001) have been reported. Normalization of calcium and parathyroid hormone (PTH) levels for two patients after allotransplantation of barium alginate microencapsulated parathyroid tissue was achieved during twelve weeks without immunosuppression (Hasse et al. 1997). On the other hand, similar but long-lasting (even over one year) effects of treatment without immuno-suppression were observed in clinics after allotransplantation of cultured and HLA class II antigen-depleted, but non-encapsulated, parathyroid cells (Tolloczko et al. 1996). Although it is a very promising approach, there are still some problems with the cell's activity because two months after transplantation it is retained in less than 40 % of recipients. Disregarding immunological reasons, this can be due to some physiological in situ problems, including limited diffusion, cells aggregation and lack of attachment to blood capillary wall. To assess the reasons for the graft (either encapsulated or not) failure it is advisable to investigate a microencapsulated cells culture as a simpler system. The topic of the actual presentation is to comment on the influence of aggregation on success or failure of parathyroid cells culture.

2 Materials and methods

2.1 Cells

Single human parathyroid cells (without tissue fragments), obtained post-operatively from a hyperparathyroidic patient, were cultured in Chang medium (Sigma, USA) in a humidified atmosphere (37°C, 5 % CO_2). A sample of cells in the medium (about 4 ml) with a concentration of $1.5x10^7$ cells/ml was collected for cell entrapment in alginate. Cells were floating freely in the culture medium without any signs of aggregation.

2.2 Microencapsulation

Concentrated cells were suspended in 1.5 ml of 1.5 % sodium alginate (Sigma, medium viscosity) in 0.9 % NaCl solution and entire cell alginate suspension was forced under gas pressure into a 1.1 % calcium chloride gellifying bath. Microencapsulation was performed using the electrostatic microcapsule generator (EMG, Figure 1) of our own construction. EMG worked in an impulse mode under the static voltage of 8000 V. Obtained alginate microbeads with entrapped parathyroid cells were carefully washed twice in 0.9 % NaCl solution and transferred to Dulbecco Minimal Essential Medium (DMEM). After one hour of incubation they were resuspeneded in Chang medium.

[1] Stefan Rosinski, Dorota Lewinska and Andrzej Werynski, Institute of Biocybernetics and Biomedical Engineering, Trojdena Str 4, 02-109 Warsaw, Poland
[2] Malgorzata Migaj and Bogdan Wozniewicz, Children Memorial Health Institute, Al.Dzieci Polskich 20, 04-736 Warsaw, Poland

Size distribution of alginate microbeads with cells was evaluated twice with the help of an crystallographic type optical microscope: in calcium chloride solution immediately after microencapsulation and after incubation in the culture medium.

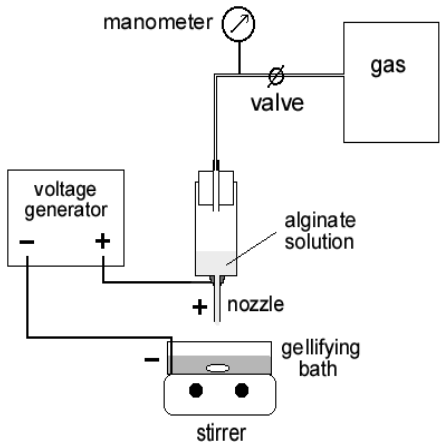

Figure 1:
Schematic diagram of electrostatic microcapsule generator

2.3 Microencapsulated cells culture

Microbeads with entrapped cells were cultured in Chang medium with the addition of human serum inside a polypropylene flask in a humidified atmosphere (37°C, 5 % CO_2) during three weeks (Figure 2).

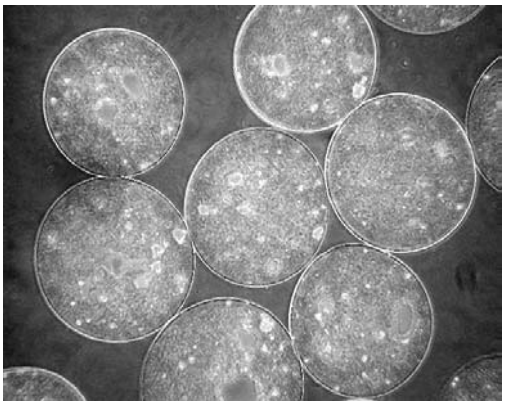

Figure 2:
Microencapsulated cells after two weeks of culture

The culture medium was exchanged every two days and samples were collected regularly during the culture period. Samples of microbeads were fixed with formaldehyde, embedded in paraffin, cut on microtome, stained in hematoxylin and eosin and examined under an optical microscope equipped with an image analysis system. Living cells in cross sections inside microbeads were counted by two methods: manually and using computer program SigmaScan Pro 5 (SPSS Science, USA) and number of cells per investigated microbead was estimated using geometrical conversion factors. Along with this, photographs of microbeads in the culture medium were analysed for cell number and distribution. PTH concentration in the samples of the culture supernatant was determined by RIA. Student t-test was used for analysis of significance of differences.

3 Results

Microbeads comprised of two fractions regarding their size: a majority was contained in the main fraction, accompanied by a small satellite fraction which contributed less than 2 % to the total volume of microbeads. In calcium chloride solution immediately after microencapsulation, the measured average diameter with standard deviation SD was 0.278 ± 0.013 mm (coefficient of variation CV, calculated as a quotient of SD and average multiplied by 100 %, was 5 %) for the main fraction and 0.070 ± 0.013 mm (18 %) for the satellite fraction (Figure 3a). After incubation of the microbeads in the culture, medium average diameters increased due to swelling to 0.415 ± 0.017 mm (4 %) and to 0.134 ± 0.021 mm (16 %) for both fractions respectively (Figure 3b).

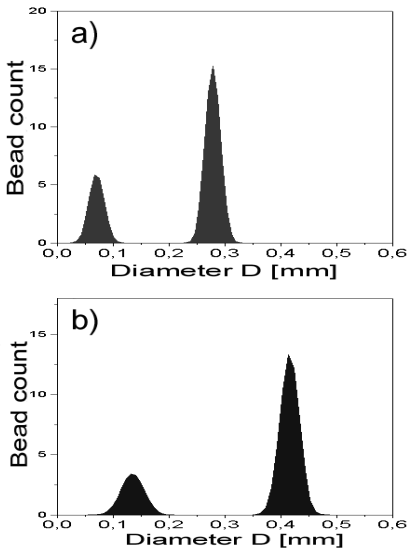

Figure 3:
Size distribution of alginate microbeads (a) in a gellifying bath after cell microencapsulation and (b) in a culture medium. Contribution of small satellite fraction exaggerated for the purpose of comparison

First of all the microscopic analysis revealed that parathyroid cells are viable and strongly aggregated inside microbeads after the microencapsulation process. For the purpose of analysis, the cells found inside microbeads were divided into three groups according to the following convention: single cells (abbreviated

Sing), small clusters of several tens (Teen, between 2 and 50) of cells and aggregates (Aggr)-big clusters of more than 50-100 cells. The number of cells in each group was counted using individual microcapsule cross sections (Figure 4) and average numbers of cells inside each of the groups were determined. This analysis was performed for both fractions of microbeads separately and in different times during the culture period. Results of analysis concerning percent contributions of the Sing, Teen and Aggr groups to the average number of cells per single microbead (taken as 100%) are presented in Figure 5.

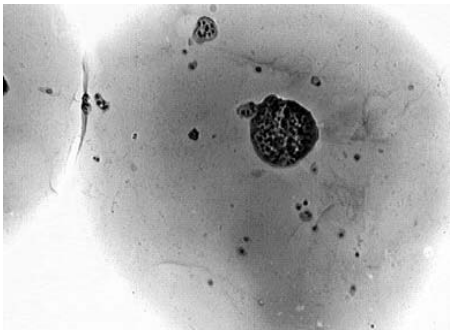

Figure 4:
Sample of microbead prepared for microscopic analysis for cell viability and distribution

Calculation of average total numbers of cells per bead (main fraction) gives the values 1190 ± 520 cells/bead at the beginning of culture and 1080 ± 460 cells/bead at the end (the difference non-significant according to Student t-test at p = 0.02). Corresponding values for the small microbead fraction are one cell on average at the beginning and 70 ± 26 cells/bead, concentrated in clusters, at the end of culture.

Concentration of PTH in the culture medium outside microbeads decreased gradually during the culture period. It was 2700 pg/ml on the 3rd day, 2590 pg/ml on the 6th day, 560 pg/ml on the 10th day, 310 pg/ml on the 13th day, 160 pg/ml on the 16th day and below the determination level on the 21st day. Cells were viable until the 21st day and after 23 days were all dead.

3 Discussion and conclusions

According to the authors knowledge, previous encapsulations of parathyroid cells and tissue were performed using air jet microencapsulation devices for droplet formation (e.g. Fu 1989; Gaumann et al. 2001; Hasse et al. 1997,1998; Kobayashi et al. 2000). In this work it was proven that one can use also the electrostatic droplet formation device for this purpose. After encountering high static voltage of 8 kV, more than 95 % of all microencapsulated cells were viable and able to produce PTH. The best proof of the proliferation ability of parathyroid cells after encapsulation is the seventy-fold increase in their number inside microbeads of small size fraction (Figure 5c and Figure 5d). Another interesting aspect of electrostatic microencapsulation is the spatial distribution of big cell

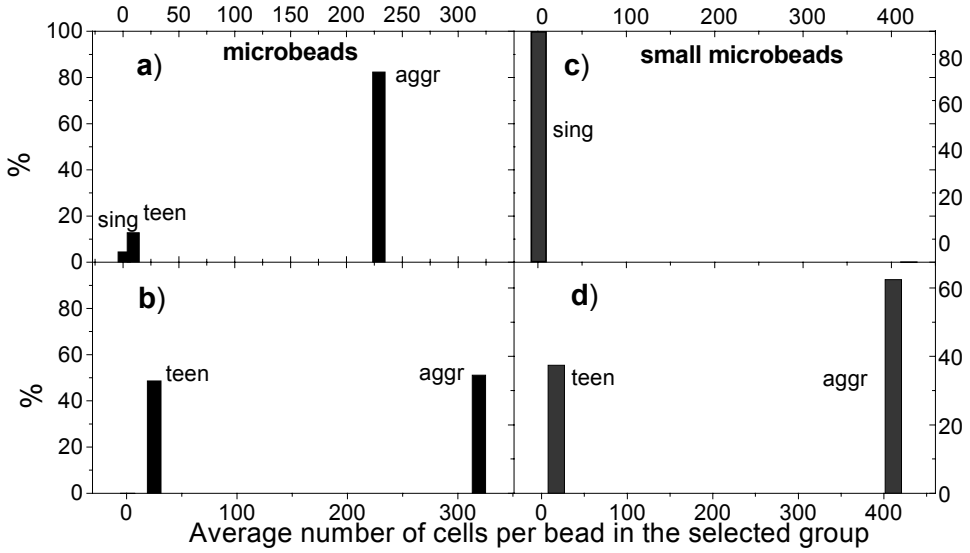

Figure 5:
Cell distribution in both fractions of microbeads. In the main fraction: at the beginning of culture (a) cells are mostly in big clusters (average number of cells 230 per bead), the minority are single cells and small clusters (average 9 per bead); at the culture end (b) number of small clusters significantly increases (with 25 inside on average) while single cells disappear and number of big clusters (with average 320 cells per bead) decreases. In small microbeads: there are only single cells at beginning (c), during culture period develop (d) small and big clusters

clusters inside microcapsules. As the detailed inspection of microbead photographs shows, they are located inside beads with no clusters penetrating the bead surface. Inclusion of cells in the microcapsule boundary is a known problem by the common air jet encapsulation of e.g. Langerhans islets.

Parathyroid cells do not leave the beads during culture, no single cells or clusters were found outside alginate beads during the culture period. This is contrary to the behaviour of, e.g., microencapsulated by the similar procedure hybridoma WEHI cells which were able to move out of beads (Lewinska et al. 2000).

It is not easy to explain the observed behaviour of microencapsulated parathyroid cells in *in vitro* cultures. Concentration of PTH decreases but the number of living cells does not. Cells can grow intensively in small microbeads as Figure 5 shows. As this is only a fraction of a few percent of the total cell number, they do not contribute significantly to the total PTH release. On the other hand, as the results show, cells in microbeads of the main fraction maintain a kind of dynamic equilibrium state and do not decrease significantly in number. There seem to be two parallel processes: intensive growth of cells in small clusters and accompanying decline of big clusters inside microbeads. On average, there are four big clusters per microbead at the beginning, and at the end there are only two. Nevertheless, one can hardly explain the decreasing level of PTH by the decrease of the total number of cells. Starting level of PTH concentration equal to 2700 pg/ml per total of 1.5 ml volume of microbeads is quite satisfactory, especially compared with the same cells encapsulated in polypropylene hollow fibers. In such experiments, the PTH level was between 53 and 59 pg/ml (Granicka et al. 2000), with $1.8x10^5$ cells in total volume of fibers equal to 47 ml (fiber outer diameter 1 mm, fiber length 1 cm). Comparing the efficiency of cells in microbeads with an estimated level of physiological PTH release per active parathyroid cell, one observes that it is about two orders of magnitude lower.

One possible reason for the observed cell behaviour could be that parathyroid cells really “do not like” to exist in clusters and big aggregates. Interestingly enough there are examples of failures of in vitro cultures in the case of encapsulation of tissue fragments. Gradual decrease of the PTH concentration over three weeks was noted for human parathyroid tissue in carrageenan capsules complexed with phenyl-ethylene derivatives (Kobayashi et al. 2000). Another group (Gaumann et al. 2001) observed much better functioning of encapsulated single parathyroid cells than tissue fragments. Further experiments are planned to see how a better dispersion of cells in an encapsulation matrix influences the results. Another goal is to gain more insight into the possibility of undesired interactions between the encapsulation matrix, cells and medium.

Acknowledgements

This work was partially supported by research grant 4 P05C 003 15 from Polish State Committee for Scientific Research for Children Memorial Health Institute

References

Fu XW, Sun AM (1989) Microencapsulated parathyroid cells as a bioartificial parathyroid. In vivo studies. Transplantation 47(3):423-425

Gaumann A, Laudes M, Jacob R, Pommersheim R, Laur C, Vogt W, Schrezenheimer J (2001) Xenotransplantation of parathyroids in rats using barium-alginate and polyacrylic acid multilayer microcapsules. Exp Toxic Pathol 53:35-43

Granicka LH, Migaj M, Wozniewicz B, Zawitkowska T, Tolloczko T, Werynski A, Kawiak J (2000) Encapsulation of parathyroid cells in hollow fibers: a preliminary report. Folia Histochem Cytobiol 38(3):129-131

Hasse C, Kloeck G, Schlosser A, Zimmermann U, Rothmund M (1997) Parathyroid allotransplantation without immunosuppression. Lancet 350:1296-1297

Hasse C, Zielke A, Kloeck G, Schlosser A, Barth P, Zimmermann U, Sitter H, Lorenz W, Rothmund M (1998) Amitogenic alginates: key to first clinical application of microencapsulation.. World Journal of Surgery 22(7):659-665

Kobayashi S, Amano J, Minoru F, Kazuhiko A, Shingu K, Itoh K, Hama Y, Takemoto M, Iwasaki T, Teramoto A, Abe K (2000) Microencapsulated parathyroid tissue in vitro. Biomed Pharmacother 54 supp.1:66-68

Lewinska D, Rosinski S, Granicka L, Kawiak J,. Bukowski, J, Werynski A (2000) Influence of electrostatic encapsulation process on viability of WEHI cells. Int Journal of Artif Organs 23(8):583

Tolloczko T, Wozniewicz B, Gorski A, Sawicki A, Nawrot I, Migaj M, Zawitkowska T (1996) Cultured parathyroid cells allotransplantation without immunosuppression for treatment of intractable hypoparathyroidism. Annals of Transplantation 1(1):51-53

Comparison of different encapsulation strategies for living cells and mechanical characterization of microspheres by scanning acoustic microscopy

Christian Schwinger[1], Albrecht Klemenz[2], Kay Raum[2], and Jörg Kressler[1]

Abstract

Microencapsulation is a novel strategy for immobilization and immunoprotection of cells where microcapsules are used for long term production of recombinant proteins, hormones, and growth factors in culture or in vivo.

The focus of this study was the comparison of three different strategies for the production of calcium cross-linked alginate beads of a small size (< 350 mm) to immobilized and immunoprotected mammalian cells. The following strategies for bead production have been used, a) the AirJet technology (coaxial gas flow extrusion), b) the vibrating nozzle technology, and c) the JetCutter technology and for the successful immunoprotection of the cells were used the established alginate/poly-L-lysine/alginate complexation as the polymeric system.

It was shown that all three methods may be used for production of homogeneous beads with a diameter < 350 mm. While the vibrating nozzle technique was limited to an alginate viscosity of 0.2 Pa·s or less, the AirJet and JetCutter technology were less sensitive to higher viscosities. Optimum parameters for production of beads with specific characteristics were defined for the three methods.

In conclusion, this study describes optimized methods for alginate microencapsulation of genetically modified mammalian cells, which may be used for treatment of human diseases *in vivo*.

High frequency Scanning Acoustic Microscopy is used for mechanical characterization of the microspheres as well as for investigation of surface properties. The mechano-elastical properties are measured in terms of acoustic impedance. Additionally, 2- and 3D images show the surface of the microspheres with a spatial resolution of 1.5 µm. Mechanical stiffness is obtained from bulk measurements of acoustic velocity and mass density.

Keywords: alginate, microcapsule, AirJet, vibrating nozzle, JetCutter, viscosity, scanning acoustic microscopy, acoustic impedance

1 Introduction

Microencapsulation is a procedure where materials, such as enzymes, bacteria, yeast, or eucaryotic cells are enclosed within microscopic, semipermeable containers. Microencapsulation of mammalian cells is a novel and versatile means of delivering therapeutically important natural or recombinant molecules *in vivo*. It can also have numerous applications as a platform for gene therapy of metabolic or neurological disorders and cancer (Vallbacka et al. 2001, Lohr et al. 2001). Most of the previous work done on encapsulation of transgenic mammalian cells was concentrated on protection against the immune response of the host and on minimizing local inflammatory reactions generated by the microcapsules (Kulseng et al. 1999, Sakai et al. 2000). However, encapsulation techniques additionally are limited by physical factors, e. g. viscosity of the biopolymer solution, size distribution, or mechanical strength of the produced microcapsules. With the prevalent methods for bead formation, such as vibrating nozzles, gas jet droplet generators or laminar jet break-up, rather low-concentrated alginate solutions can be employed (Klock et al. 1997). In addition, beads with a small diameter (< 300 mm) are more difficult to produce than those with a larger diameter (> 500 mm) although smaller microcapsules may have several advantages, such as better oxygenation of encapsulated cells, smaller implant volume, and easier application to organs *in vivo* (De Vos et al. 1996, Robitaille et al. 1999).

A serious disadvantage of low viscosity alginate solutions is the lack of mechanical stability of the alginate hydrogel which is formed by cross-linking of the alginate molecules with polyvalent cations (Peirone et al. 1998). Therefore, covering solid beads with outer alginate layers and protective polycationic shells resulting in alginate-poly-L-lysine-alginate (APA) microcapsules, or the use of Ba^{2+}- instead of Ca^{2+}-alginate has been suggested for improving the mechanical stability of hollow core microcapsules (Thu et al. 1996a and b, Gaumann et al. 2001).

The purpose of this study is to evaluate the physical properties of alginate microcapsules produced by

[1] Christian Schwinger and Jörg Kressler, Institute of Bioengineering, Department of Engineering Science, Martin-Luther-University Halle-Wittenberg, 06097 Halle, Germany

[2] Albrecht Klemenz and Kay Raum, Institute of Medical Physics and Biophysics, Department of Medicine, Martin-Luther-University Halle-Wittenberg, 06097 Halle, Germany

three different methods, shown in Figure 1, laminar gas flow (AirJet), vibrating nozzle, and JetCutter with the aim of optimizing the production of small size (< 350 µm) microcapsules suitable for biomedical applications in humans, and to investigate the proliferation of normal, neoplastic, or transgenic cells in these granules.

High-frequency Scanning Acoustic Microscopy (SAM) was used for investigation of mechanical properties in terms of acoustic impedance and 3D-surface topography of full alginate microspheres (diameter: 350 µm). Mean surface impedance was measured with SAM at 900 MHz with a spatial resolution of 1.5 µm. The sensitivity and reproducibility of SAM had to be increased considerably to receive and quantify signals in the very low impedance region. A multi layer analysis method was developed to get quantitative data with SAM at a microscopic level. 3D images show details of structure and surface topography.

The mechanical stiffness c_{11} was obtained from mass density and longitudinal ultrasound velocity, measured with a pulse echo method at 6 MHz.

2 Materials and methods

2.1 Encapsulation materials

Sodium alginate powder was obtained from Inotech AG (Dottikon, Switzerland) and from Fluka (Buchs, Switzerland). Preparation and further dilution of all alginate solutions was done with *aqua dest.* All alginates as well as a 0.1 % (w/v) poly-L-lysine solution (PLL; M_W 25.700 g/mol; Sigma) were sterilized by filtration through a 0.22 µm filter (Merck), and stored at 4°C. The MOPS buffer used for rinsing the microcapsules between single encapsulation steps consisted of 10 mM MOPS (ICN Biomedicals, Eschwege, Germany) and 0.85 % (w/v) NaCl (pH = 7.3). Calcium chloride (ICN Biomedicals, Eschwege, Germany) was dissolved in 10 mM MOPS to 100 mM concentration. Trisodium citrate (Merck Eurolab) was dissolved with 10 mM MOPS and 0.45 % (w/v) NaCl to 50 mM concentration. The solutions were adjusted to pH 7.4, sterilized by autoclaving, and stored at room temperature.

2.2 Viscosity measurements

The zero shear viscosity of the described alginates, with the solution range between 1.0 and 2.0 % (w/v), was determined by a temperature of 20°C with a CSL 100 - Rotational Rheometer from Carri-Med (Düsseldorf, Germany) with a cone-plate measuring system (cone diameter 60 mm, angle 2°, gap 57 µm).

2.3 Cell line and culture

The murine fibroblast cell line GLI 328 (PA317; Rainov 2000, Ram et al. 1997) used in this study was from Dr. E. Otto, GTI Inc., Gaithersburg, MD. It was maintained in DMEM with 1 g/L glucose (Biochrom KG, Berlin, Germany) with addition of 10 % (w/v) donor calf serum (CS; Gibco BRL Life Technologies, Karlsruhe, Germany) and 1 % penicillin/streptomycin (Gibco BRL) at 37°C in humid atmosphere containing 5 % (v/v) CO_2.

2.4 Encapsulation methods and procedure

Three methods for preparing alginate microcapsules are shown in Figure 1. The AirJet (A) apparatus was self-made and was described elsewhere (Prokop et al. 1998, Schwinger et al. 2001, Wolters et al. 1992). The vibrating nozzle apparatus was from Inotech AG (Dottikon, Switzerland; Inotech 2001) and the JetCutter system (Prüsse et al. 2000), was from geniaLab GmbH (Braunschweig, Germany).

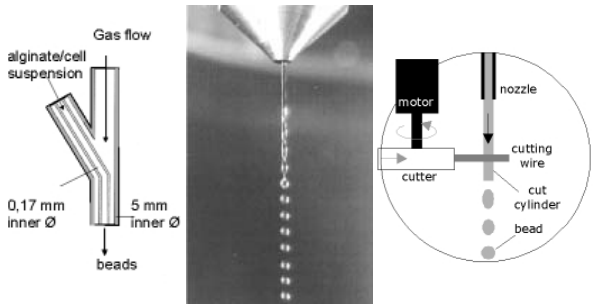

Figure 1:
Left: Principle of AirJet method, middle: Vibrating nozzle, right: Principle of the JetCutter

Microspheres from alginate type Fluka 71238 were produced by the AirJet and the JetCutter method with a concentration of 1.5 (w/v). For the vibrating nozzle method 1.5 % (w/v) sodium alginate from Inotech was used. 8 ml of a suspension with 2.0 x 10^6 GLI 328 cells/ml were added to all alginate solutions. The JetCutter and the AirJet systems were placed in a class two clean bench to allow bead production under semi sterile conditions The vibrating nozzle system was operated under sterile GMP conditions. The droplets were collected in 200 ml sterile calcium chloride solution (100 mM) containing 10 mM MOPS buffer.

2.5 Post-processing of alginate beads

Beads were separated from the collection bath by sieving. Subsequent formation of outer layers was carried out according to a simplified alginate-poly-L-

lysine-alginate (APA) protocol (Lim and Sun 1980). In brief, the beads were incubated in 0.1 % (w/v) poly-L-lysine (PLL) for 10 min and then washed twice with 10 mM MOPS buffer. An outer layer of alginate was formed by incubation for 10 min in a 0.03 % (w/v) alginate solution, and followed by washing with MOPS. The alginate core was then dissolved with trisodium-citrate buffer for 30 min, and capsules were washed once with MOPS. At the end of the encapsulation procedure, the microcapsules were transferred to standard culture medium in 75 cm^2 tissue culture flasks (Biochrom KG). The medium was changed weekly.

2.6 Scanning Acoustic Microscopy

The acoustic microscope SAM 2000 (Kraemer Scientific Instruments, Herborn, Germany) with a broadband lens (0.8 - 1.3 GHz, 100° aperture angle) was operated at 900 MHz. It works in burst mode. The principle has been described elsewhere (Lemons and Quate 1974). Distilled and degassed water was used as coupling fluid. This provides a lateral resolution of 1.5 µm at the applied frequency.

The contrast of SAM primarily depends on the ultrasound reflection of the insonified region, which is related to the angle of incidence and the acoustic impedances of the coupling fluid and the specimen, respectively. In focal position all incident waves have no phase differences and the resulting wave can be considered as plane. Then the signal amplitude is determined by the angle-dependent reflectance function. At normal incidence this function simplifies to the reflection factor r (Briggs 1992):

$$r = \frac{p_r}{p_0} = \frac{Z_m - Z_w}{Z_m + Z_w} \qquad (1)$$

p_r and p_0 are the reflected and incident pressure amplitudes, Z_m and Z_w are the impedances of the specimen (microsphere) and the coupling fluid (water), respectively.

The focal distance of the lens is 40 µm. During scanning of the lens, the microspheres under investigation were moving too, caused by shear forces in the coupling fluid. Therefore the spheres were fixed right at their bottoms in an agarose matrix (2.0 % (w/v) agarose in aqua dest.). Because of high attenuation, GHz-ultrasound penetrates alginate by only a few microns (Gracewski et al. 1988, Daft et al. 1989) so that the reflected signals represent surface properties. Additionally, device and environmental parameters must be considered for quantitative data analysis. Since attenuation and sound velocity are strongly temperature dependent, all measurements were performed in a temperature controlled water tank at 25.0 ± 0.1°C and at constant room temperature. Signal drifts were eliminated by temperature stabilization of the electronic circuitry.

For every alginate concentration a total of 15 microspheres were investigated and mean values and standard deviations calculated.

2.7 Bulk Method

Acoustic velocity and bulk density were measured to estimate the mechanical stiffness. Alginate concentration varied from 1.0 to 2.0 % (w/v) in steps of 0.25.

2.8 Acoustic velocity

The bulk longitudinal wave velocity was estimated with a pulse-echo method. A total of 30 cylinders (6 per concentration step) were investigated and the sound velocity was measured at 3 positions per cylinder. The alginate sample was placed in a water tank on a plain polished steel reflector. The transducer (diameter: 5 mm) was set normally to the reflector on the top of the alginate sample and the pulse runtime tp1 between transducer and reflector was estimated with a digital oscilloscope (LeCroy 9430). Then the transducer was shifted down by a definite but small z-distance. Since at small deformations alginate is elastic, no significant change in density is expected. t_{p2} is measured and the longitudinal wave velocity c_l is calculated from:

$$c_l = \frac{2z}{t_{p1} - t_{p2}} \qquad (2)$$

Assuming alginate to be isotropic, the elastic stiffness in longitudinal direction c_{11} is (Zimmermann et al. 1990):

$$c_{11} = \rho c_l^2 = Z c_l \qquad (3)$$

3 Results and Discussion

3.1 Viscosity of alginate

Owing to the fact that the shear field in nozzles is very high, it can be assumed that the tailoring of viscosity is extremely important for the successful application of different microencapsulation techniques.

In Figure 2 can be seen, that there are significant differences between the zero shear viscosity of the two investigated alginate types and that the differences have serious implications on the flow behaviour of the solutions. As an example, the viscosity of algi-

nate from Inotech remains below 0.2 Pa·s even at a concentration of 2.0 % (w/v) and the viscosity of alginate from Fluka at 2.0 % (w/v) increases to a value of more than 1.6 Pa·s.

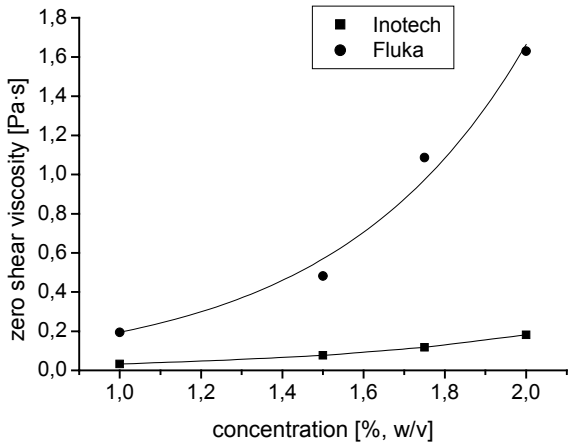

Figure 2:
Zero shear viscosity as a function of alginate concentration for the two different species

3.2 Bead Size of the different encapsulation strategies

3.2.1 AirJet method

This method was refined for producing microcapsules smaller than 450 µm, because these capsules have an optimal secretion kinetics of insulin (Chicheportiche and Resch 1988). The size distribution of the produced microcapsules is shown in Figure 3.

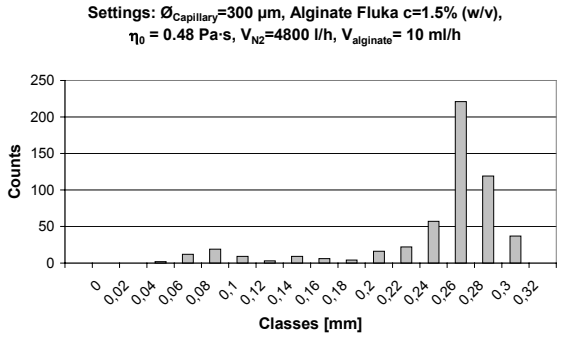

Figure 3:
Size distribution with optimal settings of the AirJet apparatus

The particle diameter and the arising size distribution are not only dependent on the volume flow of alginate and gas and the viscosity of the alginate. In this study a significant influence of the outer diameter of the capillary on the size distribution was found. It can be shown that under laminar gas flow conditions a monodisperse distribution only can be obtained if the capsule size is smaller then the diameter of the capillary. The optimal parameter settings of the AirJet apparatus are shown in the Figure 3 and Figure 1.

3.2.2 Vibrating nozzle method

The microcapsules are very homogeneous in size, as shown in Figure 4, together with the optimal settings. The disadvantage of the vibrating nozzle method is the strong dependence on the viscosity. In this study alginate solutions were capable with a very low zero shear viscosity, e. g. solutions from the Inotech alginate with a range of the zero shear viscosity between 0.08 and 0.18 Pa·s for concentrations between 1.00 and 2.00 % (w/v).

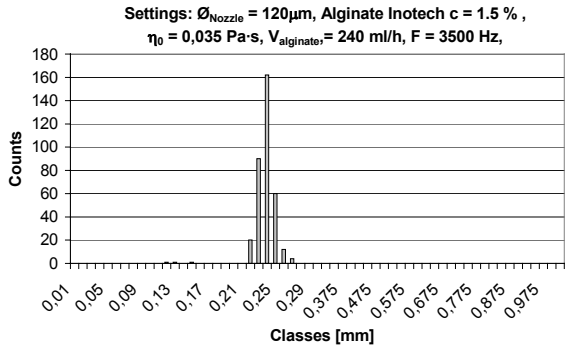

Figure 4:
Size distribution with optimal settings of the vibrating nozzle apparatus

3.2.3 JetCutter method

Beads produced with the JetCutter method with settings as shown in Figure 5 are also uniform in size.

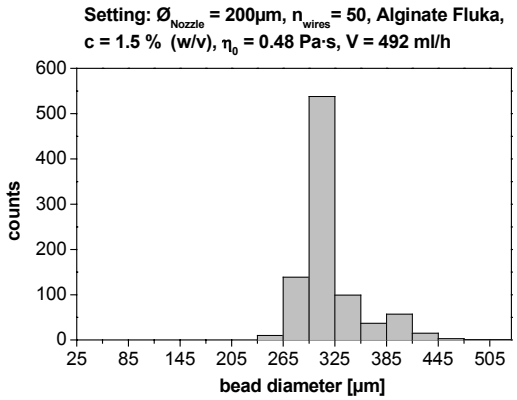

Figure 5:
Capsule size distribution and optimal parameters of the JetCutter

Beads were used for the determination of size distribution. More than 60 % of the beads were within a range of 295 to 325 µm in diameter, and only 1 % are

smaller than 265 µm. Larger beads are probably caused by collision and coalescence of falling droplets. As an example, two merging beads of 320 µm result in one bead of 400 µm diameter which possibly may explain the relatively high percentage of this fraction.

3.3 Cell growth after encapsulation

After encapsulation of the cells by the different strategies, the cell growth shows a similar behaviour. After one day, the cells formed a compact aggregate in the middle of the capsule. After approximately one week a significant cell growth can be seen and after four weeks the cells fill the whole capsule, as shown in Figure 6.

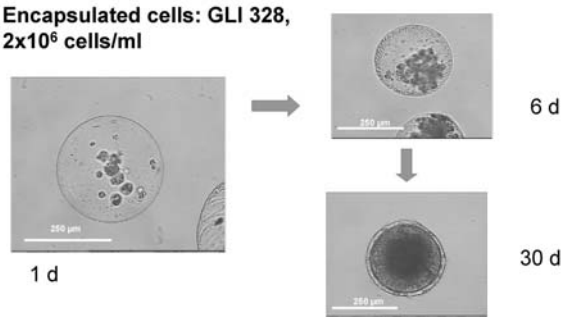

Figure 6:
Cell growth in a period of 30 days after encapsulation

3.4 Scanning Acoustic Microscopy

Figure 7 left shows the impedance image of an alginate sphere (1.5 % (w/v)) as plane projection of the reflected ultrasound signals. The concentric steps represent the z-increment of the scans. The surface of the sphere is not ideally smooth. It contains some depressions and elevations. Local changes of grey level represent inhomogeneities in the membrane structure. The bright dots are microbubbles of air that adhere on the surface. The real diameter of the sphere is 300 µm. To show the entire sphere is not possible because of the inclination of the surface: with increasing angle of incidence, fewer signals are reflected back to the transducer and the signal amplitude decreases more and more down to the noise level.

The topography profile in Figure 7 right along the dotted line in Figure 7 left indicates that the z-distance from the center to the margin of the registered part of the sphere is 15 µm. Figure 8 shows the 3D image of the sphere.

The results of the impedance measurements in dependence of alginate concentration are shown in Figure 9.

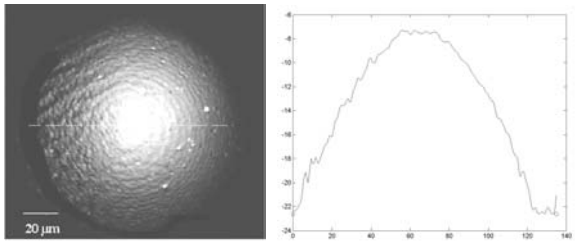

Figure 7:
Left: 2D-picture of an alginate sphere, right: Topography profile along the dotted line in left part of the figure

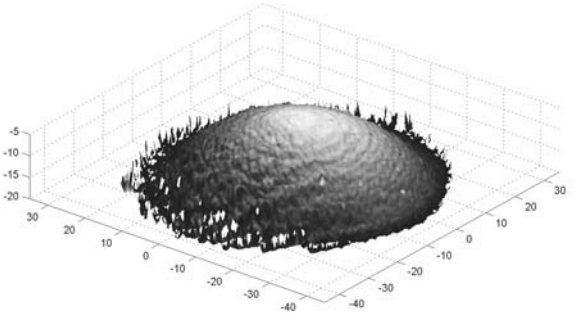

Figure 8:
3D image of the top of an alginate microsphere. Structural analysis shows surface inhomogeneities and topographical details

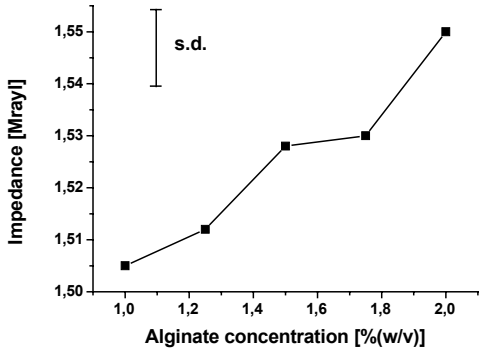

Figure 9:
Impedance versus concentration of alginate microspheres. Results from SAM

Table 1:
Densities and longitudinal sound velocities of alginate specimens, conc. = concentration

Alginate conc., % (w/v)	Density, g/cm³	Sound velocity x 10^3, m/s
1.0	1.0110 ± 0.0003	1.4916 ± 0.0095
1.25	1.0113	1.4978
1.5	1.0114	1.5006
1.75	1.0123	1.5094
2.0	1.0142	1.5284

3.5 Bulk method

The measured densities and longitudinal sound velocities are presented in Table 1. The stiffness data of alginate samples are shown in Figure 10.

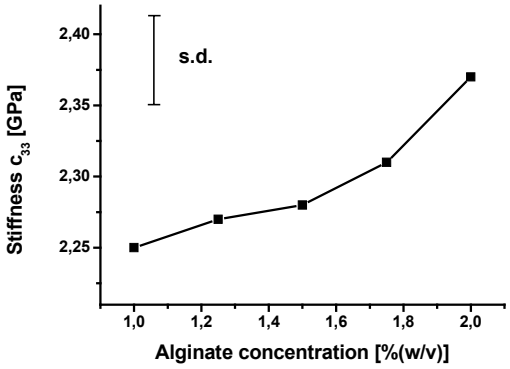

Figure 10:
Mechanical stiffness of alginate samples. Data are measured with the bulk method (see text)

4 Conclusions

The results demonstrate that a custom made encapsulation AirJet device is well suitable for alginate encapsulation of mammalian cells and that it is comparable with a commercially available vibrating nozzle device (IEM-40, Inotech AG). Both encapsulation methods show the feasibility of generating uniform alginate microbeads for APA microcapsules.

The vibrating nozzle method is one of the most frequently used methods for large scale production of microbeads. It requires low viscosity of the biopolymer, however. Extrusion by coaxial gas flow (AirJet) is less sensitive against high viscosity polymers, but has a low throughput. It is therefore suitable for experimental purposes, but not for large scale production of microcapsules.

The JetCutter technology also seems to be appropriate for alginate encapsulation of living mammalian cells. Small alginate beads (320 µm) containing viable cells could be produced at a very high throughput. The encapsulated murine fibroblasts formed colonies and proliferated at a considerable rate, which indicates that the mechanical stress during the encapsulation procedure is well tolerated and does not irreversibly damage the cells.

Sterilisation or autoclaving of the parts of the JetCutter being in contact with the alginate-cell suspension, usage of sterile working solutions, and placement of the whole set-up in a clean bench may prevent contamination of the cultured beads and allow for microcapsule mass production under GMP conditions.

Another important aspect is the mechanical stability of the beads. One possible and rather straightforward approach is to increase the polymer content of the hydrogel, e. g. to use higher concentrated alginate solutions (2 to 5 %). At present the JetCutter is the only technology that is able to process alginate at such concentrations.

Scanning Acoustic Microscopy is a suitable and sensitive tool for measuring elasto-mechanical properties of alginate specimens in terms of quantitative acoustic impedance. Measurements on different concentrations of alginate are presented. The alginate spheres are investigated in their presumed environment, i.e. water. There is no further preparation required that could possibly change mechanical properties, as for electron microscopic methods. The topography of the surface as well as detailed structural information with a resolution of 1.5 µm can be obtained. The latter can be helpful for detailed studies of the surface inhomogeneities caused by material and by topography as well as for the optimization of the production process of the spheres.

Bulk mechanical stiffness is estimated with low frequency ultrasound.

However, SAM is not only able to provide information on surface impedance of full microspheres but it also has the potential of investigating the elastic properties of capsule membranes. Because the SAM can be applied with both low- and high-frequency ultrasound, there are measurements at different stages of spatial resolution possible, beginning from bulk up to high resolution surface measurements.

Acknowledgements

The authors thank S. Koch and Ph.D. N. Rainov for the cultivation of cells and immobilized cells. Additionally we thank for the technical support and discussions of this work.

References

Briggs A (1992) Acoustic Microscopy. Oxford: Clarendon Press

Gracewski SM, Waag RC, Schenk EA (1988) High-frequency attenuation measurements using an acoustic microscope. J Acoust Soc Am 83:2405-2409

Chicheportiche D, Resch G (1988) In vitro kinetics of insulin release by microencapsulated rat islets: effect of the size of the microcapsules. Diabetologia 31:54-57

Daft CMW, Briggs GAD, O'Brien Jr WD (1989) Frequency dependence of tissue attenuation measured by acoustic microscopy. J Acoust So. Am 85:2194-2201

De Vos P, De Haan B, Pater J, Van Schilfgaarde R (1996) Association between capsule diameter, adequacy of encapsulation, and survival of microencapsulated rat islet allografts. Transplantation 62(7):893-899

Gaumann A, Laudes M, Jacob B, Pommersheim R, Laue C, Vogt W, Schrezenmeir J (2001) Xenotransplantation of parathyroids

in rats using barium-alginate and polyacrylic acid multilayer microcapsules. Exp Toxicol Pathol 53(1):35-43

Inotech (2001): www.inotech.ch/products.htm

Klock G, Pfeffermann A, Ryser C, Grohn P, Kuttler B, Hahn HJ, Zimmermann U (1997) Biocompatibility of mannuronic acid-rich alginates. Biomaterials 18(10):707-13

Kulseng B, Skjak-Braek G, Ryan L, Andersson A, King A, Faxvaag A, Espevik T (1999) Transplantation of alginate microcapsules: generation of antibodies against alginates and encapsulated porcine islet-like cell clusters. Transplantation 67(7): 978-984

Lemons RA, Quate CF (1974) Acoustic microscope-scanning version. Appl Phys Lett 24:163-165

Lim F, Sun AM (1980) Microencapsulated islets as a bioartificial pancreas. Science 210:908-910

Lohr M, Hoffmeyer A, Kroger J, Freund M, Hain J, Holle A, Karle P, Knofel WT, Liebe S, Muller P, Nizze H, Renner M, Saller RM, Wagner T, Hauenstein K, Gunzburg WH, Salmons B (2001) Microencapsulated cell-mediated treatment of inoperable pancreatic carcinoma. Lancet 357(9268):1591-1592

Peirone M, Ross CJ, Hortelano G, Brash JL, Chang PL (1998) Encapsulation of various recombinant mammalian cell types in different alginate microcapsules. J Biomed Mater Res 42(4):587-596

Prokop A, Hunkeler D, DiMari S, Haralson MA, Wang TG (1998) Water soluble polymers for immunoisolation I. Advances in Polymer Science 136:1

Prüsse U, Dalluhn J, Breford J, Vorlop K D (2000) Production of spherical beads by JetCutting. Chem Eng Technol 23:1105-1110

Rainov NG (2000) on behalf of the GLI328 International Study Group: A Phase III clinical evaluation of herpes simplex virus type 1 thymidine kinase and ganciclovir gene therapy as an adjuvant to surgical resection and radiation in adults with previously untreated glioblastoma multiforme. Hum Gene Ther 11:2389-2401

Ram Z, Culver KW, Oshiro EM, Viola JJ, DeVroom HL, Otto E, Long Z, Chiang Y, McGarrity GJ, Muul LM, Katz D, Blaese RM, Oldfield EH (1997) Therapy of malignant brain tumors by intratumoral implantation of retroviral vector-producing cells. Nat Med 3:1354-1361

Robitaille R, Pariseau JF, Leblond FA, Lamoureux M, Lepage Y, Halle JP (1999) Studies on small (< 350 mm) alginate-poly-L-lysine microcapsules. III. Biocompatibility of smaller versus standard microcapsules. J Biomed Mater Res 44(1):116-120

Sakai S, Ono T, Ijima H, Kawakami K (2000) Control of molecular weight cut-off for immunoisolation by multilayering glycol chitosan-alginate polyion complex on alginate-based microcapsules. J Microencapsulation 17(6):691-699

Schwinger Chr, Kressler J, Koch S, Rainov N, Klemenz A (2001) Strategies for encapsulation of living cells with polymeric systems - microencapsulation. Proc ACS, PMSE 84:894

Thu B, Bruheim P, Espevik T, Smidsrod O, Soon-Shiong P, Skjak-Braek G (1996a) Alginate polycation microcapsules. I. Interaction between alginate and polycation. Biomaterials 17(10): 1031-1040

Thu B, Bruheim P, Espevik T, Smidsrod O, Soon-Shiong P, Skjak-Braek G (1996b) Alginate polycation microcapsules. II. Some functional properties. Biomaterials 17(11):1069-1079

Vallbacka JJ, Nobrega JN, Sefton MV (2001) Tissue engineering as a platform for controlled release of therapeutic agents: implantation of microencapsulated dopamine producing cells in the brains of rats. J Control Release 72(1-3):93-100

Wolters GHU, Fritschy WM, Gerrits D, van Schilfgaarde RJ (1992) A versatile alginate droplet generator applicable for microencapsulation of pancreatic islets. J Appl Biomat 3:281-286

Zimmermann MC, Meunier A, Katz JL, Christel P (1990) The evaluation of cortical bone remodeling with a new ultrasonic technique. IEEE Trans Biomed Eng 37:433-441

Downstream processing of microcapsules: Quality control of capsule morphology, permeability and mechanical properties as a function of raw material endotoxin levels

David Hunkeler[1], Christine Wandrey[2], Ion Ceausoglu[2], Dianelys Sainz Vidal[2], and David Espinosa[2]

Abstract

The large-scale production of microcapsules with defined membrane thickness and permeabilities, both decoupled from the mechanical resistance, is demonstrated. Specifically, a novel apparatus, which controls the downstream part of the microencapsulation process has been developed. The oscillating reactor system permits the formation of capsules with controlled membranes based on pre-cast microbeads. The precise manipulation of the reaction time, and its distribution, between polyanion beads and the cationic receiving bath has been found to be critical. Given this, microcapsule diameters can be produced within ± 10 %, both within and between batches. The membrane thickness can also be controlled to a tolerance of ± 5 micrometers. The Automatic Reaction Control has been tested on polysaccharide blends of alginate and cellulose sulfate, and found to produce identical capsules, independent of the endotoxin level of the biomaterial. When this is combined with the demonstration that alginate and cellulose sulfate can be depyrogenated to fractions of the limit imposed by the FDA, the novel technology enables, for the first time, the production of clinical quantities of sterile microcapsules suitable for transplantation. The downstream control of microcapsule reaction parameters can be coupled with any front-end system for bead generation, based on air-stripping, electrostatics or jet cutting. It is demonstrated on the former, using calcium and poly(methylene-co-guanidine) hydrochloride as the cations.

Keywords: Alginate, bioartificial pancreas, cellulose sulfate, endotoxin, microencapsulation

1 Introduction

The transplantation of encapsulated cells for therapies aimed at the treatment of hormone deficient and neuro-degenerative diseases, such as type I diabetes, Alzheimer's and Parkinson's, have been the topic of extensive research over the past two decades. Following the pioneering work on the bio-artificial pancreas (Lim and Sun, 1980), significant attention has been devoted to the pairing of transplant site with a biocompatible capsule with the appropriate morphology and permeability (Schuldt and Hunkeler, 2000), as well as the centering of the cells within the microcapsules of the more commonly applied microbeads. However, the production of immuno-isolated cells, or bio-artificial organs, under clinically relevant conditions has not been addressed. Furthermore, despite the advances in the depyrogenation of polysaccharides such as alginate on a small scale using multi-step procedures (Klock et al., 1994), the method has yet to be scaled up or generalized to other polyanions.

Microencapsulation technologies are generally categorized into the means by which the droplet is produced, with air stripping, vibrating nozzles and electrostatics the most common methods (Hunkeler, 1997). While these techniques can yield excellent sphericity and control of bead size, with polydispersities as low as 3% for the air and vibration-based methods, there has been little work on the control of membrane properties. Given that membrane growth is a function of microcapsule size, and that membrane thickness correlates with reduced diffusion, the control of downstream process conditions is essential if the diffusional characteristics of the microcapsule are to be tuned to a specific application (Stegemann and Sefton, 1996).

This paper summarizes work on the development of a large-scale, by medical standards, downstream encapsulation device, which can control the microcapsule reaction conditions. It will be demonstrated that the membrane characteristics can be concomitantly regulated with the microcapsule morphology. The technique will be shown to be applicable to depyrogenated polysaccharides without any loss in performance of the microcapsule. A scaled-up method for the endotoxin reduction of alginate, and cellulose sulfate, will also be highlighted.

[1] David Hunkeler, AQUA+TECH Specialties, 4 Chemin du Chalet du Bac, 1283 La Plaine, Geneva, CP 117, Switzerland

[2] Christine Wandrey, Ion Ceausoglu, Dianelys Sainz Vidal, and David Espinosa, Laboratory of Polyelectrolytes and BioMacromolecules, Swiss Federal Institute of Technology, 1015 Lausanne, Switzerland

2 Experimental

2.1 Materials and purification

Sodium alginate (SA) (Keltone HV Kelco/NutraSweet, San Diego, CA, USA) and sodium cellulose sulfate (SCS) (Across Organics, Geel, Belgium) were employed as polyanions. The polycation poly(methylene-co-guanidine) hydrochloride (PMCG) was purchased as 35 % aqueous solution from Scientific Polymer Products, Inc. (Ontario, NY, USA).

SA and SCS were dissolved in highly purified deionized water from a Milli-Q PF water purification system (Millipore, Switzerland). The solutions, having concentrations of 1.5 % (SA) and 2 % (SCS), were successively filtered through filters with decreasing pore size in the range 30 to 0.22 mm. The filtration was followed by precipitation in solvent/non-solvent mixtures, polymer isolation, and drying (patent pending). The endotoxin content was determined by a standard kinetic turbidimetric method (LAL-5000 Series 2), and as recommended by the new FDA guidance (FDA, 1987). Each test was performed in duplicate.

2.2 Polymer solutions

All solutions were prepared, one day prior to encapsulation, with purified water with a resistance greater than 18 Mohm·cm from the Millipore model Milli-Q (Volketswil, Switzerland). A 0.22 mm cellulose acetate membrane was used to filter solutions of unpurified polymers with an applied pressure of 5 bars. The membranes (from Winiger ref. C26027) were autoclaved with the entire air pressure system to ensure sterility. Volumes up to 50 mL were filtered using the sterile vacuum-based devices from Schleicher&Schuell (ref. 443401). For experiments requiring less than 5 mL of solution Schleicher&Schuell filters (ref. 462200) were also employed. The stock NaCl, PBS and $CaCl_2$ solutions (Fluka, Buchs, Switzerland) were "Bio" labelled (green top). Depyrogenated polymers were stored in solution, at 10 °C, and applied after warming to room temperature without further modification.

Alginate/cellulose sulphate/poly(methylene-co-guanidine) hydrochloride/calcium chloride (Alg/CS// $CaCl_2$/PMCG) microcapsules (diameter 400 µm) were produced in a two-stage procedure, which comprised the formation of calcium/polyanion beads, followed by a membrane generation stage where the beads are suspended in a solution of polycation (in our case PMCG). A polyanion solution containing 0.6 % Alg and 0.6 % CS in 0.9 % NaCl, was employed for bead formation, with a gelation batch consisting of 1.5 % $CaCl_2$ in 0.9 % NaCl. The PMCG concentration in the reacting solution was 1.2 %. All solutions, as well as the equipment, were sterilised by filtration or autoclaving prior to use and the capsule production unit was placed inside a laminar flow hood, during sterile production.

2.3 Droplet generation

Droplet formation proceeds by first generating liquid spheres. A droplet generator, which comprises a droplet "sizer" connected with an air-flow regulator and a syringe pump, was employed. The sizer is composed of a movable needle holder and a fix gas chamber and gas jacket. Two microstages allow accurate positioning of the needle within the gas jacket on the y- and z-axes. The gas jacket shape and the accurate positioning together with flow control are critical for the droplet production without satellites and within a narrow size distribution. Microlance® 21 gauge needles with a length of 40 mm, from Becton Dickinson, were employed for droplet generation.

2.4 Microencapsulation

A scaled-up apparatus, referred to as the Automatic Reaction Control (ARC) method has been specifically developed to permit production rates in the range of 500,000 capsules per hour. The method, based on oscillating semi-batch reactors, ensures the highest reproducibility and the lowest contamination risk, as minimal handling is needed. Briefly, the droplets were collected during 30 seconds and gelled for a further 30 seconds in a bath containing 15 ml of 1.5 % calcium chloride, 0.9 % sodium chloride and 1 % polyethylene glycol (MW 1000) and which was stirred at 100 rpm with a magnetic stirring bar. To the same bath was then added 50 ml of 1.2 % PMCG in 0.9 % sodium chloride (pH adjusted with NaOH to 7.4) which was stirred at 100 rpm with a magnetic stirring bar. The reaction time was 15 s in order to obtain 20µm membrane thickness. The final step was washing with 150 ml 0.9 % NaCl, during 10 seconds and collecting the capsules from the bath. A diagram detailing the ARC is shown in Figure 1.

2.5 Microcapsule characterization

The variation of the capsule diameters within each experiment were determined visually by examination under a standard inverted-light microscope (Axiovert 100, Carl Zeiss Jena GmbH, Jena, Germany). Pools of forty eight empty capsules, randomly selected from the same batch, were measured with an estimated

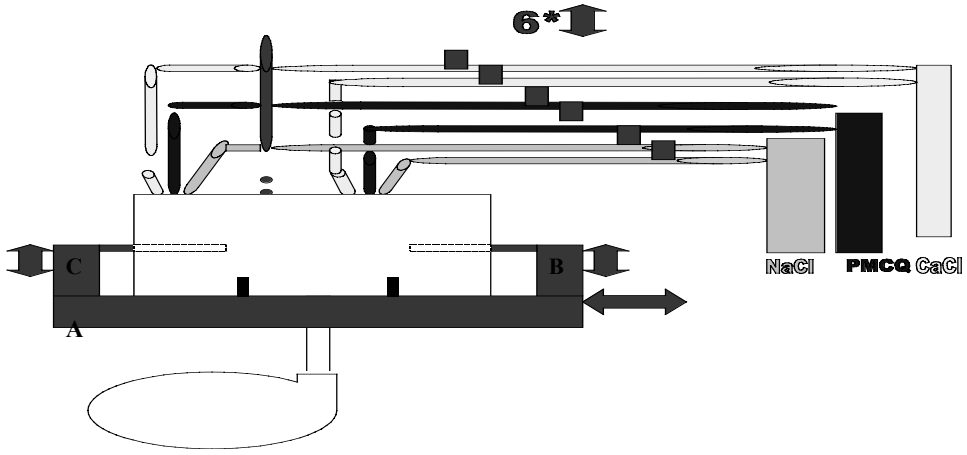

Figure 1:
A diagram detailing the large scale Automatic Reaction Control microencapsulator. The sketch illustrates that the flow of the liquid microcapsule precursors is regulated through a set (1-4) of bevelled 21 gauge needles. This enters the first "reactor", which contains the polycation solution. After a sufficient number of microcapsules are collected, the reactors shift place so that the droplets fall into the second reservoir, which is washed and contains a virgin polycation solution. After a pre-set time the reaction is stopped by dilution and the solution is drained. The gelled membrane-containing capsules are collected in the reservoir. The horizontal oscillation of the two reservoirs, to control the reaction time and membrane thickness, is noted by the symbol A. The sequentially filling of the two reaction reservoirs is noted, respectively, by the symbols B and C

accuracy of ± 5µm. The desired production requirements were set at 400 µm size, within a tolerated range of ± 10%. The choice of 400 µm came as the best compromise between the necessity to reduce the ingress/egress distance for nutrients and oxygen, which is 200 µm in hydrogels. The upper tolerance of 440 µm is governed by the maximum volume that one lobe of the human liver can withstand, if it were to require half a million microencapsulated islets, as would be the case for a diabetes therapy. A lower limit of 350 µm provides assurance that the largest islets will have full immunoprotection. In order to control the reproducibility of the production technique, we have determined the variation of capsule size between the experiments, as will be demonstrated herein. The mechanical resistance of microcapsules to compression was determined on a texture analyzer (Ta-XT2I, Stable Micro Systems, Godalming, U.K.). Each single capsule was compressed until bursting applying a speed of 0.4 mm/s. Force values at the bursting point were registered. The mechanical tests were performed after an equilibrium phase of five days. Further discussion of mechanical testing of microcapsules is provided in Rehor et al. 2001.

3 Results and discussion

The control of microcapsule size, in inter-batch experiments performed under independent conditions, over eighteen consecutive months, is shown in Fig. 2.

Relative to the target value of 400 micrometers, which is ideal for oxygen ingress and nutrient egress, the box plots demonstrate excellent quality control. Specifically, the majority of the capsules, in all batches, are below the maximum transplant tolerance of 440 micrometers, with an overall deviation of ± 10 % (Ceausoglu and Hunkeler, in press).

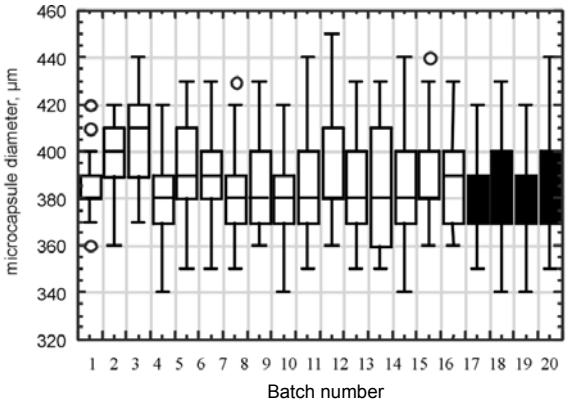

Figure 2:
Intra- and inter-batch microcapsule size distribution. The "box" within the plots contain 50 % of the data with the vertical lines the upper, and lower, 25 % of the distribution. Outliers are denoted with discrete symbols. This quality plot demonstrates that 20 batches, prepared over twenty months with completely independent solutions and same device settings are within the quality bands (400 µm ± 10 %), y-axis = range

Figure 3 demonstrates that the membrane thickness can also be maintained, within a tolerance of ± 25 %. The latter is possible due to the fact that the distribution of reaction times of the microcapsules is controlled. Specifically, the period during which the anionic is added to the reactive cationic solution is much shorter than the reaction time. The oscillating reactor principle, which is equivalent to several continuous stirred tanks in series, or a long tubular reactor, therefore provides a means to continuously produce membrane-containing microcapsules with controlled permeabilities and mechanical properties, as is detailed in a publication (Ceausoglu and Hunkeler, in press) and a submitted patent application.

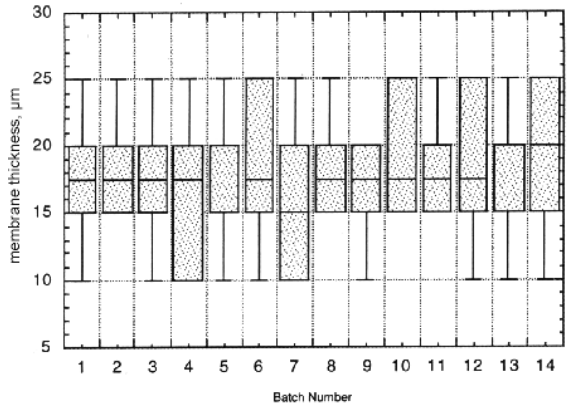

Figure 3:
Intra- and inter-batch membrane thickness distribution. The "box" within the plots contain 50 % of the data with the vertical lines the upper, and lower, 25 % of the distribution. Outliers are denoted with discrete symbols. This quality plot demonstrates that 20 batches, prepared over twenty months with completely independent solutions and same device settings are within the quality bands (20 ± 5 micrometers)

The microcapsules produced with the new ARC technology have good mechanical properties (data not shown). The effect of reducing the endotoxin level to $1/10^{th}$ of that required by the FDA (FDA, 1987) does not alter at all the mechanical properties of the microcapsules, nor the membrane thickness or its distribution (data not shown). This indicates that the removal of endotoxin is selective, since high yields of SA and SCS were obtained. Figure 4 illustrates examples of microencapsulated islets of Langerhans as well as empty alginate/cellulosesulfate//poly(methylene-co-guanidine) capsules. The control of the capsule size and membrane thickness, within a batch, is evident. The random distribution of islets between capsules is acceptable provided the diameters are within tolerance and there is no tissue protruding the membrane, as is the case.

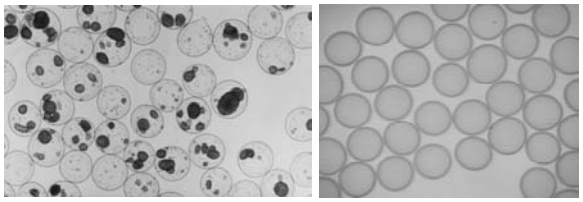

Figure 4:
Photographs of a typical family of empty microcapsules produced with the ARC apparatus (right) as well as microencapsulated islets of Langerhans (left)

4 Conclusions

The present study demonstrates that the downstream processing of membrane containing microcapsules is critical for the production of clinical grade, transplantable, immunoprotection systems. By controlling the reaction time of the polyanion precursor beads in the oligocation solution, the membrane thickness, and hence permeability and mechanical resistance, of the microcapsules can be manipulated both within, and between, batches. These microcapsules, containing islets, have been transplanted intraperitoneally in rats, revealing long term diabetes reversal (Wang et al., 1997). Results of a research cooperation with Professor Morel's group at the University Hospital in Geneva (HUG) will be published separately, and document the lack of any acute or chronic side effects during the transplantation of ten thousand empty capsules per kilogram of body weight in large white pigs.

References

Ceausoglu I, Hunkeler D, J. Microencapulation (in press)

FDA Guidelines 1987; FDA Guidance 1991. USP: Bacterial endotoxins tests

Hunkeler D (1997) Polymers for bioartificial organs. Trends in Polymer Science 5:286-293

Klock G, Frank H, Houben R, Zekorn T, Horcher A, Siebers U, Wohrle M, Federlin K, Zimmermann U (1994) Production of purified alginates suitable for use in immunoisolated transplantation. Appl Microbiol Biotechnol 40:638-643

Lim F, Sun A (1980) Microencapsulated islets as bioartificial endocrine pancreas. Science 210:908-910

Rehor A, Canaple L, Zhang Z, Hunkeler D (2001) The compressive deformation of multicomponent microcapsules: Influence of size, membrane thickness, and compression speed. J Biomaterials Science, Polymer Ed 12:157-170

Schuldt U, Hunkeler D (2000) Characterization methods for microcapsules. Minerva Biotech 12:249-264

Stegemann JP, Sefton M (1996) Video analysis of submerged jet microencapsulation using HEMA-MMA. Cdn J Chem Eng 4:518-525

Wang T, Lacik I, Brissova M, Anilkumar AV, Prokop A, Hunkeler D, Green R, Shahrokhi K, Powers AC (1997) An encapsulation system for the immunoisolation of pancreatic islets. Nature Biotechnology15:358-362

Application of polycarbamoylsulfonate (PCS) for fabrication of enzyme sensors

Bernd Gründig[1]

Abstract

Operational stability of enzyme sensors is usually the single most important factor in limiting their applicability. A promising material for a careful and stable immobilization of proteins was found with Polycarbamoylsulfonate (PCS)-prepolymers. These form synthetic, self-adhesive, polyurethane-based hydrogel layers on planar structured electrochemical sensors. The self-adhesive characteristics of the PCS-hydrogel play a key role in its usability in combination with reusable planar sensors chips which are fabricated by means of mass production technologies as known from microelectronics. Both the careful entrapment and the covalent cross-linking during the gelating process may account for the good stability of different enzymes in the PCS-matrix, as it was found for a range of oxidases, oxygenases and hydrolases which were applied as sensitive layers of thick-film chip sensors developed for applications in food industry, bioprocess monitoring and clinical diagnostics. The operational stability of the different sensors was tested under conditions of flow injection analysis. Depending on the enzyme / enzyme system, most of the different enzyme sensors operate stably between 7 days and 35 days at room temperature, retaining at least more than 50 % of their initial sensitivity.

Keywords: Polycarbamoylsulfonate, enzyme immobilization, thick film sensors, operational stability

1 Introduction

Over the medium to long term, an increasing demand can be expected for rapid, inexpensive analytical tools for application in almost every field of analytical science including; clinical diagnostics, environmental control, food-quality control and monitoring of biotechnological processes, which can only be satisfied by innovative solutions. Biosensor technology, which is increasingly being transferred from basic research into commercial products, represents one such innovative, alternative solution.

Nevertheless, the widespread application of biosensors is still limited by the instability of their biological compounds. Enzymes used in an artificial environment undergo more or less rapid unfolding of their structures. Unfortunately, our knowledge of the factors affecting the protein integrity is far from complete. A sum of various forces like hydrophobic forces, hydrogen bonding, salt bridges, dipole-dipole, and other electrostatic interactions together with the binding of metal ions, substrates and cofactors contribute to the structural integrity of an enzyme (Fig 1).

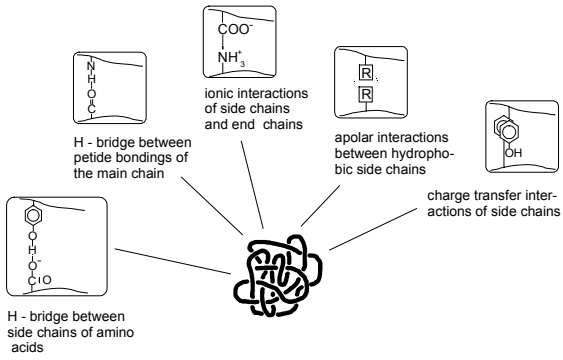

Figure 1:
Bondings responsible for protein integrity

Factors such as temperature, ionic strength, and pH, but also chemical reagents and solvents of the surrounding medium, affect the protein stability (Zaborski 1975, Kennedy and Carbal 1987, Weetall 1975, Schellenberger 1989).

Initial steps of enzyme deactivation are the breaking down of hydrogen bondings, which cause the disruption of large molecule domains, the unfolding of the protein, and the dissociation of the prosthetic groups or catalytic ions (Craig et al. 1998). The resulting decrease of catalytic activity of the enzyme is associated with a loss in sensitivity and linearity of the corresponding biosensor.

2 Strategies for enzyme immobilisation in biosensors

Therefore, a range of different immobilization procedures has been established in order to minimize such conformational changes but to maintain functional stability (Figure 2) (Kennedy and Carbal 1987, Weetall 1975, Schellenberger 1989). Widely-used procedures are based on entrapment and covalent bonding of the proteins (Table 1). Recently, a novel stabilization procedure has been commercialised based on crystallization of the protein (ALTUS.com

[1] Bernd Gründig, SensLab GmbH, Bautzner Str. 67, 04347 Leipzig, Germany

2001). The use of macroscopic crystal approaches of enzymes in biosensors are still being studied by different working groups. Two of the most widely-used procedures for biosensor applications are based on gel entrapment and chemical cross-linking of the proteins (Wong and Wong, 1992, Carr and Bowers 1980, Schmidt et al. 1992).

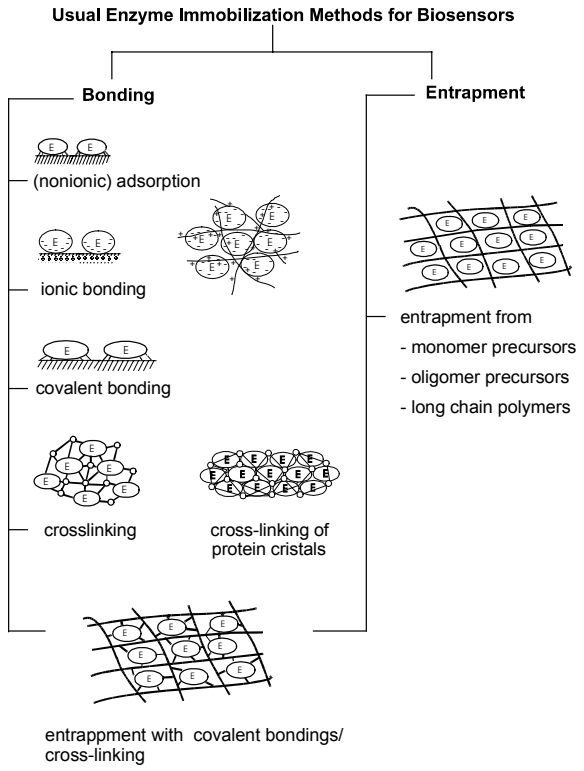

Figure 2:
Immobilization procedures for enzymes in biosensors

The gel entrapment method involves entrapping the enzyme within the lattice of a water-insoluble polymeric network without any chemical binding between the enzyme and the gel matrix. The polymeric gel framework can be obtained from monomers, oligomeric or polymeric precursors, by changing the solubility variables such as solvent, temperature, ionic strength and pH, and taking into account the cross-linking reaction (Kennedy and Carbal 1987). The application of gel entrapment methods usually lead to enzyme layers with high retention of the specific enzyme activity. But the leakage of a small sized enzyme molecules or dissociated monomers of an enzyme from the layer may occur depending on the cut off of the polymeric network. Nevertheless, gel entrapment ensures the highest enzyme loadings compared with other immobilization methods.

Chemical cross-linking of enzymes aims at preserving the secondary and tertiary structure of the protein to maintain the active conformation. The formation of intra- and intermolecular cross-links is achieved by bi- or multifunctional reagents which generate three-dimensional, cross-linked, water-insoluble enzyme aggregates. Depending on the functional groups of the enzyme which have to be activated for binding, and the chain lengths for the bracing groups of the cross-linking reagent hydrophobic or hydrophilic characteristics of the protein could be manipulated. In this way the stability of the enzyme aggregate could be markedly improved. Due to the strong bonds between the enzyme molecules, or the enzyme and a carrier protein by the cross-linker, the enzyme immobilization usually shows a good operational stability. However, owing to difficulty of controlling the intermolecular cross-linking reaction, this leads partly to non-gelatinous layers with poorly defined mass transport characteristics. In addition, the intramolecular cross-linking could also involve functional groups of the catalytically active centre of the enzyme decreasing the activity of the enzyme layer (Wong and Wong 1992).

Considering the advantages and drawbacks of the

Table 1:
Comparison of the three most applied immobilization procedures for biosensors, considering results from Kennedy and Cabral, 1987

Characteristics	Immobilization Method		
	Covalent bonding	Cross-linking	Entrapment
Preparation	difficult	intermediate	intermediate
Binding Force	strong	strong	intermediate
Enzyme activity	intermediate	intermediate	high
Stability	intermediate	high	high
Costs of immobilization	high	intermediate	low
Compatibility to mass production	limited	limited	good
Main advantages	no enzyme leaching	high enzyme stability no enzyme leaching	high enzyme activity high enzyme loading
Main drawbacks	low enzyme loading	poor reproducibility of the cross-linking reaction	enzyme leaching

entrapment and chemical cross-linking immobilization methods as compared in Table 1, it is reasonable to assume that the conjugation of both methods by entrapping the enzyme and cross-linking it with intra - and intermolecular spacer links could result in more stable enzyme immobilizations (Carr and Bowers 1980, Schmidt et al. 1992). In addition, the immobilization procedure has to be optimised for the individual target enzyme or enzyme system.

3 Criteria for enzyme layers in biosensors

The enzyme layer in planar structured biosensors for enzyme substrate detection must fulfil a range of needs. The most important criterion is the maintenance of both operational stability for a certain number of measurements, and storage stability within a defined time scale. In addition, for the application at planar structured transducers, the enzyme must be fixed directly at the planar transducer surface. Therefore, the immobilization matrix and the resulting layer must meet the following conditions:

1. careful immobilization procedure without damaging the enzyme activity
2. enzyme stabilizing effects of the framework
3. high enzyme loading / enzyme reserve ensuring nearly constant sensor sensitivity within the application period (>1000 measurements), low sensitivity towards inhibitors and variations of pH and temperature
4. diffusion controlled reaction in order to obtain a linear measuring range between two and five decades
5. no hindrance of the enzymatic function by conformational, steric, or partitioning effects of the immobilization method, accessibility of the substrate, cofactor to the active sites of the enzyme molecule
6. sufficient mass transport of substrates, cofactors, electron mediators and products of the enzyme through the layer
7. low leaching of the enzyme from the matrix / layer
8. procedure must be easy to handle and compatible with potential mass production technologies

4 Hydrogel matrix with promising characteristics

A promising material for a careful and stable immobilization of proteins was found with Polycarbamoylsulfonate (PCS)-prepolymers, forming synthetic, self-adhesive, polyurethane-based hydrogel layers (Vorlop et al. 1992).

Both the careful entrapment and the covalent cross-linking may account for the good stability of different enzymes in the PCS-matrix, as was found for a range of oxidases, oxygenases, hydrolases and reductases. Prototypes of enzyme sensors using PCS-hydrogel as an immobilization matrix have been developed for applications in environmental control, clinical diagnostics and bioprocess monitoring.

PCS is a bisulphite-blocked hydrophilic isocyanate prepolymer based on the isomers 2,4 - and 2,6 - toluene - diisocyanate and polyol. It is deblocked by neutralization, that forms an entrapping three-dimensional framework of PCS-hydrogel for the entrapment of the enzyme in an aqueous solution. Residual isocyanate groups of the prepolymer are also expected to bond covalently to amino groups of the entrapped protein (Figure 3).

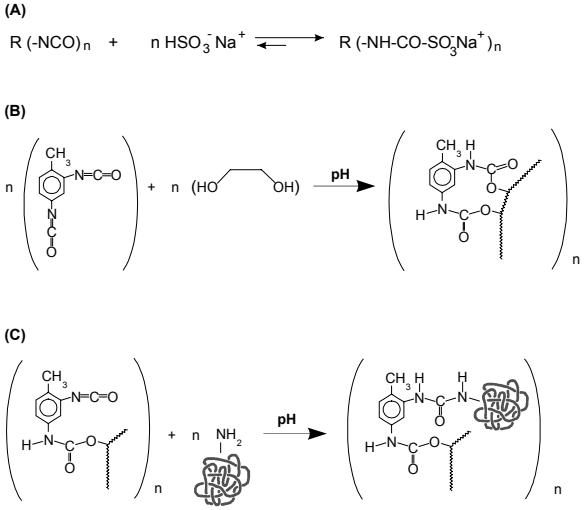

Figure 3:
Preparation and immobilization scheme of Poly(carbomoyl)sulfonate (PCS): Blocking of isocyanates by bisulfite (A), PCS framework formation entrapping the enzyme (B), formation of additional covalent bondings (C)

Adhesion of hydrogel on the surface of the transducer was significantly improved using an aqueous polyethyleneimine solution for adjusting the pH of the prepolymer solution. To reach a diffusion controlled enzyme reaction, the enzyme load applied in the hydrogel layer was varied depending on the enzyme activity and protein concentration of the purified charge. The thickness of the unsoaked layer was estimated to be about 15 to 25 µm (Kotte et al. 1995).

5 Results and Discussion

5.1 Enzyme sensors

5.1.1 Glucose / Lactate sensors

The different enzyme sensors based on planar structured amperometric signal transducers which were manufactured by polymeric thick film techniques. The enzymes or enzyme systems were immobilized by PCS as described in the previous section, forming a self-adhesive layer at the working electrode (Figure 6).

The amperometric sensors detect the formation of hydrogen peroxide of oxidase-based indicating reactions as illustrated for the glucose detection in Figure 4.

The response time of the sensors studied under conditions of a stirred batch measuring cell range between 20 sec and 60 sec (Figure 5). Depending on the enzyme or enzyme system used, most of the sensors respond linearly to concentrations of 1 mM or 5 mM (compare Table 2).

The operational stabilities of the different sensors were tested in a flow-injection analysis arrangement using flow through cells as shown in Figure 6. Usually, a measuring frequency between 30 and 60 samples of 1 mM analyte concentration per hour were applied. Long-term studies using model analyte solutions have shown that the lactate- and glucose sensors retain at least between 80 % and 90 % of their initial sensitivity after 10,000 measurements.

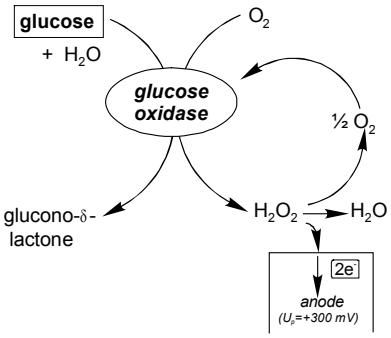

Figure 4:
Glucose oxidase based amperometric detection principle of glucose

Furthermore, during continuous long term measurement of 0.24 mM glucose, a 20 % increase of sensitivity was observed. This rare effect is likely due to a swelling effect of the working electrode material increasing the electro-active area of the working electrode (Figure 8).

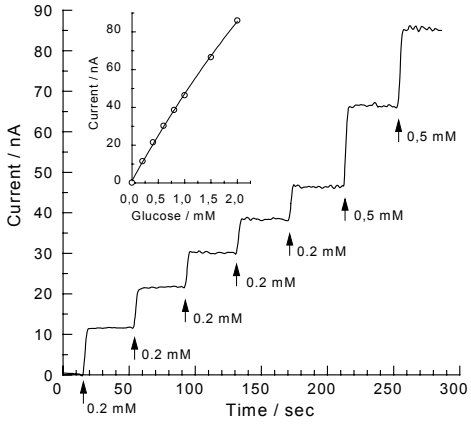

Figure 5:
Glucose oxidase based amperometric detection principle of glucose

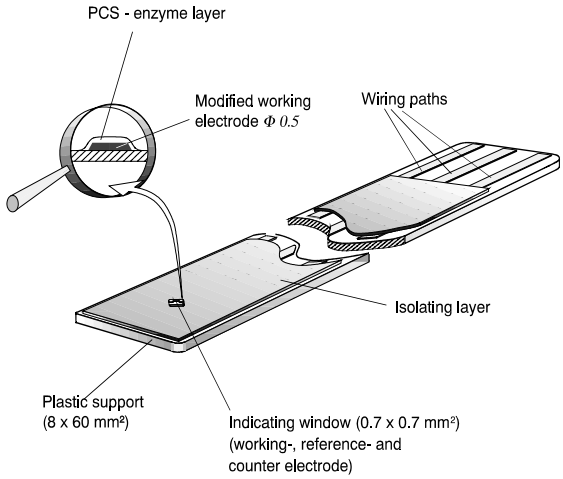

Figure 6:
Scheme of a screen printed enzyme sensor (SensLab)

Figure 7:
Sensor / flow-through cell cascade arrangement

Table 2:
Parameters of enzyme sensors based on PCS immobilization. Sensitivities and measuring ranges were obtained under steady state measuring conditions using a stirred 5 ml batch measuring cell. Operational stabilities were obtained in a FIA arrangement applying model analyte solutions (Gründig 1999)

Analyte	Enzyme / Enzyme System	Sensitivity / $\mu A\ mM^{-1}cm^{-2}$	Measuring Range / mM	Operational stability	
				Number of FIA measurements	Time / days
glucose	glucose oxidase	20…30	0.005 - 1	10.000	30
lactate	lactate oxidase	40…70	0.005 - 1	10.000	30
alcohols	alcohol oxidase	15...20	0.01 - 5	3.000	10
sucrose	fructosidase, mutarotase, GOD	35...50	0.01 - 5	> 10.000	> 21
glutamate	glutamate oxidase (GLOD)	40...70	0.005 - 1	3.000	> 21
glutamine	glutaminase, GLOD	20...30	0.01 - 1	1000	3
urea	urease	20...40	0.005 - 1	500	2
phenols	tyrosinase	400...1000	$5\ 10^{-6}$ - $1\ 10^{-3}$	300	1
nitrite	nitrite reductase	200...700	0.05 - 0.100	50	-
nitrate	nitrate reductase	30...50	0.005 - 0.100	50	-

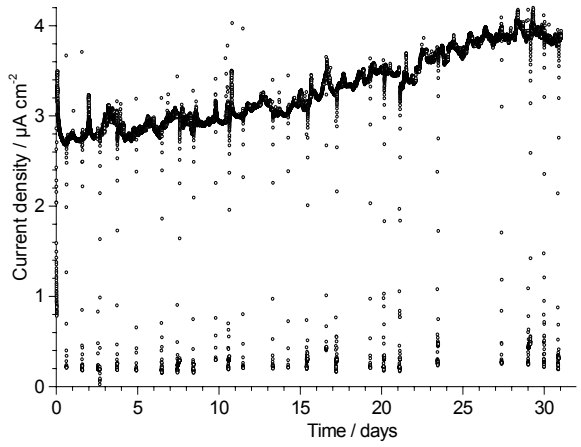

Figure 8:
Operational stability of a glucose sensor based on glucose oxidase - PCS immobilization during continuous measurement of 0.24 mM glucose in 0.1 M phosphate buffer solution pH 6.8 at room temperature, flow rate: 0.5 ml min^{-1}, three electrode arrangement on chip: AE: Pt, GE: Pt, RE: RE 32-SL, U_{pol}: 300 mV

The enzymatic lactate sensor operates more than 37 days at room temperature (20...35°C) without losing more than 10 % of its initial activity after the 37th day of continuous measurement of 1 mM lactate (Cheng et al. 2000). The baseline current was checked by exchanging the analyte solution for buffer solution. Fluctuations and variations of the sensor signal were caused by air bubbles, changes in room temperature between day and night and exchange of analyte solution. The results look promising for the employment of the sensors in clinical analyzers.

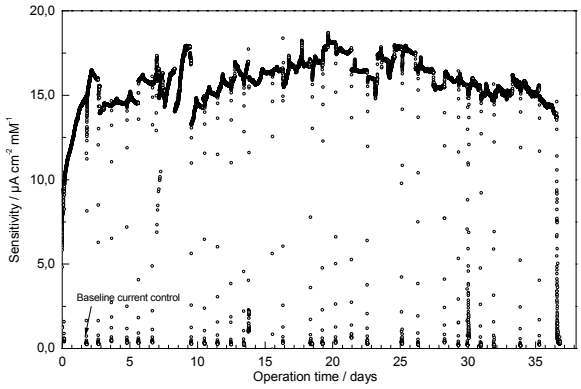

Figure 9:
Operational stability of a lactate sensor based on lactate oxidase - PCS immobilization during continuous measurement of 1 mM glucose in 0.1 M phosphate buffer solution pH 6.8 at room temperature, flow rate: 0.5 ml min^{-1}, three electrode arrangement on chip: AE: Pt, GE: Pt, RE: RE 32-SL, U_{pol}: 300 mV

5.1.2 Phenol sensor

In order to obtain highly sensitive phenol sensors with moderate operational and storage stability, but maintain the high activity of the tyrosinase, the enzyme was immobilized by PCS-hydrogel on the surface of a methoxy-methylphenazonium-phenylborate-modified working electrode which was part of a screen-printed two electrode arrangement.

The enzymatic oxidation of phenols, which generates quinoid products, was combined via the reduced electron mediator of the working electrode to an efficient chemical signal amplification system enabling the detection of subnanomolar phenol concentrations

(Figure 10). The linear response obtained by the phenol sensor ranged between 50 nM and 5 µM.

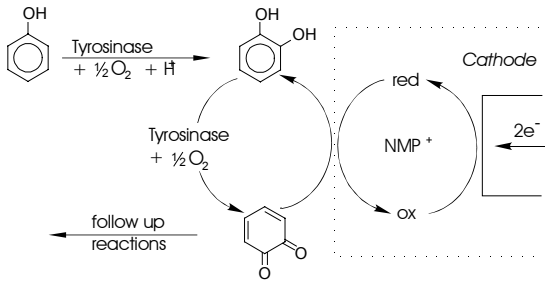

Figure 10:
Phenol detection principle applying an enzymatic–electrochemical signal amplification

Long-term stability was examined in an FIA arrangement injecting consecutive samples of 2 µM phenol with a frequency of 20 samples per hour. After 300 measurements, the sensitivity of the sensor was still 50 % of its initial sensitivity as can be seen in Figure 11. A satisfactory storage stability of more than 100 days was obtained by storing sensors both in buffer solution at + 5°C and dry at -18°C, whereas storage of the sensors at room temperature resulted in a complete loss of their sensitivity within 20 days. The conditions under which the sensors are stored significantly affects their operational stability. Obviously temperature has the strongest influence on stability of the enzyme layer.

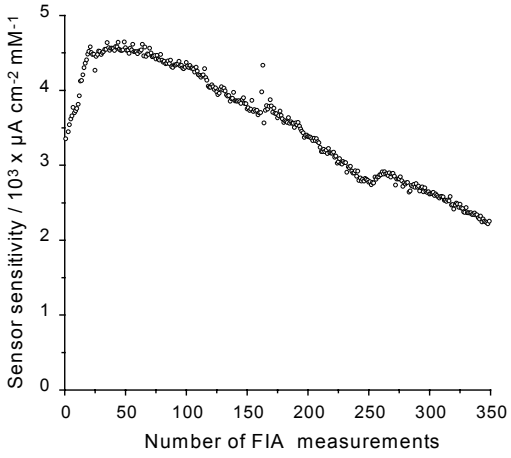

Figure 11:
Operational stability of an phenol sensor based on tyrosinase - PCS immobilization tested under FIA conditions, injection frequency: 20 samples (of 1 µM phenol) per hour at room temperature, carrier: 0.1 M phosphate buffer pH 6.8, flow rate: 0.8 ml min^{-1}, three electrode arrangement on chip: AE: Pt, GE: Pt, RE: RE 32-SL, U_{pol}: 300 mV

5.1.3 Other enzyme sensors

PCS-hydrogel was successfully applied for the immobilization of a range of further enzymes used as receptor compounds of our sensors (Gründig 1999). Table 2 gives an overview of the sensor parameters obtained with the different enzyme sensors which use PCS for the immobilization of the enzyme or enzyme system. Most of the enzyme sensors have shown remarkable operational stabilities compared with enzyme immobilizations known from the literature.

The sucrose sensor which contains a three enzyme system of fructosidase, mutarotase and glucose oxidase (Figure 12) operates stably at least for 7 days at room temperature, retaining more than 90 % of its initial sensitivity (Figure 13). After 21 days of operation in a FIA system, the sensitivity was decreased to 70 % of its initial activity.

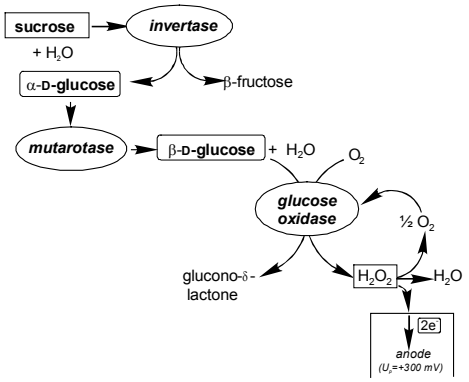

Figure 12:
Indicating principle for sucrose using a three enzyme system immobilized by PCS at the working electrode surface

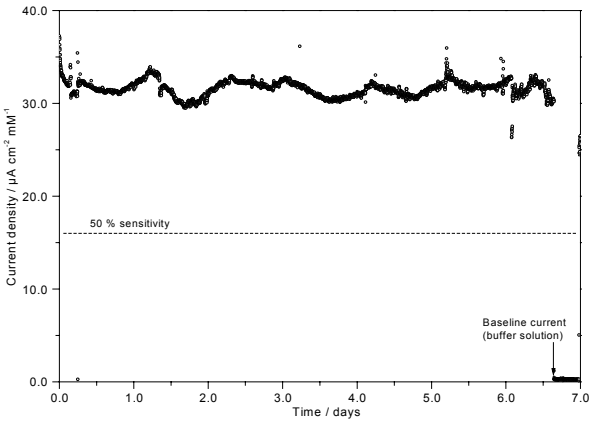

Figure 13:
Operational stability of a sucrose sensor based on fructosidase/ mutarotase/ GOD - PCS immobilization tested under FIA conditions, injection frequency: 40 samples of 5 mM sucrose per hour at room temperature, carrier: 0.1 M phosphate buffer pH 6.8, flow rate: 0.8 ml min^{-1}, three electrode arrangement on chip: AE: Pt, GE: Pt, RE: Ag/AgCl, U_{pol}: 450 mV

Storage studies of such sucrose sensors of about three months have shown a loss of sensitivity between 5 % and 10 % (Mitzkat and Strehlitz 2002).

Although the alcohol oxidase is known as an enzyme with strong limited lifespan, the alcohol sensor based on the PCS-alcohol oxidase sensing layer shows an operational stability of about 3.000 FIA-measurements within 10 days, until the sensor has lost 50 % of its initial sensitivity (Figure 14).

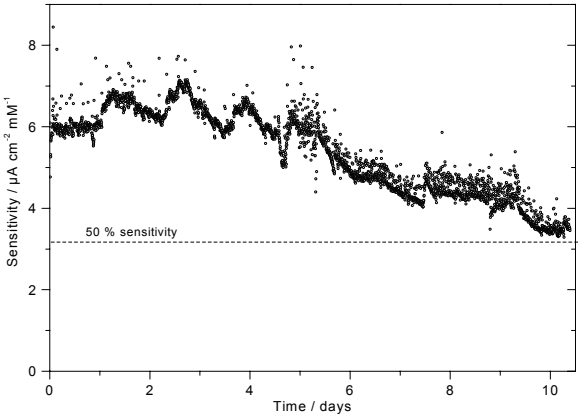

Figure 14:
Operational stability of an alcohol sensor based on alcohol oxidase - PCS immobilization tested under FIA conditions, injection frequency: 25 samples (of 2.5 mM alcohol) per hour at room temperature, carrier: 0.1 M phosphate buffer pH 6.8, flow rate: 0.8 ml min^{-1}, three electrode arrangement on chip: AE: Pt, GE: Pt, RE: RE 32-SL, U_{pol}: 300 mV

Sensitive and stable amperometric biosensors were obtained for the determination of creatine and creatinine using the three - enzyme sequence creatine amidinohydrolase and sarcosine oxidase for creatine and creatinine amidohydrolase, creatine amidinohydrolase and sarcosine oxidase for creatinine. The enzymes were co-immobilized in the PCS-hydrogel matrix onto the surface of a platinum working electrode for the amperometric detection of enzymatically generated hydrogen peroxide. Both sensors showed a detection limit of 0.3 µM. The sensor response has a linear range of 1-150 µM, which corresponds to the relevant physiological range for the monitoring of kidney function. The sensors retained about 50 % of their initial sensitivity after 24 h continuous flow at 37°C. The storage stability at 8°C was found to be 6 months without loss of sensitivity (Schneider et al. 1996).

Similar results were obtained for glutamate sensors based on glutamate oxidase - PCS immobilization (Kwong et al. 2000). The immobilization of urease at an amperometric ammonia sensor yielded an operational stability of about 500 FIA measurements within 2 days (Strehlitz et al 2000). In contrast, the immobilization of nitrite and nitrate reductases has not really been successful up to now. It is reasonable to assume that the instability of the very delicate enzymes is caused mainly by the number and complex arrangement of their redox centres.

Also, the PCS-hydrogel is a suitable matrix for preparing membranes loaded with microorganisms as detecting layers of sensors (Vorlop et al. 1992, König et al. 1996).

6 Conclusions

The results obtained from studies, started 6 years ago, have shown that PCS-hydrogel is a favourable matrix for the preparation of enzyme immobilization layers or membranes for biosensors. The immobilization procedure using PCS-prepolymer can easily be handled. The PCS-hydrogel framework shows only a low toxicity towards the biological compounds, which ensures a careful entrapment of the delicate proteins. The most interesting sensor features revealed by the application of the PCS-matrix are summarized as follows:

- high storage and operational stability
- fast response time (90 % steady state response within 20-60 s, depending on protein loading)
- submicromolar concentrations are detectable
- sensor can be stored dry after use
- short rehydration / swelling time

Moreover, the self-adhesive characteristic of the PCS-hydrogel is an important aspect in view of cost-effective strip-sensors with improved stability and mass production compatibility.

Acknowledgements

The author is greatful to Prof. Vorlop (FAL Braunschweig) for introducing his PCS immobilization technique to enzyme sensor applications. I thank Mrs. S. Wollermann and Dipl.-Ing. H. Kopinke for skillful technical assistance.

References

ALTUS.com (2001) Protein technologies, biomedical applications

Carr PW, Bowers LD (1980) Immobilized Enzymes in Analytical and Clinical Chemistry, Chemical Analysis. A Series of Monographs on Analytical Chemistry and its Applications Vol.56, John Wiley & Sons, New York

Cheng S, Kaptein WA, Gruendig B, Yuen Y, Korf J, Renneberg R (2000) Continuous lactate measurement that combines a portable ultrafiltration storage device with an enzyme sensor. Analytical Letters 33:2153-2168

Craig DB, Arriaga E, Wong JCY, Lu H, Dovichi, NJ (1998) Life and Death of a single enzyme molecule. Anal Chem 75:39A-43A

Gründig B (1999) Amperometrische Enzymsensoren. In: Henze G, Köhler M, Lay JP (eds) Umweltdiagnostik mit Mikrosystemen, Wiley-VCH, Weinheim, pp. 257-303

Kennedy JF, Carbal JMS (1987) Enzyme Immobilization. In: Rehm H-J, Reed G (eds): Biotechnology, Vol. 7a, J.F. Kennedy (volume editor), VCH Weinheim, pp. 347-404

König A, Zaborosch C, Muscat A, Vorlop K-D, Spener F (1996) Microbial sensors for naphthalene using Sphingomonas sp. B1 or Pseudomonas fluorescens WW4. Appl Microbiol Biotechnol 45:844-850

Kotte H, Gründig B, Vorlop K-D, Strehlitz B, Stottmeister U (1995) NMP^{+}-Y zeolite modified enzyme sensor based on polymer thick films for subnanomolar detection of phenols. Anal Chem 67:65-70

Kwong AW, Gründig B, Hu J, Renneberg R (2000) Comparative study of hydrogel-immobilized l-glutamate oxidases for a novel thick-film biosensor and its application in food samples. Biotechnol Letters 22:267-272

Mitzkat L, Strehlitz B (2002) Biosensoren messen Saccharose. LaborPraxis 2, in press

Schellenberger A (ed) (1989) Enzymkatalyse: Einführung in die Chemie der Biochemie und Technologie der Enzyme. Gustav-Fischer-Verlag, Jena

Schmidt H-L, Schuhmann W, Scheller F (1992) Binding of biomolecules to transducer surfaces. In: Göpel W (ed): Sensors, Vol. III: Chemical and Biochemical Sensors, VCH Weinheim, pp. 755-770

Schneider J, Gründig B, Renneberg R, Cammann K, Madaras MB, Buck RP, Vorlop K-D (1996) Amperometric Biosensing of Creatine and Creatinine. Anal Chim Acta 325:161-167

Strehlitz B, Gründig B, Kopinke H (2000) Sensor for amperometric detection of ammonia-forming enzyme reactions. Anal Chim Acta 403:11-23

Vorlop K-D, Muscat A, Beyersdorf J (1992). Entrapment of microbial cells within polyurethane hydrogel beads with the advantage of low toxicity. Biotechnol Tech 6:483-488

Wong SS and Wong L-JC (1992) Chemical crosslinking and the stabilization of proteins and enzymes. Enzyme Microb Technol 14:866-874

Weetall HH (1975) Immobilised enzymes, antigens, antibodies and peptides. Marcel Dekker, New York

Zaborski OR (1975) Immobilized enzymes. CRC Press, Cleveland, Ohio

Preparation of monodisperse controlled release microcapsules

Thorsten Brandau[1]

Abstract

Since the handling of many active agents in their pure form causes many problems, microencapsulation is used to have better properties in the product. With the patented BRACE-Processes it is possible to encapsulate a very wide range of materials in monodisperse microspheres or microcapsules in a diameter range of 50-6000 µm with a very narrow size distribution. The microsphere units from BRACE can be custom-tailored to the materials and all necessary specifications such as FDA, GMP/GLP, EX, CIP, WIP, etc. The throughput of the BRACE microsphere Units ranges from between 10 ml/h (small laboratory scale) up to over 1000 l/h (production scale) while the production cost are very low, especially if compared directly to competitive processes such as spray-drying or fluidized bed coating.

Keywords: microspheres, microencapsulation, pharmaceuticals, food, cell encapsulation

1 Introduction

Most technically or industrially available products take the form of grains, flakes, blocks or powders. With this granulometry, many disadvantages surface. Especially when handling of active agents is required, the difficulties are enormous. Not only is the application itself in many cases troubled, e.g. due to instabilities of the active agent in air, but also the dosage with potent or expensive agents or the handling of oily substances leads to expensive machinery with many problems.

2 The BRACE-processes

The solution to these problems can be achieved with microencapsulation with BRACE microspheres and microcapsules. The microspheres are solid spheres with a matrix encapsulated active agent, while the microcapsules consist of a solid shell with a liquid or solidified core (Figure 1).

The main difference between these two types of microgranules is their release profile. While microspheres usually have diffusion controlled release profiles with a permanent release rate kinetically controlled by the particle size, microcapsules expel their content in a single high burst as the shell breaks (Figure 2).

Figure 1:
Schematic drawing of microcapsules and microspheres. From left to right: microcapsule with solution as core, microcapsule with cell suspension as core, microsphere with matrix encapsulated active agent

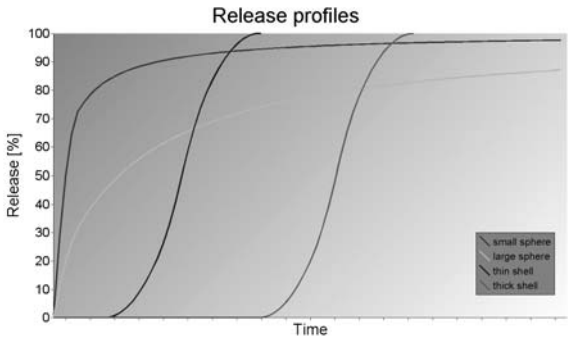

Figure 2:
Release profiles of different types of microspheres and microcapsules. While small microspheres have a fast release profile (bright red), larger microspheres have slower release rates (bright green). The burst time of microcapsules depends on the thickness of their shell (dark red and dark green)

The patented BRACE-Processes for producing microspheres and microcapsules are basically vibrating nozzle processes. These processes produce particles with monomodal grain size distributions with a single sharp maximum. d_{min}/d_{max}-values lower 1.10, 1.05 or even 1.01 are common for spherical granules produced with the BRACE microsphere units. It is possible to obtain microspheres or microcapsules in a diameter range of 50-6000 µm. With special nozzles, larger and smaller particles are possible. A wide range of shell materials are usable with this highly scalable process. The BRACE-Processes combine low space and energy consumptions with high throughput and

[1] Thorsten Brandau, BRACE GmbH, Taunusring 50, D-63755 Alzenau, Germany

very high flexibility concerning the materials to be used. All installations can be customer-tailored to meet all necessary requirements like GMP/GLP, FDA, pharmaceutical, food-, nuclear-, chemical or other industrial standards.

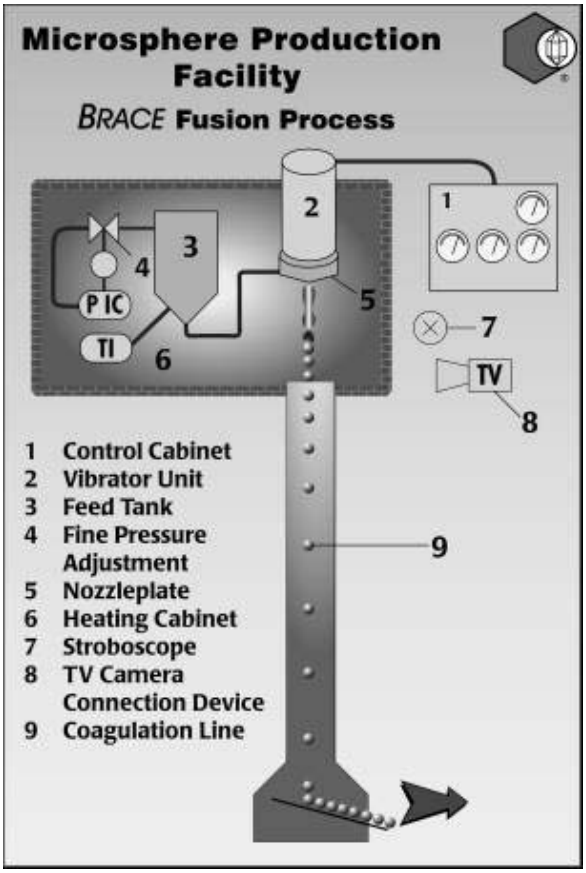

Figure 3:
BRACE microsphere process (fusion process)

The process itself can be described schematically as follows (Figure 3): A liquid feed is pumped from a feed tank (3) to the nozzle head (5) where the vibrating device (2) induces the break-up of the flow into uniform droplets. These are formed into spheres by the surface tension of the feed. The droplets are solidified during falling (9). This can be realized depending on the materials and/or coagulation system used by cooling, chemical reaction or drying. The head of the microsphere unit can be placed in a heating chamber (6), the visual control of the process can be either done by a stroboscopic lamp or with a camera set for remote control. The electronic cabinet (1) controls the microsphere unit and can be integrated in existing control systems.

3 Suitable materials and properties

There are few limitations for the materials that can be used for the BRACE microsphere processes. The materials have to be liquid, the viscosity has to be lower than 10,000 mPa·s, emulsions and dispersions have to be stable over the duration of the process, dispersed particles should have diameters lower than one quarter of the nozzle size to be used and the presolidification should be a fast process so that the particles are not deformed.

The resulting list of chemicals is very long. To name just a few of the usable materials:

- Alginates
- Gelatines
- Agar-Agar
- Cellulose sulfates
- Wax/Thermoplastics
- Oxides: Si-, Al-, Ti-, Zr-, Hf-, Ce-, In-, Y-Oxides, mixtures
- Sols
- Polyethylenimine
- Polyethersulfone
- PEG, PVA
- Polyacrylate, -methacrylate
- Polyamid
- Polystyrene

Suitable active agents depend on the encapsulation technique. For matrix-encapsulation (microspheres) the active agent can be dispersed, dissolved or emulsified into the shell material. For microcapsules, the core material can consist of a liquid like a solution, an emulsion, a dispersion or a fusion/melt. The only restriction is that the core material should not react with the shell material (i.e., to weaken it).

4 Postprocessing

After the production of the microspheres they can be treated with any available technology. This includes drying with all standard dryers (Circulated air, Belt dryer, Drum dryer, Fluidized bed dryer...), calcining, sintering, coating, impregnation, sorting, chemical treatment etc.

5 Types of installations

All microsphere units from BRACE are customer-tailored to the specific needs of the customer. Depending on the application they are built to conform to GMP/GLP, FDA, CIP, WIP, as continuous or batch wise installations, fully automatically or semi automatically. They can be adapted into existing production facilities and scaled from laboratory scale up to

large production scale. All machinery parts are made as the customer requires. Materials as stainless steel, glass, plastic, ... are used.

6 Production capacity

The production capacity of a BRACE microsphere installation ranges from about 10 ml/h up to over 1000 l/h. A comparison of different nozzle sizes to throughput are shown in Figure 4. The example is calculated for a thermoplastic but can be transferred to other materials. With a 500 µm nozzle a throughput of 11 l/h with about 8000 microspheres per second of 1 mm diameter can be produced. With a 200 µm nozzle (resulting in about 400 µm microspheres) it is only about 2,8 l/h but with 30000 microspheres per second.

7 Manufacturing cost

The manufacturing cost depends on the material and the production capacities. For industrial scale production, the manufacturing costs start at 2,66 €/kg for a production of 50 tons/year and reach 0,31 €/kg at 1000 tons/year (Table 1). This calculation is based on a thermoplastic with a melting point of about 80°C including a turn-key installation with building, storage and packing facilities, quality control and operator cost.

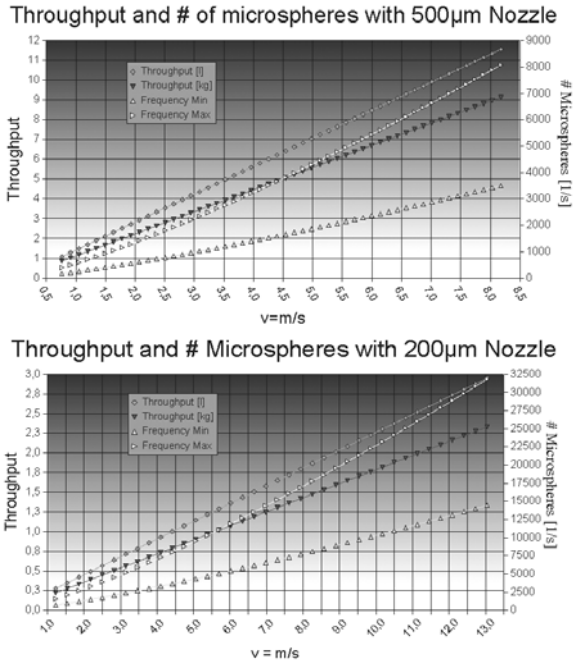

Figure 4:
Comparison of throughput and number (#) of microspheres per second to the nozzle diameter. As a calculation base, a thermoplastic with a melting point of 80°C has been chosen

8 Examples

The BRACE-Processes are widely used in the chemical, pharmaceutical and food industries. For example waxes are used in cosmetic (Figure 5, left) or

Table 1:
Manufacturing cost for different production scales. A thermoplastic with a melting point of about 80°C is assumed

Investment, Description	**Manufacturing Capacity, 1 shift, 2000 h/a**				
Tons per year	50	100	300	500	1000
kg per hour	**25**	**50**	**150**	**250**	**500**
Nr of Nozzles	12	24	72	120	240
Feed preparation	20.000 €	25.000 €	40.000 €	50.000 €	80.000 €
Microsphere Unit	150.000 €	180.000 €	240.000 €	290.000 €	380.000 €
Storage and Packing	10.000 €	15.000 €	20.000 €	30.000 €	50.000 €
Total I	**180.000 €**	**220.000 €**	**300.000 €**	**370.000 €**	**510.000 €**
Laboratory, Quality control	10.000 €	12.000 €	16.000 €	24.000 €	30.000 €
Total II	**190.000 €**	**232.000 €**	**316.000 €**	**394.000 €**	**540.000 €**
Building (rent)	**15.000 €**	**15.000 €**	**20.000 €**	**20.000 €**	**25.000 €**
Raw material 1€/kg	**50.000 €**	**100.000 €**	**300.000 €**	**500.000 €**	**1.000.000 €**
Operators per shift	**2**	**2**	**2**	**3**	**3**
Operator cost per shift	80.000,00 €	80.000,00 €	80.000,00 €	120.000,00 €	120.000,00 €
Maintenance 5% of Total II	9.500,00 €	11.600,00 €	15.800,00 €	19.700,00 €	27.000,00 €
Amortisation 5a, 8% (0,2505)	**47.595 €**	**58.116 €**	**79.158 €**	**98.697 €**	**135.270 €**
Amortisation 10 a, 8 % (0,14903)	28.316 €	34.575 €	47.093 €	58.718 €	80.476 €
Manufacturing cost per kg (5a)	**3,04 €**	**1,65 €**	**0,65 €**	**0,52 €**	**0,31 €**
Cost including material	**4,04 €**	**2,65 €**	**1,65 €**	**1,52 €**	**1,31 €**
Manufacturing cost per kg (10a)	**2,66 €**	**1,41 €**	**0,54 €**	**0,44 €**	**0,25 €**
Cost including material	3,66 €	2,41 €	1,54 €	1,44 €	1,25 €

dental application or as catalysts with active ingredients. Agar-Agar is used to encapsulate oils or other volatile ingredients for cosmetic applications (Figure 6, right), gelatine or alginates are used to encapsulate oils, fragrances or flavours for food technology applications. Polymer beads (Figure 6, left) are used in combinatorical synthesis since the BRACE-Process produces monomodal grains of high quality polystyrene microspheres with defined binding capacities. In the pharmaceutical industry the BRACE-Process is used to encapsulate active agents either against the destructive forces in the digestive system or as taste masking for very bitter materials (Figure 6, right). The adjustable size of the microspheres is used to produce defined release profiles. Chemical and petrochemical industries use catalyst carriers (Figure 7) and grinding balls produced by the BRACE-Processes to obtain maximum performance and low wear and tear in process. Medical industries use inorganic microspheres in bone surgery applications while food technologist prepare toothpaste with “crunch”.

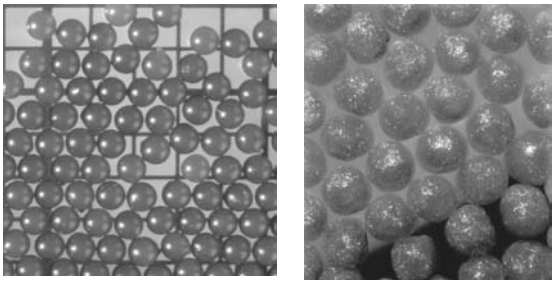

Figure 5:
Left: Cosmetic waxes; right: Agar-Agar with oils

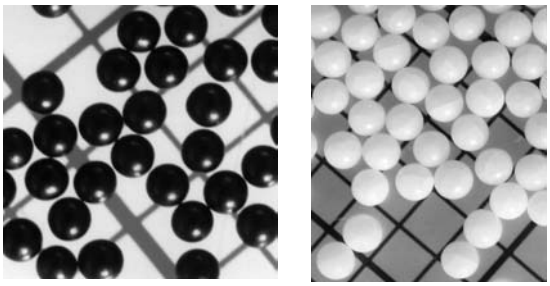

Figure 6:
Left: Polymer beads for combinatorical synthesis; right: Pharmaceutics encapsulated in wax

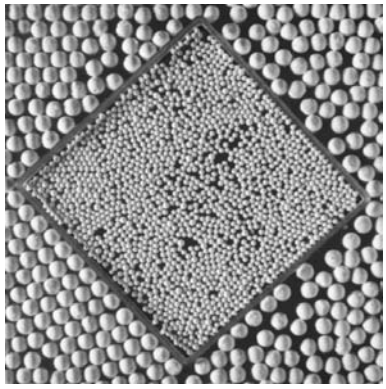

Figure 7:
Inorganic microspheres as catalyst carriers

List of relevant patents

EP585264; US5,420,086; DE 4125133; EP 597911; US 5,472,648; JP 503224/93; EP 556222; US 8,039,498; JP 2766909; EP 687246; US 8,424,435; JP 510647/94

Production of Isomalt

Thomas Rose and Markwart Kunz[1]

Abstract

Sucrose is not only an important raw material in food industry and nutrition, but also an excellent starting material for the synthesis of special oligo- and polysaccharides. Modification of disaccharides. e. g.. sucrose. is possible by reorganising or conserving the carbohydrate structure.

Production of isomaltulose is an example for the enzymatic modification of sucrose by reorganisation of the carbohydrate structure. Isomaltulose is used as a precursor for the production of the sugar replacer isomalt. Isomalt is manufactured in a two-stage process: first, sucrose is enzymatically transformed into isomaltulose. The reaction can be carried out by the enzyme glycosyltransferase (sucrosemutase) for example from *Protaminobacter rubrum*. Isomaltulose yield is about 80 to 85 %. For the industrial process it is advantageous to use immobilized non viable cells of *P. rubrum* in a packed bed reactor. Isomaltulose is hydrogenated in a second step to produce isomalt, an equimolar mixture of GPM (1-O-alpha-D-glucopyranosyl-D-mannitol) and GPS (6-O-alpha-D-glucopyranosyl-D-sorbitol).

Isomalt is an odourless, white, crystalline substance containing about 5 % water of crystallisation. It tastes just as natural as sugar, is not sticky, tooth-friendly, suitable for diabetics and has only about half as many calories as sugar because it cannot be completely metabolised. Because it is similar to sucrose, isomalt is particularly suitable for making products such as candies, chewing gum, chocolate, compressed tablets or lozenges, baked goods, baking mixtures, and pharmaceutical products using conventional equipment.

Keywords: isomalt, isomaltulose, palatinose, sucrose, bioconversion, immobilization, Protaminobacter rubrum

1 Introduction

About 95 % of the annually grown biomass are saccharides, but only 3 % are exploited (Lichtenthaler 1991a). Sucrose extracted from sugar cane or sugar beets is one of the most common saccharides. World production of sucrose was about 148 million tons in 1999/2000; the European Union's share was about 18 million tons. Südzucker (Southern Sugar) is the largest producer of sucrose/saccharides in the European Union (Zuckerwirtschaft Europa 2001 2000). Even though sucrose is the most produced pure organic compound, its application as a bulk chemical is not yet very common (Reinefeld 1987).

Sucrose is not only an important raw material in the food industry and nutrition but also an excellent renewable raw material for the synthesis of special oligosaccharides, polysaccharides, and building blocks for the production of, for example, fatty acid esters, surfactants, and polymers. Many syntheses are available in modern organic chemistry to modify carbohydrates. The sugar derivative HMF (5-hydroxymethyl-furfural), for example, acts as a key substance between carbohydrate chemistry and modern industrial organic chemistry (Kunz 1988, Schiweck et al. 1990, Clarke et al. 1991, Kunz 1991, Lichtenthaler 1991a, 1991b, Schiweck et al. 1991, Cartarius et al. 2001, Nicolaou and Mitchell 2001).

Because of the high functionality of the sucrose molecule and the instable (alpha-1-> beta-2)-intersaccharide bond, classical chemical reactions are difficult to manage. However, modification reactions are realizable in many cases by applying a sequence of a biochemical transformation of sucrose into reducing disaccharides followed by chemical modification (Buchholz et al. 1991, Kunz 1991).

The biochemical transformation of sucrose can be carried out enzymatically whereby the carbohydrate structure is either retained or rearranged. An example of retaining the carbohydrate structure during modification is the enzymatic oxidation using *Agrobacterium tumefaciens* (Buchholz et al. 1991). The product 3-ketosucrose contains a carbonyl group for further chemical reactions such as the reductive amination to 3-aminosucrose.

Production of isomaltulose (palatinose) is an example of the enzymatic modification of sucrose by reorganisation of the carbohydrate structure. Although isomaltulose (palatinose) is a sugar replacement in its own right, it is currently being used as a precursor for the production of the sugar replacer isomalt.

2 Production of isomaltulose (palatinose)

The microorganism *Leuconostoc mesenteroides* was found to produce an unknown disaccharide in

[1] Thomas Rose and Markwart Kunz, Südzucker AG Mannheim/Ochsenfurt, Research, Development and Services Department, Wormser Str. 11, 67283 Obrigheim/Pfalz, Germany

1952 (Stodala et al. 1952). In 1957 Weidenhagen and Lorenz found independently that a bacterium they had isolated from sugar beet raw juice effects a conversion of sucrose to an unknown reducing disaccharide. The disaccharide was identified as isomaltulose and given the trivial name palatinose. It was identical with the unknown disaccharide Stodala, Koepsell, and Sharpe had isolated in 1952. The name palatinose is derived from „palatinum", the latin name of the German province where Weidenhagen and Lorenz found the disaccharide (Weidenhagen and Lorenz 1957a and 1957b, Lorenz 1958a, 1958b).

In 1958 Windisch identified the isolated bacterium as *Protaminobacter rubrum* den Dooren de Jong. Depending on culture conditions, *P. rubrum* produces a red pigment. The bacterium is also able to degrade and modify amines. But its most remarkable property is the transglycosylation of sucrose to palatinose (Windisch 1958). The first patent for the production of palatinose was awarded to Süddeutsche Zucker AG, Mannheim, Germany in 1957 (Weidenhagen and Lorenz 1957c) (Figure 1).

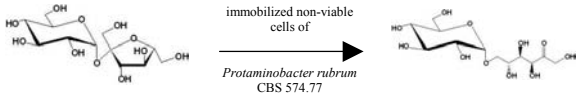

Figure 1:
Conversion of sucrose to palatinose

In addition to *P. rubrum* the microorganisms *Leuconostoc mesenteroides* (Stodala et al. 1952, 1956), *Serratia plymuthica* (Schmidt-Berg-Lorenz and Mauch 1964), *Serratia marcescens* (Schmidt-Berg-Lorenz and Mauch 1964), *Erwinia carotovera* (Schmidt-Berg-Lorenz and Mauch 1964, Lund and Wyatt 1973), and *Erwinia rhapontici* (Cheetham et al. 1982) have been reported to be capable of transforming sucrose into palatinose.

The enzymatic transglycosylation of sucrose to palatinose effected by the glycosyltransferase (sucrosemutase) is described with the molecules in their steric representation in figure 2 for a better understanding. The glucosyl group of the sucrose (alpha-D-glucopyranosyl-1,2-beta-D-fructofuranoside) changes from alpha(1->2) to alpha(1->6) position. The enzymatic reaction results in the thermodynamically more stable palatinose (alpha-glucopyranosyl-1,6-D-fructofuranose) (Schiweck et al. 1990, Lichtentaler 1991a, 1991b, Schiweck et al. 1991).

Of all the microorganisms reported, only the strain of *P. rubrum* originally isolated by Weidenhagen and Lorenz in 1957 (Weidenhagen and Lorenz 1957a and 1957b, Lorenz 1958a, 1958b) has been foreseen for industrial scale use thus far (Nakajima 1984, Kaga and Mizutani 1985).

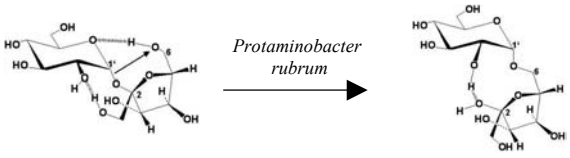

Figure 2:
Enzymatic transglycosylation of sucrose to palatinose (Schiweck et al. 1990, Lichtentaler 1991a, 1991b, Schiweck et al. 1991)

Earlier processes using viable, free microorganisms have the disadvantage of higher product purification costs and lower yield. More cost-effective are techniques using immobilized non-viable cells (Schiweck *et al.* 1990, 1991). This is in agreement with many other authors who prefer the use of immobilization techniques for other processes (Vorlop and Klein 1983, Scott 1984, Chibata et al. 1986, 1987, Hartmeier 1986, Klein and Vorlop 1986, Wiesmann 1994, Buchholz and Kasche 1997, Liese et al. 2000).

The process starts with the propagation of the cells (Figure 3). *P. rubrum* can be cultivated either on thick juice supplemented with corn steep liquor or on molasses with additional nitrogen and phosphate e. g. $(NH_4)_2HPO_4$. Molasses is a byproduct of the sugar industry. The growth medium is adjusted to a concentration of 5 % total solids and pH of 7.2. Sterilization of the medium is, of course, necessary. Growth parameters are given in Table 1 (Schiweck, et al., 1990, 1991).

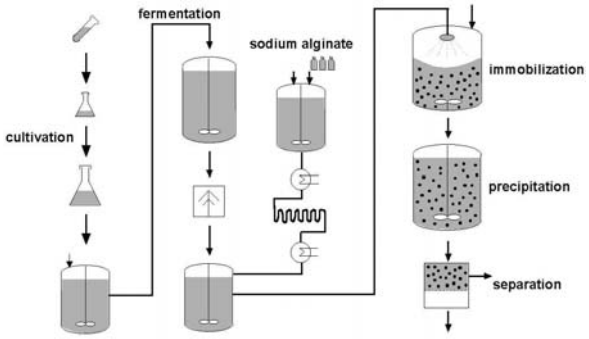

Figure 3:
Fermentation and immobilization of *P. rubrum*

Table 1:
Growth parameters for fermentation of *P. rubrum*

optimum temperature	30 °C
optimum pH	7.0 – > 5.5
optimum aeration rate	1 vvm
growth rate	0.69 h^{-1}
doubling time	1.59 h
fermentation time	12 h

Because there is no need to isolate the enzyme affecting the conversion of sucrose to palatinose, whole cells of *P. rubrum* are immobilized. Almost all immobilization methods described in the literature are suitable for *P. rubrum*. But one limitation has to be regarded: The enzyme is sensitive to glutaraldehyde. The best technique so far is the immobilization in classical calcium alginate beads according to the method of Lim and Sun (1980) (Schiweck et al. 1990, 1991).

After fermentation, cells of *P. rubrum* are separated, mixed with sterilized sodium alginate solution and sprayed into a precipitation bath containing calcium acetate (Figure 3). The biocatalyst is separated and transferred to a packed bed reactor (Figure 4). All manipulations are carried out under sterile conditions.

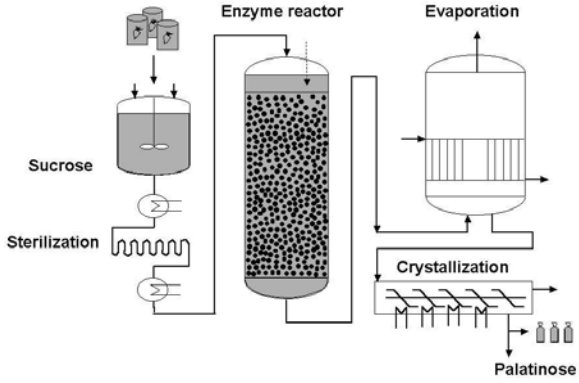

Figure 4:
Production of palatinose with immobilized *P. rubrum*

The sucrose used for conversion to palatinose is dissolved and pH is adjusted to 6.0 before it is sterilized and pumped into the reactors. Downflow operation has been found to be advantageous. Flow rate is adjusted individually for each reactor to convert almost all sucrose being supplied. The product pattern of the solution leaving the reactors is shown in Table 2. The formation of byproducts cannot be avoided even when using the purified enzyme. The product pattern can be slightly influenced by operating parameters like substrate concentration, temperature, mean residence time, residence time distribution and to some extent, the method of immobilization.

The long-time stability of the immobilized enzyme is remarkably high even if high concentrations of sucrose up to 550 g/L are used. A half-life of more than 5,000 hours is absolutely common (Cheetham 1987). The extent of byproduct formation determines not only the yield but also the extent of purification required (Schiweck et al. 1990, 1991). Crystallization from aqueous solutions is the most efficient method for isolation of pure isomaltulose from the product solution leaving the column reactors. Although conventional evaporation technology can be applied to concentrate palatinose solutions, heat sensitivity of palatinose has to be taken into account. Heat sensitivity is caused by the fructose part of the palatinose molecule. After evaporation and crystallization palatinose is separated (Figure 4).

Table 2:
Product pattern of the glycosyltransferase of *P. rubrum*.

product	% on total solids
isomaltulose (palatinose)	79.0 – 84.5
trehalulose	9.0 – 11.0
fructose	2.5 – 3.5
glucose	2.0 – 2.5
isomaltose	0.8 – 1.5
sucrose	0.5 – 1.0
isomelezitose	0.5
others	0.7 – 1.5

Palatinose can be dried in conventional drying equipment e. g. rotary drum dryers. However drying and packaging of palatinose is only required if it is stored for further use. If palatinose is processed to isomalt moist crystals from crystallization are used directly (Figure 4).

Recent research and development resulted in a modified method of production, so called isomalt 2 process (Figure 5). The palatinose solution from the enzyme reactor is used for hydrogenation without evaporation and crystallization. To produce sucrose free isomalt, the sucrose has to be removed before hydrogenation. The removal is achieved in a second enzyme reactor containing immobilized non-viable cells of *Saccharomyces cerevisiae*. Sucrose is enzymatically hydrolysed to glucose and fructose. During the hydrogenation process glucose and fructose are converted to sorbitol and mannitol. The biocatalyst containing *S. cerevisiae* is prepared in the same way as the *P. rubrum* biocatalyst (see above).

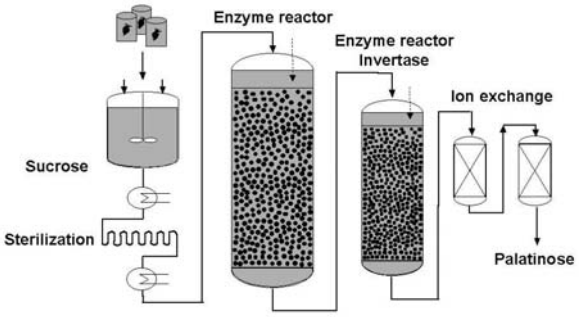

Figure 5:
Alternative method for the production of palatinose with immobilized *P. rubrum*

Currently both processes for the production of palatinose are in use. Properties of palatinose are

given in Table 3. Most palatinose is used as a precursor for the production of the sugar replacer isomalt.

3 Production of isomalt (palatinit)

Following the discovery of palatinose in the fifties, research activities focussed on its benefits during the sixties. With the properties of palatinose being similar to those of fructose, production of palatinose did not seem to be commercially reasonable. However the hydrogenation of palatinose to isomalt (palatinit) in the sixties by Schiweck gave fresh impetus to research activities. In the seventies, the process for production of isomalt was established and in the eighties the production on a technical scale started. At the same time, Südzucker applied for approval of isomalt as food ingredient. In 1990, a large scale plant for production of isomalt went on stream in Offstein/ Rhineland-Palatinate (Bruhns 1991). Current isomalt production is about 35,000 tons yearly.

Hydrogenation of palatinose solutions can be done easily under moderate temperature and pressure conditions and at neutral pH or under mildly alkaline conditions. Any of the usual hydrogenation catalysts is suitable for carrying out the reaction. Quite suitable is Raney-Nickel in pelletized form in a fixed bed reactor. Theoretically the reduction of palatinose should yield an equimolar mixture of 1-O-alpha-D-glucopyranosyl-D-mannitol (1,1-GPM) and 6-O-alpha-D-glucopyranosyl-D-sorbitol (1,6-GPS) but depending on the conditions of hydrogenation the rate of each component can vary between 43-57 % (Schiweck et al. 1990, 1991, Figure 6, 7).

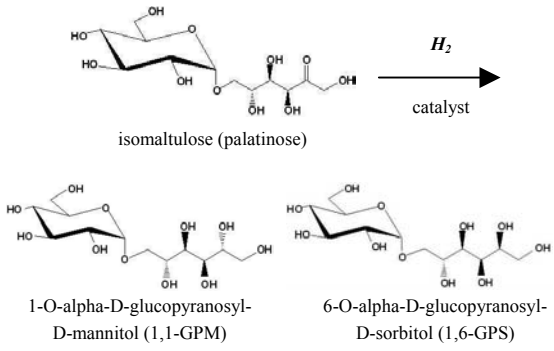

Figure 6:
Hydrogenation of isomaltulose (palatinose) to isomalt (palatinit)

Traces of nickel may dissolve during the hydrogenation process as slight acid formation cannot be excluded. This nickel together with the anions must be removed completely from the solution before crystallisation. Purification of the isomalt solution is possible by ion exchange. The ion exchange is carried out by using strong acid cation and medium-to-strong base anion resins. After filtration and ion exchange the isomalt solution is evaporated to appropriate concentration. Evaporation is carried out in a multi-stage falling film evaporator operating at reduced pressure (Figure 7).

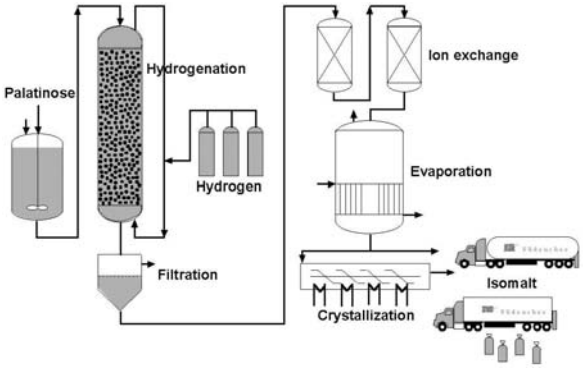

Figure 7:
Production of isomalt: Hydrogenation and down-stream processing

The isomalt solution is either sold as such or evaporated to super saturation and sent to crystallization. Isomalt crystallizes readily from aqueous solutions. The GPM part of isomalt crystallizes with two mols of crystal water (Lindner and Lichtenthaler 1981) whereas GPS crystals are anhydrous (Lichtenthaler and Lindner 1981). This results in a water content of 5 % in crystalline isomalt. Because the crystal water of GPM is integrated into the molecule via hydrogen bonding it is very difficult to produce anhydrous GPM (Schiweck et al. 1990, 1991).

4 Properties and applications of isomalt/palatinit

Isomalt is an odourless, white, crystalline substance containing about 5 % water of crystallisation. It tastes just as natural as sugar, is not sticky, tooth-friendly (it helps to prevent cavities and plaque), suitable for diabetics and has only about half as many calories as sugar because it cannot be completely metabolized.

Isomalt is a bulk sweetener and can substitute sugar in a 1:1 mass ratio. It should not be mistaken for intense sweeteners, which have much greater sweetening power (between a hundred and a thousand times as high). For this reason these intense sweeteners are only used in small quantities. Because isomalt is similar to sucrose, it is particularly suitable for making products such as candies, chewing gum, chocolate, compressed tablets or lozenges, baked goods, baking mixtures, and pharmaceutical products using conventional equipment. Isomalt's nutritional and physio-

logical benefits are ideal for use in sugarfree, low-calorie and diabetic products. It is particularly suitable for food and pharmaceutical applications and also offers many advantages for technical uses (Table 3, http://www.isomalt.com).

Table 3:
Properties and applications of isomaltulose (palatinose) and isomalt/palatinit compared to those of sucrose (Schiweck et al. 1990, 1991)

property	sucrose	isomaltulose/ palatinose	isomalt/ palatinit
sweetening power	100	42	45-60
sweetening character	round, balanced	neutral	neutral sweetness
melting point (range)	160-185°C	123-124°C	145-150°C
specific rotation	+ 66.5 °	+ 103 °	
solution enthalpy	-18.2 kJ/kg	-21.7 kJ/kg	-39.4 kJ/kg
cooling effect on dissolving	none	none	low
solubility at 20 °C	appr. 2 g/g_{water}	0.49 g/g_{water}	0.33 g/g_{water}
hydroscopicity in powder	low	very low	very low
viscosity in solution	low	low	low
browning reactions	+	+	–
calories/g DS	4	4	2
suitable for diabetics	–	+	+
tooth-friendly	–	+	+

References

Bruhns J (1991) Eröffnung der Palatinit-Anlage in Offstein. Zuckerindustrie 116(8):736-737

Buchholz K, Stoppock E, Matalla K, Reh KD, Jördening, HJ (1991) Enzymatic sucrose modification and saccharide synthesis. In: Lichtenthaler FW (ed) Carbohydrates as organic raw materials. VCH, Weinheim, Germany, pp. 155-168

Buchholz K, Kasche V (1997) Biokatalysatoren und Enzymtechnologie. VCH, Weinheim, Germany, pp. 141-233

Cartarius R, Krause T, Vogel H (2001) Bioabbaubare Tenside durch heterogenkatalysierte reduktive Aminierung von Isomaltulose. Chemie Ingenieur Technik 73(1+2):118-123

Cheetham PSJ, Imber CE, Isherwood, J (1982) The formation of isomaltulose by immobilized Erwinia rhapontici. Nature 299:628-631

Cheetham PSJ (1987) Production of isomaltulose using immobilized microbial cells. In: Mosbach K (ed) Methods in enzymology. Academic Press 136:432-454

Chibata I, Tosa T, Sato T (1986) Immobilized cells and enzymes. Journal of Molecular Catalysis 37:1-24

Chibata I, Tosa T, Sato T (1987) Application of immobilized biocatalysts in pharmaceutical and chemical industries. In: Rehm H-J, Reed G (ed) Biotechnology. VCH, Weinheim, Germany, 7 a: pp. 653-684

Clarke MA, Bailey AV, Roberts EJ, Tsang WS (1991) Polyfructose: a new microbial polysaccharide. In: Lichtenthaler, FW (ed) Carbohydrates as organic raw materials VCH, Weinheim, Germany, pp. 169-182

Hartmeier W (1986). Immobilisierte Biokatalysatoren. Heidelberg: Springer

Kaga T, Mizutani T (1985) Proceedings of the Research Society of Japan Sugar Refineries Technologists 34:45-57; Chemical Abstracts (1986) 105:224782f

Klein J, Vorlop K-D (1986) Immobilization techniques. In: Moo-Young M (ed) Cells in comprehensive biotechnology. Pergamon Press, Oxford, Great Britain, Vol. II, pp. 203-224

Kunz M (1988) Saccharosederivate – Zucker als hydrophiler Baustein/Sucrose derivates – sugar as hydrophilic building block. Zuckerindustrie 113(4):273-278

Kunz M (1991) Sucrose-based hydrophilic building blocks as intermediates for the synthesis of surfactants and polymers. In: Lichtenthaler, FW (ed) Carbohydrates as organic raw materials. VCH, Weinheim, Germany, pp. 127-154

Lichtenthaler FW, Lindner HJ (1981) Liebigs Annalen der Chemie 2372-2383

Lichtenthaler FW (1991a) Perspectives in the utilization of low-molecular-weight carbohydrates as raw materials for chemical industry. Zuckerindustrie 116(8):701-712

Lichtenthaler FW (1991b) Carbohydrates as organic raw materials. VCH, Weinheim, Germany

Liese A, Seelbach K, Wandrey C (2000) Industrial biotransformations. VCH, Weinheim, Germany, pp. 74-79

Lim F, Sun AM (1980) Microencapsulateted islets as bioartifical endocrine pancreas. Science 210:908-910

Lindner HJ, Lichtenthaler FW (1981) Extended zigzag conformation of 1-O-alpha-D-glucopyranosyl-D-mannitol. Carbohydrate Research 93:135-140

Lorenz S (1958a) Über bakteriologische Betriebskontrolle in Zuckerfabriken und papierchromatographische Studien zu Saccharoseumwandlung der dabei gefundenen Bakterienstämme. Zeitschrift für die Zuckerindustrie 8:490-494

Lorenz S (1958b) Über bakteriologische Betriebskontrolle in Zuckerfabriken und papierchromatographische Studien zu Saccharoseumwandlung der dabei gefundenen Bakterienstämme. Zeitschrift für die Zuckerindustrie 8:535-541

Lund BM, Wyatt GM (1973) The nature of reducing compounds formed from sucrose by Erwinia carotovora var atroseptica. Journal of General Microbiology 78:331-336

Nakajima Y (1984) Proceedings of the Research Society of Japan Sugar Refineries Technologists 33:55-63; Chemical Abstracts (1984) 103:213357d

Nicolaou KC, Mitchell HJ (2001) Abenteuer in der Kohlenhydratchemie: Synthesestrategien, Synthesemethoden, Molekueldesign und biologische Chemie. Angewandte Chemie 113:1624-1672

Reinefeld E (1987) Zur Verwendung von Saccharose in der chemischen Industrie. Zuckerindustrie 112(12):1049-1056

Scott, C (1984) Immobilized cells: a review of recent literature. Enzyme Microbiology and Technology 9:66-72

Schiweck H, Munir M, Rapp KM, Schneider B, Vogel M (1990) New developments in the use of sucrose as an industrial bulk chemical. Zuckerindustrie 115(7):555-565

Schiweck H, Munir M, Rapp KM, Schneider B, Vogel M (1991) New developments in the use of sucrose as an industrial bulk chemical. In: Lichtenthaler FW (ed) Carbohydrates as organic raw materials. VCH, Weinheim, Germany, pp. 57-94

Schmidt-Berg-Lorenz S, Mauch W (1964) Ein weiterer Isomaltulose bildender Bakterienstamm. Zeitschrift für die Zuckerindustrie 14:625-627

Stodala FH, Koepsell HJ, Sharpe ES (1952) A new disaccharide of Leuconostoc mesenteroides. Journal of the American Chemical Society 74:3202-3203

Stodola FH, Sharp S, Koepsell, HJ (1956) The preparation, properties and structure of the disaccharide leucrose. Journal of the American Chemical Society 78:2514-2518

Vorlop K-D, Klein, J (1983) New developments in the field of cell immobilization – formation of biocatalysts by ionotropic gelation. In: Lafferty RM (ed) Enzyme technology. Springer, Berlin, Germany, pp. 219-235

Weidenhagen R, Lorenz S (1957a) Ein neues bakterielles Umwandlungsprodukt der Saccharose. Angewandte Chemie 69:641

Weidenhagen R, Lorenz S (1957b) Palatinose (6-(alpha-Gluco-pyranosido)-fructofuranose), ein neues bakterielles Umwandlungsprodukt der Saccharose. Zeitschrift für die Zuckerindustrie 7:533-534

Weidenhagen R, Lorenz S (Süddeutsche Zucker AG) (1957c) Process for the production of Palatinose. German Patent DE 1,049,800. Chemical Abstracts (1961) 55:2030b

Wiesmann R (1994) Einfluß der Immobilisierung auf den Stofftransport in biotechnischen Prozessen. Fortschritt-Berichte VDI Reihe 17 Nr. 113. VDI Verlag, Düsseldorf, Germany

Windisch S (1958) Über einen Farbstoffbildner von Zuckerrüben, Protaminobacter rubrum (den Dooren de Jong). Zeitschrift für die Zuckerindustrie 14:446

Zuckerwirtschaft Europa 2001 (2000) Berlin: Dr Albert Bartens

Significant reduction of energy consumption for sewage treatment by using LentiKat® encapsulated nitrifying bacteria

Michael Sievers[1], Sven Schäfer[1], Ulrich Jahnz[2], Marc Schlieker[3], and Klaus-Dieter Vorlop[3]

Abstract

Bacteria from an external fermentation were employed in entrapped form to specifically increase the nitrification rate in nitrifying waste water treatment plants. For maximum biological and mechanical stability a matrix consisting of polyvinyl alcohol (PVA) was chosen. Stable hydrogels were obtained by room-temperature gelation according to the LentiKat® method. Waste water from a municipal waste water treatment plant was used directly for the lab-scale set-up and the parameters ammonia, nitrate and COD were measured regularly. The set-up was run with different parameters over a period of 650 days. A specific volumetric nitrate production rate of approx. 25 to 30 mg/(L·h) was achieved at maximum nitrification. The residence time was between 30 and 60 minutes which is ten times shorter compared to conventional methods. For real waste water treatment plants this means a significant reduction in size for the nitrification reactors. The COD consumption showed values between 10 and 50 % due to specific nitrification. The remaining COD is available for the subsequent denitrification step. The LentiKats® showed no deterioration over the complete time span.

Keywords: Nitrification, immobilisation, LentiKats®, energy

1 Introduction

1.1 Situation regarding WWTPs

Stringent environmental regulations regarding effluent nitrogen concentration of wastewater treatment plants (WWTPs) were established in many countries in the last decade. Moreover, the growth of the population mostly requires upgrading of existing sewage treatment plants. Therefore, to achieve complete nitrogen removal in a conventional single-sludge WWTP, a significant increase of the reaction volume compared to chemical oxygen demand (COD) removal has been commonly established.

Presently, new solutions for cost-effective nitrogen removal are necessary both for less investment and lower operational costs to ensure sustainable wastewater treatment not only in highly industrialised but also well developed countries. One possibility for a new process at WWTPs is the use of nitrifying microorganisms encapsulated in LentiKats®.

1.2 Encapsulated nitrifiers

The advantages of the use of encapsulated microorganisms compared to conventional systems are as follows:

1. It is possible to nitrify with much less water hydraulic retention time due to the high concentration of encapsulated organisms and their high activity.
2. The high age of the sludge, which is necessary in single sludge systems to ensure complete nitrification due to the low growth of nitrifying microorganisms could be reduced. Therefore, the additional aeration for endogenous respiration, which increases with the sludge age, could be reduced substantially.
3. A more selective nitrification process with less biological oxygen demand (BOD) reduction due to at this stage unwanted heterotrophic microorganisms becomes possible. As a result, post denitrification can be done with the internal use of organic compounds.
4. The internal recycling of nitrified wastewater as commonly established for pre-de-nitrification processes is not always necessary with respect to waste water concentration of carbon ions and capacity to equalise alkalinity.

2 Operations for sewage treatment

A typical flow scheme of a sewage treatment plant is shown in Figure 1. The sewage is treated firstly by mechanical processes such as sieving and primary settling, and secondly by biological processes. The mechanical processes eliminate suspended particles of

[1] Michael Sievers and Sven Schäfer, CUTEC-Institut GmbH (Clausthal Environmental Technology Institute), Leibnizstraße 21, 38678 Clausthal-Zellerfeld, Germany

[2] Ulrich Jahnz, geniaLab Biotechnologie GmbH, Bundesallee 50, 38116 Braunschweig, Germany

[3] Marc Schlieker and Klaus-Dieter Vorlop, Institute of Technology and Biosystems Engineering, Federal Agricultural Research Centre (FAL), Bundesallee 50, 38116 Braunschweig, Germany

raw wastewater while the biological processes mainly eliminate dissolved nitrogen and organic compounds of raw wastewater. Sludge would be produced in these processes. This sludge is commonly treated through anaerobic digestion and sludge de-watering.

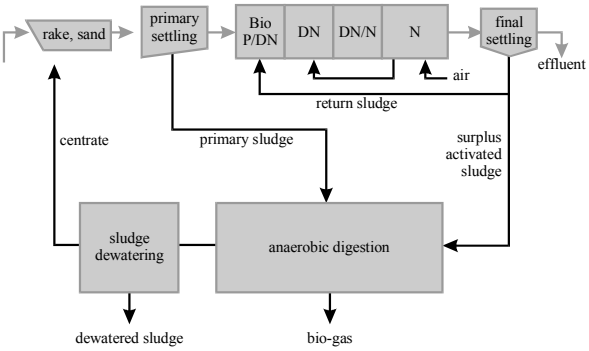

Figure 1:
Mass-flow scheme in a waste water treatment plant

2.1 Cost for waster water treatment

A typical distribution of operational costs is shown in Figure 2. It is obvious that energy consumption plays a substantial role in operational costs. Moreover, more than 65 % of overall energy consumption is needed for the biological processes and mainly for the aeration of biological processes.

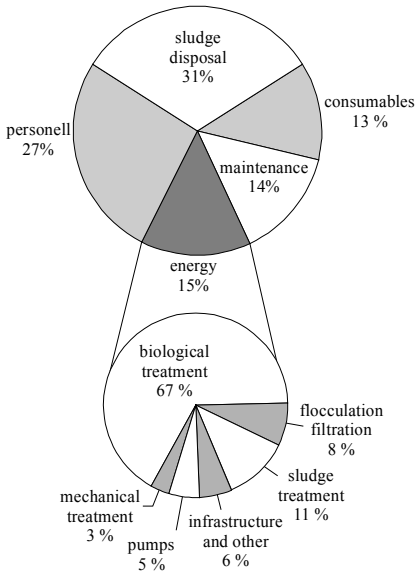

Figure 2:
Distribution of cost arising in a WWTP

2.2 Cost optimisation

Therefore, optimisation of aeration and oxygen supply could lead to a substantial reduction of energy consumption at WWTPs, but the minimum of oxygen consumption is limited to the amount of ammonia, BOD (biological oxygen demand) and COD (chemical oxygen demand), which has to be oxidised. Optimisation of energy consumption itself on WWTP could be done in two ways:

1. The operation of WWTPs could be optimised via analysis of the energy consumption and certain methods of saving energy. This potential is not the subject of this paper and it has to be dealt with carefully, because of the need to treat wastewater efficiently today and even more so in the future.
2. Further energy-savings could only be realised by altering the process configuration itself. The main approach is to optimise the biological processes, for which 70 to 80 % of the energy is used for air supply.

2.3 Sludge age and air supply

For example, the potential of energy reduction would be explained on the basis of published results on aeration experiments at domestic WWTPs. The specific oxygen consumption related to the BOD in raw wastewater is one key parameter to evaluate the energy consumption for aeration. Some data published by wastewater treatment plant operators and the organisation "Abwassertechnische Vereinigung" (ATV) are listed in Table 1 for different sludge ages. It is obvious that up to 46 % of energy for BOD oxidation could be saved just by reducing the sludge age from 25 to 4 days.

Table 1:
Specific oxygen consumption in kg O_2 per kg of BOD for different sludge ages in single sludge WWTPs

sludge age	10°C	15°C	20°C
4 days	0.81–0.83	0.89–0.94	0.97–1.05
8 days	0.97–1.05	1.05–1.20	1.13–1.35
25 days	1.21–1.55	1.26–1.60	1.31–1.60

This different oxygen consumption is caused by two main effects:

a) The oxygen consumption for endogenous respiration would be decreased for lower sludge ages.
b) The BOD of raw wastewater would be less oxidised into carbon dioxide but more into additional bio-mass. The latter has the potential for higher bio-gas production during anaerobic digestion of sludge.

3 Nitrogen elimination at WWTPs

The nitrogen to be removed from raw waste water is commonly ammonia, which can be decomposed conventionally by the following two-step overall reaction scheme:

nitrification:
$NH_4^+ + 2\ O_2 \rightarrow NO_2^- + 2\ H_2O + 2\ H^+$ and
$NO_2^- + 0.5\ O_2 \rightarrow NO_3^-$

denitrification:
$5\ CH_3COOH + 8\ NO_3^- \rightarrow 10\ CO_2 + 6\ H_2O + 8\ OH^-$

The formula for the denitrification step is shown for the case of acetic acid as carbon source. For nitrification, dissolved oxygen is relevant and therefore aeration is essential (aerobic conditions). For denitrification, solute oxygen must be avoided (anoxic conditions), otherwise denitrification will not occur due to the fact that the affinity of the electrons donated by acetic acid is much higher to molecular oxygen than to nitrate.

The electron donator, usually a carbon source, is substantially only present in raw wastewater, but not in the nitrified wastewater. To reduce nitrate of nitrified wastewater with the internal utilisation of raw wastewater carbon source three possible processes for nitrogen elimination have been established:

a) pre-denitrification
b) post-denitrification
c) simultaneous denitrification.

The first process implies a re-circulation of wastewater containing nitrate back from the nitrification to the denitrification step at the inlet of the biological basin. The effluent of such processes would always contain nitrate, the amount depending on the level of concentration and the re-circulation rate. Treatment of wastewater containing high nitrogen concentrations would need a high re-circulation rate to fulfil regulations for the effluent.

The post denitrification has the advantage of making possible an almost complete nitrogen removal through the optimisation of every single process step of the treatment process. The main disadvantage of this process is the low level of carbon sources in the nitrified wastewater and external carbon sources are commonly needed for substantial denitrification. Moreover, additional BOD compared to BOD of raw wastewater has to be oxidised, leading to more sludge and a less cost-effective process.

For the simultaneous denitrification, nitrification and denitrification would take place in the same reactor by alternating aerobic and anaerobic conditions through different aeration modes or zones.

The limitation of the growth of the nitrifying organisms, especially at lower temperatures, is common to all processes. To avoid washing out of nitrifiers compared to the faster growing heterotrophs, the need for a higher age of the sludge arises resulting in a low rate of denitrification and higher expenses for aeration needed for endogen respiration.

4 Nitrification by encapsulated nitrifiers

4.1 Demands for the encapsulation

Nitrification rates can be increased by specifically favouring those bacteria responsible for the biological oxidation of ammonia, namely *Nitrosomonas spec*. and *Nitrobacter spec*. These bacteria can be encapsulated for this purpose within a matrix. The microscopic bacteria become manageable by macroscopic means. The matrix used for this immobilisation procedure has to fulfil the following demands:

1. It must be permeable for the nutrients required by the microorganisms but it must hold back the enclosed bacteria effectively at the same time.
2. The material itself and the methods necessary to make a stable matrix must not harm the microorganisms irreversibly.
3. Since nitrification is a process mainly carried out by growing cells, the matrix must be flexible enough to allow the formation of colonies within the inner volume.
4. The material must be stable under the conditions of a WWTP, i.e., they must have resistance against mechanical forces and must also be resistant against biological degradation.
5. The resulting matrix particles must be small enough to prevent limitation effects resulting from means of diffusion which are too long.

A hydrogel on the basis of poylvinyl alcohol (PVA) meets all of these requirements. Different methods are known to produce stable hydrogels from PVA, but only the method of room-temperature gelation by controlled partial drying provides conditions mild enough to ensure good survival rates for susceptible nitrifiers. Due to their shape, the resulting particles are called LentiKats®.

4.2 Preparation of LentiKats®

For preparation of LentiKats® ready-to-use LentiKat®Liquid solution (geniaLab, Braunschweig, Germany) is mixed with a highly active fermentation broth of externally cultivated nitrifiers and small droplets are floored on a suitable surface. When these droplets are exposed to air, the water starts to evapo-

rate and thus leads to enhanced formation of hydrogen bonds. Once the hydrogel is stable enough, it is re-swollen in a stabilising solution.

The particles formed by this procedure combine the advantages of both large and small beads as can be seen from Figure 3: On the one hand, they measure about 3 to 4 mm in diameter and can be retained by established sieve technology or rapidly by settling. On the other hand, they are only 200 to 400 µm thick and thus cause hardly any diffusional limitations to the enclosed biocatalysts (Jahnz et al., 2001).

LentiKats® were successfully used for the immobilisation of microorganisms like *clostridia* (Wittlich et al., 1998) and *Oenococcus sp.* (Durieux et al., 2000) and also enzymes (Gröger et al., 2001). Initial results for the process of nitrification were also obtained in the past (Jekel et al., 1998) but those experiments were done with artificial media and not with real waste water as described in the present work.

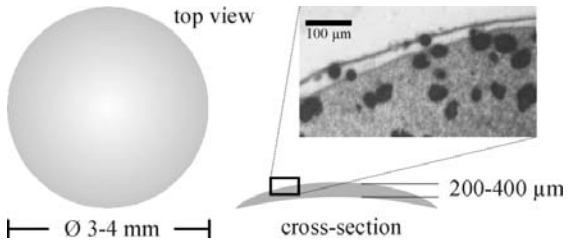

Figure 3:
Schematic view and image of a LentiKat® and microscopic view of nitrifier colonies within the hydrogel

5 Nitrogen elimination process with LentiKats®

The flow scheme of the lab-scaled process using LentiKats® is shown in Figure 4. The elimination of nitrogen is achieved by a post-de-nitrification process.

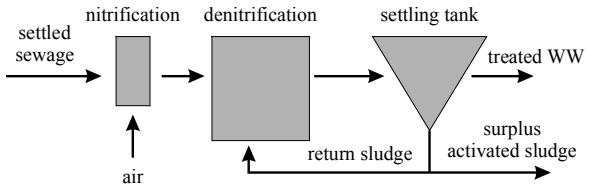

Figure 4:
Flow scheme of the laboratory set-up

A selective nitrification in the first stage of the process increases the efficiency of the process, which is catalysed by encapsulated nitrifying micro-organisms. Minimisation of BOD-removal in this stage by low concentration of heterotrophic micro-organisms is needed to ensure complete de-nitrification at the second stage by using the original BOD as an electron-donator. To minimise BOD removal in the first stage, no thickened sludge from clarifier would be cycled back to this stage. Therefore, this process should be called "pre-nitrification" instead of post-de-nitrification.

6 Experimental

Continuously driven lab scale experiments have been carried out with municipal wastewater. The volume of the reactors were 2.8 L and 9 L for the first and second stage, respectively. The wastewater was collected twice a week from a WWTP after primary settling and fed to the system via a continuously stirred tank of 1,000 L volume. The first reactor was filled with 800 g of LentiKats® equal to 1.5 L. This reactor for nitrification was continuously stirred and aerated. During the selected period of day 500 to day 650, the volumetric flow rate was about 120 L per day, which is equivalent to a hydraulic retention time in the first reactor of 34 minutes.

The main experimental parameters are shown in Table 2. The probes were collected as a spot check once a day. The flow rate of the inflow was measured by an inductive flow-meter, the pH with the instrument pH 91 and the electrode SenTix 50, dissolved oxygen and temperature with Oxi 96 and the electrode EO 96 (all equipment WTW, Germany). Different vessel tests were used to measure ammonia, nitrate and nitrite (MERCK, Darmstadt, Germany) and COD (HACH, Colorado, US). Dilution of 1:10 with demineralised water was done as necessary. After analysis, the probes from the last month were kept frozen to render possible reanalysis.

Table 2:
Main experimental results

	min	max	average
		inflow	
pH	6.88	8.45	7.5
NH_4^+, mg/L	1	191	46.3
COD, mg/L	9	278	74.6
		nitrification	
pH	5.2	8.4	6.9
NH_4^+, mg/L	0	75	11.5
NO_3^-, mg/L	14	58	30.8
NO_2^-, mg/L	0	5	1.8
COD, mg/L	7	121	53.2

7 Results

As shown in Figure 5, a nearly complete nitrification of ammonia to nitrate has been established with

an average volumetric reaction rate of about 45 mg nitrogen per litre reaction volume and hour. The hydraulic retention time was always at approx. 30 or 60 minutes. This is approx. 10 times lower than the conventional adjusted hydraulic retention times in aeration zones of sewage treatment plants.

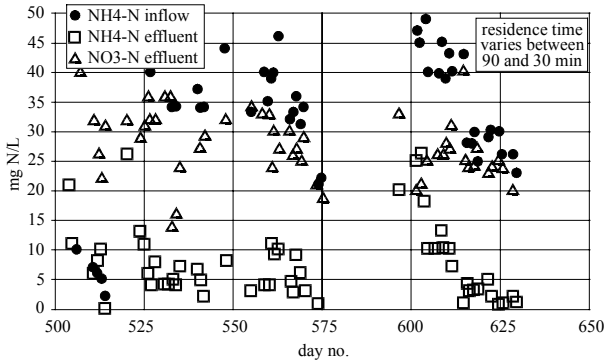

Figure 5:
Nitrification of ammonia

This figure also implies that nitrification could always be stable within a period of two years at present. Many disturbances, including an interruption of the treatment process have taken place, but never destructed the LentiKats®. Moreover, full treatment efficiency was in most cases reached at the next sampling period a day later. The high ammonia effluent at days 600 to 610 shows that maximum nitrification rate was reached with a specific volumetric nitrate production rate of approx. 25 to 30 mg/(L·h).

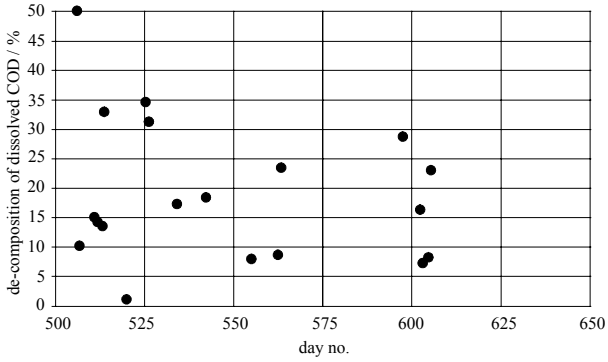

Figure 6:
Elimination of COD

To evaluate the COD elimination in this stage, the soluble COD was measured in influent and effluent. Figure 6 shows the COD degradation efficiency, which is between 10 and 50 %. Further optimisation is necessary to reduce COD degradation. However, this COD reduction does not include most of the particular COD and it is well known, that firstly a BOD uptake in heterotrophic microorganisms could take place, especially at high loading rates, and secondly, this BOD is usable for de-nitrification. Earlier experiments with acetic acid as BOD have shown that it is possible to fulfil a low dissolved COD-reduction of about 30 %.

8 Conclusions

Continuous lab scale experiments with encapsulated nitrifying microorganisms have shown a complete nitrification for more than 650 days. During that period, the nitrification operated stably, whether the denitrification was respective to the reactor design and operation due to the occurrence of floating sludge during that period.

The evaluation of lab results shows that it is possible to ensure complete nitrification by encapsulated nitrifiers with a hydraulic retention time of 0.5 hours, which is approx. 10 times lower than the the model sewage plant for the equivalent 100,000 people. Based on a flow rate of 24,500 m^3 per day, a nitrification reactor of 580 m^3 volume compared to common 5,000 to 7,000 m^3 has been calculated. However, this result has to be confirmed at pilot scale under realistic sewage treatment conditions onsite. It is expected that the efficiency of the process would decrease, but otherwise, there is also a high potential for optimisation of LentiKats® with much higher maximum reaction rates.

The results show also that the proposed process of de-nitrification after nitrification with LentiKats® would be possible due to low COD removal efficiency of 10 to 50 % in the nitrification reactor. This enables the internal use of wastewater's carbon sources for de-nitrification. However, the denitrification process has to be optimised with regard to kinetic study and avoidance of sludge flotation in final clarifier.

The energy consumption for aeration could be reduced substantially based on published results for different sludge ages for specific oxygen consumption for degradation of organic compounds. The reduction of the sludge age from 20 to less than 4 days would enable an energy reduction of 30 to 50 %. This needs to be investigated in pilot scale experiments.

References

Durieux A, Nicolay X, Simon J-P (2000), Continuous malolactic fermentation by *Oenococcus oeni* entrapped in LentiKats®, Biotechnol Lett 22(21):1679-1684

Gröger H, Capan E, Barthuber A, Vorlop K-D (2001) Asymmetric synthesis of an (R)-cyanohydrin using enzymes entrapped in lens-shaped gels. Organic Letters 3(13):1969-1972

Jekel M, Buhr A, Willke T, Vorlop K-D (1998) Immobilization of Biocatalysts in LentiKats®. Chem Eng Technol 21 (3):275-278

Jahnz U, Wittlich P, Pruesse, U, Vorlop K-D (2001), New matrices and bioencapsulation processes. In: Focus on Biotechnology Vol. 4, Hofmann M and Anne J (eds), Kluver Academic Publishers, Dordrecht, pp. 293-307

Wittlich P, Reimann C, Willke T, Vorlop K-D (1998), Bioconversion of raw-glycerol to 1,3-propanediol by immobilized bacteria. Biospektrum (special edition), p. 128

Biocatalytic asymmetric hydrocyanation in the presence of (R)-oxynitrilases entrapped in lens-shaped gels

Harald Gröger[1], Emine Capan[2], Anita Barthuber[3], and Klaus-Dieter Vorlop[2]

Dedicated to Dr. Stefan Weiss on the occasion of his 60th birthday

Abstract

This contribution contains a brief review of our results on the recent development of a cross-linked and subsequently polyvinylalcohol-entrapped (R)-oxynitrilase and its application in the asymmetric hydrocyanation. In the presence of this novel LentiKat®-entrapped oxynitrilase as a biocatalyst, and benzaldehyde as an aldehyde component, the desired (R)-mandelonitrile was obtained in good yields and with high enantioselectivities. This new type of immobilized lens-shaped biocatalyst has a well-defined macroscopic size in mm-range, and can be re-used efficiently.

1 Introduction

The fine chemicals industry is highly interested in efficient immobilization methods since immobilization offers a broad variety of advantages, e.g., easy catalyst separation and its reuse, simple work up procedures, stabilization of the biocatalyst and so on. Although numerous immobilization methods have been reported so far, only a few of them were applied on technical scale – In spite of the high potential of immobilized biocatalysts, in a United Nations publication (Klyosov 1989), only eight industrial processes have been reported which are based on immobilized enzymes or microbial cells. The manufacture of 7-aminocephalosporanic acid represents (probably) the most important industrial process which is based on the use of an immobilized enzyme. – which indicates the need for more efficient immobilization technologies.

Recently, a promising, industrially feasible immobilization concept for cells was reported by the Vorlop group (Jekel et al. 1998, Wittlich et al. 1999a & b, Welter et al. 1999) This immobilization is based on the entrapment of cells in a hydrogel matrix consisting of polyvinylalcohol. This method, which has been commercialized by geniaLab® (geniaLab 2001), represents a cheap and efficient immobilization technique. In addition, a negligible catalyst leaching is observed, and macroscopically well-defined and flexible lens-shaped particles with a high activity are obtained (type: LentiKats®; diameter: 3 - 5 mm; thickness: 300 - 400 mm). Several successful applications of this concept were already reported by Vorlop and co-workers (Wittlich et al. 1999b, Welter et al. 1999) and Durieux et al. 2000, e.g. for the synthesis of itaconic acid and 1,3-propanediol. Further advantages are that these lens-shaped hydrogels, which can be easily separated, show no abrasion and have a minimized diffusion limitation due to a low thickness of < 0.5 mm. We envisioned that this immobilization concept could be extended to a suitable immobilization method for enzymes in general, and oxynitrilases in particular. Oxynitrilases represent versatile biocatalysts for the preparation of optically active cyanohydrins which find a wide range of pharmaceutical and agrochemical applications (Effenberger 1994a & b, Gregory 1999, Gröger 2001, Hamashima et al. 2000). For example, (R)-mandelic acid - a derivative of (R)-mandelonitrile - represents a fine chemical which is produced on multi-hundred ton scale.

Several substituted optically active (R)-mandelic acids are intermediates in the synthesis of pharmaceuticals. In addition, the (S)-enantiomer of phenoxybenzyladehyde cyanohydrin represents an intermediate in the production of enantiomerically pure pyrethroids which are used as insecticides. A graphical summary of cyanohydrin applications is given in Figure 1.

The immobilization of oxynitrilases as biocatalysts for the synthesis of chiral cyanohydrins has been known for a long time. However, many of those immobilization methods for oxynitrilases have practical problems on a large scale – Among the main problems of immobilized methods are the non-satisfied long-term stability, catalyst leaching, abrasion of the immobilisate, and a wide particle distribution (instead of a well-defined macroscopic size) in the case of powdered immobilisates –. In the following, we report a summary of our results on the first development of LentiKat®-entrapped enzymes (here: oxynitrilases)

[1] Harald Gröger, Degussa AG, Project House Biotechnology, Rodenbacher Chaussee 4, 63457 Hanau-Wolfgang, Germany
[2] Emine Capan and Klaus-Dieter Vorlop, Institute of Technology and Biosystems Engineering, Federal Agricultural Research Centre (FAL), Bundesallee 50, 38116 Braunschweig, Germany
[3] Anita Barthuber, Degussa AG, R&D Department FC-AG-RD, Dr.-A.-Frank-Str. 32, 83308 Trostberg, Germany

and their application in the asymmetric biocatalytic synthesis of (R)-mandelonitrile (Gröger et al. 2001a & b, Capan et al. 2001).

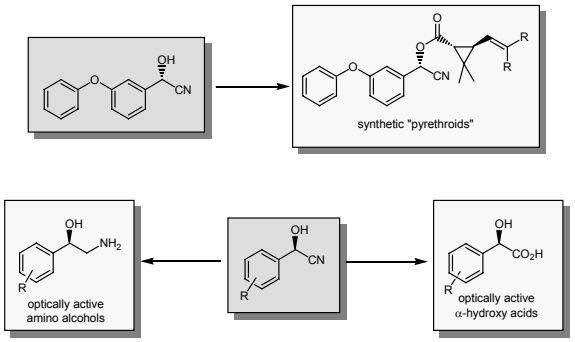

Figure 1:
Graphical summary of cyanohydrin applications

2 Results and Discussion

2.1 The concept for entrapping oxynitrilases

For our studies we used a non-purified (R)-oxynitrilase purchased from ASA Spezialenzyme GmbH, Braunschweig for economic reasons. This oxynitrilase has a specific activity of 13.6 U/mg protein, and an amount of protein of 7.6 mg/mL. In order to prepare an efficiently entrapped oxynitrilase, a two-step procedure was chosen. In a first step, a cross-linking process was carried out which led to an increased molecular weight of the (cross-linked) enzymes. This cross-linking procedure is necessary since enzymes with a molecular weight of max. 50,000 (as in case of oxynitrilases) would not be restrained in the hydrogels. At first the cross-linking process was carried out with glutaraldehyde only, but the resulting cross-linked enzymes showed a drastically decreased activity. Probably the enzyme is deactivated under those conditions. However, a combination of glutaraldehyde and chitosan led to an improved cross-linked enzyme which showed 89 % of its native activity.

In a subsequent step, this cross-linked enzyme was entrapped in a hydrogel matrix which is (mainly) based on polyvinylalcohol. After entrapping the cross-linked oxynitrilase 65 % of its activity remains. The concept of this two-step immobilization method is shown in Figure 2 (Gröger et al. 2001). These lens-shaped hydrogels are highly elastic and flexible towards mechanical treatment.

The general protocol for the preparation of (R)-oxynitrilase-containing, lens-shaped PVAL-hydrogels reads as follows: The cross-linking step of the (R)-oxynitrilase was carried out using chitosan and glutardialdehyde. At first 1.5 g of chitosan are dissolved in 98.5 g acetic acid solution (0.5 %), and 1 M NaOH are added until a pH 5.5 has been obtained. Subsequently 7.89 g of a non-purified oxynitrilase solution (60 mg protein; purchased from ASA Spezialenzyme GmbH, Braunschweig; specific activity: 13.6 U/mg protein; amount of protein: 7.6 mg/mL) are added to 4 g of the chitosan solution. The resulting mixture was treated with 200 µL of a glutardialdehyde solution (50 %; pH 5.5). After stirring for 16 h at 4 °C the cross-linked (R)-oxynitrilase (after centrifugation) is entrapped in LentiKat® by addition of 2.07 g of the chitosan/glutardialdehyde-crosslinked enzyme solution and 7.9 g of water to 74 g of LentiKat®Liquid (a polyvinylalcohol-containing aqueous solution which is commercially available from geniaLab; geniaLab 2001).

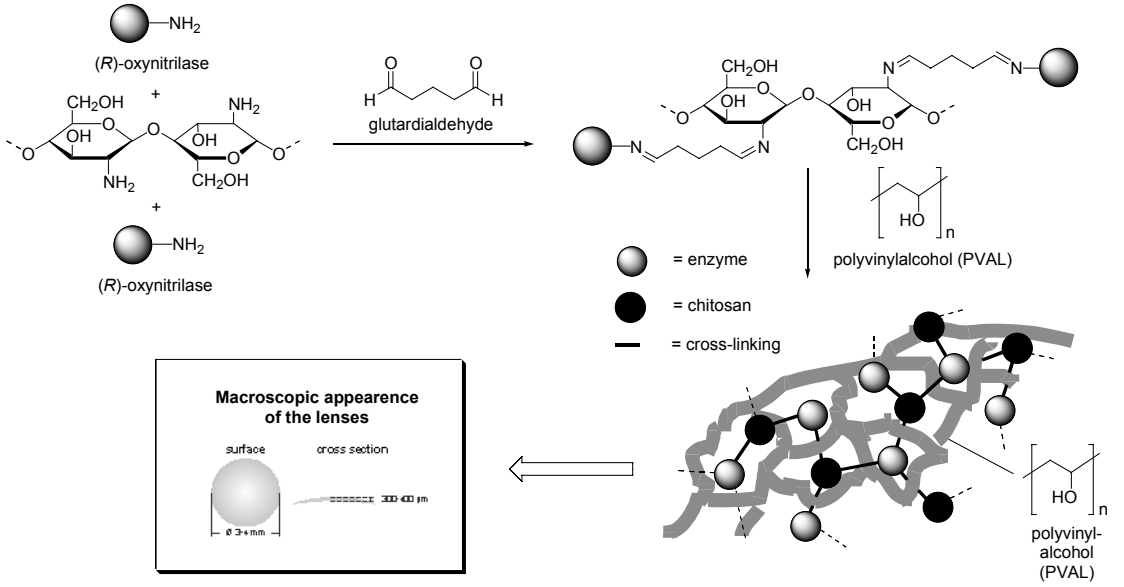

Figure 2:
Scheme of the two-step immobilization method inside LentiKats®

The lens-shaped gels are obtained after dropping the polymeric suspension on a plate using a LentiKat®-printer. For further details on the steps of preparation of the lenses, see Jekel et al. 1998, Wittlich et al. 1999a & b, Welter et al. 1999, Durieux et al. 2000, and geniaLab 2001. The entrapped (R)-oxynitrilases have been obtained on highly elastic, lense-shaped gels with a defined diameter of 3 to 5 mm. The activities of the lenses varied between 8 and 40 U per g lenses. A picture of the shape of those polyvinylalcohol-based lenses is given in Figure 3. The lens-shaped, oxynitrilase-containing catalyst shows a well-defined particle diameter of 3 or 5 mm and a thickness of 0.3-0.4 mm. Further physical properties of such type of lens-shaped hydrogels in general have been described earlier (Jekel et al. 1998, Wittlich et al. 1999a, Welter et al. 1999).

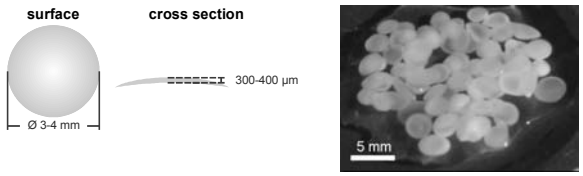

Figure 3:
Scheme and photo of LentiKats®

2.2 Properties of entrapped (R)-oxynitrilases in LentiKats®

A potential catalyst leaching was investigated with respect to the dehydrocyanation reaction of mandelonitrile (in general, the catalytic activity of oxynitrilases is determined via this cleavage reaction of mandelonitrile). A photometrical determination of the reaction course showed that no catalyst leaching occurs after a stirring time of up to 143 h. This conclusion was supported by the (nearly) identical course of the enzyme activities determined from the reactions with "fresh" hydrogels and hydrogels after stirring for 143 h, respectively. For more details regarding this investigation see (Gröger et al. 2001b and Capan et al. 2001). In conclusion, a catalyst leaching or a decrease of the catalyst activity due to a deactivation process was not observed.

2.3 Hydrocyanation with entrapped (R)-oxynitrilases in aqueous media

The lens-shaped oxynitrilases have subsequently been applied as a biocatalyst for the reaction at a low pH of pH 3.75 in aqueous media. The low pH is required in order to prevent the formation of the racemic mandelonitrile which would led to lower enantioselectivities. This effect has been described previously by Kula and co-workers in detail (Niedermeyer and Kula 1990a & b).

In the presence of the cross-linked and subsequently entrapped oxynitrilases, the hydrocyanation in aqueous media at a low pH proceeds well, leading to the desired optically active product (R)-mandelonitrile with an high enantioselectivity of > 99 % ee (Figure 4 and Figure 5, batch 1, see also Capan et al. 2001).

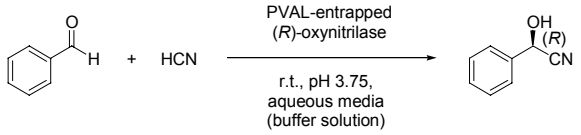

Figure 4:
Reaction scheme for the enzymatic conversion of benzaldehyde to (R)-cyanohydrin in aqueous media

As a next step, the long-term stability and the recycling abilities – a crucial economical criterion – have been investigated. We were pleased to find that the lens-shaped PVAL-entrapped oxynitrilases can be re-used repeatedly in at least 9 batches (Capan et al. 2001). It is noteworthy that the enantioselectivity remained unchanged at high 99 % ee (Figure 5).

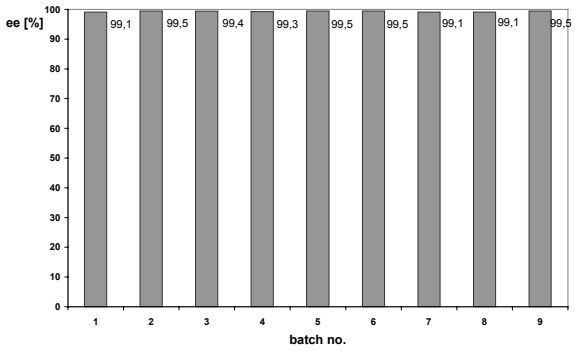

Figure 5:
Long-term stability of the PVAL-entrapped oxynitrilase in aqueous media

2.4 Hydrocyanation with entrapped (R)-oxynitrilases in a biphasic media

Another interesting concept of biocatalytic hydrocyanation reactions is based on a biphasic reaction system, consisting of a water-immiscible organic phase and an aqueous phase, as a reaction media. The presence of an organic solvent guarantees a high enantioselectivity in spite of carrying out the reaction at higher pH values (Effenberger et al. 1987a & b, Griengl et al. 1997, Loos et al. 1995). This beneficial effect of an organic solvents, found by Effenberger in 1987, is due to the fact that the formation of the undesired racemic mandelonitrile is supressed under those conditions (Effenberger et al. 1987a & b). The appli-

cation of biphasic reaction systems for the asymmetric hydrocyanation using oxynitrilases was reported by Griengl et al. 1997 for (S)-oxynitrilases, and Loos et al. 1995 for (R)-oxynitrilases, respectively.

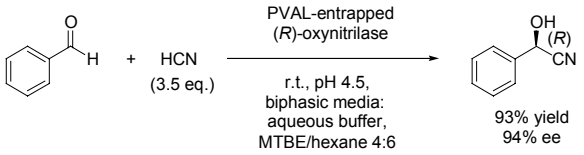

Figure 6:
Reaction scheme for the enzymatic conversion of benzaldehyde to (R)-cyanohydrin in a biphasic media

In the presence of the cross-linked and subsequently entrapped oxynitrilase-catalyst (with an activity of 8.16 U per g lenses) at pH 4.5 in a biphasic system, the desired product (R)-mandelonitrile was obtained in 93 % yield and with 94 % ee (Figure 6, Gröger et al. 2001a & b). The general procedure for the asymmetric hydrocyanation using oxynitrilases entrapped in lens-shaped gels reads as follows: To a solution of the PVAL-entrapped (R)-oxynitrilases (lens-shaped capsules; g lenses per mmol substrate: entries 2 and 4-5, 1.84 g; entry 3, 3.67 g; entry 6, 2.47 g) in 4 mL of a citric buffer, subsequently 4 mL of the organic solvent, 1 mmol of benzaldehyde, and 3.5 mmol of HCN (as an 20 % aqueous solution) are added. After stirring the reaction mixture for two hours, the organic layer is separated, and the aqueous layer is washed with 2 x 20 mL MTBE (subsequently, the aqueous layer is treated with NaOCl solution in order to decompose HCN which has been used in excess amount). The organic phases are dried over magnesium sulfate, and after filtration the volatile materials are removed in vacuo. The product (R)-mandelonitrile is obtained with a purity of > 90-95 % (in some cases of up to 99 %).

It is noteworthy that this result is comparable to the one obtained with "free" oxynitrilases. Thus, in spite of modifying the enzyme by cross-linking and entrapping a comparable synthetic, results with respect to enantioselectivity and yield were obtained with "free" and PVAL-entrapped oxynitrilases, respectively (Gröger et al. 2001a & b).

The "catalyst loading" of the entrapped oxynitrilase has an influence on the reaction course of the asymmetric hydrocyanation. When using an entrapped oxynitrilases with a somewhat higher catalyst loading of 40 U per g lens, a yield of 74 % yield and slightly decreased 91 % ee were obtained. In addition, the organic solvent plays an important role. Under optimized conditions an enantioselectivity of 99 % ee can be obtained when carrying out the reaction in a biphasic media with diisopropylether as an organic solvent (Gröger et al. 2001b).

As in case of the study in an aqueous media, investigation with respect to the recycling abilities of the entrapped oxynitrilases were carried out in a biphasic media. In total, the lens-shaped hydrogels were recycled 20 times without a decrease of enantioselectivity (Figure 7, Gröger et al. 2001b). In contrast, the ee slightly increased from 91 % ee to 95 % ee which might be due to an increased stabilization of the enzyme within the hydrogel matrix. The yield remains in the same range of ca. 80 %. It is further noteworthy that the oxynitrilase-containing hydrogels do not change their elasticity, size and flexibility.

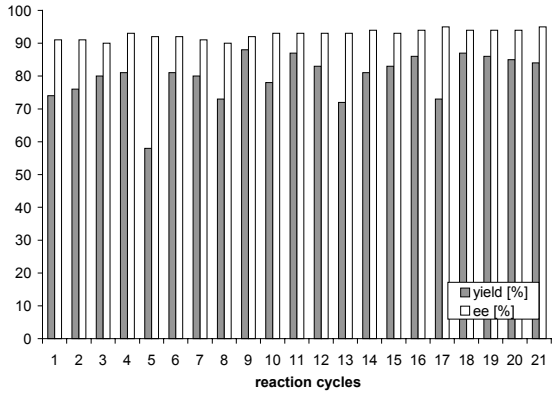

Figure 7:
Long-term stability of the PVAL-entrapped oxynitrilase in a biphasic system

3 Conclusions

In conclusion, a cross-linked and subsequently PVAL-entrapped oxynitrilase catalyst was developed and applied successfully for the asymmetric hydrocyanation of benzaldehyde. These new LentiKat®-entrapped oxynitrilases show the following properties:

- Macroscopic well-defined size (diameter in mm-range)
- High yields, and high enantioselectivity of up to 99 %
- High synthetic efficiency
- Recyclable without loss of enzymatic activity
- Suitable for technical reactors due to high elasticity
- Leaching of the oxynitrilase has not been observed
- Encapsulation materials are cheap and non-toxic
- Simple encapsulation protocol.

Thus, the asymmetric biocatalytic hydrocyanation via LentiKat®-entrapped oxynitrilases represents an attractive access to the commercially important optically active mandelonitrile.

Acknowledgements

The authors are grateful to Dr. Stefan Buchholz, Dr. Benedikt Hammer, Dr. Reinhard Kröner, and Dr. Stefan Weiss, for their support and help in connection with this project.

References

Capan E, Vorlop K-D, Barthuber A, Gröger H (2001) BioTrans 2001: The 5th International Symposium on Biocatalysis and Biotransformation (September 2nd-7th 2001), TU Darmstadt

Durieux A, Nicolay X, Simon J-P (2000) Continuous malolactic fermentation by *Oenococcus oeni* entrapped in LentiKats®. Biotechnol Lett 22:1679-1684

Effenberger F (1994a) Synthese und Reaktionen optisch aktiver Cyanohydrine. Angew Chem 106:1609-1619

Effenberger F (1994b) Synthesis and reactions of optically-active cyanohydrins. Angew Chem Int Ed Engl 33:1555-1564

Effenberger F, Ziegler T, Förster S (1987a) Enzym-katalysierte Cyanhydrinsyntehse in organischen Lösungsmitteln. Angew Chem 99:491-492

Effenberger F, Ziegler T, Förster S (1987b) Enzyme-catalyzed cyanohydrin synthesis in organic solvents. Angew Chem Int Ed Engl 26:458-460

geniaLab (2001) Product information about LentiKats®, http://www.geniaLab.de

Griengl H, Hickel A, Johnson DV, Kratky C, Schmidt M, Schwab H (1997) Enzymatic cleavage and formation of cyanohydrins: a reaction of biological and synthetic relevance. Chem Commun 1933-1940

Gregory RJH (1999) Cyanohydrins in nature and the laboratory: Biology, preparations, and synthetic applications. Chem Rev 99:3649-3682

Gröger H (2001) Enzymatic routes to enantiomerically pure aromatic alpha-hydroxy carboxylic acids: A further example for the diversity of biocatalysis. Adv Synth Catal 343:547-558

Gröger H, Vorlop K-D, Capan E (2001a) Method for producing optically active cyanhydrins. PCT Pat. Appl. WO01/38554

Gröger H, Capan E, Barthuber A, Vorlop K-D (2001)) Asymmetric synthesis of an (R)-cyanohydin using enzymes entrapped in lens-shaped gels. Org Lett 3:1969-1972

Hamashima Y, Kanai M, Shibasaki M (2000) Catalytic enantioselective cyanosilylation of ketones. J Am Chem Soc 122:7412-7413

Jekel M, Buhr A, Willke Th, Vorlop K-D (1998) Immobilisation of biocatalysts in LentiKats. Chem Eng Technol 21:275-278

Klyosov AA (1989) Report, UNIDO/IPTC. 93, V-89-61316; Order No. PB90-210360

Loos WT, Gelluk HW, Ruijken MMA, Kruse CG, Brussee J, van der Gen A (1995) Synthesis of otically-active cyanohydrins using R-oxynitrilase in a liquid-liquid biphasic system. 1. An industrial useful procedure. Biocatal Biotransform 12:255-266

Niedermeyer U, Kula MR (1990a) Enzym-katalysierte Synthese von (S)-Cyanhydrinen. Angew Chem 102:423-425

Niedermeyer U, Kula MR (1990b) Enzyme-catalyzed synthesis of (S)-cyanohydrins. Angew Chem Int Ed Engl 29:386-387

Welter K, Willke Th, Vorlop K-D (1999) Production of itaconic acid by LentiKats®. SchrR Nachwachsende Rohstoffe 14:520-521

Wittlich P, Schlieker M, Jahnz U, Willke Th, Vorlop K-D (1999a) Bioconversion of raw glycerol to 1,3-Propanediol by immobilized bacteria. Proceed. 9th Eur Congr Biotechnol No. P2762, ISBN 805215-1-5

Wittlich P, Schlieker M, Lutz J, Reimann C, Willke Th, Vorlop K-D (1999b) Bioconversion of glycerol to 1,3-propanediol by LentiKats®. SchrR Nachwachsende Rohstoffe 14:524-532

Aerial conidia of *Metarhizium anisopliae* subjected to spray drying for encapsulation purposes

Andrea Horaczek and Helmut Viernstein[1]

Abstract

This research deals with the preservation and formulation of an isolate of an entomopathogenic fungus. The suitability of spray drying as formulation technology for *Metarhizium anisopliae* BIPESCO 5 was tested. Therefore, an aqueous binary mixture composed of skim milk and polyvinylpyrrolidone (PVP K90) was evaluated as a means of preserving and encapsulating conidia. Due to the formulation technology it was possible to encapsulate the fungal propagules resulting in a dust free, water soluble/oil dispersible formulation for spray application.

The influence of different inlet/outlet temperature adjustments and the composition of the carrier system were investigated due to their influence on spore viability. Results of spray drying experiments showed that air outlet temperatures up to 53°C resulted in a slight reduction of approximately 3 % of the conidial viability. Maintaining these operating conditions resulted in microcapsules of germination rates of 76 % and moisture contents of 18.11 to 21.22 %. Microencapsulated conidia were subjected to storage tests with and without the addition of silica gel capsules at various temperatures. Results showed that survival was inversely related to the storage temperature and residual moisture levels. The highest survival rates of stored conidia were observed at moisture contents of 3 % and a temperature of 6°C. Moreover, production characteristics like entrapment efficacy, shape and size were investigated.

The results show that spray drying is a possible encapsulation technology for aerial conidia of *Metarhizium anisopliae* resulting in highly concentrated spray dried powders with 76 % viability.

Keywords: Metarhizium anisopliae, formulation, spray drying, encapsulation, skim milk, PVP K90, shelf life

1 Introduction

There is great interest in the use of entomopathogenic fungi as biocontrol agents to avoid the negative effects of chemical pesticides. The range of target pests of *Metarhizium anisopliae* includes *Coleoptera* and *Lepidoptera* (Copping, 1998). Entomogenous fungi may be introduced in the field as conidia, mycelial fragments or blastospores (Li et al., 1993; Butt et al., 1994). Environmental conditions like sunlight, temperature, humidity, substratum and chemical pesticides, however, all influence the stability, sensitivity and persistence of these propagules. Therefore, the widespread acceptance and use of mycoinsecticides will depend on the improvement of the environmental stability of the pathogen by the development of appropriate formulations. To make biocontrol agents competitive, the formulation must enhance virulence, extend the shelf life of the active agent, improve efficacy of application, prolong field persistence and moreover must be cost efficient (Butt et al., 1999). Therefore, the formulation process must be carefully designed for the particular requirements and limitations of an organism (Rhodes, 1993).

From the great variety of formulation technology, the authors chose spray drying to convert the propagules in practical formulations. Although most often considered a dehydration process, spray drying can also be used as an encapsulation method when it entraps 'active' material within a protective matrix. Compared to other conventional microencapsulation techniques it offers the attractive advantage of producing microcapsules in a relatively simple, inexpensive, continuous processing operation (Ré, 1998). However, there are obviously challenges associated with using spray drying to formulate microorganisms, including the requirements that the processed organisms have to survive the temperatures occurring during the process.

In the present study, a spray drying process was developed which allowed the encapsulation of conidia of *Metarhizium anisopliae*. A mixture of skim milk and polyvinylpyrrolidone was used as carrier vehicle. Skim milk was chosen because it is a well known membrane stabiliser during cryopreservation. Furthermore, milk proteins possess numerous functional properties, i.e., solubility, emulsification, film formation, the ability to interact with water, small ions and other polymers that are desirable for a wall material. Furthermore, skim milk also exhibits UV-protection (Burges, 1998). Burges (1998) also mentioned the second component of the carrier matrix, PVP, as a protective colloid. Furthermore, Millqvist-Fureby

[1] Andrea Horaczek and Helmut Viernstein, University of Vienna, Institute of Pharmaceutical Technology and Biopharmaceutics, Althanstraße 14, 1090 Vienna, Austria

(1999) observed the tendency of PVP combined with other polymers to form the continuous phase during the spray drying process, resulting in a better protection of the sensitive biological material due to the protection from interactions with the spray-droplet surface.

The aim of the present study was to optimise the spray drying process as a formulation method for the production of preparations guaranteeing a higher environmental stability, an easy application method and a prolonged shelf life for the contained pathogen.

2 Materials and methods

2.1 Fungal isolate

Metarhizium anisopliae (BIPESCO 5) was supplied by Prophyta Biologischer Pflanzenschutz GMBH (Malchow/Poel, Germany) at 4.7 x 1010 CFU g^{-1} dry spores.

2.2 Preparation of fungal dispersions for spray drying

1 g conidia of *Metarhizium anisopliae* was dispersed in 99 ml of an aqueous 0.1 % sterile TWEEN 80 (Merck; Darmstadt, Germany) solution. With the help of a Thoma haemocytometer, the number of spores per ml was specified. The suspension contained $4.3x10^8$ spores ml^{-1}. The carrier matrix used for the encapsulation of the conidia was composed of two aqueous solutions. The solutions were prepared with skim milk (10 % w/v; Merck; Darmstadt, Germany) and polyvinylpyrrolidone PVP K90 (10 % w/v; Fluka; Buchs, Switzerland). The skim milk solution was sterilised at 120°C for 15 min and PVP K90 was added to sterilised water. 10 ml of the fungal suspension were mixed with 90 ml of the carrier matrix solution consisting of 45 ml of skim milk and 45 ml of PVP K90 solutions. The polymer/fungus compatibility was verified just before the process of microencapsulation. The mixtures of the carrier matrix were continuously stirred when subjected to spray drying. The experiment was performed in triplicate.

2.3 Spray drying technique

The fungal dispersions were spray dried with a laboratory scale spray dryer (model Büchi mini spray dryer; Flawil, Switzerland) equipped with a 0.7 mm nozzle by adjusting air-flow to 700 Nl/h and aspirator setting to 35 m^3/h. The inlet temperature, the flow rate of feed suspension and the composition of the carrier matrix were varied. The microcapsules precipitated into the collecting flask were harvested and stored in polypropylene flasks (Semadeni; Vienna, Austria) with and without the addition of silica gel capsules.

2.4 Effect of different inlet/outlet temperatures on the viability of fungal propagules

The influences of five different outlet/inlet temperature regimes were investigated due to their influence on the conidial germination behaviour. Therefore, the spore suspensions were exposed to inlet temperatures of 40, 60, 80, 100 and 120°C during the spray drying process. The feeding rate of the spore solution varied from 3 to 10 ml min^{-1} depending on the increase of the inlet temperature to keep the outlet temperature as low as possible but avoiding condensation in the spray dryer. The development of the outlet temperature was monitored. The moisture content and the germination rate were examined directly after the spray drying process. The assay was performed in triplicate.

2.5 Effect of the carrier matrix composition on the viability of fungal propagules

In order to investigate the membrane stabilising function of each component of the carrier matrix, spray drying experiments were carried out with conidia dispersed in aqueous solutions of skim milk (5 % w/v) or PVP K90 (5 % w/v). Therefore, 5 ml of the conidia suspension were mixed with 45 ml skim milk or PVP K90 solution. The resulting suspensions were subjected to the following inlet temperatures: 40, 60, 80, 100 and 120°C. The feeding rate of the spore solution varied from 3 to 10 ml min^{-1}. The development of the outlet temperature was monitored. After spray drying the germination rate was determined. The assay was performed in triplicate.

2.6 Viability test

Spray dried conidia were dispersed in an 0.1 % aqueous Tween 80 (Merck) solution. Afterwards 50 µl of the resulting suspension were spread on agar plates (1 % glucose, Merck; 0.5 % peptone, Merck; 1.5 % agar, Merck; and 0.5 % yeast extract, Oxoid; amended with 30 mg l^{-1} of streptomycin sulphate, Merck; and 50 mg l^{-1} of chloramphenicol, Merck) and incubated for 24 hours at 25°C. The viability of 300 spores was assessed after staining with lactophenol cotton blue using a Nikon 104 light microscope. Only spores with germ tubes longer than their width were considered to have germinated.

2.7 Microcapsule characterisation

2.7.1 Microscopic studies

Scanning electron microscopy (SEM) was performed on a Zeiss DSM 940 scanning electron microscope. This technique was used to investigate the microstructure properties and particle size of spray dried products. Specimens were sputtered with gold. The operating conditions for the electron microscope were: 9 mm working distance and 10 kV acceleration voltage.

The SEM work was performed at the Centre for Ultrastructure Research of the University of Agricultural Sciences Vienna, Austria.

Optical microscopy was also used to check the shape and the particle size of the batches. A Nikon 104 light microscope was used. Therefore, 0.1 g of the specimens were dispersed in 100 ml of a non-solvent, in this case paraffin, sonicated and stirred for 5 minutes and afterward investigated at a x 400 magnification. 100 particles of each sample were characterised. The size distribution was expressed in percent. Prior a calibrated stage micrometer was used to calibrate the ocular micrometer.

To check the encapsulation efficacy, fluorescence microscopy was performed. Therefore, conidia were incubated with flourescein isothiocyanat (FITC) (Sigma-Aldrich; Vienna, Austria) prior to spray drying. 8 mg conidia were dispersed in 4 ml 0.1 M Na_2CO_3 (Merck; Darmstadt, Germany). Afterward 200 µl of a solution of FITC dissolved in DMSO (2.5 mg/ml) were added. The conidia were incubated at 4°C over night. Then the conidia were separated by centrifugation at 10.000 g and washed three times with an aqueous 0.1 % Tween 80 solution. The resulting labelled conidia were subject to spray drying.

2.7.2 Dissolution and dispersing profile of the microcapsules

In a 250 ml beaker 100 mg of the specimens were put into tap water (4°C) or paraffin (Kwizda; Vienna, Austria) and stirred continuously with a magnetic stirrer. Furthermore, the property of skim milk to act as an emulsifying agent was assessed.

2.8 Residual moisture content of microcapsules

These measurements were made with a moisture analyser (Sartorius MA 30, Sartorius; Göttingen, Germany). The residual moisture was obtained after drying a sample of 0.1 g at 130°C, and was expressed as a percentage. The water desorption kinetics varied according to the sample (from 0 to 99 min).

2.9 Evaluation of storage stability

Microcapsules produced by spray drying at a constant air outlet temperature of 80°C were stored with or without the addition of silica gel capsules at different temperatures (6, 20 and 30°C). The viability was assessed over a period of 3 months.

2.10 Statistical analysis

Statistical analysis was carried out with Statgraphics® Plus 4.0 for Windows. For analysis of the spore viability, arcsine√p-transformed data of percentage germination were analysed using one-way analysis of variance (ANOVA). When homogeneity of variance was achieved by a Hartlett's test ($P < 0.05$), the Fisher's least significant difference procedure ($P < 0.05$) was used to separate means of transformed data.

3 Results and discussion

3.1 Effect of different inlet/outlet temperatures on the viability of fungal propagules

High temperatures and thermal stress are extremely detrimental to *Metarhizium anisopliae*. Therefore, the initial spray drying experiments were performed to determine the outlet temperature optimum for spore viability. The authors noted that the spraying conditions had an effect on spore viability and the residual moisture of the microspheres obtained. Results demonstrate that the outlet air temperature is the most important parameter to be varied. It is a function of inlet air temperature, the delivery rate of sample dispersions and the aspirator capacity. The effects of various inlet and outlet temperatures on the viability and water content of microencapsulated conidia of *Metarhizium anisopliae* are given in Table 1. The survival decreases as the outlet temperature increases. Spores show germination rates of 72 and 0.7 %, at inlet/outlet temperatures of 40/30°C and 120/75°C, respectively.

3.2 Effect of the carrier matrix composition on the viability of fungal propagules

In order to investigate the membrane stabilising function of each excipient of the carrier matrix system, the spray-drying experiments were carried out with conidia dispersed exclusively in PVP K90 (5 % w/v) solutions or skim milk (5 % w/v) solutions. Reflected from the germination rates given in Table 2, only skim milk shows a membrane stabilising function for the fungus. Also Stephan (1998) showed the

Table 1
Conditions of the spray drying process and the effect of inlet and outlet temperatures on the water content of the spray dried powders and on the viability of aerial conidia of BIPBESCO 5, suspended in skim milk (5 % w/v) and PVP K90 (5 % w/v) solutions. Control: untreated conidia.

Inlet, °C	Outlet, °C	Suspension feed, ml/min	Mean germination at 24 h		Moisture content	
			%	± SEM [a,b]	%	± SEM [a]
Control			79.38	2.50a		
40	28 ± 2	3	72.0	2.59a	21.22	2.38
60	40 ± 2	5	67.3	2.45a	20.06	1.95
80	50 ± 3	6	75.8	2.00a	18.11	2.38
100	62 ± 2	8	13.5	2.57b	14.29	1.68
120	75 ± 2	10	0.7	2.57c	13.40	1.68

[a] Standard error of the mean for three assays.
[b] Means of the arcine√p-transformed data within a column followed by the same letter are not significantly different following Fisher's least significant difference procedure ($P < 0.05$).

excellent protective function of skim milk for submerged spores subjected to spray drying and Gardiner (2000) reported high viability levels for lactic acid bacteria embedded in skim milk matrices via spray drying. Encapsulation with skim milk results in germination percentages of 64 % to 1 % at inlet temperatures ranging from 40°C to 120°C.

PVP K90 provided insufficient protection against the membrane damages. In comparison to spray drying experiment carried out with skim milk viability, rates of 35 % were obtained at an inlet temperature of 40°C and only 6 % of the conidia remained viable when subjected to 80°C. These results demonstrate clearly that that PVP K90 is an insufficient protectant.

Table 2
Comparison of different carrier materials according to their protective function at different temperature regimes. Control: untreated conidia of 79.38 % viability

Inlet, °C	Outlet, °C	Carrier matrix	Mean germination at 24 h	
			%	± SEM [a,b]
40	28 ± 2	SM/PVP K90	72.0	2.59a
40	28 ± 2	SM	63.8	2.94a
40	28 ± 2	PVP K90	34.9	3.57b
60	40 ± 2	SM/PVP K90	67.3	2.45a
60	40 ± 2	SM	75.6	2.77a
60	40 ± 2	PVP K90	40.3	3.57b
80	50 ± 3	SM/PVP K90	75.8	2.00a
80	50 ± 3	SM	84.7	3.39a
80	50 ± 3	PVP K90	5.6	2.91b
100	62 ± 2	SM/PVP K90	13.5	2.57a
100	62 ± 2	SM	27.9	3.39b
100	62 ± 2	PVP K90	1.2	2.91c
120	75 ± 2	SM/PVP K90	0.7	2.57a
120	75 ± 2	SM	1.0	3.14a
120	75 ± 2	PVP K90	0.0	3.57a

[a] Standard error of the mean for three assays.
[b] Means of the arcine√p-transformed data within a column followed by the same letter are not significantly different following Fisher's least significant difference procedure ($P < 0.05$).

But PVP exhibits the following functional properties useful for a formulation for spray application: adhesiveness, binding power, film formation, affinity to hydrophilic and hydrophobic surfaces and it increases viscosity (Bühler, 2001).

3.3 Microcapsule characterisation

3.3.1 Microscopic studies

The outer structure of the spray dried particles was investigated by scanning electron microscopy. The surface of capsules showed surface dents reported for spray dried skim milk powders. This behaviour had been attributed to the effect of conditions of atomisation and drying on casein. Furthermore, spherical indentations were visualised that have been observed on the surface of PVP K90 particles. The scanning electron micrographs of the composite particles revealed that the particle size was relatively uniform, ranging between 3 µm and 30 µm. Furthermore, conidial presence could not be detected on the surface of the microcapsules (Figure 1).

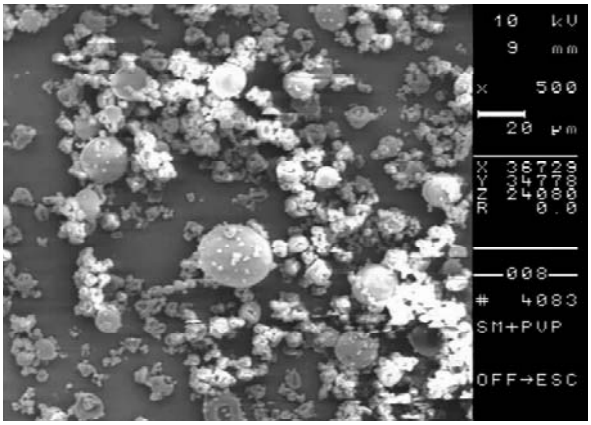

Figure 1:
Scanning electron imagine of conidia (0.01 % w/w) embedded in a matrix composed of a mixture of skim milk and PVP K90 in the ration 1:1. The conditions to operate the microscope were: working distance 9 mm and acceleration voltage 10 kV

Optical microscopy allowed visualisation of the spherical character of the microparticles. Microscopical particle analysis showed that 72 % (s = ± 4 %) of the microcapsules were within the range of 10-17 µm. As the average diameter of conidia is approximately 6 µm, the spray dried particles are large enough to accommodate spores.

Fluorescence microscopy revealed the good encapsulation property of the used carrier system. Skim milk and polyvinylpyrrolidone are both known for their functional property to form films (Bühler, 2001). With the help of this technique, the eccentric position of the conidia in the microcapsules could be visualised as it is shown in Figure 2.

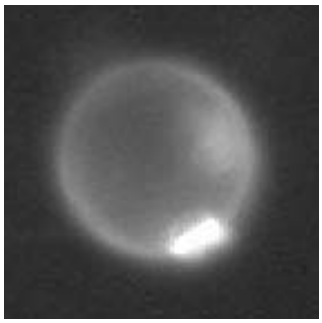

Figure 2:
Microencapsulated FITC labelled conidium of *Metarhizium anisopliae*. Diameter of microcapsule 9 µm.

3.3.2 Dissolution and dispersing profile of the microcapsules

Due to the solubility of the used matrix material, the spray dried powder has the property to dissolve in water, resulting in a burst release of microencapsulated conidia and to disperse in oil based carriers resulting in the controlled release of propagules. As Prior (1988) stated, formulation in oil increases efficacy and reduces dependence on humid conditions. Skim milk worked well as a surfactant as no conidia could be observed to be floating on the surface as in the control. As a control dried untreated conidia were used.

3.4 Residual moisture content of microcapsules

The moisture contents of the powders increase as the outlet temperature decrease. Results are given in Table 1.

3.5 Conidia survival in microcapsules during storage

Microcapsules produced at constant outlet temperatures of 50 to 53°C were stored at different temperature levels (6, 20 and 30°C) with and without the addition of silica gel capsules. The addition of silica gel capsules resulted in moisture contents of 3 % of the spray dried powders. The germination rate was assessed over a 3 month period. Maximum survival rates of 95 % were found at storage temperatures of 6°C and moisture contents of 3 %. In comparison, spray dried powders stored under the same conditions, but with residual moisture levels of 18 % showed germination rates of 0 % after a storage period of 4

weeks. Storage conditions of 20 and 30°C generally resulted in a fast decline in conidial viability. Microencapsulated conidia with moisture contents of 3 % showed germination rates of 0 % after two months storage at 20°C and 0 % after two weeks storage at 30°C. Storage without the addition of silica gel capsules resulted in 0 % viability after two weeks storage at 20 and 30°C. Therefore, shelf life seemed to be inversely related to the moisture content of the stored material and the storage temperature.

4 Conclusion

The results of the present study show that spray drying is a useful formulation method for the microencapsulation of conidia of *Metarhizium anisopliae*. In consideration of the special requirements for *Metarhizium anisopliae*, it was possible to produce highly concentrated spray dried powders with 76 % viability. The temperature stress has been noted as the key factor during the formulation process and the importance of the addition of membrane stabilising agents has been shown. Furthermore, storage tests demonstrate that conidial formulations require a residual moisture content of approximately 3 % and low temperatures for prolonged storage.

Acknowledgements

The SEM work was performed at the Centre for Ultrastructure Research of the University of Agricultural Sciences Vienna, Austria. This work was part of the EU-project BIPESCO (FAIR6-CT-4105). The authors would like to express thanks to the enterprise F. Joh. Kwizda GmbH for the possibility to take part in the EU-project BIPESCO.

References

Burges HD (1998) Formulation of microbial biopesticides. Dordrecht: Kluwer, ISBN 0-412-62520-2

Butt TM, Ibrahim L, Ball BV, Clark SJ (1994) Pathogenicity of the entomogenous fungi Metarhizium anisopliae on the surface of aphid and flea beetle cuticles. Mycol Res 99:945-950

Butt TM, Harris J, Powell K (1999) Microbial biopesticides: The European Scene. In: Hall FR, Menn JJ (eds) Methods in Biotechnolgy Vol. 5 Biopesticides: Use and Delivery. Totowa NJ: Human Press, pp 23-44, ISBN 0-89603-515-8

Bühler V (2001) Kollidon®: Polyvinylpyrrolidone for the pharmaceutical industry. Vol. 6. Ludwigshafen: BASF Aktiengesellschaft, 71 p

Copping LG (1998) The biopesticide manual: a world compendium. Bracknell: BCPC, 149 p, ISBN 1-901396-26-6

Gardiner GE, O`Sullivan E, Kelly J, Auty MAE, Fitzgerald GF, Collins JK, Ross RP, Stanton C (2000) Comparative survival rates of human-derived probiotic Lactobacillus paracasei and L. salivarius strains during heat treatment and spray drying. Appl Environ Microbiol 66(6):2605-2612

Li Z, Butt TM, Beckett A, Wilding N (1993) The structure of dry mycelia of the entomophtoralean fungi Zoophthora radicans and Eryinia neoaphidis following different preparatory treatments. Mycol Res 97:1315-1323

Millqvist-Fureby A, Malmsten M, Bergenståhl B (1999) An aqueous polymer two-phase system as a carrier in the spray-drying of biological material. J Colloid Interface Sci 225:54-61

Prior C, Jollands P, Le Patourel G (1988) Infectivity of oil and water formulations of Beauveria bassiana (Deutromycotina: Hyphomycetes) to the cocoa weevil pest Pantorhytes pultus Coleoptera: Curculionidae). J Invertebr Pathol 52:66-72

Ré MI (1998) Microencapsulation by spray drying. Drying Technology 16(6):1195-1236

Rhodes DJ (1993) Formulations of biological control agents. In: Jones DG (ed) Exploitation of Microorganisms. London: Chapman and Hall, pp 411-438, ISBN 0-412-45740-7

Stephan D, Zimmermann G (1998) Development of a spray-drying technique for submerged spores of entomopathogenic fungi. Biocontrol Science and Technology 8:3-11

Beads from natural hydrogels as encapsulation matrices for cofactor-dependent enzymes in organic solvents

Marion B. Ansorge-Schumacher, Gesine Pleß, Daria Metrangolo, and Winfried Hartmeier[1]

Abstract

Due to their simple polymerization process and low toxicity, natural hydrogels are favorable matrices for the encapsulation of biocatalysts in organic synthesis. In organic solvents, they form stable compartments which protect entrapped enzymes from detrimental effects of their environment. Material and encapsulation method, however, affect stability and activity of the biocatalyst itself as well as mass transfer in and mechanical stability of the immobilization matrix. When an alcohol dehydrogenase from *Lactobacillus kefir* and its cofactor, $NADPH+H^+$, were entrapped in alginate, agar, gellan, and κ-carrageenan by dropping into aqueous hardening baths, enzyme as well as cofactor loss from the hydrogels was observed. However, immobilization yields of 100 % were easily achieved by adapting four different methods. Best results were obtained with two-phase dispersions of sunflower oil and solutions of gellan or κ-carrageenan. With regard to the low thermostability of the entrapped alcohol dehydrogenase, the gelling temperature of both materials was decreased below 40 °C by changing polymer and ion concentrations. Influences on the mechanical strength of the hydrogels were investigated by comparing the critical compression forces of gel cylinders with standard sizes. Reasonable gelling temperatures as well as mechanical strengths was observed for 1.5 % (w/v) gellan including 0.05 % (w/v) $CaCl_2$. Encapsulating the alcohol dehydrogenase and its cofactor with this hydrogel composition, stereoselective production of R-phenylethanol from acetophenone was performed with a yield of 80-85 % and an enantiomeric excess of 98 %.

Keywords: hydrogel, encapsulation, alcohol dehydrogenase, organic solvent

1 Introduction

Organic solvents are widely used as reaction media in chemical synthesis. They (I) increase the solubility of hydrophobic substrates, (II) enable reactions that are unfavorable in water, e.g., the reversal of hydrolysis reactions in favor of synthesis and (III) simplify product and catalyst recovery. Regarding biocatalytic conversions, some isolated enzymes show reasonable activity and even enhanced thermostability in the presence of organic solvents (Kvittingen 1994), but many others are rapidly deactivated (Ghatorae et al. 1994). A general use of biocatalysts in such media requires an efficient separation of the biocatalyst from direct contact with the surrounding solvent.

In medical and biotechnological applications, natural hydrogels like alginate or agarose are often employed when a separation of whole cells from aqueous reaction media is necessary (Jen et al. 1996). Hertzberg et al. (1992) demonstrated that such hydrogels can also be used to encapsulate isolated enzymes for an application in organic solvents. The resulting aqueous, but stable, compartments protect the biocatalyst from detrimental effects of its environment. They should therefore enable the conversion of poorly water-soluble compounds with enzymes that are deactivated in the presence of organic solvents or aqueous-organic interfaces. Additionally, it should be possible to apply multi-enzyme systems or biocatalysts that require cofactors for activity to syntheses in organic solvents. Material and encapsulation method, of course, have to be selected carefully, as they may affect the stability and activity of the biocatalyst itself as well as mass transfer in and mechanical stability of the immobilization matrix.

Dehydrogenases are versatile tools for the synthesis of many chiral compounds (Hummel and Kula 1989), but suffer from both a poor stability in organic solvents (Hummel 1999) and the essential need for hydrophilic cofactors. In this work, the encapsulation of an alcohol dehydrogenase [ADH, E.C.1.1.1.1] from *Lactobacillus kefir* and its cofactor, $NADPH+H^+$, in beads of the natural hydrogels alginate, gellan gum, agar and κ-carrageenan was performed. The encapsulation process and different hydrogels were investigated and optimized with special regard to enzyme and cofactor loss, ADH stability and productivity towards the stereoselective synthesis of R-phenylethanol, as well as hydrogel properties, such as the mechanical strength.

[1] Marion B. Ansorge-Schumacher, Gesine Pleß, Daria Metrangolo, Winfried Hartmeier, Department of Biotechnology, Aachen University of Technology (RWTH), Worringerweg 1, 52056 Aachen, Germany

2 Experimental

2.1 Chemicals

Gellan was a generous gift from Kelco (Hamburg, Germany). Manugel® DJX sodium alginate was purchased from Monsanto (Waterfield, UK), BECO®-agar from Behrens & Co. (Hamburg, Germany) and κ-carrageenan from Fluka (Neu Ulm, Germany). ADH from *L. kefir* was obtained from Sigma-Aldrich Chemie (Deisenhofen, Germany), NADPH+H^+ from BIOMOL (Hamburg, Germany) and the protein assay (Bradford reagent) from Biorad (München, Germany). Sunflower oil was a product from Brökelmann Oelmühle (Hamm, Germany). All other chemicals were obtained from Fluka Chemie (Neu Ulm, Germany).

2.2 Preparation of hydrogels

Hydrogel solutions were prepared by dissolving the respective matrices in 0.1 M Tris-HCl, pH 7.0, heating to appropriate temperatures and mixing for 10 minutes on a magnetic stirrer. 7.1 mg/ml (3 U/ml) ADH and 3.0 mg/ml NADPH+H^+ were added after letting the gel solutions cool down to maximum temperatures of 40-50 °C. Beads were produced (1) by dropping the mixtures into aqueous hardening baths, buffered with 0.1 M Tris-HCl, pH 7.0 and containing 2 % (w/v) calcium chloride for alginate and gellan gels or 1 % (w/v) potassium chloride for κ-carrageenan gels, (2) by dropping the hydrogel solutions into stirred sunflower oil or (3) by adapting a two-phase dispersion process (Audet and Lacroix 1989). Gel cylinders of 1 cm in height and 0.8 cm in diameter were formed by pouring the gel mixtures into molds, which were removed after gel formation.

2.3 Determination of enzyme and cofactor loss

Enzyme and cofactor loss from hydrogels were determined by quantifying protein and NADPH+H^+ concentrations in the hardening baths after gel addition. In aqueous solutions, a commercial protein assay was used to measure the protein content, in sunflower oil relative protein concentrations were calculated from measurements with a Beckman DU® 7400 spectrophotometer (Fullerton, CA, USA) at a wavelength of 280 nm. NADPH+H^+ was determined spectrophotometrically at a wavelength of 340 nm in all solutions.

2.4 Determination of the hydrogel strength

Hydrogel cylinders were fixed on a balance and compressed by a metal disc (Ø 1 cm). The time-force curve was recorded by a personal computer and the data evaluated using FlexPro 2.0 (Educational Version, Greitmann, Menden, Germany). The critical compression force (CCF) leading to the breakage of the gel was identified by the resulting sudden drop in the time-force curve. The gel strength (tB) was calculated according to Christanson et al. (1985) using the equation $\tau_B = CCF/pR_0^2$, R being the initial radius of the cylinders (0.4 cm).

2.5 Determination of ADH productivity and stereoselectivity

Beads resulting from 1 ml hydrogel solution were added to 10 ml of solvent containing 10 mM acetophenone as substrate and 20 mM decane as internal standard. Acetophenone decrease and R-phenylethanol increase were measured by gas chromatography using an HP 5890 series II gas chromatograph (Hewlett Packard, Walbronn, Germany), equipped with an autosampler and a flame ionization detector (FID), on a chiral FS-Cyclodex-beta-I/P capillary column (25 m x 0.25 mm i. d.; CS GmbH, Langerwehe, Germany). Nitrogen was used as carrier gas.

3 Results and discussion

Hydrogel beads were obtained from alginate, agar, gellan and κ-carrageenan by dropping 2 % (w/v) buffered gel solutions into an aqueous hardening bath. However, despite improved gel formation due to calcium or potassium ions in the hardening solutions (Smidsrød and Skjåk-Bræk 1990; Michel et al. 1997; Morris et al. 1995), up to 60 minutes were necessary to form solid beads from agar, gellan and κ-carrageenan. During this time, considerable leakage of enzyme and cofactor from the hydrogels can be expected (Dashevsky, 1998).

3.1 Enzyme and cofactor loss

When ADH from *L. kefir* and its cofactor NADPH+H^+ were entrapped in alginate beads, only 1 % of the enzyme, but 21 % of the cofactor were lost from the matrix within 60 minutes. Cofactor loss mainly occurred within the first 30 seconds after dropping the gel solution into the hardening bath. During the remaining hardening time, NADPH+H^+ was almost completely retained in the hydrogel (Figure 1).

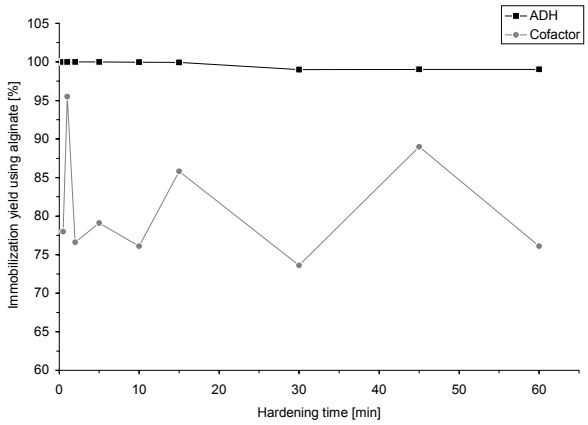

Figure 1:
Enzyme and cofactor loss from alginate beads during the hardening in an aqueous solution containing 2 % (w/v) of calcium chloride

Most probably, the unexpected retention of the low molecular size cofactor did result from its specific binding to the entrapped enzyme rather than from the alginate network. From gellan beads, enzyme and cofactor were continuously lost during their exposition to the hardening solution (Figure 2). After 60 minutes, an immobilization yield of only 62 % of the cofactor and 87 % of the ADH was determined. The exponential decrease indicated a free diffusion of both compounds approaching equilibrium.

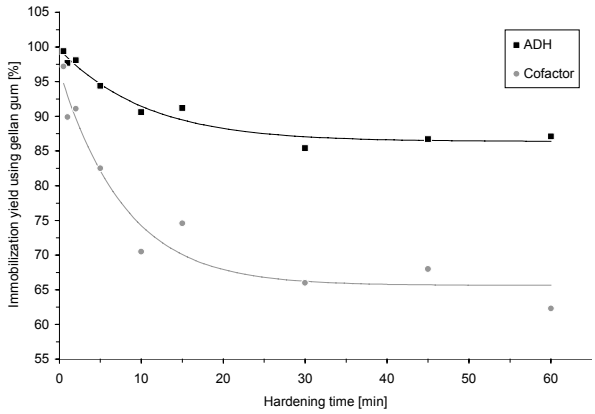

Figure 2:
Enzyme and cofactor loss from gellan beads during the hardening in an aqueous solution, containing 2 % (w/v) of calcium chloride

Similar curves, but enhanced losses, were observed for κ-carrageenan. The immobilization yields of cofactor and enzyme were 52 % and 73 %, respectively (data not shown). As the formation of agar beads according to the described production process affected both protein and cofactor determination, enzyme and cofactor loss were not quantified. However, a rapid leakage of both compounds can be assumed.

3.2 Optimisations of the immobilization yield

The immobilization yield in all hydrogels was increased to 100 % by (1) saturating the hardening baths with enzyme and cofactor according to the initial concentrations in the gel, (2) swelling dry gel beads containing enzyme in cofactor solutions, (3) dropping the gel solutions into hydrophobic hardening baths or (4) adapting a two-phase dispersion process (Audet and Lacroix 1989).

(1) Despite the simplicity of preventing enzyme as well as cofactor loss from hydrogels by saturating the hardening baths with appropriate concentrations of both compounds, the method was abandoned due to economical considerations. (2) The same argument holds true for the second preparation method. Besides, cofactor uptake by drying beads under mild conditions (30 °C, 72 hours) and swelling them in a $NADPH+H^+$ solution was successfully performed with alginate gel, but severely affected the structure of gellan as well as κ-carrageenan beads. (3) Dropping hydrogel solutions into pure sunflower oil resulted in the production of heavily deformed beads. Regular shapes were obtained by the addition of surfactants (dish washing) to the sunflower oil. However, as the presence of surfactants during gel formation might affect the gel properties (Manca et al. 2001) as well as the entrapped enzyme, the method was not further investigated. (4) Best results with regard to bead shape and size distribution were obtained by preparing two-phase dispersions of sunflower oil and hydrogel solution with a magnetic stirrer. However, as cations necessary for bead formation or stabilization were hardly soluble in the hydrophobic phase, they had to be added directly to the hydrogel solutions. Subsequently, the production of two-phase dispersions was only possible for polymer solutions with slow gel formation in the presence of ions. No two-phase dispersion was obtained with alginate.

3.3 Enzyme and hydrogel stability

The low thermostability of ADH from *L. kefir* (Tarhan and Hummel 1995) demands gelling temperatures below 40 °C. They were achieved by changing the polymer as well as ion concentrations of the hydrogels. However, the concomitant determination of the critical compression forces also revealed strong effects on the hydrogel strength. The results are summarized in Table 1.

Table 1:
Gelling temperature (TG) and critical compression force (CCF) at varying polymer and cation concentrations (c_{cation}) in two-phase dispersion systems

Hydrogel, %	c_{cation}, %	T_G, °C	CCF, N/cm^2
4.0 κ-carrageenan	-	43	48.4
3.0 κ-carrageenan	-	38	29.2
2.0 κ-carrageenan	-	31	10.8
2.0 κ-carrageenan	1.0 K^+	52	21.4
1.5 κ-carrageenan	0.2 K^+	45	14.5
1.5 κ-carrageenan	0.3 K^+	46	14.6
1.2 κ-carrageenan	0.2 K^+	41	5.5
1.2 κ-carrageenan	0.3 K^+	46	5.2
1.2 κ-carrageenan	0.4 K^+	48	8.6
3.0 Gellan gum	-	43	9.9
2.0 Gellan gum	-	38	3.34
2.0 Gellan gum	0.3 Ca^{2+}	66	12.5
1.7 Gellan gum	0.05 Ca^{2+}	44	14.5
1.5 Gellan gum	0.05 Ca^{2+}	39	11.2
1.2 Gellan gum	0.05 Ca^{2+}	39	6.9
3.0 Agar	-	37	13.25
2.0 Agar	-	33	9.7
1.0 Agar	-	-	3.3

Best results considering both low gelling temperatures and critical compression forces above 10 N/cm^2 were obtained with 1.5 % gellan gum, containing 0.05 % $CaCl_2$.

3.4 Enzyme productivity and stereoselectivity

Enzyme productivity and stereoselectivity were investigated with regard to the stereoselective synthesis of R-phenylethanol from acetophenone. Using 1.5 % gellan gum, containing 0.05 % $CaCl_2$, a product yield of 80-85 % and an enantiomeric excess of 98 % were achieved.

4 Conclusions

The encapsulation of ADH from *L. kefir* and its cofactor, NADPH+H$^+$, in natural hydrogels like alginate, gellan, κ-carrageenan and agar can be performed without loss of enzyme or cofactor during the production process. The adaptation to the low thermostability of the entrapped enzyme, however, requires low polymer and ion concentrations. Subsequently, high productivity and stereoselectivity towards the production of R-phenylethanol, but only low mechanical strength of the respective hydrogels can be achieved. For technical applications, an optimisations of the hydrogel matrix needs to be performed to enhance the resistance against mechanical stress. This might be achieved by mixing natural gels with synthetic compounds to combine the non-toxic and mild gellation conditions of natural polymers with the favourable mechanical properties of many synthetic materials. Also, cofactor regeneration in the resulting beads has to be investigated.

References

Audet P, Lacroix C (1989) Two-phase dispersion process for the production of biopolymer gel beads: Effect of various parameters on bead size and their distribution. Proc Biochem 24:217-226

Christianson DD, Casiraghi EM, Bagley EB (1985) Uniaxial compression of bonded and lubricated gels. J Reol 29(6):671-684

Dashevsky A (1998) Protein loss by the microencapsulation of an enzyme (lactase) in alginate beads. Int J Pharm 161:1-5

Ghatorae AS, Bell G, Halling PJ (1994) Inactivation of enzymes by organic solvents: New techniques with well-defined area. Biotechol Bioeng 43:331-336

Hertzberg S, Fuskevag O M, Anthonsen T (1992) Hydrophilic gels as immobilization materials and stabilizers for enzyme-catalysed esterification in organic media. In: Tramper J (ed) Biocatalysis in non-conventional media. Elsevier, Amsterdam, pp 347-354

Hummel W (1999) Large-scale application of NAD(P)-dependent oxidoreductases: Recent developments. Trends Biotechnol 17:487-492

Hummel W, Kula M-R (1989) Dehydrogenases for the synthesis of chiral compounds. Eur J Biochem 184:1-13

Jen AC, Wake MC, Mikos AG (1996) Review: Hydrogels for cell immobilization. Biotechnol Bioeng 50:357-364

Kvittingen L (1994) Some aspects of biocatalysis in organic solvents. Tetrahedron 50(28):8253-8274

Manca S, Lapasin R, Partal P, Gallegos C (2001) Influence of surfactant addition on the rheological properties of aqueous Welan matrices. Rheol Acta 40:128-134

Michel A-S, Mestdagh MM, Axelos MAV (1997) Physico-chemical properties of carrageenan gels in presence of various cations. Int J Biol Macromol 21:195-200

Morris VJ, Tsiami A, Brownsey GJ (1995) Work hardening effects in gellan gum gels. J Carbohydrate Chem 14(4+5):667-675

Smidsrød O, Skjåk-Bræk G (1990) Alginate as immobilization matrix for cells. Trends Biotechnol 8:71-78

Tarhan L, Hummel W (1995) Immobilisation and characterisation of phenylethanol dehydrogenase from *Lactobacillus kefir* and its application in a flow-injection-analysis system. Proc Biochem 30(1):49-55

Continuous hydrolysis of concentrated sucrose solutions by alginate immobilized yeast cells

Marek Wójcik[1]

Abstract

An immobilized biocatalyst with invertase activity was obtained by the entrapment of native bakers' yeast cells *Saccharromyces cerevisiae* in calcium alginate beads. Silica was added as an inert material to increase density of the biocatalyst. Bead formation was achieved by using a previously developed technique (Klein at al. 1983). The diameter of obtained beads was 1.2 mm and varied within ± 0.1 mm. Freezing and thawing of the biocatalyst was used to enhance diffusivity of sucrose in the beads. The effect of pH on the biocatalyst activity was investigated by determining the amount of reducing sugars liberated by biocatalyst beads in sucrose solution of 500 g l^{-1} in a stirred batch reactor at 50°C. The optimum pH value for invertase activity was 5.0. The biocatalyst was used for continuous sucrose hydrolysis in tubular packed bed reactor at pH 5.0, substrate concentrations of 500-890 g·l^{-1} and reaction temperatures of 50-65°C. The biocatalyst shows a good stability for temperature range 50-65°C. The half-life was 2200 h for temperature 60°C and inlet sucrose concentration 890 g·l^{-1}. The mechanical stability of the biocatalyst particles was very good during 3072 h of operation in a packed bed. The results of the biocatalyst investigations confirmed its full applicability for hydrolysis of concentrated sucrose solutions.

Keywords: Sucrose hydrolysis, alginate, immobilized cells, biocatalyst, invertase

1 Introduction

Invert sugar syrups are commercial products which can be obtained by acid or enzymatic hydrolysis of sucrose and used mainly in the confectionery, beverage, and bakery industries. The acid hydrolysis often yields syrups contaminated with unwanted by-products. Better product quality can be achieved with the use of enzymatic hydrolysis because the reaction is carried out under milder conditions. In order to economize the process, a number of authors have considered the use of immobilized invertase. Reutilization of the biocatalyst and increase in half-life of immobilized invertase can lead to a cost reduction in the hydrolysis of sucrose.

There are numerous reports on invertase immobilization (Abdellah et al. 1992, Arruda and Vitolo 1999, Imai et al. 1986, Iqbal and Saleemuddin 1985, Mansfeld and Schellenberger 1987, Mansfeld et al. 1991). Most of the studies have been carried out using dilute sucrose solution. Relatively few reports have appeared on the use of immobilized invertase for hydrolysis of concentrated sucrose solutions (Godbole et al. 1990, Mansfeld et al. 1992, Monsan and Combes 1984).

The immobilization of whole cells containing invertase offers several advantages over immobilization of soluble invertase (Hasal et al. 1992). Yeast cells with invertase activity have been immobilized by the adhesion or covalent bonding to the surface of insoluble carriers: glass (D'Souza et al. 1986), tuff (Parascandola et al. 1987), cotton (D'Souza and Kamath 1988, Melo et al. 1992), and wool (Krastanov 1997). Immobilization of cells by entrapment in synthetic or natural hydrophilic gels such as polyacrylamide (Ghosh and D'Souza 1989), pectate (Polakovič et. al 1993), and alginate (Báleš et al. 1991, Lazcano et al. 1993) was also used. Except for the immobilization of cells in calcium alginate with added molecular sieves (Lazcano et al. 1993), none of the biocatalysts mentioned here have sufficient density to be used for continuous hydrolysis of concentrated sucrose solution in a conventional packed bed reactor with flow from the bottom to the top. Hazel et al. (1992) tested the biocatalyst bed which was fixed between two adjustable piston-like closures covered with nylon cloth sieves. This paper demonstrates a simple method which was used for preparation of immobilized biocatalyst with invertase activity. The biocatalyst was found to be capable of sucrose hydrolysis in a packed bed reactor at high substrate concentrations.

2 Experimental

2.1 Materials

Sodium alginate (Type DMF from KELCO) was used as the hydrocolloidal gelling material. Silica from SIGMA with a particle size range of 0.5 to 10

[1] Marek Wójcik, Department of Chemical and Biochemical Engineering, University of Technology and Agriculture, 85-326 Bydgoszcz, ul. Seminaryjna 3, Poland

mm diameter was added as an inert material to control density of the biocatalyst. Sucrose of commercial grade was purchased from local sources. Other chemicals were of reagent grade.

2.2 Microorganism

Cells of the yeast *Saccharomyces cerevisiae* were used for the immobilization in the form of squeezed bakers' yeast. They were purchased on local market.

2.3 Analytical method

The concentrations of reducing sugars in the reaction syrups were determined by the spectrophotometric method of Nelson and Somogyi. Solutions with equimolar amounts of glucose and fructose were used as standards.

2.4 Immobilization

Sodium alginate (5 g) was first completely dissolved in 375 ml deionized water at 50°C. Then, the temperature was reduced to approximately 30°C and appropriate amounts of yeast cells (90 g) and silica (15 g) were added with continuous stirring. The desired final alginate concentration (10 $g \cdot l^{-1}$) was obtained by adding deionized water. This suspension was used to form the beads of biocatalyst. Bead formation was achieved by using a previously developed technique (Klein et al. 1983). The apparatus used for immobilization is shown in Figure 1.

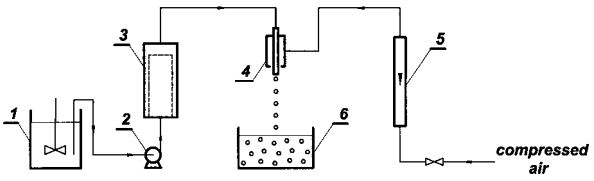

Figure 1:
Schematic diagram of the immobilisation apparatus: (1) mixer with suspension of yeast and silica, (2) peristaltic pump, (3) sieve filter, (4) concentric orifice, (5) rotameter, (6) $CaCl_2$ solution

The viscous suspension was fed through the sieve filter (3) into the concentric orifice (4) by a peristaltic pump (2). The size of the droplets was controlled by applying a coaxial air stream. The gel beads were obtained by allowing droplets of suspension to fall into an aqueous solution of $CaCl_2$ (0.2 M). The formed beads were left in calcium chloride solution for 12 h to complete gelation within the whole bead volume. The diameter of obtained beads was 1.2 mm and varied within ± 0.1 mm. The beads of biocatalyst were then removed from the precipitation bath and stored at temperature –20°C. Freezing and thawing of biocatalyst was used to enhance diffusivity of sucrose in the beads.

3 Results and discussion

3.1 Effect of pH on the biocatalyst activity

The effect of pH on the biocatalyst activity was investigated at 50°C. The activity was determined by the amount of reducing sugars liberated by biocatalyst beads in sucrose solution of 500 $g \cdot l^{-1}$ in a stirred-batch reactor. Figure 2 shows that the maximum activity of biocatalyst was 5.0. Around this value the pH influence to the initial reaction rate is weak.

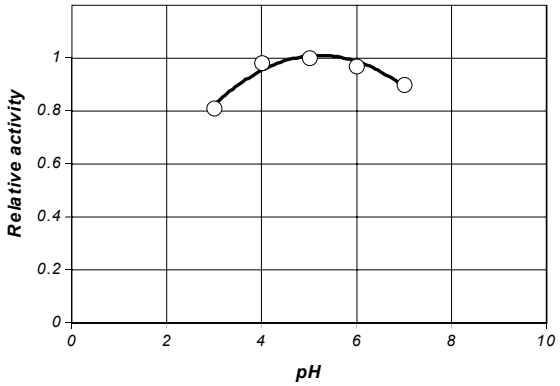

Figure 2:
Effect of pH on the biocatalyst activity

3.2 Continuous hydrolysis of sucrose solution

Continuous hydrolysis was studied at pH 5.0 using different concentrations of sucrose syrup. Experiments were performed in a jacketed plexiglass column bioreactor with inner diameter 20 mm. Sucrose solutions were prepared by dissolving sucrose in warm tap water and adjusting the pH to the desired volume by addition of citric acid. Figure 3 shows the experimental set-up for hydrolysis of sucrose. The substrate solution from reservoir (1) was pump with a peristaltic pump (2) through the heat exchanger (3) into the reactor (4). Reaction temperature was maintained constant using thermostat (5) with water circulation system.

At the reactor outlet samples were taken and reducing sugars concentration was determined. The conversion X was calculated from the equation 1.

$$X = \frac{S_0 - S}{S_0} \cdot 100\% \qquad (1)$$

Here S_0 represents the substrate concentration at reactor inlet and S the substrate concentration at reactor outlet.

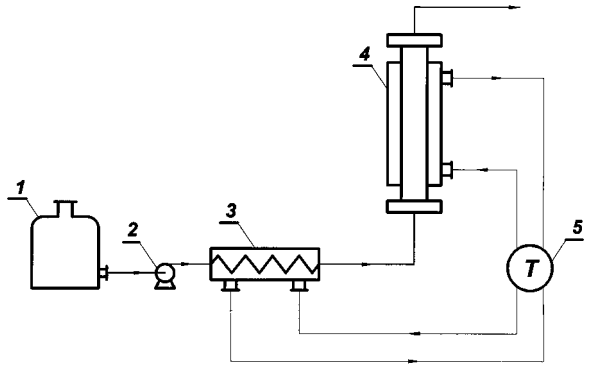

Figure 3:
Experimental set-up for hydrolysis of sucrose in packed bed reactor: (1) substrate reservoir, (2) peristaltic pump, (3) heat exchanger, (4) packed bed reactor, (5) thermostat

In this experimental study, attention was mainly paid to the influence of the process parameters on conversion. The industrial production of invert syrups involves the need to operate the biocatalyst in the presence of high sucrose concentrations to avoid microbial contamination and expensive concentration of the product. For this reason the experiments were performed using concentrations sucrose solutions above 500 $g \cdot l^{-1}$. The effect of flow rate and inlet substrate concentration on the output reactor conversion is presented in Figure 4.

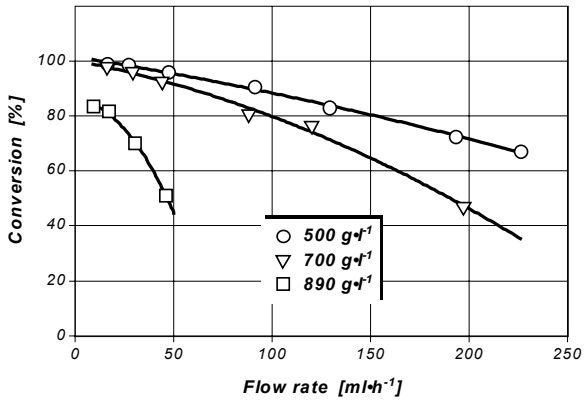

Figure 4:
Effect of flow rate on conversion at 50°C

Similar results have been published by other authors (Mansfeld and Schellenberger 1987) for immobilized invertase. Considerable decrease of conversion with increasing substrate concentration occurs, especially at high flow rates. By increasing the temperature, the productivity and conversion can be enhanced. On the other hand, with increasing temperature the half-life of the biocatalyst reduces. The operational stability of the biocatalyst was tested by long-term sucrose hydrolysis at temperature 60°C and inlet sucrose concentration of 890 $g \cdot l^{-1}$. Dependence between conversion and time is presented in Figure 5.

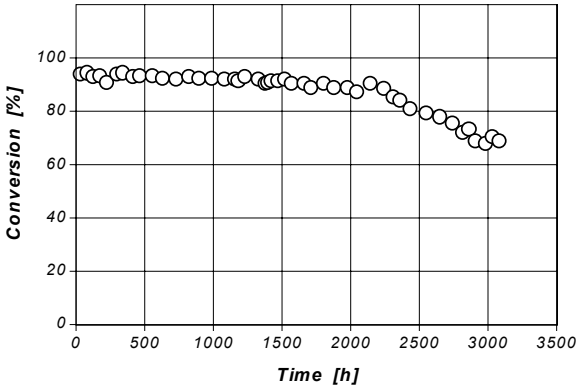

Figure 5:
Operational stability of the biocatalyst at 60°C

The initial productivity of reactor was 0.7$kg \cdot l^{-1} \cdot h^{-1}$. The half-life of the enzyme activity was estimated to be about 2200 h. This value is comparable with determinations of other researchers (Hazel et al. 1992) for immobilized yeast cells with invertase activity. The mechanical stability of the biocatalyst particles was very good during 3072 h of operation in packed bed.

4 Conclusions

As demonstrated by the results presented here, the biocatalyst with invertase activity obtained by entrapment of whole yeast cells in calcium alginate can be effectively used for continuous hydrolysis of concentrated sucrose solutions in packed bed reactor. The immobilization costs are very low, whereas the properties of the biocatalyst are comparable to those of biocatalyst prepared by more sophisticated methods. Production of invert syrups promises to be economically attractive by using this kind of biocatalyst.

References

Abdellah HA, Baker TMA, Shekib LA, El-Iraqi SM (1992) Characteristics of invertase immobilized on three different types of supports. Food Chem 43:369-375

Arruda LMO, Vitolo M (1999) Characterisation of Invertase Entrapped into Calcium Alginate Beads. Applied. Biochem Biotechnol 81:23-33

Báleš V, Polakovič M, Štefuca V (1991) Study of hydrolysis of sucrose in packed bed immobilized cell bioreactor. Chem Biochem Eng Q 5:53-57

D'Souza SF, Kamath N (1988) Cloth bioreactor containing yeast cells immobilized on cotton cloth using polyethyleneimine. Appl Microbiol Biotechnol 29:136-140

D'Souza SF, Melo JS, Deshpande A, Nadkarni GB (1986) Immobilization of yeast cells by adhesion to glass surface using polyethyleneimine. Biotechnol Lett 8:643-648

Ghosh S, D'Souza SF (1989) Crushing strength as a tool for reactor height determination for invertase containing yeast cells immobilized in polyacrylamide. Enzyme Microb Technol 11:376-378

Godbole SS, Kubal BS, D'Souza SF (1990) Hydrolysis of concentrated sucrose syrups by invertase immobilized on anion exchanger waste cotton thread. Enzyme Microb Technol 12:214-217

Hazel P, Vojtišek V, Čejková A, Kleczek P, Kofroňová O (1992) An immobilized whole yeast cell biocatalyst for enzymatic sucrose hydrolysis. Enzyme Microb Technol 14:221-229

Imai K, Shiomi T, Uchida K, Masamitsu M (1986) Immobilization of enzyme into poly (vinyl alcohol) membrane. Biotechnol Bioeng 28:1721-1726

Iqbal J, Saleemuddin M (1985) Sucrose hydrolysis using invertase immobilized on concanavalin α-Sepharose. Enzyme Microb Technol 7:175-178

Klein J, Stock J, Vorlop K-D (1983) Pore size and properties of spherical Ca-alginate biocatalysts. Appl. Microbiol. Biotechnol. 18:86-91

Krastanov A (1997) Continuous sucrose hydrolysis by yeast cells immobilized to wool. Appl Microbiol Biotechnol 47:476-481

Lazcano R.R, Perez AC, Baele NF (1993) Method and apparatus for the production of glucose - fructose syrups from sucrose using a recombinant yeast strain. US Patent 5 270 177

Mansfeld J, Förster M, Schellenberger A, Dautzenberg H (1991) Immobilization of invertase by encapsulation in polyelectrolyte complexes. Enzyme Microb Technol 13:240-244

Mansfeld J, Schellenberger A (1987) Invertase immobilzed on macroporous polystyrene properties and kinetic characterization. Biotechnol Bioeng 29:72-78

Mansfeld J, Schellenberger A, Römbach J, (1992) Application of polystyrene-bound invertase to continuous sucrose hydrolysis on pilot scale. Biotechnol Bioeng 40:997-103

Melo JS, Kubal, D'Souza (1992) Production of inverted sucrose syrups using yeast cells adhered to polyethylenimine treated cotton threads. Food Biotechnol 6:175-186

Monsan P, Combes D (1984) Application of immobilized invertase to continuous hydrolysis of concentrated sucrose solutions. Biotechnol Bioeng 26:347-351

Parascandola P, Scardi V, Tartaglione O (1987) Immobilization of yeast cells by adhesion on tuff granules. Appl Microbiol Biotechnol 26:507-510

Polakovič M, Štefuca V, Báleš V, Kurillova L, Gemeiner P (1993) Heterogenous enzymic hydrolysis in a biocatalytic packed bed formed by Ca-pectate gel beads. Proc Biochem 28:549-552

Investigations into the applicability of polyesters for the immobilization of enzymes

Peter Grunwald[1], Michael Arp[1], Yiyan Yang[2], and Katrin Hensen[1]

Abstract

In this paper the application of microspheres fabricated from biodegradable polyesters like poly(DL-lactic acid) and poly(DL-lactic-co-glycolic acid) as carrier materials for the enzymes urease and phytase is described. The microspheres were prepared by a recently developed water-in-oil-in-water emulsion technique. The mean diameter of the obtained ball-shaped particles was between 50 and 200 µm, depending on the reaction conditions. The entrapment of urease within poly(DL-lactic acid)-beads results in a water-insoluble biocatalyst of good operational stability. The kinetic data (Michaelis-Menten constant, activation energy) as well as the determined low effective diffusion coefficient indicate a considerable mass transfer limitation whereas partitioning effects could not be detected. Further, phospholipids being present in the reaction mixture lead to a decrease in activation energy and with this to a remarkable increase in the reaction rate. This was observed for immobilized phytase too. The use of poly(DL-lactic-co-glycolic-acid) instead of poly(DL-lactic acid) turned out to be not as advantageous for the entrapment of urease concerning its repeated application, however, in case of phytase immobilized by the same technique within the co-polymer catalysts with an efficiency of up to 40 % could be produced. On the other hand their operational stability is not yet satisfactory. This contribution also contains first results regarding the entrapment of ß-D-galactosidase within poly(DL-lactic acid) microspheres.

Keywords enzyme immobilization, emulsion techniques, polyesters, urease, phytase

1 Introduction

Nowadays the employment of immobilized biocatalysts is firmly established in many fields such as medicine, pharmacy, the analytical area, the synthesis of organic compounds, etc. An essential prerequisite for an economical application of enzymes and cells bound to, or entrapped within a water-insoluble matrix is that they be reusable and catalytically active over a longer period of time. Different biocatalysts often need specially designed carriers depending on the properties of the catalyst as well as on the actual reaction conditions. Because of this, it is still of great interest to search for new carrier materials. A commonly applied immobilization method for enzymes is the covalent attachment to the surface of a matrix of organic or inorganic origin, which is often accompanied by a considerable loss of activity due to the rigid chemistry used. A good alternative is the immobilization of enzymes or whole cells by entrapment or encapsulation. Materials, often used for this purpose are polysaccharides like alginate, chitosan or carrageenan. This contribution deals with the entrapment of the enzymes urease (EC 3.5.1.5), phytase (EC 3.1.3.8), and ß-galactosidase (EC 3.2.1.23) within the polyesters poly(DL-lactic-acid) (PDLLA) and poly(DL-lactic-co-glycolic-acid) (PDLLGA). These polyesters are normally used successfully in the area of controlled drug release. However, the number of papers describing their preparation with the aim to permanently retain the catalysts within the matrix is low so far. In a recent publication (Cooper 2001) the entrapment of enzymes in PDLLA with supercritical CO_2 was mentioned without going into details concerning the properties of the obtained biocatalysts. There are several areas of application for these enzymes in an immobilized, and with this, reusable state. Urease is of interest in connection with the development of an artificial kidney, and phytase may be used for the synthesis of definite inositol phosphates. ß-D-galactosidase that does not only catalyze the hydrolysis of disaccharides, but can also be 'persuaded' by appropriate reaction conditions to act in the reverse direction so that it is a useful tool for the synthesis of oligosaccharides and neo-glycoconjugates.

2 Experimental

The preparation of microspheres was carried out by use of a modified water-in-oil-in-water double-emulsion extraction/evaporation method (Yang et al. 2000). Typical assay conditions are as follows: A solution of 600 mg polyester in 6 ml methylene chloride is added to 60 mg of the enzyme (urease: Sigma U1500; phytase: Natuphos® 5000 from *Aspergillus niger*, Gist-brocades; ß-D-galactosidase from *Asper-*

[1] Peter Grunwald, Michael Arp and Katrin Hensen, Department of Physical Chemistry, University of Hamburg, Bundesstraße 45, 20146 Hamburg, Germany
[2] Yiyan Yang, Institute of Materials Research & Engineering, No. 3 Research Link, National University of Singapore, 119260 Singapore

gillus oryzae: Sigma) dissolved in 300 µl distilled water. After sonication (Bandelin sonoplus HD 2200) for 20 s at an output power of 20 Watt the W/O emulsion is injected with a glass syringe under stirring at 500 rpm (reduction to 300 rpm after 5 min), using a propeller type agitator with four blades, into 240 ml of a phosphate buffer solution (PBS, pH = 7.4, T = 15°C), containing 0.05 w/v % polyvinyl alcohol (PVA: M_w 49,000, degree of hydrolysis 86-89 mol %, Fluka). In order to extract CH_2Cl_2, 640 ml of the PBS/PVA is added after 30 min continuously over a period of 4 hours via an elastic tube pump (Ismatec). The obtained microspheres are separated by filtration, washed three times with PBS-buffer, dried, and stored at 4°C).

For an analysis of the physicochemical properties of the microspheres, the average particle size was determined by a laser light-scattering particle size analyzer (Coulter LS 230, Beckmann) after soaking the microspheres in aqueous solution containing 0.1 w/v % Tween 80. The surface topography was observed by taking scanning electron micrographs (SEMs) using a Philips SEM 515 after spattering the surface of the dried samples with a gold layer, the thickness of which was about 100 Å.

Both urease and phytase catalyze the hydrolysis of the corresponding substrates urea and phytic acid, leading to an increase of charged particles in the reaction solution. Therefore, the activity was determined by conductivity measurements (Hans and Rey 1971, Grunwald 1984) with a microprocessor conductivity meter (LF 3000, WTW) and a Pt-electrode, the cell constant of which was 0.6 cm^{-1}. The catalytic activity of these two enzymes is given in µS/min. The activity of ß-D-galactosidase was determined photometrically measuring the amount of o-nitrophenol liberated by the enzyme from the substrate o-nitrophenyl-ß-D-galactopyranoside via the absorbance at 405 nm.

The effective diffusion coefficient D_e was determined by effusion measurements (Vorlop and Klein 1982, Vorlop 1985) using a modified method of evaluation (Grunwald 1997). For this purpose, the microspheres containing the enzyme, which was inactivated before by heat treatment, were equilibrated over night in the corresponding substrate solution and then transferred to a given volume of distilled water. In the case of phytic acid, the effusion could be simply followed by the time course of electric conductivity. The necessary data for urea were obtained by taking samples in time intervals and after complete hydrolysis that was achieved by adding urease, the measured conductivity values ‚G_t' were treated as equivalent to the urea concentration in the sample. D_e was calculated from the slope of the following equation (Grunwald 1997):

$$\ln \frac{G_\infty - G_t}{G_\infty} = -\frac{\pi^2 \cdot D_e}{r^2} t + const \qquad (1)$$

‚G_∞' can be obtained from a plot of ‚G_t' versus 1/t from extrapolation to 1/t = 0, and represents the situation when the substrate is equally distributed in both phases, the microspheres and the surrounding solution. The diffusion coefficients for substrate molecules in solution were obtained by equation 2 (Vorlop 1985) were h is the viscosity of the solvent at a given temperature T:

$$D_0 = 1.7 \cdot 10^{-7} \frac{T}{M_w^{0.41} \cdot \eta} \qquad (2)$$

3 Results and discussion

Figure 1 shows a PDLLGA-particle prepared by the W/O/W double emulsion extraction/ evaporation method described above whereas Figure 2 depicts a view of the cross-section of a PDLLA-microsphere.

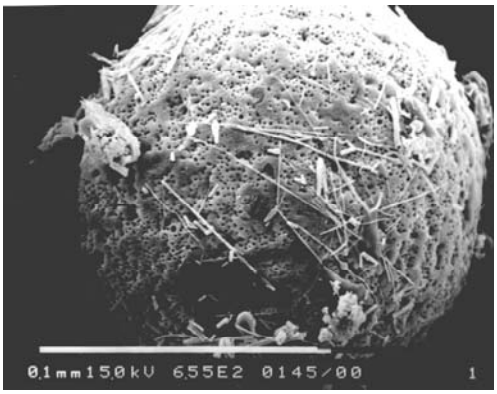

Figure 1:
SEM of a PDLLGA particle with a magnification of x 655, acceleration voltage: 15 kV

The particles are ball-shaped with a mean diameter of about 100 µm, and exhibit a porous surface, necessary for the mass exchange between the catalyst within such beads and the bulk solution. Further, the cross-section SEM reveals a porous internal network structure with cavities of different size which is outwardly surrounded by a skin with a thickness of some few µm. This microporous skin may cause a considerable diffusion limitation. Corresponding data for the system phytase/PDLLGA are compiled in Figure 3.

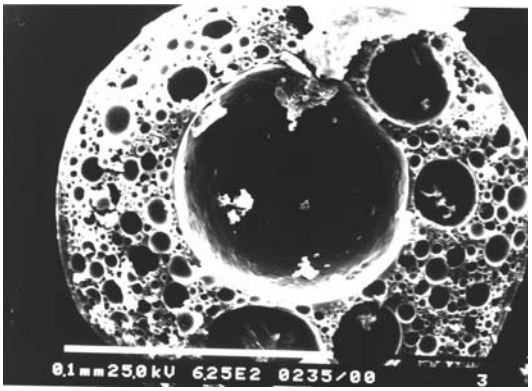

Figure 2:
SEM of a cross-section through a PDLLA-microsphere, acceleration voltage: 25 kV

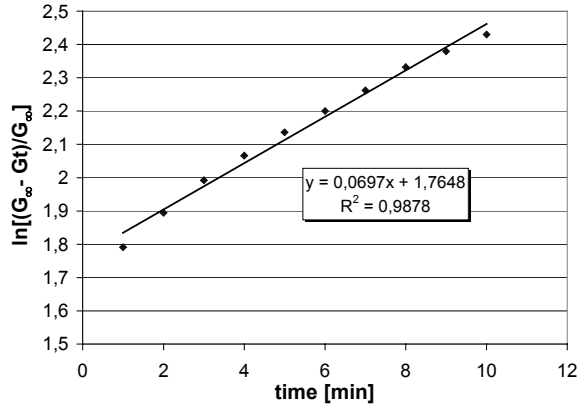

Figure 3:
Evaluation of the effusion of phytic acid from PDLLGA-microspheres according to equation 1

The slope of the straight line $\pi^2 \cdot D_e/r^2$ allows the calculation of the effective diffusion coefficient for the substrate phytic acid which is $2.92 \cdot 10^{-9}$ cm^2/s (with r = 0.005 cm). The D_e-value for urea in a PDLLA was found to be $4.18 \cdot 10^{-9}$ cm^2/s. A comparison with the diffusion constants D_0 for phytic acid and urea in the aqueous solution which were calculated from equation 2 as $10.6 \cdot 10^{-6}$ cm^2/s and $3.83 \cdot 10^{-6}$ cm^2/s, respectively, indeed indicates a strong diffusion barrier, caused by the polyester matrix.

The course of the phytic acid hydrolysis versus the substrate concentration within a substrate concentration range between 80 µmol/l and 1.4 mmol/l (Figure 4) exhibits a maximum for the native enzyme at 1 mmol/l. This value is reduced by about 200 µmol/l when the reaction is catalyzed by phytase immobilized by insertion into the PDLLGA-polyester.

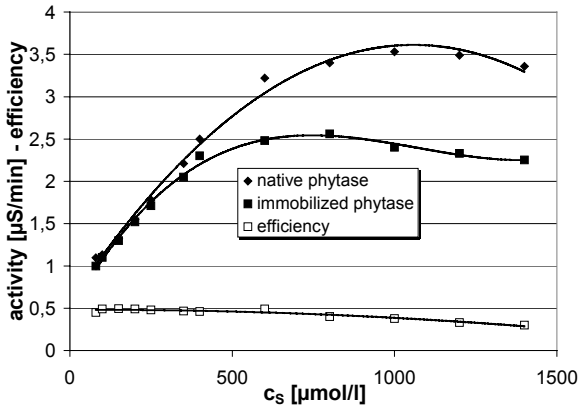

Figure 4:
Activity of native and immobilized phytase as a function of phytic acid concentration, and efficiency η (on the scale from 0 to 1) at 298 K. The experiments with native phytase were performed with a diluted Natuphos® solution containing 10 mg of the enzyme. The corresponding activity values were divided by a factor of 100. For the series of measurements with immobilized phytase 5 mg of the biocatalyst with a protein content of 0.2 mg were applied.

This shows that substrate inhibition as a characteristic of phytase is not changed by entrapment. Within the concentration ranges of $0.1 \cdot 10^{-3}$ mol/l to $0.6 \cdot 10^{-3}$ mol/l (native phytase), and $0.15 \cdot 10^{-3}$ mol/l to $0.5 \cdot 10^{-3}$ mol/l (immobilized phytase) both catalysts seem to obey the Michaelis-Menten mechanism. From corresponding Lineweaver-Burk plots, the K_m-values are calculated to be 2.40 mmol/l and 4.97 mmol/l, respectively. This increase of the K_m-value can also be considered as an indication for diffusion limitation leading to a decrease in efficiency (the ratio of r_i, the reaction rate in presence of the immobilized enzyme, and r_0 the reaction rate in solution). The data in Figure 4 show that the efficiency for the phytase/polyester system is about 50 % and decreases to less than 40 % when substrate inhibition takes effect.

Another interesting parameter is the temperature dependence of the activity of an immobilized biocatalyst. In some cases, an increase in temperature stability due to immobilization has been reported (Buchholz and Kasche 1997). In contrast, the optimum temperature of phytic acid hydrolysis in presence of phytase entrapped within PDLLGA is slightly diminished from 60°C (for the native enzyme) to 55°C, as shown in Figure 5.

This was found for the phytase/PDLLA system, too (see Table 1). The exponential increase of the activity allows the calculation of the activation energies from the corresponding Arrhenius law, which are 53.5 kJ/mol (for native phytase) and 59.6 kJ/mol.

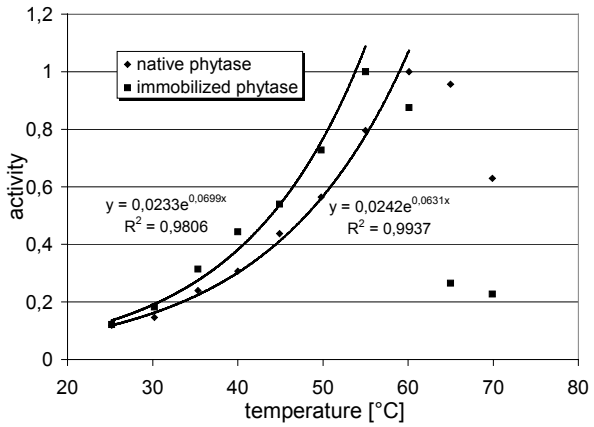

Figure 5:
Temperature dependence of the activity of native phytase und phytase immobilized within the PDLLGA-polyester matrix. The maximum activity was set equal to 1

The kinetics of immobilized biocatalysts may not only be influenced by diffusion limitation, but also by partitioning effects. As the reaction solution and the specific carrier material are two different phases, depletion as well as enrichment of substrate, products, etc. in one of the phases are possible, leading to a change in the microenvironment of the biocatalyst on the surface of a carrier or within a carrier matrix. As a consequence, the measured catalyst-specific data are apparent values. Among other things, these partitioning effects sometimes cause a distinct shift of the pH-optimum. The pH-dependence of the urea hydrolysis catalyzed by native urease and urease/PDLLA-microspheres is given in Figure 6.

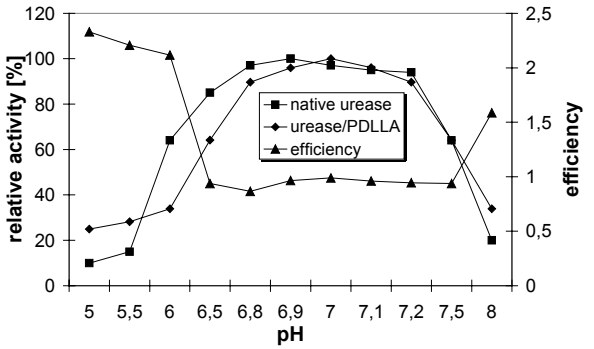

Figure 6:
The activity of native urease and urease entrapped within PDLLA-microspheres and the efficiency for the immobilized enzyme

The pH-optima for native urease and urease fixed within the PDLLA-matrix are 6.9 and 7.0, respectively. This reveals that the microenvironment of the PDLLA-beads has no major effect on the properties of the entrapped urease. However, the decline of the pH-course of the reaction rate is somewhat steeper towards lower pH-values and the polyester seems to stabilize the enzyme at pH-values below 5.5. As a consequence, the efficiency – that is already quite high in the area around the pH-optimum – increases above 1.

An important criterion for immobilized biocatalysts is their reusability. Corresponding tests were carried out with a flow injection analysis device containing between 20 mg and 100 mg of the immobilized catalysts as fixed bed. The substrate solution was injected by use of a µl-syringe. The results compiled in Figure 7 exhibit that the activity loss of the urease/PDLLA-system after seven repeated applications is negligible.

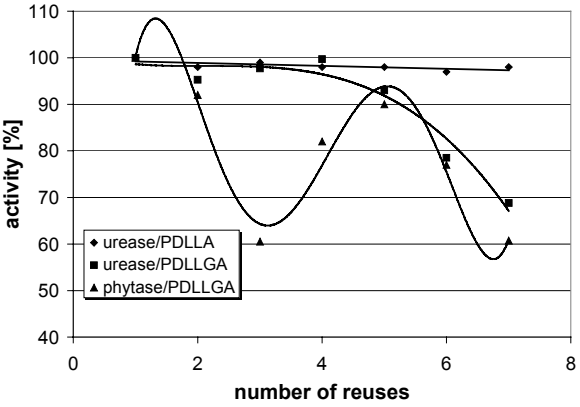

Figure 7:
Examples for the operational stability of the enzymes urease and phytase immobilized within polyester microspheres

However, if PDLLGA is applied the activity deteriorates continuously and after ten applications the residual activity is 50 %. If such a series of measurements is interrupted for 50 hours, the activity decreases again down to 30 % and then remains nearly constant up to 40 further repeated uses. Thereafter, the obtained signal was still inversely proportional to the substrate flow rate which allowed enhancement of the sensitivity of urea detection by changing this parameter. An investigation into the operational stability of phytase-containing PDLLGA-microspheres exhibited that the activity undergoes considerable variations during repeated application between 30 % and 80 %, even after a twenty-fold reuse. The reason for this behaviour is not yet clear.

Table 1 contains a summary of kinetic data for the three investigated enzymes phytase and urease, together with first results concerning ß-D-galactosidase. The best results with respect to the efficiency and the temperature stability were obtained with urease inserted into PDLLA- and PDLLGA-microspheres. However, the data for the PDLLGA-urease system are

not uniform for preparations made by different operators. Furthermore, the application of PDLLGA leads to a decrease of temperature stability if urease or phytase are entrapped within this polyester – a phenomenon that was not found for immobilized ß-D-galactosidase, the efficiency of which is rather poor. A possible reason might be a leakage of the small enzyme molecules from the polyester particles during the immobilization procedure. Therefore, cross-linking reactions with glutar dialdehyde (Khare and Gupta 1990) were performed in order to enhance the apparent molecular weight. The obtained catalyst revealed an efficiency of about 30 % as well as a high temperature stability. Experiments dealing with the immobilization of such products by use of different polyester microspheres are in preparation.

Table 1:
Kinetic data for the enzymes urease, phytase, and ß-D-galactosidase in their native as well as immobilized state, eff. = efficiency

catalyst	K_m (mol/l)	E_a (kJ/mol)	T_{opt} (°C)	eff. (%)
native urease	0.0031	34.2	65	100
urease/PDLLA	0.0069	24.2	65	> 90
urease/PDLLGA	0.005-0.01	25-40	55	50-70
native phytase	0.00024	53.5	60	100
phytase/PDLLA	0.0005	59.6	55	17
phytase/PDLLGA	0.0005	59.6	55	40-50
native ß-D-galac	0.0042	23	65	100
ß-D-galac/PDLLA	0.00083	14,3	70	4
ß-D-galac-crossl.	0.0028	19.83	>70	32

One of the problems that surfaced during work-with polyester beads in an aqueous solution was their low wettability. This means that in a stirred tank reactor the stirring rate has to be high in order to achieve a homogeneous distribution of the catalyst. The situation could be improved by adding surfactants to the reaction mixture. Especially the application of phosphatidyl choline was successful. If this phospholipid is present during the hydrolysis of urea by the urease-PDLLA system, the activation energy decreases from 24 kJ/mol to 19 kJ/mol as a consequence of which the reaction rate is enhanced by nearly 50 % at room temperature and still 15 % at 65°C. A similar result was found for phytase entrapped within this polyester. However, as the diminution of the activation energy in this case is even higher, the positive effect of phosphatidyl choline on the reaction rate is restricted to a temperature range around 300 K.

4 Conclusions

The experimental results shown in this contribution confirm that polyesters are, in principle, well suited for the entrapment of enzymes. This is especially valid for biocatalysts with a high molecular weight like urease. In the case of small protein molecules, leakage into the surrounding bulk solution must be expected. This could be avoided either by coating the polyester beads with a second thin polymer layer by which the wettability might also be improved, or by changing the preparation conditions for microspheres with the aim of reducing the pore size of the polyester surface. Another possibility is to insert enzymes in their cross-linked state. Corresponding experiments are in preparation.

Acknowledgements

We have to thank the companies Gist-brocades (Delft) and Purac (Gorinchem) for providing us with phytase, and poly(DL-lactic acid), respectively, as well as the students Theresa Heckmann, Arne Reuman, and Dirk Schulze for their support in performing experiments.

References

Buchholz K, Kasche V (1997) Biokatalysatoren und Enzymtechnologie. Weinheim: VCH

Chang TMS (1998) Pharmaceutical and therapeutic applications of artificial cells including microencapsulation. Eur J Pharm Biopharm 45:3-8

Cooper AI (2001) Recent developments in material synthesis and processing using supercritical CO_2. Adv Mater 13(14):1111-1114

Grunwald P (1984) Imparting of some biochemical fundamentals in the course of basic education of chemistry students with the system urea/urease as example. Biochem Educ 12:170-173

Grunwald P, Hansen K, Gunßer W (1997) The determination of effective diffusion coefficients in a polysaccharide matrix used for the immobilization of biocatalysts. Solid State Ionics 101-103:863-867

Hanns M, Rey A (1971) Application de la conductoétrie à l'étude des réactions enzymatiques, système urée-uréase. Biochim Biophys Acta 227:630-638

Khare SK, Gupta MN (1990) An active insoluble aggregate of E. coli ß-galactosidase. Biotechnol Bioeng 35:94-98

Vorlop K-D (1985) Entwicklung von Verfahren zur Polymerfixierung von Mikroorganismen und Anwendung der Biokatalysatoren zur Spaltung von Penicillin G und Synthese von L-Tryptophan. Thesis, Technische Universität Carolo-Wilhelmina zu Braunschweig: pp. 64-75

Vorlop K-D, Klein J (1982) New developments in the field of cell immobilization – formulation of biocatalysts by ionotropic gelation. In: Lafferty RM (ed) Enzyme technology. Springer Verlag, Berlin, pp. 219-235

Yang Y-Y, Chung T-S, Bay X-L Chan W-K (2000) Effect of preparation conditions on morphology and release profiles of biodegradable polymeric microspheres containing protein fabricated by double emulsion method. Chem Eng Sci 55:2223-2236

Process development for production of DFA from inulin on an industrial scale: Screening, genetic engineering and immobilisation

Ulrich Jahnz, Milada Schubert and Klaus-Dieter Vorlop[1]

Abstract

The bioconversion of renewable resources for industrial applications increasingly often demands the availability of suitable technologies for the usage of enzymes. This paper presents results obtained from the development of a process designed to convert inulin into difructose anhydrid (DFA III).

In a broad screening programme, strain Buo141 was isolated which expresses a thermo stable enzyme carrying out the desired conversion. To increase the formation of enzymes the inulase gene was cloned into *E. coli* XL1-blue, inulase II was expressed and its activity was detected. After optimising the enzyme with genetic engineering techniques, the GMO was fermented and an activity of 1.76 Mio U/L was observed.

To allow permanent immobilisation the enzyme was flocculated from cell-free extract by co-cross-linking with chitosan and glutardialdehyde. Subsequently the enzyme was entrapped in calcium alginate hydrogels. To enable the production of uniform and small bead shaped particles, novel JetCutter technology was used with a production rate of 5600 beads/(s·nozzle). The influence of bead diameter on the activity was investigated and an activity of 196 U/g was measured for 600 µm beads. The figures obtained from the experiments were in wide consistency with theoretical data.

Keywords: inulin, DFA, screening, thermotolerant enzyme, genetic engineering, immobilization, JetCutter

1 Introduction

1.1 Bioconversions for industrial raw materials

The growing awareness of limited fossil resources and environmental problems connected to carbon dioxide have caused an increased interest in renewable resources. For many applications, crop-based products have to be refined first. Refining steps can either be chemical or use whole cells or isolated enzymes. Before establishing a process to convert agricultural products for non food applications, proper cells or enzymes have to be found and optimised for optimal operation. This paper shows the schedule of such a development for the conversion of inulin into a disaccharide called DFA III.

1.2 Origin and usage of inulin

Inulin is a linear β-2,1-linked polyfructan terminated with a glucose residue. Large amounts of inulin are contained as reserve carbohydrates in the roots and tubers of such crops as chicory and Jerusalem artichoke. The degree of polymerisation depends on the originating plant and is usually in the range from nine to some thirty fructose units. Inulin has various applications in food and non-food areas.

Carboxylated inulins act as tensides and can be used as replacements for polyacrylates in washing agents or can be further functionalised with sulfonic groups and employed as chelating agents. Ether-products of long-chained inulins with epoxides can be used as plasticisers for thermoplasts or in textile industries. Further chemical products from inulin like furandialdehyde or furandicarbonic acid are accessible via the intermediate 5-hydroxymethylfurfural.

Numerous works deal with the bioconversion of inulin to obtain products for the non-food-market. Possible fermentation products are butanol (*Clostridium pasteurianum*), acetone (*C. acetobutyricum*), and 2,3-butanediol (*Bacillus polymyxa*) (Oiwa et al., 1987). Ethanol for fuel purposes can be produced by *Klyuveromyces marxianus* without the need for prior hydrolysing of the inulin chains (Bajpai and Bajpai, 1989).

The uses of inulins in human nutrition have long been known, and they have, since the 19th century, for instance, been used in coffee-surrogates. Fructooligosaccharides are added to various food products, mainly in the dairy area as dietary fibres in probiotics. As an alternative to high-fructose corn syrups (HFCS) high-fructose syrups can be gained from either chemical or enzymatic hydrolysis of inulins or inulin-containing crops like the Mexican agave and their juices are fermented directly to yield alcoholic drinks like tequila.

However, inulins have a very limited market thus far in both the food and the non-food-area. This is

[1] Ulrich Jahnz, Milada Schubert and Klaus-Dieter Vorlop, Institute of Technology and Biosystems Engineering, Federal Agricultural Research Centre (FAL), Bundesallee 50, 38116 Braunschweig, Germany

mainly due to the high cost connected with expensive separation and purification steps. For 1.5 to 2 €/kg it is about four times as costly as competing glucose, starch or sucrose. This also explains why short oligofructoses for probiotic products are synthesized enzymatically from sucrose rather than obtained by partial hydrolysis of inulins.

Future use of inulin-derived products is thus either in high-value markets like the functional food segment or by converting inulin into intermediates which can be separated and purified at lower costs.

1.3 DFA III

One promising compound derived from inulin for this purpose is di-D-fructofuranose-1,2':2,3'-dianhydride (DFA III). The formation of DFA III is catalysed by the enzyme inulase II as a kind of an intramolecular transfructosylation (Tanaka et al., 1975). DFA III can be used as a substitute for sucrose in human nutrition. It has half the sweetness of sucrose and thus gives a comparable volume when used as a food-additive. Since it is not metabolised by the human body it is clearly reduced in calories. Like the fibre inulin itself, DFA III has a positive effect on the intestinal microbial flora and was shown to enhance the uptake of calcium (Suzuki et al., 1998).

On the other hand, DFA III can be the basis for plastics and tensides. After ion exchange it can be crystallised as easily as sucrose and hence it can be produced at a price well below that of inulin. So far DFA III has not been introduced onto the market since no efficient enzyme and biotechnical process was available for the necessary bioconversion of inulin.

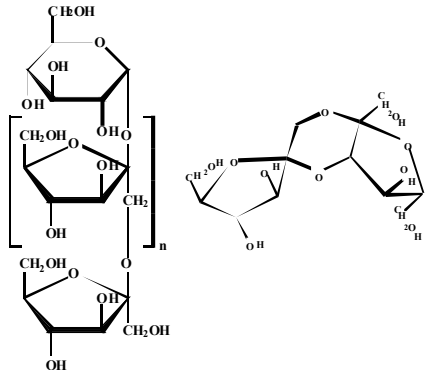

Figure 1:
Chemical structure of inulin (left) and the enzymatic conversion product DFA III (right)

1.4 Catalysts in continuous processes

To establish a large scale process based on a biochemical reaction it is preferable to have means available to hold back the catalyst in the bioreaction vessel. By immobilising catalysts like growing, resting or dead cells or enzymes it is possible to retard them. Besides the advantage of easy retention, immobilised catalysts often also show an increased stability with regard, for instance, to pH-value and temperature.

As a matrix for entrapment, the biopolymer alginate can be chosen. Sodium alginate is mixed with the catalyst solution and then solidified by dripping into a solution of calcium chloride. The resulting particles are bead-shaped and the biocatalyst is equally distributed throughout the volume of the bead.

However, encapsulation of catalysts also has disadvantages. Depending on the used matrix system the catalyst may be inactivated during the process of matrix formation. Even if this is not the case, the overall activity of the bead in case of calcium-alginate entrapment is less than that of the free catalyst due to diffusional limitations. To minimise this negative effect, particles have to be kept as small as possible and as is reasonable for the later application.

Continuous processes are preferably run in packed bed reactors. Since these build up significant pressure, it is important to have as stable beads as possible. The stability of the beads can be increased by using higher concentrated polymer solutions, which simultaneously makes it more difficult to fulfil the above claim for small particles.

1.5 Enzyme immobilisation

Using hydrogels, the majority of enzymes used in bioconversion processes shows a too low molecular weight and is thus not suitable for direct entrapment. In natural form, the enzyme would readily diffuse from the matrix. To increase the molecular weight, several enzymes can either be linked with each other or co-crosslinked covalently with polymers. Among suitable materials, the naturally derived polymer chitosan is favourable since its amino groups provide a good reaction site for linkage to the amino groups of lysine residues of enzymes as depicted in Figure 2. The exact reaction conditions depend on the enzyme and have to be optimised specifically.

1.6 Aims of the work

To isolate strains producing inulase II enzymes, a broad screening-programme was started. Of special interest were thermo-tolerant enzymes which are stable at a temperature of at least 60°C for a prolonged period of time. By cloning the corresponding *ift* gene into *E. coli* the production of this enzyme should be enhanced. To facilitate the use of the enzyme in a future industrial process, the basics for its immobilisa-

tion were investigated and the practical results compared to theoretical values.

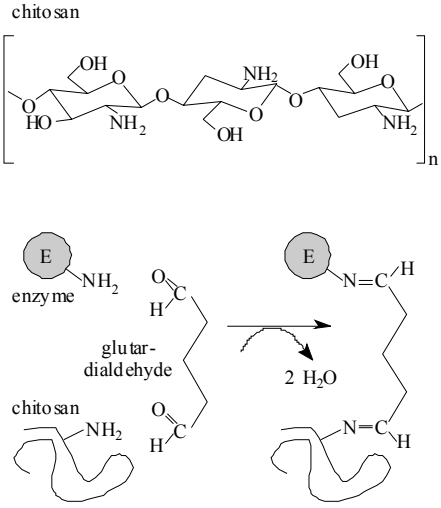

Figure 2:
Chemical structure of chitosan and reaction with glutardialdehyde and enzyme-bound amino groups, simplified scheme

2 Materials and methods

2.1 Screening for microorganisms

For selective enrichment, a mineral salt medium with inulin from dahlia tubers as the sole source for carbon and energy was used. Samples were plated on a solidified medium and incubated at 30, 45 and 60°C under aerobic and anaerobic conditions. Grown colonies were then subcultured to liquid media and screened for formation of DFA III by HPLC analysis (column CHO611, Interaction Chromatography, San Jose; eluent 1 mM NaOH; 0.5 mL/min; RI detector). Supernatant of positive strains was tested after incubation at different elevated temperatures to determine temperature stability. DFA was verified by NMR measurement.

2.2 Genetic engineering

For cloning of the *ift* gene, a genomic library was constructed from partially digested Arthrobacter genome in phage l. By phylogenetic analysis of published data, a universal *ift* gene-specific primer pair was designed and used to amplify a homologous *ift* gene-specific probe from Arthrobacter chromosomal DNA. This probe was used to screen the genomic library and a hybridizing clone, bearing an approximately 15 kBp large genomic fragment with the complete *ift* gene, was isolated. The genomic subfragments were subcloned into the plasmids pUC18 and pUC19, respectively. Based on these *ift*-subclones, expression vectors were constructed and the enzyme expressed in *E. coli* XL1-blue and its activity detected. Activity tests were done by measuring the amount of DFA III formed in 30 minutes from a 10 % (w/v) solution of inulin at 50°C.

Enzyme design was accomplished on the DNA level in two steps: The sequence for the original signal peptide was partially removed by exonuclease activity. Based on results obtained from these experiments, the entire region coding for the transfer peptide was subsequently deleted by means of specific endonucleases. Additionally a point mutation in the coding region of the *ift* gene was generated by error-prone PCR.

To obtain large quantities of the enzyme, the genetically modified organism was fermented in 10-L-scale (NLF22, Bioengineering, Wald) using a medium consisting of technical yeast (Ohly, Hamburg) extract and glycerol as carbon source. Cells were harvested and disrupted with a high pressure homogenizer (LAB60, APV Gaulin, Lübeck; 3 passages of 65 MPa; 0.5 L/min).

2.3 Enzyme immobilisation

For immobilisation the enzyme was co-cross-linked. Chitosan (geniaLab, Braunschweig) was dissolved in 0.5 % (w/w) acetic acid and mixed with enzyme solution as a cell free extract. After addition of glutardialdehyde from a 50 % stock solution cross-linking was accomplished over 24 h at 4°C while stirring and afterwards 3 % sodium alginate (LF20/60, FMC Biopolymer, Drammen) was added. Small droplets of 500 to 850 µm in diameter were formed with a JetCutter (geniaLab Braunschweig; nozzle 300 µm; flow of liquid 0.9 g/sec; cutting tool 48 wires of 100 µm; rotation speed 7000 rpm) and hardened in a 2 % calcium chloride solution. To evaluate the effect of diffusional limitation, the activity of beads of different diameters was measured.

Alginate beads were dissolved for 30 min in a mixed solution of 100 mmol/L sodium citrate and 100 mmol/L sodium chloride.

3 Results and discussion

3.1 Screening and genetic optimisation

The screening programme resulted in strain Buo141 expressing an extracellular enzyme which is stable at temperatures of 60°C. Using metabolic data and 16S-rRNA-sequencing, the strain was identified as a new Arthrobacter species, growing aerobically at ambient temperatures.

To gain access to the gene coding for inulase II (*ift* gene) primers for a PCR-reaction were needed. Suitable sequences for primers were phylogenetically reasoned from two highly divergent sequences:

- a DFA III producing inulase enzyme, in its function identical and in its phylogenetic origin closely related to our enzyme (Sakurai et al., 1997)
- a DFA I producing inulase enzyme, in its phylogenetic origin only distantly related to our enzyme (Haraguchi et al., 1995)

Using this universal *ift* gene-specific primer pair, a region of approx. 500 bp was amplified from the Arthrobacter chromosomal DNA. The complete *ift* gene was obtained by screening the genomic library with this probe. As a result a plasmid was constructed in pUC19 which expressed an enzyme of 477 amino acids when transferred to *E. coli* XL1 blue. A cell-free extract of such a culture showed an activity of 3000 U/L, whereas the majority of this activity was detected intracellularly.

For optimisation the sequence coding for a signal transfer-peptide, which is responsible for transport of the enzyme via the membrane in Arthrobacter, was identified and removed resulting in a hundred fold increased activity. A further increase in activity of approx. 35 % was achieved by a point-mutation which was induced by error-prone PCR. On position 221 of the enzyme a glycine was exchanged with arginine. A new a-helix region can be generated in the region of amino acids 216 to 224 according to the model of Garnier et al. (1978). The resulting GMO was named *E. coli pMSiftOptR*.

3.2 Production of enzyme

The recombinant *E. coli* was fermented using an inexpensive technical medium. During the fermentation the inulase activity was monitored, a typical fermentation run is depicted in Figure 3. A final biomass concentration of 11 g/L (dry weight) and an overall activity of $1{,}76 \cdot 10^6$ U/L was measured.

Since high-density fermentations of *E. coli* are known to reach biomass concentration of 100 g/L, it seems reasonable that after optimising the fermentation an activity of at least 15 million units per litre seems to be possible.

3.3 Co-cross-linking of enzyme

Initially it was tested if the covalent binding of the enzyme inulase II has an influence on its activity. If lysine residues are located in the enzyme's active site a reaction of their amino groups may lead to a readily inactivation. As can be seen from Figure 4, our enzyme is not susceptible to glutardialdehyde over a broad range of concentration and thus the envisaged method of co-cross-linking was viable.

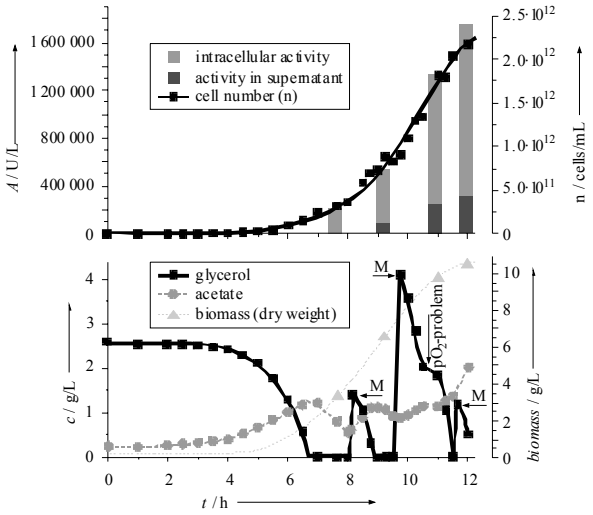

Figure 3:
Run of fermentation of *E. coli pMSiftOptR*, (M) indicates addition of new medium to the fermenter

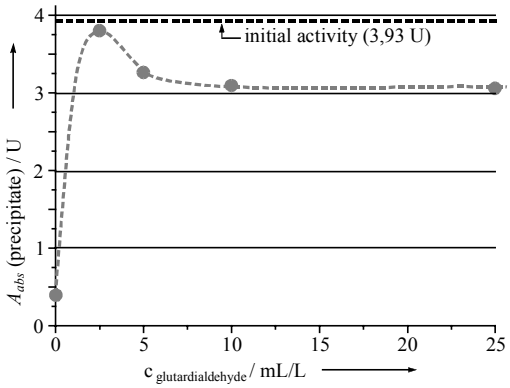

Figure 4:
Effect of glutardialdehyde on enzyme activity

Subsequently the optimal ratio of enzyme, chitosan and glutardialdehyde was determined in a matrix experiment. Using the enzyme solution derived from the above described fermentation ($1{,}76 \cdot 10^6$ U/L) precipitates were obtained in combination with varying amounts of chitosan and glutardialdehyde. To investigate the quality of the co-cross-linking alginate, beads were made in manual operation from each preparation, washed thoroughly and dissolved again for activity testing. As can be seen from Figure 5, a maximum of activity could be found at a chitosan concentration of 0.45 % (w/w) and at a glutardialdehyde usage of 25 mL/L (50 % (w/w) solution), respectively. This corresponds to approx. 30 mmol/L of reactive amino groups in the chitsoan and approx. 280 mmol/L aldehyde groups from glutardialdehyde. The protein concentration in this preparation was 2.8 g/L.

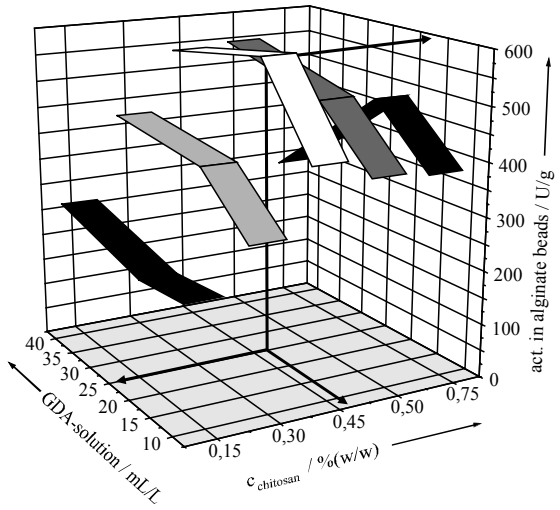

Figure 5:
Activities obtained from matrix experiments with varying concentrations of chitosan and glutardialdehyde

3.4 Mass production of beads

Based on these findings, a larger batch of co-cross-linked enzyme was prepared. To accomplish the task of producing the tiny droplets from the highly viscous alginate-enzyme-mixture, novel JetCutter technology was employed (Vorlop and Breford, 1984). In comparison to other techniques like blow-off devices, vibrating nozzles or electrostatic forces, the JetCutter uses a mechanical cutting of a continuous jet of liquid to produce small droplets (Prüße et al., 1998; Jahnz et al., 2001). It is possible to work with liquids which have a viscosity of up to several Pa·s. The jet of liquid escapes from the nozzle (50 to 1200 µm in diameter) at a constant velocity of 10 to 30 m/s and the cutting tool with 48 wires rotates with a constant speed of up to 10 000 rpm. Due to these parameters the JetCutter has a tremendous throughput.

The resulting particles were sieved and the different fractions weighed. As can be seen from Figure 6 the distribution in particle size is small and in the desired range of 600 to 700 µm.

3.5 Kinetic investigation of entrapped inulase II

Beads with diameters in the range of 500 to 800 µm were analysed and the activities compared as is shown in Figure 7. For beads of 600 µm diameter an activity of 196 U/g was measured for wet matter. Comparing the initial slopes of the curves an effectiveness h factor can be calculated. While beads of 600 µm in diameter showed an effectiveness factor of 0.44, for beads of 850 µm this value dropped to 0.34.

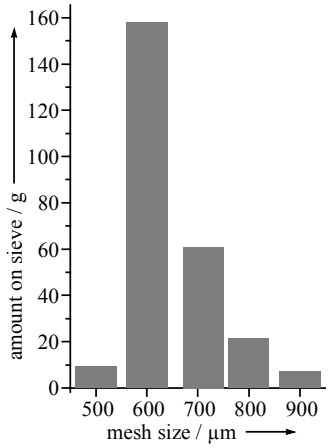

Figure 6:
Distribution of alginate beads (sieve analysis)

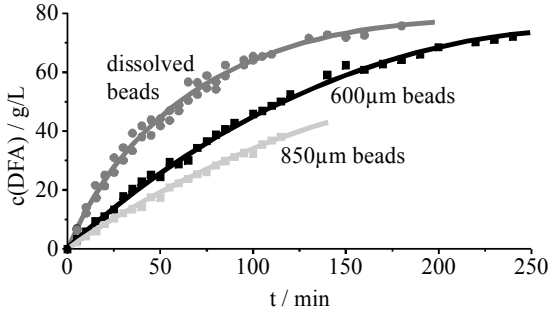

Figure 7:
Activity of beads with encapsulated inulase II at different diameters (shown are results for dissolved beads and for diameters of 600 and 850 µm, respectively)

These results were reviewed from a theoretical point of view. The diffusion coefficient for inulin in pure water at the elevated temperature of 50°C was calculated according to the following equation using the known dynamic viscosity values ϖ_{T1} and ϖ_{T2} for water.

$$D_{0,T2} = \frac{D_{0,T1} \cdot T2 \cdot \eta_{T1}}{T1 \cdot \eta_{T2}} = 4.64 \cdot 10^{-6}\ \mathrm{cm^2/s}$$

$D_{0,T1}$ = $2.30 \cdot 10^{-6}$ $\mathrm{cm^2/s}$ (Chaplin, 2001)
$T1$ = 293 K
$T2$ = 323 K
ϖ_{T1} = 1.002 mPa·s
ϖ_{T2} = 0.5468 mPa·s (Treybal, 1980)

To take into account the hindering influence of the matrix consisting of alginate and co-cross-linked chitosan, the effective diffusion coefficient was calculated according to the equation of White and Dorion (1961), where a is a parameter for the molecular weight of the substrate and Vp is the concentration of

solid matter in the particle. It is estimated by summing up the concentrations for alginate, protein, glutardialdehyde and chitosan:

$$D_{eff} = D_0 \cdot e^{-a \cdot Vp} = 2.11 \cdot 10^{-7}\ cm^2/s$$

a = 69 (extrapolated from Vorlop, 1984)
Vp = 0.0448 kg/L

Based on Michaelis-Menten kinetic the Thiele modulus Φ is calculated according to the following equation for spherical particles (data shown for beads of 600 µm in diameter):

$$\Phi = \frac{r_P}{3} \cdot \sqrt{\frac{v_{max}}{K_M \cdot D_{eff}}} = 9.63$$

r_P = 0.03 cm
v_{max} = $4.5 \cdot 10^{-4}$ mol/(min·g)
K_M = $2.3 \cdot 10^{-3}$ mol/L
D_{eff} = $2.11 \cdot 10^{-7}$ cm²/s

Figure 8 shows the relation of the Thiele modulus Φ and the key figure β, which is the ratio of the concentration in the solution surrounding the particle and the K_M-value for the considered enzyme:

$$\beta = \frac{c_0}{K_M} = 7.7$$

c_0 = $1.78 \cdot 10^{-3}$ mol/L
K_M = $2.3 \cdot 10^{-3}$ mol/L

Recapitulating, the following figures are calculated for different particles:

d_{bead}	$\eta_{exp.}$	β	Φ	$\eta_{calc.}$
600 µm	0.44	0.77	9.63	0.34
850 µm	0.34	0.77	13.65	0.23

As can be seen the values obtained from the experiments and those calculated differ significantly but are in the same order of magnitude. However, it has to be considered that the following assumptions and estimations were made:

- The beads used in the experiments were selected by sieve analysis and thus they do not have an exact diameter.
- For obtaining the parameter a for the molecular weight of the substrate inulin, a far-ranging extrapolation was necessary.
- The content of solid matter within the particles was only roughly calculated.

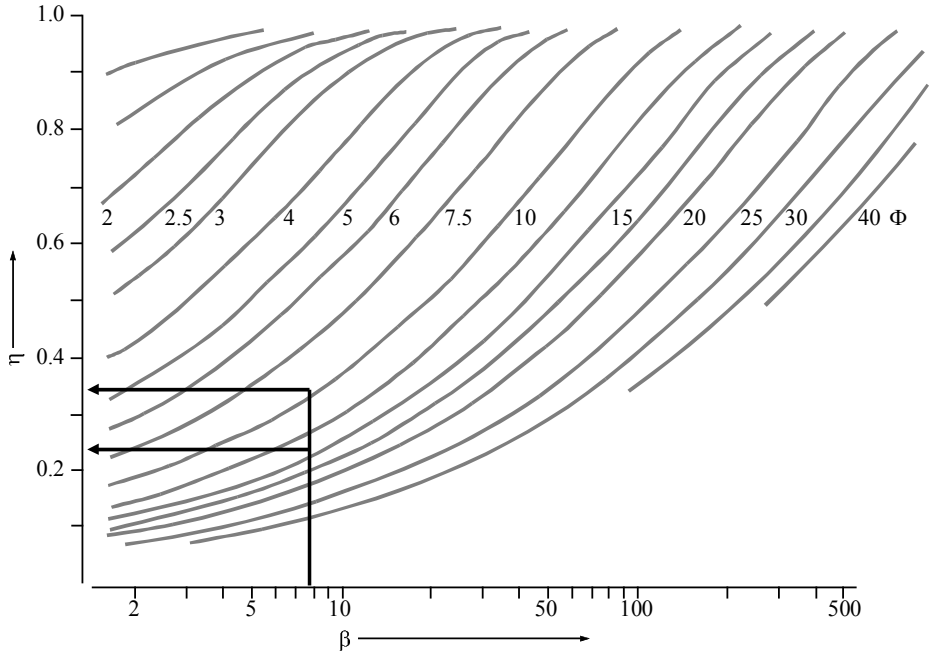

Figure 8:
Calculated effectiveness factors η with respect to different values for Thiele modulus and substrate key figures β (taken from Vorlop, 1984). The results for particles of 600 and 850 µm diameter, respectively, are pointed out.

4 Summary

We have shown the complete work starting from screening for an enzyme with the desired characteristics, i.e., an inulase II converting inulin to DFA III at elevated temperatures of 60°C. Next we successfully optimised the enzyme by genetic engineering and constructed a genetically modified organism which expresses the enzyme in very high numbers. We fermented this strain and showed the benefits of entrapping the enzyme in hydrogel particles which had an activity of 196 U/g (wet matter).

For different particles the effectiveness factor was measured and also calculated on a theoretical basis. The values matched each other satisfactorily.

5 Conclusions

To produce DFA III at a technical and industrial scale, large amounts of encapsulated enzyme are needed. The work described in this paper gives a basis for satisfying this need. Due to results from genetic engineering, a standard fermentation technique is capable of producing unlimited enzyme which can then be encapsulated on an industrial scale by using the novel JetCutter technology. The prospect of producing DFA III on an industrial scale has been accelerated greatly.

Acknowledgements

We are thankful to Fachagentur Nachwachsende Rohstoffe e.V. (FNR), Gülzow, and Nordzucker AG, Braunschweig, for partially financing the work.

List of Symbols and Units

a	parameter for molecular weight (-)
β	ratio of concentration and enzymatic activity
c_0	concentration in solution (mol/L)
$D_{0,Tx}$	diffusion coefficient at given temperature Tx (cm^2/s)
D_{eff}	effective diffusion coefficient within matrix (cm^2/s)
Φ	Thiele modulus (-)
K_M	Michaelis Menten constant (mol/L)
η	effectiveness factor (-)
rpm	rotations per minute
r_p	radius of particle (cm)
Tx	temperature (K)
U	enzyme units (1 U = 1 µmol/min)
µ...	micro...
V_p	concentration of solid matter (kg/L)
v_{max}	maximum enzymatic activity (mol/(min·g))
ϖ_{Tx}	dynamic viscosity at given temperature Tx
% (w/w)	weight percentage

References

Bajpai P, Bajpai PK (1989), Utilization of Jerusalem artichoke for fuel ethanol production using free and immobilized cells. Biotechnol Appl Biochem 11:155-168

Haraguchi K, Seki K, Kishimoto M, Nagata T, Kasumi T, Kainuma K, Kobayashi S (1995), Cloning and nucleotide sequence of the inulin fructransferase (DFA I-producing) gene of *Arthrobacter globiformis* S14-3. Biosci Biotech Biochem 59:1809-1812

Jahnz U, Wittlich P, Pruesse, U, Vorlop K-D (2001) New matrices and bioencapsulation processes. In: Focus on Biotechnology Vol. 4, Hofmann M and Anne J (eds), Kluver Academic Publishers, Dordrecht, pp. 293-307

Oiwa H, Naganuma M, Ohnuma S (1987), acetone-butanol production from dahlia inulin by *Clostridium pasteurianum* var. I-53. Agr Biol Chem Tokyo 51(10):2819-2820

Prüße U, Fox B, Kirchhoff M, Bruske F, Breford J, Vorlop K-D (1998), New Process (Jet Cutting Method) for the production of spherical beads from highly viscous polymer solutions. Chem Eng Technol 21:29-33

Sakurai H, Yokota A, Tomita F (1997), Molecular cloning of an inulin fructotransferase (de-polymerizing) gene from *Arthrobacter sp.* H65-7 and its expression in Escherichia coli. Biosci Biotech Biochem 61:87-92

Suzuki T, Hara H, Kasai T, Tomita F (1998) Effects of difructose anhydride III on calcium absorption in small and large intestines of rats. Biosci Biotechn Biochem 62:837-841

Tanaka T, Uchiyama T, Kobori H, Tanaka K (1975) Enzymic hydrolysis of di-D-fructo-furanose 1,2':2,3' dianhydride with *Arthrobacter ureafaciens*. J Biochem 8:1201-1206

Vorlop K-D (1984) Entwicklung von Verfahren zur Polymerfixierung von Mikroorganismen und Anwendung der Biokatalysatoren zur Spaltung von Penicillin G und Synthese von L-Tryptophan. PhD-Thesis, Technical University Braunschweig.

Vorlop K-D, Breford J (1984), Verfahren zur Herstellung von Teilchen aus einem flüssigen Medium. German Patent DE4424998

White ML, Dorion GH (1961) Diffusion in a crosslinked acrylamide polymer gel. J Polym Sciences 55:731-740

Encapsulation of very soft cross-linked enzyme aggregates (CLEAs) in very rigid LentiKats®

Lorena Wilson[1], Andrés Illanes[2], Olga Abián[1], Roberto Fernández-Lafuente[1], and José M. Guisán[1]

Abstract

Aggregation of enzymes and further chemical cross-linking may a very simple and very useful method for preparation of industrial enzyme derivatives. Aggregation of semi-purified enzymes might allow: the preparation of very active enzyme derivatives, the very easy co-immobilization of several enzymes, the stabilization of multimeric enzymes against sub-unit dissociation, and the co-aggregation of enzymes and polymers in order to generate different enzyme micro-environments. In spite of this number of practical advantages, these enzyme derivatives are too soft and hence very difficult to handle both in conventional stirred tanks or in packed bed reactors. In order to overcome these technical limitations, the additional encapsulation of the very soft CLEAs into very rigid polyvinylalcohol polymers (LentiKats®) is proposed.

Keywords: Cross-linked enzyme, penicillin acylase, Lentikats®, dextran sulfate, polyethyleneimine

1 Introduction

Enzymes are biological catalysts with outstanding properties of specificity, activity under mild conditions and biodegradability (Polastro, 1989). These properties make them highly appealing as industrial catalysts. However, they suffer from a serious drawback, they are rather unstable (certainly much more than chemical catalysts) under process conditions. Several strategies have been considered to improve biocatalyst stability, going from screening, genetic and protein engineering of producing strains (Vieille and Zeikus, 1996; Adams and Kelly, 1998) to medium engineering (Klibanov, 1997; Rosell et al, 1998). Insolubilization has been a major technology of enzyme stabilization since the late sixties (Chibata and Tosa, 1976) and a few large-scale processes met with industrial success (Katchalsky-Katzir, 1993). However, recent advances in the rational design of matrices and insolubilization schemes (Fernández-Lafuente et al., 1999; Tischer and Kasche 1999) are now paving the way for a broader spectrum of industrial applications (Bruggink, 2001). Cross-linked enzyme aggregates (CLEA) are a new, very promising type of biocatalyst for industrial application, which combines the high stability of immobilized enzymes and cross-linked enzyme crystals (CLEC), with the fact that neither a solid matrix nor a highly purified enzyme is required. CLEA are produced by physical aggregation of enzyme molecules under non-denaturating conditions followed by chemical crosslinking. CLEA can be produced from semi-purified enzyme preparations allowing the preparation of very active enzyme derivatives, the simple co-inmobilization of several enzymes, the stabilization of multimeric enzymes against sub-unit dissociation and the co-aggregation of enzymes and polymers to generate different enzyme micro-environments. The latter aspect is very significant when using enzyme biocatalysts in reactions of synthesis in organic media. A hydrophilic microenvironment can be created around the enzyme molecules using polyfunctional charged polymers like dextran sulfate and polyethyleneimine. Then, even at high bulk concentrations of water-miscible organic cosolvents, which would otherwise be highly denaturant, enzymes will remain active and stable submerged in this protective hydrophilic microenvironment.

In spite of these practical advantages, CLEA are too soft and hence very difficult to handle, both in stirred tanks or in packed bed reactors. In order to overcome these technical limitations, encapsulation of the very soft CLEA into a very rigid polyvinyl alcohol (PVA) network, is here proposed as a suitable immobilization system for the production of robust process biocatalysts. These hydrogels have been widely used, especially in whole cell immobilization, because they are very elastic, stable and non-biodegradable (Lozinsky et al. 1998). Lens-shaped PVA hydrogels, under the trade name LentiKat®, are produced by gelation and partial drying at room temperature over a flat surface. Advantages of LentiKat® are: low cost of matrix, simple preparation, excellent mechanical and chemical stability, easy separation from the reaction medium and low diffusional limitations (Jekel et al. 1998, Gröger et al. 2001).

Penicillin acylase (Penicillin amidohydrolase; E.C. 35.1.11) is used as a case study. It is a remarkably versatile enzyme (Fernandez-Lafuente et al., 1998) whose primary industrial use is in the production of β-lactam nuclei for the chemical synthesis of second-

[1] Lorena Wilson, Olga Abián, Roberto Fernández-Lafuente, and José M. Guisán, Department of Biocatalysis. Institute of Catalysis, CSIC, Madrid, Spain
[2] Andrés Illanes, School of Biochemical Engineering, Universidad Católica de Valparaíso, Chile

generation β-lactam antibiotics (Shewale et al., 1990). However, if properly managed, this hydrolase can catalyze the reverse reaction of synthesis, so that now it is being used for the synthetic reaction as well (Bruggink et al., 1998; Wegman et al., 2001).

Two protocols to prepare crosslinked aggregates of the enzyme Penicillin G acylase (PGA) will be presented and discussed and different aggregating and cross-linking agents will be compared. Different protocols for the encapsulation of cross-linked PGA aggregates into LentiKats® will be evaluated as well. Finally, key functional properties of these novel immobilized derivatives (activity, thermal stability, cosolvent stability) and its behaviour in the synthesis of Cephalosporin G will be reported.

2 Materials and methods

2.1 Materials

Penicillin G acylase (PGA) (250 IUH/mg) was kindly donated by Antibioticos S.A. (Leon, Spain). Polyethyleneimine 25,000 was from Aldrich. Dextran sulfate and sodium borohydride were from Sigma. Polyethylenglycol 600 (PEG) was from Merck. Glutaraldehyde solution was from Fluka. All other reagents were of analytical grade.

2.2 Assay of hydrolytic enzyme activity

Enzyme activity was determined using a pHstat (Mettler Toledo, DL50) to titrate the H^+ produced by the hydrolysis of 10 mM Penicillin G in 0.1 M sodium phosphate at pH 8 and 25ºC. 50 mM NaOH was employed as titrant. One international unit of hydrolytic activity (IUH) of PGA was defined as the amount of enzyme that hydrolyzes one mmol of Penicillin G per minute under the above conditions.

2.3 Assay of enzyme activity of synthesis (for LentiKats® and CLEA)

The enzyme activity of synthesis was determined using a batch reactor thermostatted at 4ºC, with 25 mM 7-ADCA and 25mM AFA at 75 % v/v dioxane in 100 mM phosphate buffer, pH 7.0. The reaction mixture was gently stirred and samples were taken at intervals, dissolved in acetronitrile-water, 25:75 v/v, 10 mM phosphate buffer pH 3.0 and residual substrates and product assayed by HPLC. The enzyme activity of synthesis was determined as the initial rate of antibiotic synthesis under the above conditions.

2.4 Preparation of CLEA-PGA

Under agitation, 10 mL of PEG were added to 10 mL of PGA solution with 250 IU/mL to precipitate the enzyme. Glutaraldehyde (2 mL) was then added to cross-link the enzyme precipitate. Then, the reaction volume was duplicated by adding 100 mM sodium bicarbonate a solution pH 9.0 and 1 mg/mL of sodium borohydride. After 30 minutes, the CLEA-PGA produced was repeatedly washed, with 100 mM sodium phosphate pH 7.0, and centrifuged (Cao et al., 2000).

2.5 Preparation of dextran sulfate-polyethileneimine CLEADP-PGA

The same protocol as above is followed, but 10 minutes before adding PEG, 1.5 mL of dextran sulfate (100 mg/mL) and 1.5 mL of polyethyleneimine (100 mg/mL) are added to the PGA solution (Fernández-Lafuente et al. 1999).

2.6 Preparation of LentiKats®

CLEA-PGA and CLEADP-PGA LentiKats® were produced according to the protocol given by geniaLab, Braunschweig (Lentikats®, Tips & Tricks). Lentikat®Liquid and CLEA-PGA or CLEADP-PGA suspension were mixed in a 80/20 (v/v) ratio. The mixture was then fed to the LentiKat® Printer (see below) where small droplets were dripped over a plastic dish and exposed to drying and stabilization, as shown in Figure 1.

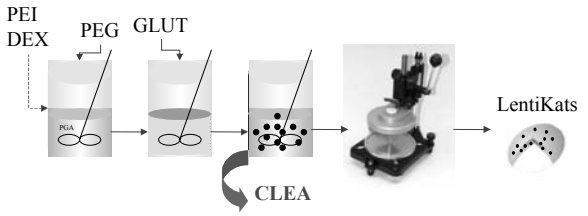

Figure 1:
Scheme for the preparation of LentiKats®, PEG: polyethyleneglycol, PEI: polyethyleneimine, DEX: dextran sulfate, GLUT: glutaraldehyde

2.7 Stability and thermal inactivation of CLEA-PGA and CLEADP-PGA LentiKats® in the presence of organic cosolvents

Stability of CLEA-PGA and CLEADP-PGA LentiKats® by prolonged incubation (50 days) at room temperature was studied in the absence and presence of organic cosolvents. Samples were taken, filtrated and the supernatants were assayed for residual enzyme activity and protein leakage.

To determine inactivation in the presence of organic cosolvents, CLEA-PGA and CLEADP-PGA LentiKats® were washed and equilibrated at 4ºC with 75 % v/v dioxane in 100 mM phosphate buffer, pH 7.0. Then, the biocatalysts were re-suspended in the same medium and temperature was raised to the desired value. Periodically, samples were withdrawn and the residual activity of synthesis was determined

Diglyme and dioxane, hydrophobic cosolvents, were selected as suitable cosolvents to study biocatalyst stability and thermal inactivation respectively. (Rosell et al., 1998). Dioxane presents the most inhibitory effect on the enzyme and it has been selected for the experiences of inactivation (Fernandez-Lafuente et al., 1991).

2.8 Synthesis of Cephalosporin G

Diglyme was selected as a suitable cosolvent to perform the synthesis of Cephalosporin G. Reaction was conducted under thermodynamic control using a batch reactor thermostatted at 20ºC, with 25 mM 7-ADCA and 25mM AFA at 75 % v/v diglyme in 100 mM phosphate buffer, pH 7.0. Reaction volume was 32 mL, with 780 and 600 mg of CLEA-PGA and CLEADP-PGA respectively. A multipoint agarose derivative of PGA (190 UI/gr), prepared as previously reported (Abián et al. 2001) was used as a standard of comparison, with 0.2 g of biocatalyst being used per 3 mL of reaction volume. Cephalosporin G was determined by HPLC.

3 Results and discussion

3.1 Yields of encapsulation

Yield of encapsulation was calculated as the percentage of expressed activity in LentiKat® biocatalyst with respect to the initial activity of the corresponding CLEA. Yields for CLEA-PGA LentiKat® and CLEA-DP-PGA LentiKat® were 60 and 80 % respectively.

3.2 Activity of CLEA-PGA and CLEADP-PGA LentiKats®

The hydrolytic specific activities of the biocatalysts were 38 and 50 IU_H/g for CLEA-PGA LentiKat® and CLEADP-PGA LentiKat® respectively.

3.3 Stability of CLEA-PGA and CLEADP-PGA LentiKats®

Stability of CLEA-PGA and CLEADP-PGA LentiKats® in buffer and organic cosolvent is presented in Table 1. No protein leakage was detected in any case and the enzyme was extremely stable in buffer. Stability in 50 % v/v diglyme was also very high in CLEA-DP-PGA LentiKats®, but much lower for CLEA-PGA LentiKats®. These results clearly reveal the protecting effect against solvent inactivation because of the ionic microenvironment in CLEADP-PG.

Table 1:
Biocatalyst stability of LentiKats® at 20ºC, in 100 mM phosphate buffer, pH 7.0 and 50 % v/v cosolvent; Digl.: diglyme

Time (days)	Stability of LentiKats® (% of initial)			
	CLEA-PGA		CLEADP-PGA	
	Bufffer 100%	Digl. 50%	Buffer 100%	Digl. 50%
50	93.65	48.33	95.15	80.64

3.4 Time-course of thermal inactivation of CLEA-PGA and CLEADP-PGA LentiKats®

Time course of enzyme thermal inactivation at 50ºC in buffer and in dioxane is presented in Figures 2 and 3 for CLEA-PGA and CLEADP-PGA LentiKats® respectively, with immobilized PGA in glyoxyl agarose (GA-PGA) being used as a standard of comparison. As seen in Figure 2, inactivation rate in GA-PGA is much higher than in any of the LentiKat® biocatalysts, with CLEDP-PGA LentiKat® being the most stable.

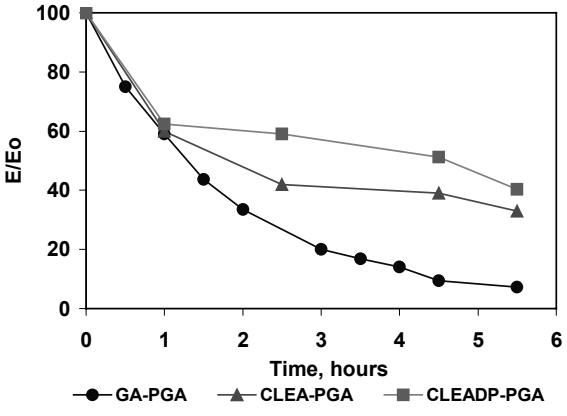

Figure 2:
Kinetics of enzyme inactivation at 50 ºC in 100 mM phosphate buffer, pH 7.0

Figure 3 shows the thermal inactivation conducted in the presence of cosolvent, inactivation rates of LentiKat® biocatalysts are much lower than in GA-PG and differences are much more pronounced than in buffer. However, in this case, inactivation of both types of LentiKat® biocatalyst is similar. Comparing the results in Figures 2 and 3, it is readily seen than

LentiKat® biocatalyst are strongly stabilized against inactivation by the presence of cosolvent. Half-life in buffer is 1.8 and 4.7 h for CLEA-PGA and CLEADP-PGA LentiKats® respectively at 50ºC, while in 75 % (v/v) dioxane projected half-lives, estimated according to first-order inactivation mechanism, increased to 407 h for CLEA-PGA and 433 h for CLEADP-PGA LentiKats®. It is yet to be determined to what extent mass-transfer limitation contributes to the apparent thermal stability of the LentiKat® biocatalysts, but certainly the differences with GA-PGA are too high to be a consequence of it. It was expected that the ionic microenvironment in CLEADP-PGA would protect the enzyme from cosolvent inactivation, but this was not seen in the case of dioxane, where inactivation kinetics of both LentiKat® biocatalysts were similar, differences being actually higher in buffer. It is still to be determined if significant differences are observed in more hydrophobic solvents, the reason for these results will be further studied.

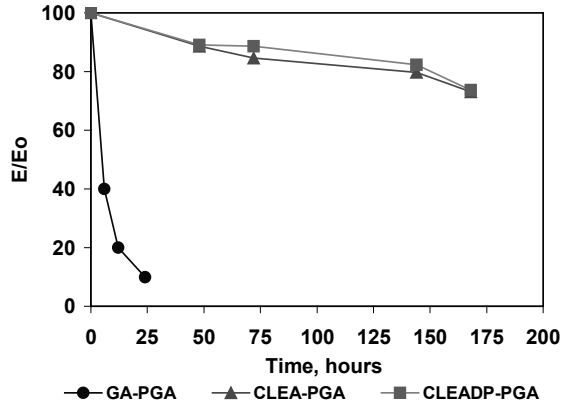

Figure 3:
Kinetics of enzyme inactivation at 4 ºC in dioxane at 75 % v/v in 100 mM phosphate buffer, pH 7.0

3.5 Synthesis of Cephalosporin G

Conditions for the synthesis under thermodynamic control of Cephalosporin G from 7ADCA and AFA, in organic media is presented in Table 2, for CLEA-PGA and CLEADP-PGA LentiKats®.

Table 2:
Conditions for the synthesis of Cephalosporine G at 25 mM 7ADCA and 25 mM AFA at 20ºC in 75 % v/v diglyme in 100 mM phosphate buffer, pH 7.0

	Hydrolysis velocity, UI/g	Synthesis velocity, UI/g
CLEA-PGA	74.66	0.20
CLEADP-PGA	67.3	0.25

4 Conclusions

Encapsulation of CLEA-PGA in PVA hydrogels produced LentiKat® biocatalysts with greatly improved mechanical properties with respect to fragile non-encapsulated CLEAs. LentiKats® produced from CLEA-PGA are quite stable with respect to thermal inactivation, especially in organic media, which makes them suitable biocatalysts for the synthesis of β-lactam antibiotics in such media. The hydrophilic microenvironment of LentiKats® from CLEADP-PGA, protects the enzyme from inactivation.

Results show that CLEAs-based LentiKat® biocatalysts are particularly suitable for synthesis of β-lactam antibiotics at a high concentration of organic cosolvents, conditions at which enzymes are usually unstable and poorly active. To our knowledge, this is the first-report of CLEA-based LentiKats®, which instead are widely used for cell immobilization. The formation of enzyme aggregates allows the use of this interesting type of matrix within the scope of enzyme biocatalysis.

Acknowledgements

We thank Antibióticos S.A. (Leon, Spain) and Hispanagar S.A. (Burgos, Spain) for their generous supply of PGA form *E.coli* and agarose gels, respectively. We gratefully recognize a fellowship for L.Wilson (AECI, Spain) and the support from the CSIC (Spain) – CONICYT (Chile) Program of International Scientific Cooperation.

References

Abián O, Mateo C, Fernández-Lorenate G, Palomo JM, Fernández-Lafuente R, Guisán JM (2001) Stabilization of immobilized enzymes against water-soluble organic cosolvents and generation of hyper-hydrophilic micro-environments surrounding enzyme molecules. Biocatal and Biotransform 19:489-503

Adams M and Kelly R (1998) Finding and using hyperthermophilic enzymes. Trends in Biotechnol 16:329-332

Bruggink A (2001) Synthesis of β-lactam antibiotics. Kluwer Acad. Publ., Dordrecht.

Bruggink A, Roos E, de Vroom E (1998) Penicillin acylase in the industrial production of β-lactam antibiotics. Organic Proc Res Develop 2:128-133

Chibata I and Tosa T (1976) Industrial application of immobilized microbial cells. In: Immobilized Enzyme Principles. Wingard L, Katchalsky E, Goldstein L (eds.) Academic Press, New York

Cao L, Van Langen F, Van Rantwijk F, Sheldon R (2001) Cross-linked aggregates of penicillin acylase: robust catalysts for the synthesis of β-lactam antibiotics. J Mol Cat B: Enz 11:665-670

Cao L, Van Rantwijk F, Sheldon R (2000) Cross-Linked Enzyme Aggregates: A Simple and Effective Method for the Immobilization of Penicillin Acylase. Org Lett 2:1361-1364

Fernandez-Lafuente R, Rosell C, Caanan-Haden L, Rodes L, Guisan J (1999) Facile synthesis of artificial enzyme nano-environments via solid-phase chemistry of immobilized derivates: Dramatic stabilization of penicillin acylase versus organic solvents. Enz Microb Technol 24:96-103

Fernandez-Lafuente R, Rosell C, and Guisan J (1991) Enzyme reaction engineering: synthesis of antibiotics catalized by stabilized penicillin G acylase in the presence of organic cosolvents. Enz Microb Technol 13:898-905

Fernandez-Lafuente R, Rosell C, and Guisan J (1998) Modulation of the properties of penicillin G acylase by acyl donor substrates during N-protection of amino compounds. Enzyme Microb Technol 22:583-587

geniaLab (2001) Manual: Lentikats®, Tips & Tricks. geniaLab Biotechnologie - Produkte und Dienstleistungen GmbH

Gröger H, Capan E, Barthuber A, Vorlop K-D (2001) Asymmetric synthesis of an (R)-cyanohydin using enzymes entrapped in lens-shaped gels. Org Lett 3:1969-1972

Jekel M, Buhr A, Vorlop K-D (1998) Immobilisation of biocatalysts in LentiKats. Chem Eng Technol 21:275-278

Katchalsky-Katzir E (1993) Immobilized enzymes-learning from past successes and failures. Trends in Biotechnol (11):471-478

Klibanov A (1997) Why are enzymes less active in organic solvents than in water? Trends in Biotechnol 15:97-101

Lozinsky VI, Plieva FM (1998) Poly(vinyl alcohol) cryogels employed as matrices for cell immobilization. 3. Overview of recent research and developments. Enzyme Microbiol Tech 23:224-242

Polastro E (1989) Enzymes in the fine-chemicals industry: dreams and realities. Bio/Technology 7:1238-1241

Rosell C, Terreni M, Fernández-Lafuente R, and Guisán J (1998) A criterion for the selection of monophasic solvents for enzymatic synthesis. Enzyme Microb Technol 23:64-69

Shewale J, Desphande B, Sudhakaran V, and Ambedkar S (1990) Penicillin acylases: applications and potentials. Proc Biochem 25:97-103

Tischer W and Kasche V (1999) Immobilized enzymes: crystals or carriers? Trends in Biotechnol 17:326-334

Vieille C and Zeikus J (1996) Thermoenzymes: identifying molecular determinants of protein structural and functional stability. Trends in Biotechnol 14:183-190

Wegman M, Janssen M, van Rantwijk F, and Sheldon R (2001) Towards biocatalytic synthesis of β-lactam antibiotics. Adv Synth Catal 343:559-576

Enantioselective hydrolysis of racemic epoxides with LentiKats®-encapsulated microorganisms

Thorsten Bruß[1,2], Daniel Mika[1], Bernhard Westermann[1], and Hans-Joachim Warnecke[2]

Abstract

Fungi like *Beauveria bassiana* can be used in biocatalytic kinetic resolutions of non-natural substrates. In our ongoing studies we are investigating the resolution of racemic epoxides like styrene oxide. To circumvent the classical drawbacks by using whole cell organisms, we devised a strategy to encapsulate them. Here we will report our results using the LentiKats-technology® for encapsulation of the fungi *Beauveria bassiana*. The catalytic activity remains high, in addition we will present data by which the recovered catalyst can be reused over a long period without losing its catalytic activity.

Keywords: Encapsulation, Beauveria bassiana, stereoselectivity, biohydrolysis, styrene oxide

1 Introduction

Kinetic resolution of racemic epoxides to chiral, non-racemic epoxides and their corresponding diols has been of considerable interest due to the most promising, versatile building blocks in asymmetric synthesis (Abramowicz 1990, Roberts and Wiggins 1993, Roberts et al. 1995, Kolb et al. 1994). At present, asymmetric epoxide hydrolysis can best be achieved by biocatalytic methods. On the one hand, epoxide hydrolases from mammalian sources such as rat or rabbit liver have been extensively investigated, but they are of limited use due to poor availability (microbial epoxide hydrolases are currently developed by Fluka Chemie, Switzerland). On the other hand, enzymes from microbial sources such as bacteria and fungi have only recently been identified (Faber et al. 1996, Pedragosa-Moreau et al. 1993). The latter can be produced on an almost unlimited scale by simple fermentation. The strength of enzymatic epoxide hydrolysis has recently increased tremendously due to the availability of microbial strains showing sufficient activity. Although these reactions show a strongly empirical aspect - i.e., knowledge of the substrate-selectivity pattern is limited at present - this area is heavily investigated and it can be anticipated that methods of great potential will be provided.

In reports published so far, the microorganisms are used in their native, non-immobilized form (Orru et al. 1997, Pedragosa-Moreau et al. 1996, Osprian et al. 1997, Bellucci et al. 1996). Therefore, the classical drawbacks of using microorganisms have to be encountered. Immobilisation techniques, however, are one of the most used methods to circumvent these obstacles. Despite several ways of immobilisation, there is still an urgent need for reliable and easy to carry out techniques.

We will show in this paper that the encapsulation of the fungi *Beauveria bassiana* in commercial available polyvinylalcohol mixtures (LentiKats®) is a very appropriate method for a stereoselective hydrolysis of styrene oxide (Figure 1). We use this substrate throughout our investigations. In addition, the high catalytic activity of these encapsulated catalysts, even after, several runs is shown.

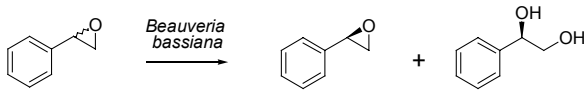

Figure 1:
Biohydrolysis of styrene oxide with *Beauveria bassiana.*

2 Experimental

2.1 Analytical monitoring

Enantiomeric excess of the styrene oxide is determined by GC (Chrompac Series 90000, He) using cyclodextrin modified materials (Heptakis-(6-*O*-butyldimethylsilyl-2,3-di-*O*-methyl)-β-cyclodextrin, Prof. König, Hamburg, Germany). Sample preparation: an aliqout of 2.0 ml of the aqueous reaction mixture is gently mixed with 2.0 ml of hexane. The retention time of (R)-styrene oxide is 8.9 min, of (S)-styrene oxide is 9.6 min.

Enantiomeric excess of the corresponding diol is determined by HPLC (Merck-Hitachi LaChrom) using cellulose modified materials (Chiracel OB-H, Daicel Inc., Japan). Sample preparation: the reaction mixture is extracted with dichloromethane as descrybed above. Mobile phase: hexane - *i*-propanole 9:1, 0.6 ml/min. Detection: UV detector, 219 nm. The (R)-

[1] Thorsten Bruß, Daniel Mika, and Bernhard Westermann, University of Paderborn, Department of Organic Chemistry, 33095 Paderborn, Germany
[2] Thorsten Bruß and Hans-Joachim Warnecke, University of Paderborn, Department of Technical Chemistry, 33095 Paderborn, Germany

phenylethane diol has a retention time of 26.5 min, the (S)-enantiomer of 36.0 min.

2.2 Encapsulation process (geniaLab 2001)

After melting at 80°C, 80 ml of commercially available polyvinyl alcohol is cooled down to 30°C. At the same time, 3.0 g of fungal cake, well dispersed in 20 ml of ringer solution, is added and reaction mixture is agitated gently. This mixture is applied with a LentiKat®-printer (geniaLab, Braunschweig, Germany, 400 spikes) on petri dishes. Afterwards the droplets are dried to 20 % of their weight on a laminar flow bench. For stabilisation of the droplets, the LentiKats® stabiliser is added. The stabilisation process is carried out for 2 hours by stirring the reaction mixture at room temperature. Afterwards, the LentiKats® are washed with phosphate buffer (0.1 m, pH 8.0) and kept in this solution for further reactions.

2.3 Biocatalytic reaction with styrene oxide

The batch hydrolysis is carried out in a 100 ml Erlenmeyer flask in a orbital shaker. 20 g of wet LentiKats® are mixed with 50 ml of 0.1 m phosphate buffer (pH 8.0). To start the reaction styrene oxide dissolved in ethanol (50 % aliquot) and added to the mixture. The concentration in the reaction mixture should be 1.0 g/l. The reaction is monitored as explained above. After the reaction, the LentiKats® were isolated by filtration and stored at 6°C in ringers solution. For all reactions, a strain of *Beauveria bassiana* taken from DSMZ in Braunschweig, Germany (DSM 1344) is used. Styrene oxide is obtained from Aldrich Chemicals and used without further purification.

3 Results and discussion

In all runs employing free and immobilised fungi *Beauveria bassiana*, the resolution of styrene oxide (Figure 1) was carried out under identical conditions. It could be shown that both free and encapsulated fungi are able to resolve the racemic substrate to an observed enantiomeric excess of ee > 98 %. However the reaction time differs slightly. In the case of free fungi, the resolution of the epoxide is achieved in 100 min, whereas encapsulated fungi needs 250 min (Figure 2). The enantiomeric excess of the phenylethane diol is, in both cases, very high, too. Free and immobilised fungi afford the diol in ee > 96 % (Figure 3). There is a little decrease of the enantiomeric excess of the diol in the reaction runs. This is because of the non selective autohydrolysis of the epoxide in water.

The differences in the reaction time, observed as enantiomeric excess of styrene oxide (Figure 3), can be explained as mass transport phenomena in the LentiKat® particles.

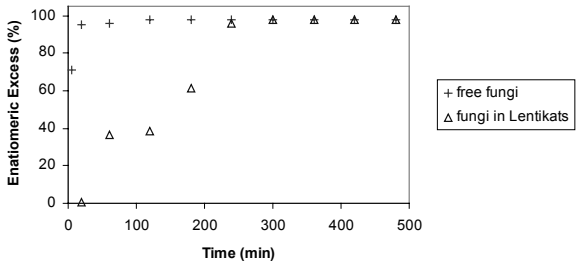

Figure 2:
Comparison of free and immobilised fungi, ee-value of styrene oxide.

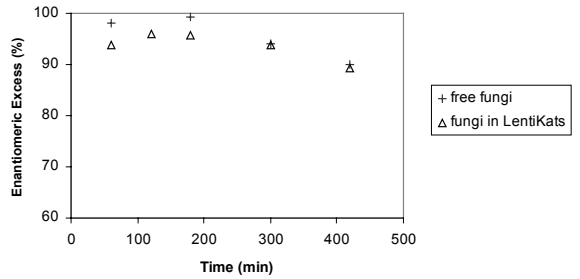

Figure 3:
Comparison of free and immobilised fungi, ee-value of phenylethane diol.

After the reaction, the lens shaped LentiKats® are recoverd by simple filtration, washed and stored in ringer´s solution at 6°C overnight and reused the next day. Again, the resolution reaction runs to high enantiomeric excess of styrene oxide and phenylethane diol (Figure 4 and 5).

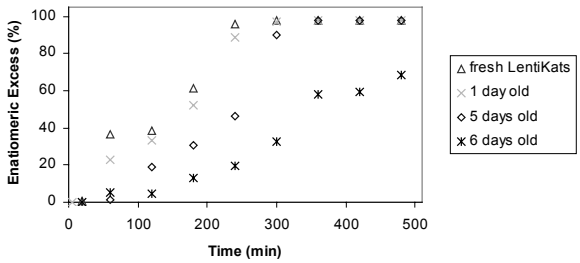

Figure 4:
Recycling experiments with the encapsulated biocatalyst, ee-value of styrene oxide.

The reaction rates decrease with the number of cycles. This indicates a decrease of activity of the immobilised biocatalyst. The high enantiomeric excess of styrene oxide (ee ≅ 98 %) is achieved in all runs. The reaction times increase from 250 min to 350 min.

Afterwards the reaction runs to an enantiomeric excess of 70 % in the experimental time of 500 min while steadily increasing.

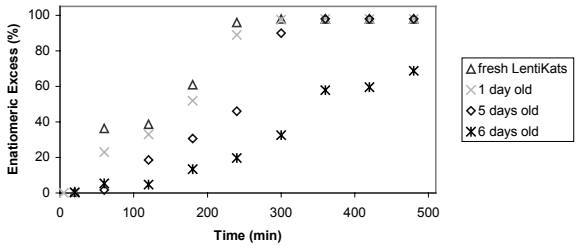

Figure 5:
Recycling experiments with the encapsulated biocatalyst, ee-value of phenylethane diol.

4 Conclusions

Our results show that the reaction with LentiKats® immobilised fungi *Beauveria bassiana* kinetically resolves racemic styrene oxide in very high enantiomeric excess to the chiral, non-racemic styrene oxide and to the corresponding phenylethane diol. The reaction rate of the immobilised fungi is only slightly lower than of free fungi, mainly due to mass transport limitations.

The stability of the PVA encapsulated *Beauveria bassiana* is very high, at least five runs can be carried out without notable decrease in activity. The biocatalyst can be recovered easily. In our future research, we will try to set up a semi-continous reaction.

References

Abramowicz DA (1990) Biocatalysis, New York, Van Nostrand Reinhold

Bellucci G, Chiappe C, Cordoni A (1996) Enantioconvergent Transformation of Racemic cis-beta-alkyl substituted Styrene Oxides to (R,R) Threo Diols by Microsomal Epoxide Hydrolase Catalysed Hydrolysis. Tetrahedron: Asymmetry 7:197-202

Faber K, Mischitz M, Kroutil W (1996) Microbial Epoxide Hydrolases. Acta Chem Scand 50:249-258

geniaLab (2001) Product information about LentiKats®; http://www.genialab.de

Kolb HC, Van Nieuwenhze MS, Sharpless KB (1994) Catalytic Asymmetric Dihydroxylation. Chem Rev 94:2483-2547

Orru RVA, Kroutil W, Faber K (1997) Deracemization of (+/-)-2,2-disubstituted Epoxides via Enantioconvergent Chemoenzymatic Hydrolysis using Nocardia EH1 Epoxide Hydrolase and Sulfuric Acid. Tetrahedron Lett 38:1753-1754

Osprian I, Kroutil W, Mischitz M, Faber K (1997) Biocatalytic Resolution of 2-Methyl-2-(aryl)alkyloxiranes using novel Bacterial Epoxide Hydrolases. Tetrahedron: Asymmetry 8:65-71

Pedragosa-Moreau S, Archelas A, Furstoss R (1993) Enantiocomplementary Epoxide Hydrolyzes as a Preparative Access to both Enantiomers of Styrene Oxide. J Org Chem 58:5533-5536

Pedragosa-Moreau S, Archelas A, Furstoss R (1996) Use of Epoxide Hydrolase Mediated Biohydrolysis as a Way to Enantiopure Epoxides and Vicinal Diols: Application to Substituted Styrene Oxide Derivatives. Tetrahedron 52:4593-4606

Roberts SM, Turner NJ, Willetts AJ (1995) Introduction to Biocatalysis Using Enzymes and Microorganisms. Cambridge University Press, Cambridge

Roberts SM, Wiggins K (1993) Preparative Biotransformations: Whole Cells and Isolated Enzymes. Wiley, Chichester

Continuous malolactic fermentation by *Oenococcus Oeni* entrapped in LentiKats®

Alain Durieux, Xavier Nicolay, and Jean-Paul Simon[1]

1 Introduction

The malolactic fermentation (MLF) which features in cider-making and in winemaking consists in the conversion of L-malic acid into L-lactic acid and CO_2; this reaction is catalysed by the activity of a lactic acid bacterium, *Oenococcus oeni* (Salou *et al.* 1994 , Davis *et al.* 1985). This strain possesses the malolactic enzyme to accomplish the malic acid conversion in a one step reaction. (Lonvaud–Funel & Strasser de Saad 1982, Spettoli *et al.* 1984). The benefit of the malolactic fermentation is a partial de-acidification of the cider, a greater aroma complexity and some limitation of other bacterial spoilage (Jarvis *et al.* 1995).

Oenococcus oeni must reach a cell concentration of 10^6 c.f.u. ml^{-1} in order to start malolactic fermentation. But even in the case of inoculation with a starter, the onset of bacterial growth is unreliable due to hostile conditions in the cider (acidic pH, presence of other inhibitors and ethanol) which limit the specific growth rate of the starter. Earlier studies proposed to immobilise *Oenoccocus oeni* in an alginate matrix, as this immobilised cell technology offers the opportunity to use a high cell density system in a continuous process (Carbranes *et al.* 1998, Durieux *et al.* 1996, Nedovic *et al.* 2000). It has the advantage of separating the malic acid bioconversion step and the cell propagation steps.

The choice of the immobilisation matrix has to be made in accordance with the long term conservation of cell viability and, for beverage production, its acceptance as GRAS (Generally Recognised As Safe). The development of new polymeric materials such as polyvinylalcohol (PVA) is very attractive. Ding and Vorlop (1995) developed a new gelation technique for entrapment of biomass in PVA characterised by the suppression of the repeated freezing and thawing of the aqueous PVA solution as traditionally required (Plieva *et al.* 2000). This present study investigates the performance of LentiKats® as an immobilisation matrix for *Oenococcus oeni* to develop a continuous reactor.

2 Materials and methods

2.1 Strains

Oenococcus oeni (Malolactine O) supplied by Groupement des Laboratories Oenologiques (G.L.O., Rueil-Malmaison, France). *Saccharomyces bayanus* supplied by Danstar Ferment AG (Zug, Switzerland), was used as a typical ethanol producer.

2.2 Feeding medium

Apple juice was purchased from Stassen Cidrerie (Aubel, Belgium). Apple juice contained per litre: 93.6 g of sugars (6.9 g saccharose, 64.5 g fructose, 22.2 g glucose) and 6.70 g of malic acid. The pH was adjusted before sterilisation (120 °C during 20 min) to give values of 4.46, 3.95, 3.46, 2.90 and 2.30. Cider was produced by initially fermenting the apple juice by *Saccharomyces bayanus* at 30°C under static conditions. When residual sugar concentration reached around 4 g glucose l^{-1} (7 days of incubation), the yeast was removed from the medium by centrifugation and the pH was adjusted respectively at 3.35, 3.80 and 4.40.

2.3 Immobilisation of cells

280 ml of "LentiKat®Liquid" (geniaLab, Braunschweig, Germany), available in gel form, previously melted in a water bath at 90°C and cooled to room temperature, was mixed with 70 ml of *O. oeni* suspension from the fermenter culture containing 6.5 x 10^8 c.f.u. ml^{-1}. A small portion of the polymer solution with biomass was dropped by a LentiKat® Printer with 400 wires per 143 cm^2 (geniaLab, Braunschweig, Germany) on to Petri dishes by dipping the tip of the wire into the solution and lifting it afterwards. The wires were pulled back from the polymer solution at always the same velocity, and the wires were put on to Petri dishes within 3 s. The Petri dishes containing the droplets were put in laminar airflow cabinet (Gera, Nivelles, Belgium) under a downwards vertical stream at room temperature. Under these conditions, gelation of the PVA-hydrogel occurred in half an hour with a reduction of 75 % of the initial mass due to water evaporation. The gel was stabilised for two

[1] Alain Durieux, Xavier Nicolay, and Jean-Paul Simon, Unité de BioTechnologie, Institut Meurice, Campus CERIA, Av. E. Gryzon 1, 1070 Brussels, Belgium

hours in the presence of a stabilising solution (geniaLab, Braunschweig, Germany).

2.4 Continuous reactor description

A tubular glass reactor (total volume, 170 ml; internal diameter, 2.5 cm) was composed of three successive layers (from the bottom to the top): 10 ml of glass beads (diameter = 2.5 mm) to allow a repartition of the feeding medium in the whole section of the reactor, 50 ml of loaded LentiKat® and 40 ml of glass beads in the upper layer to stabilise the LentiKat® layer. The void volume of the LentiKat® layer was 18 ml and was used to calculate the residence time in the active part of the reactor by dividing this value by the flow rate.

2.5 Analytical assays

The analysis of sugars (fructose, glucose, sucrose) and organic acids (malic, lactic, acetic) in the samples was accomplished by HPLC.

3 Results and discussion

3.1 Continuous malolactic fermentation of apple juices presenting different acidity levels

A tubular glass reactor loaded with LentiKats® containing *O. oeni* was fed with apple juices with pH values from 4.46 to 2.30. The temperature was kept at 30 °C during all the experiments. The malolactic activity (Figure 1) and the de-acidification (Figure 2) were measured for different flow rates. The malolactic activity was optimal for an initial pH between 3.95 and 4.46 corresponding to the same optimal values as those for free cells process. For initial pH between 3.95 and 4.46, residence times higher than 0.3 h allow a total conversion of malic acid into lactic acid.

The most interesting result is the malolactic activity measured at pH below 3.40. Below this value, the undissociated form of malic acid is predominant (pK_a 3.40; 5.11). In suspended cultures for homogenous process, the malolactic fermentation cannot proceed: no growth and no malolactic fermentation were detected in free cells process at pH below 3.90 after inoculation of apple juice by 10^6 c.f.u. ml^{-1} of *O. oeni* (Malolactine O) and incubation at 30°C. In the heterogeneous process, the microenvironment of the cells in the matrix and their physiology in the pseudo-stationary phase allow the malolactic fermentation. In free cell culture, the energetic requirement of the strain to grow and to maintain its internal pH could be too high to allow the malic acid conversion at acidic pH. On the other hand, the pseudo-stationary physiological state of the entrapped cell is generally characterised by a lower energetic demand due to its very low specific growth rate (Masschelein *et al.* 1994). In this special physiology state, the microorganism can thus generate enough ATP to maintain its cytoplasmic pH without any perturbation of the MLF. In addition, when the malolactic fermentation proceeds in the matrix, the local pH surrounding the cell may increase restoring the favourable malic acid / malate ratio in the microenvironment for natural uptake of the malate by the active cells, thus allowing the MLF to proceed at an apparently lower pH.

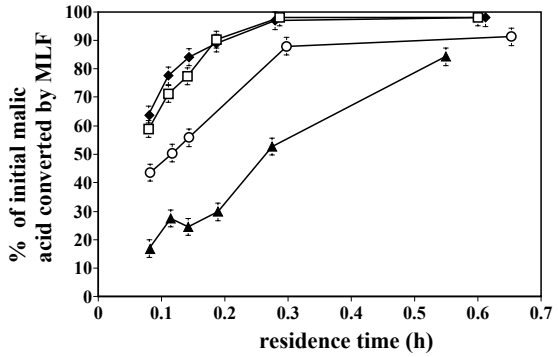

Figure 1:
Malic acid conversion rate in apple juice presenting different pH as a function of the residence time, (□) apple juice pH 4.46; (◆) apple juice pH 3.95; (❍) apple juice pH 3.46; (▲) apple juice pH 2.90

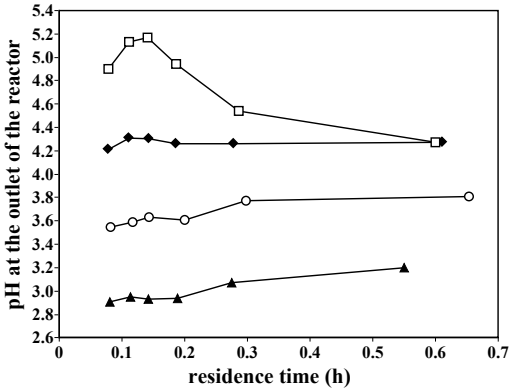

Figure 2:
pH profiles at the reactor outlet for the different apple juices as a function of the residence time, (□) apple juice pH 4.46; (◆) apple juice pH 3.95; (❍) apple juice pH 3.46; (▲) apple juice pH 2.90

The evolution of the pH at the bioreactor outlet is described in Figure 2. For longer residence time, an acidification of apple juice is detected at initial pH of 4.46, due to the heterolactic fermentation resulting in production of acetic and lactic acids from sugar. At

this pH, the malolactic fermentation is predominant at low residence time, resulting in a de-acidification. The largest pH variation between the outlet and the inlet is of 0.72, corresponding to a residence time of 0.141 h and an inlet pH of 4.46. For apple juices presenting an inlet pH below 3.95 and for the range of residence time tested, only de-acidification is detected, reflecting dominance of malolactic activity.

Thirty three percent of malic acid was converted when the initial apple juice pH was 2.30 (Table 1) with a residence time of 0.55 h, proving that the immobilised reactor could de-acidify all apple juices encountered which generally have pH values between 2.7 and 4.0.

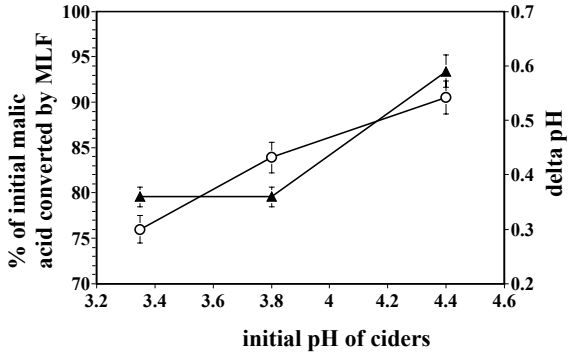

Figure 3:
De-acidification of ciders presenting initial pH of 4.40, 3.80 and 3.35 -residence time 0.195 h, (❍) delta pH (= pH at the outlet of the reactor – initial pH of cider) and (▲) % of initial malic acid converted by MLF

Table 1: Percentage of initial malic acid converted and specific malic acid consumption for the different apple juices at a residence time of 0.55 h

pH of apple juices	% of initial malic acid converted by MLF	Specific malic acid consumption (g h^{-1})
4.46	98	11.4
3.95	98	11.4
3.36	90	11.0
2.90	84	10.2
2.30	33	4.0

3.2 Continuous malolactic fermentation of cider at different pH

For this set of experiments, the immobilised bioreactor was fed with cider. This cider was produced by batch fermentation of apple juice (pH 4.40 – 3.80 and 3.35) inoculated with *S. bayanus*. As shown in Figure 3, for a residence time of 0.195 h, the de-acidification performance of the continuous bioreactor is not affected by the presence of ethanol, allowing the transposition of results obtained with apple juice at different pH to cider with similar acidity. The de-acidification level can be easily adjusted by changing the residence time.

3 Conclusions

The LentiKats® immobilisation technology represents an attractive alternative to classical alginate entrapment in view of the volumetric productivity. The LentiKats® shape allows an increased exchange surface with the medium and their low thickness reduces the diffusion barrier. No alteration of the matrix integrity was noticed after two months of working in the continuous process confirming the mechanical resistance of the LentiKats®. Biomass leakage was very low and was estimated to represent less than 0.01 % of the entrapped biomass.

References

Cabranes C, Moreno J, Mangas JJ (1998) Cider production with immobilized *Leuconostoc oenos*. J Inst Brewing 104:127-130

Davis CR, Wibowo D, Eschenbruch R, Lee TH, Fleet GH (1985) Practical implications of malolactic fermentation: a review. Am J Enol Vitic 36:290-301

Ding WA, Vorlop K D (1995) Gel aus Polyvinylalkohol und Verfahren zu seiner Herstellung. German Patent DE 4327923

Durieux A, Garre V, Mukamana J, Jourdain J-M, Silva D, Plaisant A-M, Defroyennes J-P, Foroni G, Simon J-P (1996) *Leuconostoc oenos* entrapment: applications to continuous malolactic fermentation, In: Wijffels RH, Buitelaar RM, Bucke C and Tramper J (eds.) Immobilized Cells: Basics and Applications. Elsevier, Amsterdam, pp. 679-686

Jarvis B, Forster MJ, Kinsella WP (1995) Factors affecting the development of cider flavour. J Appl Bacteriol Symp Suppl 79:5S-18S

Lonvaud-Funel A et al. (1982) Purification and properties of a malolactic enzyme from a strain of *Leuconostoc mesenteroides* isolated from grapes. Appl Environ Microbiol 43:357-361

Masschelein CA, Ryder DS, Simon J-P (1994) Immobilized cell technology in beer production. Crit Rev Biotechnol 14:155-177

Nedovic VA, Durieux A, Van Nedervelde L, Rosseels P, Vandegans J, Plaisant AM, Simon J-P (2000) Continuous cider fermentation with co-immobilized yeast and *Leuconostoc oenos* cells. Enzyme Microb Technol 26:834-839

Plieva FM, Kochetkov KA, Singh I, Parmar VS, Belokon YN, Lozinsky VI (2000) Immobilization of hog pancreas lipase in macroporous poly (vinyl alcohol)-cryogel carrier for biocatalysis in water-poor media. Biotechnol Lett 22:551-554

Salou P, Loubiere P, Pareilleux A (1994) Growth and energetics of *Leuconostoc oenos* during cometabolism of glucose with citrate or fructose. Appl Environ Microbiol 60:1459-1466

Spettoli P, Nuti MP, Zamorani A (1984) Properties of malolactic activity purified from *Leuconostoc oenos* ML34 by affinity chromatography. Appl Environ Microbiol 48:900-901

PVA-gel entrapped specific microorganisms enhancing the removal of VOCs in waste air and biofiltration systems

Benjamin Massart, Xavier Nicolay, Stefan Van Aelst , and Jean-Paul Simon[1]

Abstract

Two pilot scale biofilters are compared over a short term period (three months). The conditions applied and microorganisms used (initial quantity and nature) are similar for both biofilters. Bioaugmentation is on the one hand carried out by sparkling a liquid culture on the biofilter's bed (Uncoated Support) and on the other hand performed by coating of microorganisms immobilized in a PVA matrix (geniaLab, Braunschweig) as a thin layer around the support particles (Coated Support). This coating is achieved in a fixed bed drying system applying parameters ensuring 30 % viability for the bioaugmented strain *Ps. putida* F1, selected for its ability to degrade toluene, the model pollutant. Biofiltration efficiency is evaluated through Michaelis-Menten-like parameters considering homology between an enzymatic kinetic and the elimination capacity (EC) vs. the organic load experimental curve. Results show maximal EC of respectively 190 and 95 g/m^3 of filter bed per hour for the CS and UCS systems. Saturation constants, Ks, are identical for the two biofilters, indicating that both systems present the same affinity for the substrate. These results combined to a microbial analysis of the biofilm showing that the same quantitative and qualitative load in toluene degrading bacteria, which can lead us to the conclusion that microorganisms included in PVA still show high degradation activity after a period of three months and make the system more efficient than a classical "trickling inoculation". This also suggests that a significant part of gel entrapped biomass encounters no limitation, neither by substrate diffusion nor by oxygen diffusion.

1 Introduction

Increasingly stringent environmental legislation has stimulated investigation of technologies that reduce the emissions of toxic compounds into the environment. The use of microbial cells entrapped in a gel matrix has been investigated as an alternate technology for bioremediation of contaminated soil (Cassidy et al. 1996) and groundwater (Bettman and Rehm 1984, 1985, Chen et al. 1998, Torres et al. 1998). In these applications, gel-entrapped cells were shown to provide some advantages over the use of free cells such as: immobilization may increase the metabolic activity of cells and the stability of their plasmids, it helps to protect cells from environmental stresses, and enables a slow release of cells into their environment which reduces the possibility of accumulation of interrupting microflora. On the other hand, some limitations should also be mentioned: the diffusion of substrates may be restricted and morphological and physiological changes of cells can occur. Only little attention has been given to the application of gel-entrapped cells for waste gas treatment. Chung et al. (1996, 1997) studied the removal of hydrogen sulphide and ammonia from air using biofilters filled with Ca-alginate beads which contained microbial strains capable of degrading these pollutants

The aim of this work is an assessment of the bioaugmentation mode consisting in the inclusion of a pure Pseudomonas putida culture in a Polyvinyl Alcohol (PVA) matrix coating the biofiltration support made of expanded clay (Coated Support System; CS).

In order to achieve this study, the characteristics of the CS system are compared to a "classical" system where the biofiltration bed (expanded clay) is inoculated at start-up by trickling a liquid culture (Uncoated Support system).

2 Materials and methods

2.1 Microorganisms

The toluene degrading strain is *Pseudomonas putida* F1 (DSMZ 6899). Respirometric tests and plate counting are achieved on M1 medium containing in g/l: Beef extract, 1; Yeast extract, 2; Peptone, 5; NaCl, 5; pH is adjusted at 7.4. Agar is added for plate counting, 15 g/l. Cell growth is measured by OD (660 nm, Jenway 6100 spectrophotometer) and CFU determination after plating of diluted samples of the culture. Toluene degradation test is performed on 457 Minimal Medium containing (in g/l): Na_2HPO_4 , 2.44; KH_2PO_4, 1.52; $(NH_4)_2SO_4$, 0.50; $MgSO_4$, 7; H_2O, 0.20; $CaCl_2$, 2; H_2O, 0.05; SL4 solution, 10 ml/l; SL4 composition: EDTA, 0.5; $FeSO_4$ x 7 H_2O, 0.2; SL-6 solution, 100ml; SL6 composition: $ZnSO_4$ x 7 H_2O, 0.1; $MnCl_2$ x 4 H_2O, 0.03; H_3BO_3 , 0.3; $CoCl_2$ x 6

[1] Benjamin Massart, Xavier Nicolay, Stefan Van Aelst, and Jean-Paul Simon, Unité de Biotechnologie, Institut Meurice, CERIA, 1 Avenue Emile Gryzon , 1070 Brussels, Belgium

H_2O, 0.2; $CuCl_2$ x 2 H_2O, 0.01; $NiCl_2$ x 6 H_2O, 0.02; Na_2MoO_4 x 2 H_2O, 0.03. Toluene is added as sole carbon source: 25 µl/l.

Microbial identification is made using classical microbiology tests and API 20 E and API 20 NE (Biomérieux, France) identification kits.

2.2 Immobilization of microorganisms with coating of biofiltration support

Material: the support is made of expanded clay with granulometric distribution 4-10 mm, round-shaped (ARGEX, Belgium). *Ps. putida* culture is obtained by inoculating (100 ml culture over night) and shaking 6 l of M1 medium at 37°C. Cells are harvested by centrifugation (9000 rpm, SORVAL RC5B) and re-suspended in 200ml of physiological water. PVA polymer and stabilization solutions are provided by geniaLab, Germany.

Method: The inclusion protocol is adapted in order to achieve the support coating simultaneously with the reticulation step: 100 ml of the suspended cells solution is added to 500 ml of PVA prepolymer mix. The resulting solution is then mixed with expanded clay beads at a ratio of 20 % (w/w). This is then moulded in a PVC tube to obtain a cylinder shape adapted to the pilot biofilters geometry. The reticulation step is achieved by fixed bed drying (PRL Engineering dryer): inlet temperature is controlled at 35°C, drying time varies from 20 to 35 min, drying is completed when a 70 % weight loss of the coating solution is recorded. After drying, stabilization steps are realized as recommended by the PVA-L provider.

2.3 Respirometric analysis

The method is adapted from Tanaka et al. (1990). It consists in the measurement of pO_2 (Ingold probe) in a stirred 2 litre Scott bottle after filling it with oxygen saturated M1 medium and a pure culture in free or immobilized form.

2.4 Biofilters

Pilot scale biofilters are of cylindrical shape, made of plexiglass tubing, with a filter height of 1 m and a bed volume of 7.9 litres. It is considered a cocurrent system seeing that air flow and sparkling solution are both down-flowing. Sparkling occurs hourly with sparkling of 220 ml of salt solution. The sparkling solution (2 l) is initially in contents of (in g/l): KH_2PO_4, 10.5; $(NH_4)_2PO_4$, 2.6; $(NH_4)NO_3$, 21.5. Air flow is controlled at 500 l/h.

2.5 Analytical methods

Toluene concentrations were determined by gas chromatography. Gas chromatograph (Perkin-Elmer, Sigma 3B) was equipped with a 1/8'' 4 m stainless steel column (5 % Carbowax 20 M) and a flame ionization detector. Nitrogen was used as the carrier gas. Operating conditions were: injector, 160°C; oven, 140°C; detector, 220°C.

3 Results

3.1 Biofilters operating mode

EBRT in both biofilters is controlled at 57 s (air flow: $0{,}5 m^3 \cdot h^{-1}$). Expanded clay beads composing the filter bed material show a high internal porosity assuming high specific area. This semi-synthetic material was selected as an inert filter medium releasing no nutrient (C,N,P,K); these supplies are controlled by spraying appropriate salts solutions. Relative concentrations on N,P,K elements are adapted from optimisations achieved by Deshusses et al. (1999); it ensures no limitation on these elements according to the hypothesis of Ottengraf's model for gas biofiltration (Ottengraf, 1986). Temperature and relative humidity (HR) of incoming and outgoing air are measured daily; Hr_{in} is controlled at the inlet at a value higher than 90 % of water saturation by stripping the air through a water column. Water content of the bed material reached 50 % (w/w) during the three month experiment. pH of the sparkling solution is measured and controlled to avoid values lower than 4 (essentially at start-up). Pressure drop through the filter bed is of importance because it is related to the biomass accumulation and the compaction of the biofiltration support. These two elements are responsible for pressure drop elevation and channelling into the biofilter. It is controlled by washing the filter medium when pressure drop exceeds 1000 $Pa \cdot m^{-1}$ of bed. This operation ensures low values for the pressure drop, indicating the absence of compaction problems with the filter material used in this study.

3.2 Measurement of cell's respirometric activity

The preliminary step to this experiment was the determination of the cells' activity after inclusion in the coating matrix; that is after the drying and stabilization steps of the bed material in order to inoculate both compared systems (CS and UCS) with the same cells' activity. The biomass activity permits the evaluation of hypothetic viability losses during the support coating procedure; it is measured by a respirometric method adapted from Tanaka et al. (1990).

Table 1:
Respirometric measurements for immobilized cells activity determination

Assay	Cell density x1E10 CFU	O_2 Uptake, % $O_2 \cdot min^{-1}$	Measured SOUR, % O_2/min·1E10 CFU	Average SOUR, % O_2/min·1E10 CFU
Free cells culture 1	9.25	4.5	4.86E-1	5.03E-1
Free cells culture 2	4.63	2.4	5.19E-1	5.03E-1
Coated Support	3.58	1.8		5.03E-1

The evaluation is made on the basis of a comparison between Specific Oxygen Uptake Rate (SOUR) for a free cells culture at a known cell density and the Oxygen Uptake Rate measured for a CS-immobilized culture. Results are listed as % oxygen uptake per minute because absolute O_2 concentration of M1 medium is unknown. SOUR for free cells is measured by OD determination and a correlation with CFU is established by further plate counting. Final relation is expressed as % O_2 uptake/min.1·E10 CFU. Table 1 shows results for two distinct concentrations of free cells culture and the determination of OUR for PVA immobilized cells.

The biomass involved in the CS system before any immobilization step is 1.22E11 CFU. After reticulation and stabilization of the PVA coating matrix, this biomass shows a % O_2 uptake per min. 1E1O CFU of 1,8 % that corresponds to 3,58E10 active cells in the matrix, that is 29.3 % of active cells after inclusion in the PVA matrix. This result lead us to inoculate the UCS system at a 1/3 rate of the initial culture involved in the CS system in order to install the same bacterial activity in both biofilters at start-up.

3.3 Characterization of microbial population in the biofilm

A microbial analysis is carried out on the water used as washing solution for the filter bed (when pressure drop exceeds 1000 $Pa \cdot m^{-1}$ and the biofilter is running at steady state conditions); so that it can be considered as the microbial composition of the biofilm surrounding the support material in the UCS system and the coating matrix in the CS system.

This experiment aims to qualitatively compare biomass present in both biofilters and to assess the development of the selected *Ps. putida* strain inoculated at start-up. Results are shown in Table 2, they consist of relative appearance on plate counting of the different strains isolated from the biofilm.

Bacterial identification is achieved after a two-month period on basis of classical microbiological tests (Gram staining, oxydase test, API identification,…). These tests show that UCS strain 5 and CS strain 6 correspond to the "bioaugmented" strain *Ps. putida*. These results are corroborated by growth tests on minimal 457 medium with toluene. It indicates that UCS5 and CS6 are the only strains able to utilize toluene as sole carbon source. This lead us to the conclusion that the immobilized strain (immobilizaton by adherence for UCS and by inclusion for CS) represents only a minimal part of total biomass in the outer biofilm for both systems; but it is obvious that this strain is solely responsible for all toluene degradation. It should be noted that this experiment does not take into account any biomass included in the support material, nor the PVA immobilized cells in the CS system.

Table 2:
Qualitative analysis of biofilm in UCS and CS systems

UCS system		CS system	
Strain ID	% of total population	Strain ID	% of total population
UCS strain 1	7.69	CS strain 1	3.01
UCS strain 2	11.53	CS strain 2	11.81
UCS strain 3	66.31	CS strain 3	74.78
UCS strain 4	14.41	CS strain 4	9.04
UCS strain 5	0.06	CS strain 5	1.33
		CS strain 6	0.02

3.4 Biofiltration performances

A typical performance curve for biofiltration is given as Elimination Capacity (g toluene degraded/ $m^3_{bed} \cdot h$) vs Organic Load (g toluene in inlet gas/ $m^3_{bed} \cdot h$). These results are given in Figure 1; they are analysed as Chung et al. (1996) did for the biofiltration of H_2S containing gas. It consists of the comparison of the experimental curve with a Michaelis-Menten like enzymatic kinetic. In this model, the main parameters for characterization of a biofilter are the maximal Elimination Capacity EC_{max}, as the Vm is the maximal conversion rate for an enzyme and Ks; the "saturation constant" defined as the OL value ensuring the biofilter a EC equals to $EC_{max}/2$ and this,

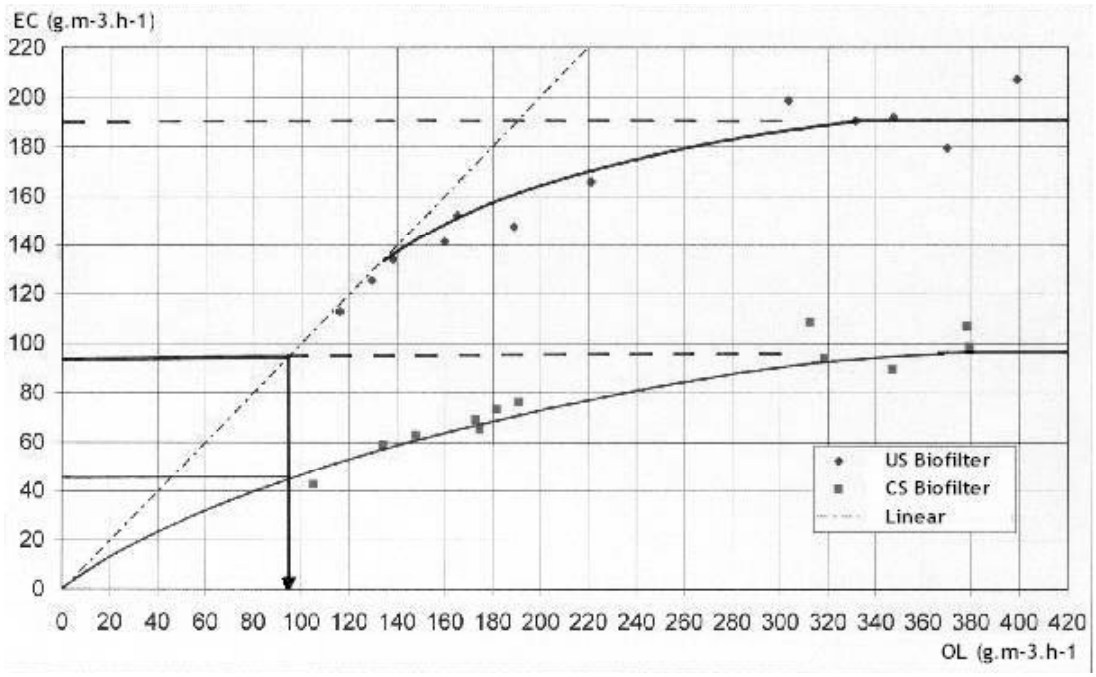

Figure 1:
EC vs. OL for UCS and CS systems

by comparison with the Michaelis-Menten constant. Figure 1 shows a EC_{max} of 190 $g/m^3_{bed}·h$ for CS biofilter, 95 $g/m^3_{bed}·h$ for UCS biofilter and an identical Ks constant of 95 $g/m^3_{bed}·h$ for both systems.

If we assume the same physical meaning of the measured parameters as for Michaelis-Menten parameters, the lower is the constant, the higher the affinity of the system for its substrate. This means that in this experiment, both systems show the same affinity for the toluene. Actually, Ks constants for UCS and CS biofilters are graphically measured at $95g/m^3_{bed}·h$; this result corroborates the previous microbial analysis and supports the fact that in both systems, the same active bacterial strain ensure toluene biodegradation, that is the "bioaugmented" *Ps. putida* strain.

As second reference parameter, EC_{max} permits the comparison of different biofiltration systems operating under various conditions for the biodegradation of the same VOC(-mix). Results reported in literature are listed in Table 3 in order to compare CS and UCS systems with other works involving different support material.

As an analysis of these results, we can conclude that both systems (UCS and CS) show high EC_{max} values and, particularly, the result obtained for the CS biofilter is the fact of active PVA immobilized cells. Actually, EC_{max} values combined to the microbial analysis showing the same relative quantity of *Ps. putida* lead us to confirm a sensibly higher activity for the CS system; as does an additional measurement of total biomass (volatile dry matter/filter volume measurement) indicating the same quantitative population for both biofilters in the outer biofilm. This microbial activity is located under the biofilm that is in the PVA coating matrix. It appears that PVA inclusion of *Ps. putida* F1 ensure stability and activity of the immobilized cells, suggesting that no restrictive limitation (substrate, oxygen,…) is occurring in this configuration.

Table 3:
Results listed in the literature on EC_{max} for the biofiltration of toluene containing air (Jorio et al.,1999), tol. = toluene

Filter Medium	EC_{max}, g tol./$m^3_{bed}·h$	Authors
Peat and compost	21	Ottengraf et al. (1986)
Compost and perlite	4	Seed et al. (1994)
Peat and perlite	25	Shareefden et al. (1994)
Compost	15	Benitez et al.(1995)
Compost and activated carbon	97	Tang et al. (1995)
Commercial peat	70	Kiared et al. (1996)
Formulated peat	165	Jorio et al. (1998)
UCS system	95	
CS system	190	

4 Conclusions

The comparison of two biofiltration systems in order to assess the inclusion of PVA cells applied as a coating element of the inert support shows high efficiency of this concept. This specific bioaugmentation method reduces the start-up period of biofilter experiment to some days. On the basis of Michaelis-Menten like development and microbial qualitative and quantitative analysis, it was shown that microorganisms included in PVA still show a high degradation activity after a period of three months. It makes the "PVA-coating bioaugmention" concept reliable and more efficient than a classical "liquid culture sparkling" bioaugmentation. This also suggests that a significant part of gel entrapped biomass encounters no restrictive limitation, neither by substrate diffusion, nor by by-products accumulation, nor by oxygen limitation.

Symbols and abbreviations

calc	calculation
VOC	Volatile Organic Compound.
CS	Coated Support
UCS	Uncoated Support
OUR	Oxygen Uptake Rate (% O_2/min)
SOUR	Specific Oxygen Uptake Rate (% O_2/min·1E10 CFU)
CFU	Colony Forming Unit
EBRT	Empty Bed Residence Time (s)
OL	Organic Load (g toluene in inlet gas/m^3_{bed}·h)
EC	Elimination Capacity (g toluene degraded/m^3_{bed}·h)

Acknowledgements

The authors would like to acknowledge Prof. Dr. K.-D. Vorlop, who is involved in this research project, especially for his advice in the field of cells entrapment matrices.

References

Bettman H, Rehm HJ (1984) Degradation of phenol by polymer entrapped microorganisms. Appl Microbiol Biotechnol 20:285-290

Bettman H, Rehm HJ (1985) Continuous degradation of phenol(s) by Pseudomonas putida P8 entrapped in polyacrylamide-hydrazide. Appl Microbiol Biotechnol 22:389-393

Cassidy MB, Lee H, Trevors JT (1996) Environmental application of immobilized cells: a review. J Ind Microbiol 16:79-101

Chen K-C, Lee S-C, Chin S-C, Houng J-Y (1998) Simultaneous carbon-nitrogen removal in wastewater using phosphorylated PVA-immobilized microorganisms. Enzym Microb Technol 23:311-320

Chung Y-C, Huang C, Tseng C-P (1996) Biodegradation of hydrogen sulphide by a laboratory-scale immobilized *Pseudomonas putida* CH11 biofilter. Biotechnol Prog 12:773-778

Chung Y-C, Huang C, Tseng C-P (1997) Biotreatment of ammonia from air by an immobilized *Arthrobacter oxydans* CH8 biofilter. Biotechnol Prog 13:794-798

Deshusses MA, Devinny J, Todd S, Webster (1999) Biofiltration for Air Pollution Control. Lewis Publishers

Jorio H, Heitz M (1999) Traitement de l'air par biofiltration. Canadian Journal of Civil Engineering 26:577-585

Ottengraf SPP, Van den Oever AHC (1896) The elimination of organic compounds in waste gases with a biological filter. Eindhoven University of Technology, The Netherlands.

Tanaka K, Tada M, Takashi K, Harada S, Fujii Y, Mizugushi T, Mori N, Emori H (1990) Development of a new nitrogen removal system using nitrifying bacteria immobilized in synthetic resin pellets. Water Sciences Technologies 23:681-690

Torres LG, Sánchez-de-la-Vega A, Beltrán NA, Jiménez BE (1998) Production and characterization of a Ca-alginate biocatalyst for removal of phenol and chlorophenols from wastewaters. Proc Biochem 33(6):625-634

Biotechnological Production of L-Tryptophane as a pharmaceutical ingredient: optimization of the process by immobilization and use of bioanalytical systems

Birgit Klaßen[1], Ulrich Seja[1], Robert Faurie[1], Thomas Scheper[2], and Klaus-Dieter Vorlop[3]

1 Introduction

L-tryptophan is an essential amino acid, which occurs naturally in all organisms. In humans, it has a sedative and antidepressive effect in higher doses although it is neither addictive nor physiologically harmful. Due to this unique combination of features, there was a fast developing market for this amino acid as a soft sleeping drug in the 1980s. A further application of L-tryptophan is as ingredient in medical infusion for pre- and postoperative, parenteral nutrition.

L-tryptophan has been produced at the AMINO GmbH for 12 years using a biotechnological method as displayed in Figure 1 (Wagner et al., 1980, Faurie and Fries, 1999).

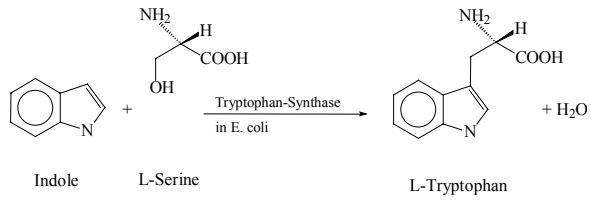

Figure 1:
Enzymatic synthesis of tryptophan

A strain of *E. coli* overproducing a highly active tryptophan synthase is fermented in a 3 m^3 scale. After separation of the biomass, the cells are mixed with a solution containing serine and indole. Serine is produced by chromatographic extraction from sugar beet molasses. Indole as a reaction partner with low solubility is added during the transformation process. The optimal dosage profile ensures a high space-time-yield and a low byproduct concentration. Cells are permeabilized in situ by indole, so that the reaction with the intracellular tryptophan synthase can take place. If indole is supplied in too high concentrations, the enzyme is inhibited whereas too low concentrations lead to a suboptimal space-time-yield and higher amounts of undesired by-products.

After the biotransformation, most of the biomass can be recovered by separation and is mixed with fresh biomass to be used again for further transformations. After several biotransformation cycles, biomass has to be discarded due to the decrease in enzymatic activity.

2 Process optimization by immobilization

The process can be optimized by increasing the stability of cells and enzyme activity. After fermentation, cells can be either cross-linked or entrapped in suitable materials. Combination of both methods can be efficient. The entrapment of the cell was achieved by using polyvinylalcohol (PVAL), the method was recently described (Jekel et al., 1998). This hydrogel provides immobilized biocatalysts with ideal features.

3 Entrapment in LentiKats®

E. coli cells are mixed with a highly viscous suspension of 1 part of polyvinylalcohol (supplied by Fa. geniaLab, Braunschweig) and 4 parts of water. By dropping or stamping, lentile shaped little tiles are formed (approx. 200 to 400 µm thick, diameter of 3 to 5 mm). At defined humidity and temperature, a hydrogel is formed by developing hydrogen bonds. These LentiKats® (Figure 2) are very resistant to mechanical and chemical stress. They can be used up to 50°C. Due to the unique shape and physical properties, they show very good diffusion features, so that transport processes are only limiting in extreme situations.

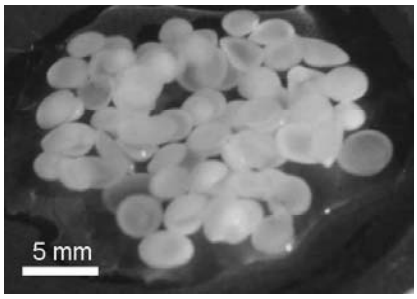

Figure 2:
Some LentiKats® shown by light microscopy

[1] Birgit Klaßen, Ulrich Seja, and Robert Faurie, Amino GmbH, Dept. R & D, Langer Kamp 5, 38106 Braunschweig, Germany and Amino GmbH, An der Zuckerraffinerie 10, 38373 Frellstedt, Germany

[2] Thomas Scheper, Institute for Technical Chemistry, University of Hannover, Callinstraße 3, 30167 Hannover, Germany

[3] Klaus-Dieter Vorlop, Institute of Technology and Biosystems Engineering, Federal Agricultural Research Centre (FAL), Bundesallee 50, 38116 Braunschweig, Germany

4 Comparison of LentiKats® and free cells

20 transformations were carried out with free cells or LentiKats® under the same experimental conditions. In both cases the cells or biocatalyst were reused each time. The result of those biotransformations are shown in Figure 3.

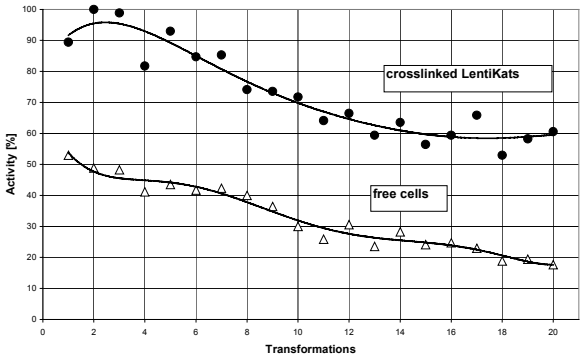

Figure 3:
Comparison of the activity of tryptophan synthase of free cells and LentiKats®

The entrapment of the cells into hydrogel results in a higher activity, decreasing in much lower degree than for free cells. Thus a higher process stability can be reached by this method.

5 Impact of cross-linking

An increased activity and higher stability of the separated cells can be achieved as well by cross-linking with glutaraldehyde. After fermentation, the separated cells were mixed with 10 mM glutardialdehyde. Activities of different treated cells were compared (Figure 4). Results are shown for a) not cross-linked, free cells; b) cross-linked, free cells; c) not cross-linked, immobilized cells; and d) cross-linked, immobilized cells. A combination of cross-linking and immobilization is most effective, stability of the biocatalysts can be increased by more than 100%.

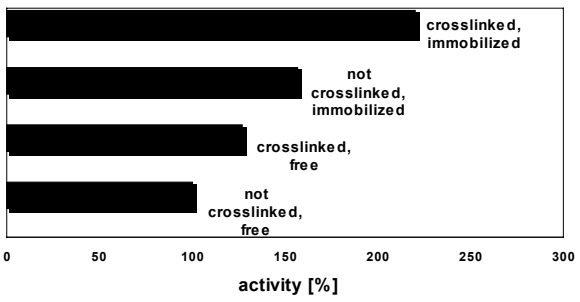

Figure 4:
Activity of different treated biocatalysts (mean of 12 transformations)

6 Process optimization by use of 2-D-process fluorimetry

During several biotransformation cycles suitable fluorescence spectra were recorded. This allowed an in-time determination of the concentrations of tryptophan and indole. The recorded data were used for the construction of a mathematical algorithm for the prediction of the process parameters. With application of this model an optimized dosage of indole can be achieved (Ulber et al., 2001).

7 Conclusions

Costs for downstream processing can be minimized by immobilization of the used biocatalysts. The separation step of the biomass after transformation can be achieved by simple sedimentation, just by turning off the stirrer. After sedimentation of the biocatalyst the product solution can be pumped out of the vessel. Time and equipment (separator) can be saved.

The costs for the biocatalysts are also decreased by minimizing the loss of bacterial cells during separation. Furthermore, the immobilized biocatalysts possess a higher long term activity which results in a lower consumption of cells. Assuming the costs for hydrogel and entrapment process to be 1-5 EUR per kg, costs for the biocatalysts can be reduced about 30 up to 80 %.

Free inactivated biomass can be released to waste water plants after use. LentiKats® are liquefied by heating to 70°C. For many biotechnological processes the step is obligatory for the inactivation of the biomass, so that additional costs will not occur. For keeping the melted polymer in liquid condition up to temperatures of 4°C, the suspension has to be diluted with one volume of water or aqueous process effluents.

In biological waste water plants, degradation of the hydrogel up to > 90 % is possible (Schonberger et al., 1997). Basic requirements are adapted microorganisms and temperatures above 12°C. The adaption phase of the microorganisms takes 3 to 6 weeks.

By application of 2-D-process fluorimetry based in-time analytics a higher product concentration can be obtained in shorter times. This leads to a significant reduction in consumption of the educts indole and serine. Additionally the power demand for downstream processing and waste water load are decreased.

8 Outlook

Whereas reaction control by use of 2-D-spectro fluorimetry could be tested on a production scale, all immobilization experiments have thus far been carried out on a laboratory scale. Prior to transfer to the

production scale, companies producing pharmaceutical ingredients must fulfil high quality GMP standards. These include that neither the use of polymers nor of glutaraldehyde affects the final quality of the pharmaceutical products.

References

Jekel M, Willke T, Vorlop K-D (1998) Immobilization of Biocatalysts in LentiKats®. Chem Eng Technol 21:275-278

Faurie R, Fries G (1999) From sugar beet to lyphan. In: Simat T, (ed.): Tryptophan: Basic Aspects and Practical Applications, Advances in Experimental Medicine and Biology. Plenum Press, New York

Schonberger H, Baumann A, Keller W (1997) Study of Microbial Degradation of Polyvinyl Alcohol (PVA) in Wasterwater Treatment Plants. American Dyestuff Reporter, pp. 9-18

Ulber R, Protsch C, Solle D, Hitzmann B, Willke B, Faurie R, Scheper T (2001) Optimierung der industriellen Tryptophanproduktion durch Einsatz bioanalytischer Systeme. Chem Ing Tech 73:524-526

Wagner F, Klein J, Bang WG, Lang S, Sahm H (1980) Verfahren zur mikrobiologischen Herstellung von L-Tryptophan. German patent DE 28 41 642

Encapsulation of *Hirsutella rhossiliensis* in hollow beads based on sulfoethylcellulose to control plant-parasitic nematodes

Anant V. Patel, Thomas Rose and Klaus-Dieter Vorlop[1]

Abstract

Plant-parasitic nematodes are important pests of a wide range of economically important plants worldwide. The endoparasitic nematophagous fungus *Hirsutella rhossiliensis* is a ubiquitous antagonist of many commercially important root-knot, cyst, and other pest nematodes. However, no commercial product containing this fungus is available because effective methods for the delivery of fungal mycelium to the soil have not yet been developed, and conidia can not be used.

The encapsulation of *H. rhossiliensis* in hollow beads should provide the following advantages:

(i) easy handling, (ii) protection from biotic and abiotic stress factors, (iii) enhanced shelf life, (iv) controlled release into the soil (controlled by environmental conditions and capsule materials) and (v) enhanced action in the soil. Amending capsules with nutrients, water-retaining substances, fillers, etc., should further enhance efficacy.

Growth experiments on petri dishes resulted in a capsule containing 15 % biomass, 15 % corn gluten and 0.5 % yeast extract. Further experiments were conducted to reduce the biomass content and capsule diameter.

During a stay at the University of California at Davis, USA (Bruce Jaffee) pathogenicity assays against *Heterodera schachtii* were conducted. The experiments indicated that high concentrations of corn gluten and yeast extract in the capsule had an adverse effect on spore transmission from fungus to nematode larvae. A reduction of nutrient content to 1.5 % corn gluten and 0.05 % yeast extract led to an increased number of infected nematode larvae of up to 50 %.

In view of the results, it may be concluded that the encapsulation of *H. rhossiliensis* in nutrient-amended hollow beads is a promising approach to the biological control of plant-parasitic nematodes.

Keywords: Hirsutella rhossiliensis, Heterodera schachtii, encapsulation, formulation, biological control

1 Introduction

The European market for biopesticides was estimated at 97.1 million US dollars in 2000 and is expected to grow by 11.7 % per year to 210.1 million US dollars in 2007 (Frost and Sullivan 2001).

While there is a wide range of microorganisms with a high biocontrol potential, the shelf life and action of cells introduced into the soil is still unsatisfactory. This is due to a lack of suitable formulation techniques (Burges 1998). The basic idea of the research presented here is to encapsulate biocontrol agents which should provide the following advantages:

- easy handling
- protection from biotic and abiotic stress factors
- enhanced shelf life
- controlled release into the soil (controlled by environmental conditions and capsule materials)
- enhanced action in the soil

The amendment of capsules with nutrients, water-retaining substances, fillers, etc., will further enhance their efficacy.

This approach was already successfully tested in our research with entomopathogenic nematodes and plant-growth promoting rhizobacteria (Patel and Vorlop 1994, Patel et al. 1995) where immobilization techniques known in classical biotechnology (Vorlop and Klein 1987) were applied. Here, this approach was to be tested for the nematophagous fungus *Hirsutella rhossiliensis* against economically important plant-parasitic nematodes.

Plant-parasitic nematodes are important pests of a wide range of plants all over the world (Oerke et al. 1994). The sugar beet nematode *Heterodera schachtii* causes an annual loss of about 90 million Euro in Europe (Müller 1999). As the hazardous chemical nematicides are being removed from the market, and the remaining control methods of integrated plant protection are not cost-effective, new control agents must be found.

The endoparasitic nematophagous fungus *Hirsutella rhossiliensis* is an ubiquitous antagonist of many commercially important root-knot, cyst, and

[1] Anant V. Patel, Thomas Rose and Klaus-Dieter Vorlop, Institute of Technology and Biosystems Engineering, Federal Agricultural Research Centre (FAL), Bundesallee 50, 38116 Braunschweig, Germany

other pest nematodes. It uses adhesive conidia to parasitize infective juveniles of the sugar beet nematode *Heterodera schachtii* and other *Heterodera spp., Meloidogyne javanica* and other *Meloidogyne spp., Globodera pallida*, etc. (Figure 1). Because the conidia lose their infectivity soon after they become detached from the mycelium (McInnis and Jaffee 1989), a liquid formulation of these conidia is impossible. It follows that the mycelium must be delivered to the field so that spores can be produced on-site in soil. Although the fungus has long been known (Minter and Brady 1980, Sturhan and Schneider 1980), no commercial product is available because methods for the delivery of mycelium to the soil have not yet been developed. Figure 2 illustrates the basic steps involved in the production of a biological control agent based on *H. rhossiliensis* to control plant-parasitic nematodes.

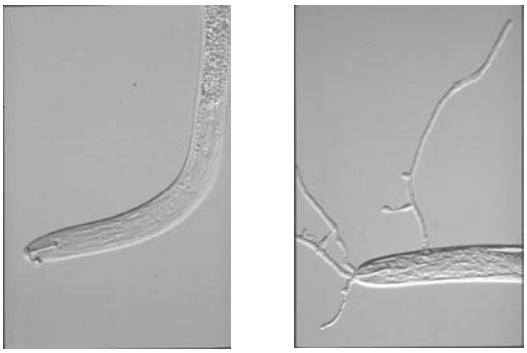

Figure 1:
Left: Spore of *Hirsutella rhossiliensis* adhering to the head of a juvenile *Heterodera schachtii*. Right: Early sporulation of *Hirsutella rhossiliensis* from a parasitized juvenile of *Heterodera schachtii*. The spore that initiated the infection is on the surface of the cuticle, to the right of the stylet. The body cavity is filled with hyphae. The first phialide and spore produced are to the right of the nematode (photos courtesy of B. Jaffee).

Earlier, a novel type of hollow bead based on sulfoethycellulose was developed (Patel 1998) and optimised (Rose et al. 2000). It was reported that *H. rhossiliensis* can be encapsulated in this type of hollow bead and that the addition of corn gluten and yeast extract enhanced growth of mycelium out of the capsules (Patel et al. 1996). Thus, this capsule system may offer an alternative to the conventional calcium alginate beads used to deliver microbes to the soil (Cassidy et al. 1996, Burges 1998). In a first pathogenicity assay, a high reduction of nematode invasion into roots of sugar beet plantlets was found. However, the transmission of spores to nematodes was not measured.

Here, we present data on the encapsulation of *H. rhossiliensis* mycelium in hollow beads based on sulfoethylcellulose together with nutrients (corn gluten and yeast extract). Then, the influence of nutrients (corn gluten, yeast extract) on the growth of fungus from capsules (colony diameter, mycelium density, sporulation) was monitored using interference contrast microscopy. Finally, the resulting formulations were tested in pathogenicity assays against *Heterodera schachtii* at the UC Davis (Prof. Bruce Jaffee) where the transmission of spores from mycelium to infective juveniles was determined in heated and unheated field soils.

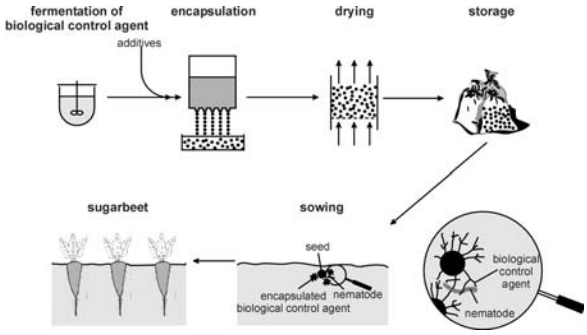

Figure 2:
Encapsulation of *Hirsutella rhossiliensis* to control *Heterodera schachtii*

2 Experimental

First, fungus was raised in a liquid shake culture (Lackey et al. 1993) and the mycelium encapsulated in hollow beads together with nutrients, resulting in a hollow bead which contained 15 % (w/w) wet biomass, 15 % (w/w) corn gluten and 0.5 % (w/w) yeast extract. Figure 3 illustrates the encapsulation of fungal mycelium in hollow beads according to Patel et al. (1996). The capsule formation is based on the reaction of the polyanion sulfoethylcelluose with a corresponding polycation such as polydiallyldimethylammoniumchloride (PDADMAC) or chitosan resulting in a semi-permeable symplex gel membrane.

Conventional calcium alginate beads were prepared according to Lackey et al. (1993) and contained no nutrients, but about 25 % (w/w) biomass.

In vitality assays, radial growth of fungus out of the capsules on water agar and soil was measured. Finally, the formulations were tested against infective juveniles of *Heterodera schachtii* (sugar beet nematode) in pathogenicity assays as described in Lackey et al. (1993): Briefly, capsules were transferred into snap cap bottles with heated or non-heated field soil and incubated for 14 d at 20°C. Then, 500-800 infective juveniles (IJ) of *H. schachtii* were added. After

another 2 d incubation, IJ were extracted and the number of IJ with one or more spores adhering to the cuticle (Figure 1, left) or with no spores adhering were counted.

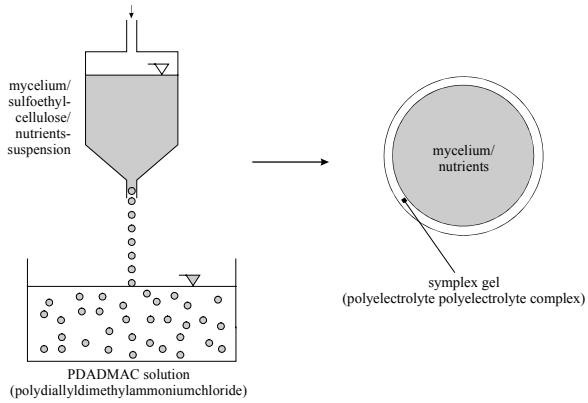

Figure 3:
Encapsulation *of H. rhossiliensis* mycelium in hollow beads based on sulfoethylcellulose

3 Results

Figure 4 shows the influence of biomass content on the growth of mycelium out of the capsules placed on water agar. It is very important to note that due to the presence of nutrients in the capsule, a reduction of biomass content from 15 % down to only 0.1 % does not reduce the growth. It illustrates one of the main advantages of such a formulation type: costly biomass can be saved. The capsule acts as a "microfermenter" where even small amounts of biomass (maybe even fermentation liquid) can multiply. The capsule also acts as a depot, because the filamentous fungus can grow out of the capsule while still using the nutrients. This gives a weak saprophyte a competitive advantage over antagonists in soil.

Figure 5 shows the influence of capsule diameter on radial growth of mycelium out of hollow beads (placed on soil at 14 % (w/w) soil moisture). Naturally, capsules with a higher diameter form bigger colonies. If the number of colonies is considered, one has to look at the "mycelium yield" per 1 ml capsule volume: Out of 1 ml encapsulation liquid, 566 capsules with 1.5 mm diameter can theoretically be formed (if shrinkage of capsules and other effects are not considered). In the other cases, with higher diameters, only 122, 71 or 30 capsules can be formed. Figure 6 shows the "mycelium volume" which is produced per ml encapsulation liquid. The same results are obtained if the surface is considered instead of the volume (data not shown). In other words: the smaller the capsules, the more mycelium will be obtained. Also, more capsules ("colony forming units") may give a better distribution of the biocontrol agent in soil. These results indicate the importance of producing small capsules, probably less than 1 mm diameter, which, to the knowledge of the authors, has not been discussed in detail in the biocontrol literature. The lowest capsule size possible will be dictated by the technological and biological limits and still needs to be investigated.

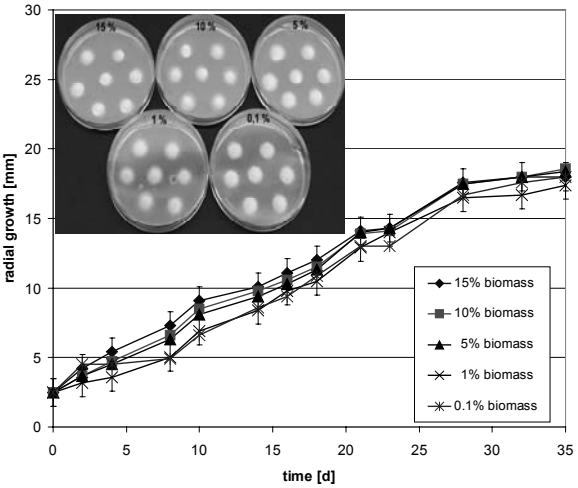

Figure 4:
Influence of biomass content on radial growth of fungal mycelium out of hollow beads containing 15 % corn gluten and 0.5 % yeast extract and placed on water agar, standard deviation for n = 10 capsules

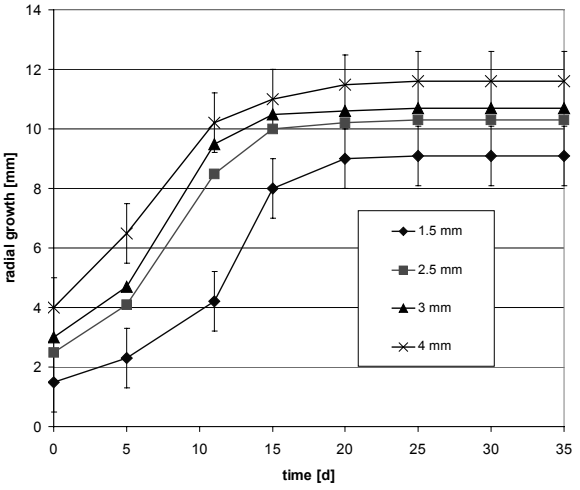

Figure 5:
Influence of capsule diameter on radial growth of fungal mycelium out of hollow beads containing 15 % corn gluten and 0.5 % yeast extract and placed on soil at 14 % (w/w) moisture, standard deviation for n = 10 capsules

The hollow beads were then tested in pathogenicity assays where the transmission of spores from mycelium to infective juveniles of *H. schachtii* was measured. In the first experiments, it was observed

that the fungus grew very well from hollow beads containing 15 % corn gluten, 0.5 % yeast extract and 15 % biomass, not only on water agar, but also in heated and unheated soil compared to alginate beads (Figure 7A,B). Surprisingly, the infection of nematode larvae was very low, despite excellent mycelial growth for hollow beads containing 15 % biomass, 15 % corn gluten and 0.5 % yeast extract (Figure 7C).

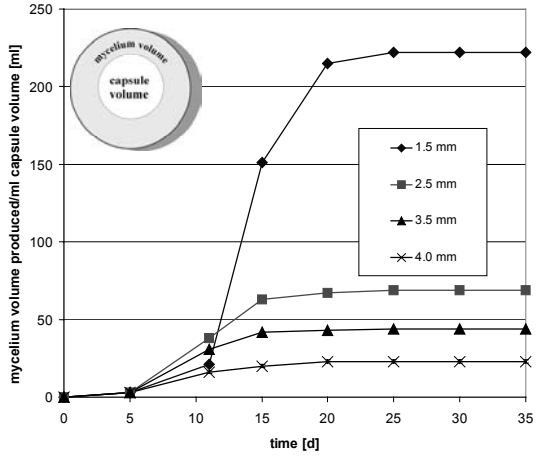

Figure 6:
Mycelium volume produced per ml capsule volume calculated for hollow beads with 1.5-4 mm diameter (explanation see text)

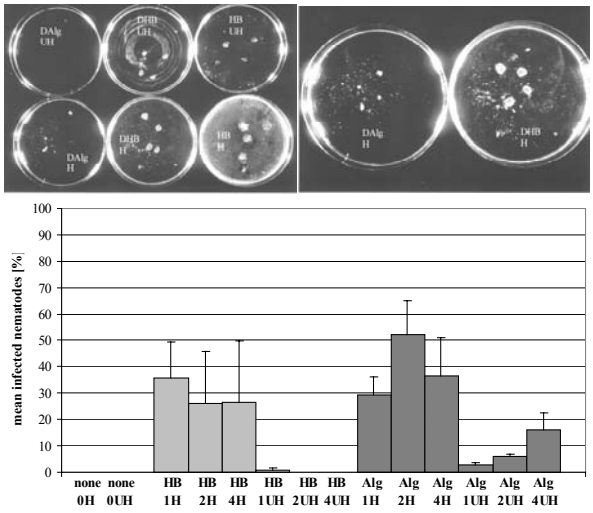

Figure 7:
Hollow beads and alginate beads extracted from soil after 16 d (A: top left, B: top right) and infection of nematode larvae in a bioassay with *H. rhossiliensis* encapsulated in hollow beads and alginate beads (C: bottom); HB: hollow bead; 1, 2, 4: number of capsules added to bioassay, H: heated soil; UH: unheated soil; Alg: alginate beads, DAlg: dried alginate beads (standard error for n=3-6)

In a "pulse experiment" it was to be investigated if the 16 d long bioassay can be accelerated by raising the temperature to 25°C. It was observed that there was a variation in the infection over time (Figure 8): There was a distinct increase in spore transmission after 5 d, which subsequently decreased. Extraction efficiency was around 50 % in all experiments (data not shown).

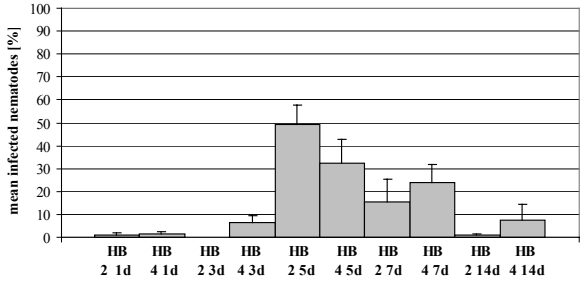

Figure 8:
Infection of nematode larvae in a bioassay after 1, 3, 5, 7 and 14 days of incubation of the hollow beads in heated soil at 25°C, HB: hollow beads, 2,4: number of capsules added to bioassay (standard error for n = 6)

In the original bioassay, the soil was tamped after addition of capsules (Lackey et al. 1993). Because of the danger of breaking moist hollow beads in the process, in the first experiments the soil was not tamped. However, it is known that porosity of the soil can have an influence on spore transmission (Tedford et al. 1992), so, in another experiment, the influence of tamping on spore transmission was investigated using dried (and thus more stable) hollow beads. No effect of tamping was observed (Figure 9).

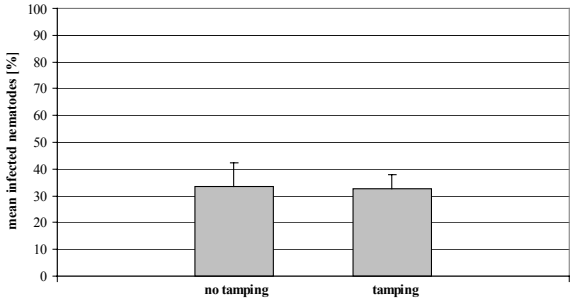

Figure 9:
Infection of nematode larvae in heated soil which was either tamped or not tamped after addition of 1 dried hollow bead (standard error for n = 6)

Finally, it was tested whether the nutrient content of the capsules has an influence on the infection of nematode larvae. It was observed that with hollow beads containing only 1/10 of the nutrients used in the experiments before (1.5 % corn gluten, 0.05 % yeast extract), the infection was significantly higher (Figure 10, Figure 11), while growth of mycelium from capsules was still good (Figure 12, Figure 13).

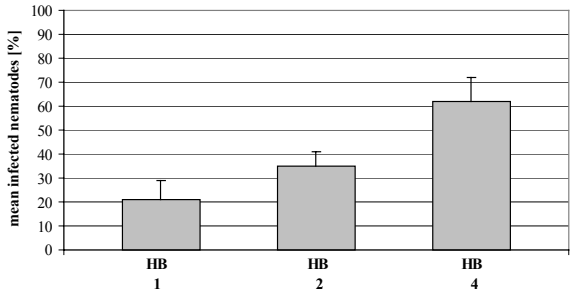

Figure 10:
Infection of nematode larvae in bioassays using 1, 2 or 4 moist hollow beads with reduced nutrient content in heated soil (standard error for n = 6)

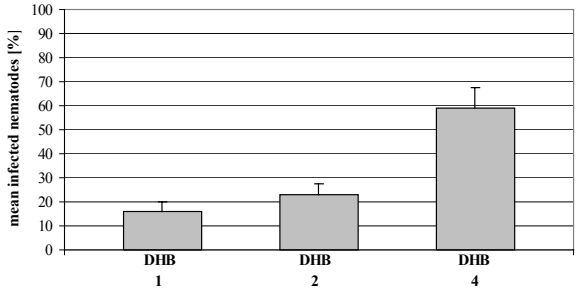

Figure 11:
Infection of nematode larvae in bioassays using 1, 2 or 4 dried hollow beads with reduced nutrient content in heated soil (standard error for n = 6)

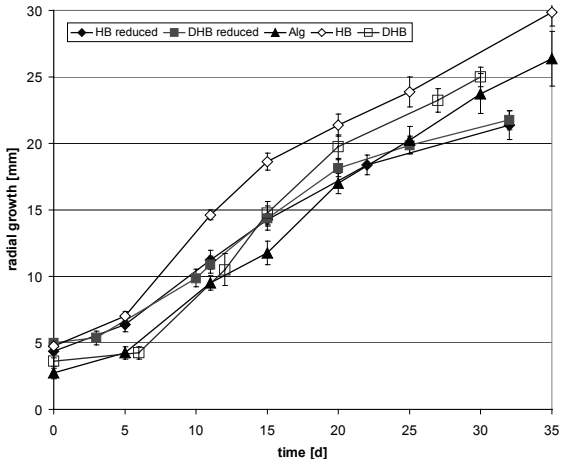

Figure 12:
Radial growth of *H. rhossiliensis* from alginate beads and from hollow beads with and without reduced nutrient content on water agar: HB: hollow beads, DHB: dried hollow beads, HB reduced: reduced nutrient content, DHB reduced: reduced nutrient content, Alg: alginate beads without nutrients (standard deviation for n = 10 capsules)

4 Discussion

We reported here that *H. rhossiliensis* can be successfully established in soil by encapsulation in a novel type of hollow bead amended with nutrients as an alternative to conventional alginate beads. The addition of nutrients to the capsule in order to give the fungus, which is reported to be a weak saprophyte (Jaffee and Zehr 1985), a competitive edge in soil is still considered a sound idea. However, care has to be taken that nutrients do not leak out of the capsule. This problem will be investigated in future research by changing membrane permeability, coating the hollow beads or introducing high molecular weight nutrients into the capsule.

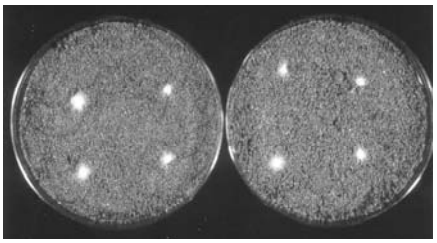

Figure 13:
Growth of *H. rhossiliensis* from hollow beads with reduced nutrient content on heated and unheated soil after 25 d

Then, in addition to the growth of mycelium, it should be investigated how the sporulation is affected by the nutrients (i.e., by the C:N ratio). Maybe (although it is considered unlikely) the poor infection in spite of excellent mycelium growth in soil can be explained with a lack of sporulation or the formation of less infectious (sticky) spores.

It also seems advisable to combine the spore transmission bioassay with a pathogenicity bioassay of *H. schachtii* where the invasion of sugar beet plantlets is investigated. This will be especially valuable in cases where the invasion of sugar beets by nematodes is very low. In these cases it should be checked if the protection of the plant is actually due to fungal activity or due to other effects such as a direct or indirect repellent effect of capsule ingredients, activity of other nematode antagonists, etc. These investigations are being carried out in the lab of J. Müller at the BBA Münster and will be published elsewhere. More systematic investigations regarding the interaction of formulation additives/fungus/nematode/host plant/rhizosphere are needed in order to develop a reliable biocontrol agent.

Finally, a focus of future research will be the capsule application. This may be done by incorporation of capsules into sugar beet pills, which may result in a release of the biological control agents only in the rhizosphere and thus in a reduction of dosage. Alternatively, dried capsules may be delivered separately as granules or powder during seed sowing or combined with an underground fertilization process as

used in maize. All formulations need to be tested in more experiments in greenhouses and in the field. More results regarding the cultivation, encapsulation and drying of *H. rhossiliensis* will be published elsewhere.

In view of the results, it may be concluded that the encapsulation of *H. rhossiliensis* in nutrient-amended hollow beads is a promising approach to the biological control of plant-parasitic nematodes.

Acknowledgements

Pathogenicity assays were conducted at the UC Davis in the lab of Prof. Bruce Jaffee whose comments are greatly acknowledged. A. Patel was funded via a fellowship under the OECD co-operative research programme Biological Resource Management for Sustainable Agricultural Systems. Part of the research was funded by the Agency for Renewable Resources (FNR) of the German Ministry of Nutrition, Agriculture and Forestry (FKZ 98 NR 067).

References

Burges HD (1998) Formulation of microbial pesticides. Dordrecht: Kluwer Academic Publishers

Cassidy MB, Lee II, Trevors JT (1996) Environmental applications of immobilized microbial cells: A review. Journal of Industrial Microbiology 16:79-101

Frost & Sullivan (2001) The European Biopesticide Market (Report 3905)

Jaffee BA, Zehr E (1985) Parasitic and saprophytic abilities of the nematode-attacking fungus *Hirsutella rhossiliensis*. Journal of Nematology 17:341-345

Lackey BA, Muldoon AE, Jaffee BA (1993) Alginate pellet formulation of *Hirsutella rhossiliensis* for biological control of plant-parasitic nematodes. Biological Control 3:155-160

McInnis TM, Jaffee BA (1989) An assay for *Hirsutella rhossiliensis* spores and the importance of phialides for nematode inoculation. Journal of Nematology 21:229-234

Minter DW, Brady BL (1980) Mononematous species *Hirsutella*. Transactions of the British Mycological Society 74(2):271-282

Müller J (1999) The economic importance of *Heterodera schachtii* in Europe. Helminthologica 36(3):205-213

Oerke E-C, Dehne H-W, Schönbeck F, Weber A (1994) Crop production and crop protection - estimated losses in major food and cash crops. Amsterdam: Elsevier

Patel AV (1998) Verkapselungsverfahren für die biologische Schädlingsbekämpfung und zur Konstruktion von „vegetativen Samen“ (Encapsulation processes for biological pest control and for the construction of artificial seeds). Sonderheft Landbauforschung Völkenrode Vol. 188

Patel AV, Vorlop K-D (1994) Entrapment of biological control agents applied to entomopathogenic nematodes. Biotechnology Techniques 8(8):569-74

Patel AV, Müller R, Vorlop K-D (1995) Einschlußimmobilisierung von biologischen Schädlingsbekämpfungsmitteln (Entrapment of biological control agents). Gesunde Pflanzen 5:167-174

Patel AV, Müller J, Müller R, Ehlers R, Vorlop K-D (1996) Entrapment of biological control agents. Proceedings of the 5th International Workshop on Bioencapsulation, Potsdam, pp. 7-12

Rose T, Neumann B, Thielking H, Koch W, Vorlop K-D (2000) Hollow beads of sulfoethylcellulose (SEC) on basis of polyelectrolyte complexes. Chemical Engineering & Technology 23(9):769-772

Sturhan D, Schneider R (1980) *Hirsutella heteroderae*, ein neuer nematodenparasitärer Pilz. Phytopath Z 99:105-115

Tedford EC, Jaffee BA, Muldoon AE (1992) Effect of soil moisture and texture on transmission of the nematophagous fungus *Hirsutella rhossiliensis* to cyst and root-knot nematodes. Phytopathologie 82(10):1002-1007

Vorlop K-D, Steinert H-J, Klein J (1987) Cell immobilization within coated alginate beads or hollow fibers formed by ionotropic gelation. Enzyme Eng 8:339-342

Pre-activated LentiKat®-hydrogels for covalent binding of enzymes

Emine Capan[1], Ulrich Jahnz[2] and Klaus-Dieter Vorlop[1]

Abstract

A mild new enzyme immobilisation technique using pre-activated poly (vinylalcohol) hydrogel (LentiKats®) as an immobilisation matrix was developed. This new technique is based on the following procedure: First chitosan is entrapped in LentiKats® as non-dissolved small particles according the standard method (Jekel et al. 1998). Subsequently, the amino-groups of chitosan are activated with glutardialdehyde. After removing non reacted glutardialdehyde in a washing step, LentiKats® are incubated with the enzyme solution. The enzyme molecules diffuse into the hydrogel matrix and are covalently bound. As model reaction we use the enantioselective synthesis of optically active (R)-cyanohydrins.

Keywords: cyanohydrin, entrapment, enzyme immobilisation, LentiKats®, (R)-oxynitrilase, pre-activated polyvinylalcohol hydrogel (PVA)

1 Introduction

PVA hydrogels as an immobilisation matrix are widely used because these hydrogels are very elastic and stable. In addition, PVA is an inexpensive material for entrapment. PVA hydrogels are mainly generated by the freeze thawing method or by cross-linking with boric acid (Muscat et al. 1996, Lozinsky and Plieva 1998). The problem with these methods is the complicated generation of the hydrogels. To overcome this shortcoming, a new and mild gelation method was developed. This gelation method, based on partial drying of LentiKat®Liquid (a polyvinylalcohol-containing aqueous solution which is commercially available from geniaLab, see also geniaLab 2001) at room temperature (Jekel et al. 1998), results in lens-shaped hydrogels (LentiKats®) and offers the following advantages: low costs for matrix and production, easy preparation, excellent mechanical stability, easy separation from reaction mixture (diameter 3-4 mm) and low diffusion limitation (thickness 200-400µm). LentiKats® were successfully used for the immobilisation of cells (Durieux et al. 2000, Wittlich et al. 1999a, Wittlich et al. 1999b, Welter et al. 1999). Due to the enzymes' small size and their subsequent diffusion out of a gel matrix, an entrapment of pure enzymes in polyvinylalcohol hydrogels (LentiKats®) often fails. A possibility to keep enzymes in LentiKats® is to cross-link the enzyme with chitosane and glutaraldehyde to obtain a supra-molecular structure prior to entrapment in LentiKats® as shown in Figure 1 (geniaLab 2001, Gröger et al. 2001).

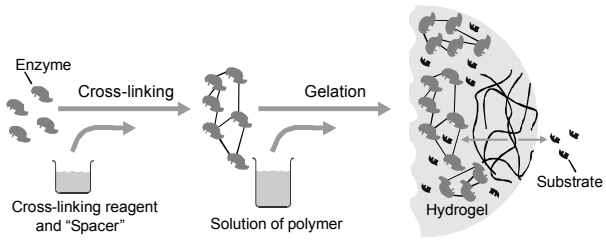

Figure 1:
Entrapment of cross-linked enzyme in LentiKats®

Instead of first cross-linking the enzyme and entrapping the resulting complex, we pursue the following alternative procedure: First chitosan is entrapped in LentiKats® as non-dissolved small particles. Subsequently, the amino-groups of chitosan are activated with glutardialdehyde.

After removing non reacted glutardialdehyde in a washing step, the LentiKats® are incubated with (R)-oxynitrilase. The enzyme molecules diffuse into the hydrogel matrix and are covalently bound (Figure 2).

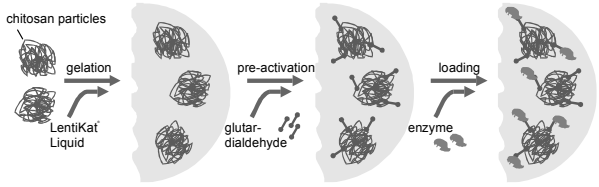

Figure 2:
Entrapment of enzyme in pre-activated LentiKats®

The (R)-oxynitrilase from almonds, E.C.4.1.2.10, which catalyses the reversible condensation of hydrogen cyanide with aldehydes, is a useful and promising enzyme for biotransformation processes (Figure 3).

[1] Emine Capan and Klaus-Dieter Vorlop, Institute of Technology and Biosystems Engineering, Federal Agricultural Research Centre (FAL), Bundesallee 50, 38116 Braunschweig, Germany

[2] Ulrich Jahnz, geniaLab Biotechnologie GmbH, Bundesallee 50, 38116 Braunschweig, Germany

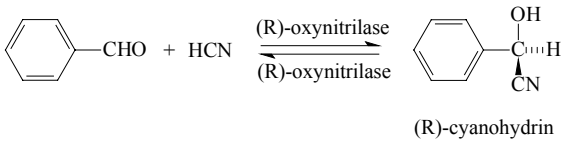

(R)-cyanohydrin

Figure 3:
Synthesis of (R)-cyanohydrin.

The resulting optically active cyanhydrins are expedient starting materials for the preparation of several important classes of compounds such as α-hydroxyketones, α-hydroxyacids, β-aminoalkohols as well as aminonitriles and aziridines.

2 Materials and methods

2.1 Preparation of LentiKats®

LentiKat®Liquid (geniaLab, Braunschweig) was liquified according to manufacturer's directions (geniaLab 2001). 5 g chitosan was shaken in 5 ml of phosphate buffer (20 mM, pH 7). The chitosan solution and 10 ml water were added under thorough mixing to 80 g LentiKat®Liquid to give a final volume of 100 ml. Using a printing device with over 400 identical pins, small droplets of approximately 4 µl were floored on a plastic dish and exposed to drying. After drying down to 30 % of the initial mass the resulting lenses were submerged in a stabilising solution (geniaLab) to reswell for 30 minutes.

Subsequently, the amino-groups of chitosan were activated with 30 ml glutardialdehyde (50 % (v/v)) for 16 h at 4 °C.

After removing non reacted glutardialdehyde by a washing step LentiKats® were incubated with (R)-oxynitrilase (purchased from ASA Spezialenzym GmbH, Braunschweig; specific activity: 51 U/mg protein; amount of protein: 14 mg/mL). At first different amounts of enzyme (3.14-15.69 mg protein) were dissolved in 8 ml of phosphate buffer (200 mM, pH 7). In a subsequent step, 2 g LentiKats® were added at the current enzyme solution. In this step, the enzyme molecules diffused into the hydrogel matrix and were covalently bound. The concept of this immobilisation method is shown in Figure 2.

2.1 Activity of the immobilised enzyme

To 400 ml of a solution of 0.1 mM benzaldehyde in citrate buffer (50 mM pH 3.75), 0.5 g KCN were added. After removing non covalently bound (R)-oxynitrilase in a washing step 1, LentiKats® were added to the reaction mixture. The reaction mixture was stirred for 30 minutes at 20°C.

The conversion of benzaldehyde was analysed by photometer (λ = 250 nm) and the formation of (R)-cyanohydrin was analysed by HPLC using a chiral column (chiralpak® AD, Merk-Eurolab, Germany). Analysis was done at 20°C (column) with hexan/2-propanol (90/10 v/v) as the eluent at a flow rate of 1.0 ml/min.

3 Results and discussion

To check whether the enzyme had really diffused into the hydrogel matrix and was covalently bound inside the pre-activated LentiKats® we measured the activity of washed LentiKats® for different concentrations of the enzyme as well as of the supernatants in relation to the activity of the free enzyme. The results are collected in Table 1. As can be seen from Table 1, the amount of bound activity was rather poor.

Table 1:
Activity of pre-activated LentiKats® incubated with different concentrations of enzyme. LK: LentiKats®, pro: protein, chi: chitosan, U: units)

Deployed activity (4 mL+1g LK), U	Activity of 1g LK, U	Covalently bonded protein, $\mu g_{prot}/g_{LK}$	Covalently bonded protein, $\mu g_{prot}/mg_{chi}$
80	1.37	27	0.54
100	1.39	27	0.54
133	1.42	28	0.56
200	1.59	31	0.62
400	1.59	31	0.62

Even a five-fold increase in enzyme concentration (80 to 400 U in total) caused an enhancement of only 15% (27 to 31 U). To investigate whether this was due to an insufficient diffusion of the enzyme into the hydrogel, the activity of soaked LentiKats® was measured as depicted in Figure 4.

The graphs clearly show that a major amount of the employed enzyme indeed diffuses into the hydrogel and that the poor results after washing are based on an inadequate binding capacity of the activated chitosan particles.

4 Conclusion and Outlook

This study proves that the idea of pre-activated LentiKats® is a viable method for enzyme immobilisation. However, further work has to focus on increasing the binding capacity inside the hydrogel. Entrapment of materials other than chitosan and other reactive compounds other than the aldehyde groups, espe-

cially nanoparticles with oxirane groups, will possibly show better results.

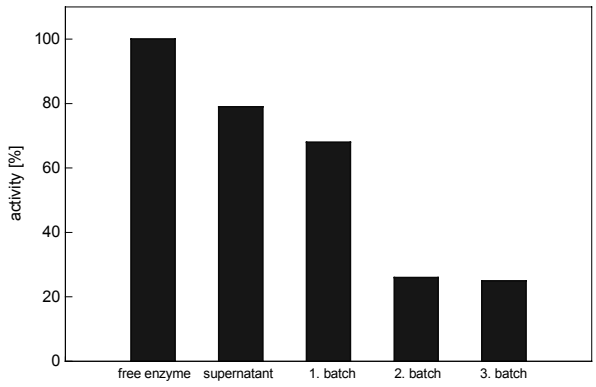

Figure 3:
Activity of free enzyme, supernatant and LentiKats®. 1.batch: without washing the LentiKats® before testing on activity, 2. and 3. batch: with washing the LentiKats® before testing on activity

References

Durieux A, Nicolay X, Simon J-P (2000), Continuous malolactic fermentation by Oenococcus Oeni entrapped in LentiKats®, Biotechnol Lett 22:1679-1684

geniaLab Biotechnologie GmbH (2001), http://www.genialab.com

Gröger H, Capan E, Barthuber A, Vorlop K-D (2001) Asymmetric synthesis of an (R)-cyanohydin using enzymes entrapped in lens-shaped gels. Org Lett 3:1969-1972

Jekel M, Buhr A, Vorlop K-D (1998) Immobilisation of biocatalysts in LentiKats. Chem Eng Technol 21:275-278

Lozinsky VI and Plieva FM (1998) Poly(vinylalcohol) cryogels employed as matrices for cell immobilisation. 3. Overview of recent research and developments. Enzyme Microb Technol 23:227-242

Muscat A, Prüße U, Vorlop K-D (1996) Stable support materials for the immobilization of viable cells. In: Wijffels R H, Buitelaar R M, Bucke C, and Tramper J (eds): Immobilized Cells: Basics and Applications, Elsevier Amsterdam, pp 55-61

Welter K, Willke T, Vorlop K D (1999): Production of itaconic acid by LentiKats®. SchrR Nachwachsende Rohstoffe 14:520-521

Wittlich P, Schlieker M, Jahnz U, Willke T, Vorlop KD (1999a): Bioconversion of raw glycerol to 1,3-propanediol by immobilized bacteria. Proceedings 9th European Congress on Biotechnology (July 11-15, Brussels) no. P2762, ISBN 805215-1-5

Wittlich P, Schlieker M, Lutz J, Reimann C, Willke T, Vorlop KD (1999b): Bioconversion of glycerol to 1,3-propanediol by LentiKats®. SchrR Nachwachsende Rohstoffe 14:524-532

Lieferbare Sonderhefte / Following special issues are available:

	Jahr 2000	€
208	Ingo Hagel Differenzierung und Charakterisierung von Weizen verschiedener Anbausysteme und Sorten durch Proteinfraktionierung	7,00
210	Ursula Pultke Freilanduntersuchungen zum Schwefelhaushalt eines Agrarökosystems mittels Analyse stabiler S-Isotope	7,00
212	Franz Ellendorff und Hartmut Stützel (Herausgeber) Workshop "Nachhaltige Landwirtschaft" vom 31.05. – 02.06.1999	10,00
213	Ulrich Dämmgen (Herausgeber) Versauernde und eutrophierende Luftverschmutzung in Nordost-Brandenburg	7,00
214	Ulf Prüße Entwicklung, Charakterisierung und Einsatz von Edelmetallkatalysatoren zur Nitratreduktion mit Wasserstoff und Ameisensäure sowie des Stahlschneideverfahrens zur Herstellung Polivinylalkohol-verkapselter Katalysatoren	10,00
215	Torsten Hemme Ein Konzept zur international vergleichenden Analyse von Politik- und Technikfolgen in der Landwirtschaft	15,00
216	Sven Dänicke und Elisabeth Oldenburg (Herausgeber) Risikofaktoren für die Fusariumtoxinbildung in Futtermitteln und Vermeidungsstrategien bei der Futtermittelerzeugung und Fütterung	7,00
218	Luit J. de Kok, Dieter Grill, Malcom J. Hawkesford, Ewald Schnug and Ineke Stulen (Editors) Plant Sulfur Research in Europe, Cost Action 829 Fundamental, Agronomical and Environmental Aspects of Sulfur Nutrition and Assimilation in Plants	7,00
219	Carsten in der Wiesche Untersuchungen zur Sanierung PAK-kontaminierter Böden mit Weißfäulepilzen	7,00
220	Ingo Hagel Auswirkungen einer Schwefeldüngung auf Ertrag und Qualität von Weizen schwefelmangel-gefährdeter Standorte des Ökologischen Landbaus	7,00
221	Franz-Josef Bockisch (Herausgeber) Beurteilung der raumklimatischen Wirkungen von Dämmstoffen aus nachwachsenden Rohstoffen	7,00
	Jahr 2001	
222	Margret Lahmann Prognose der Nachfrage nach Milch und Milcherzeugnissen in Deutschland und Frankreich bis zum Jahre 2005	12,00
223	Josef Kamphues und Gerhard Flachowsky (Herausgeber) Tierernährung – Ressourcen und neue Aufgaben	17,00
226	Jörg Hartung and Christopher M. Wathes (Editors) Livestock Farming and the Environment	7,00
229	Volker Moennig and Alex B. Thiermann (Editors) Safeguarding Animal Health in Global Trade	7,00
230	Nežika Petrič Pränatale Regulation der sexuellen Differenzierung von Luteinisierungshormon und Wachstumshormon, Genexpression und Sekretion beim Schwein	7,00
231	Bernhard Osterburg und Hiltrud Nieberg (Herausgeber) Agrarumweltprogramme – Konzepte, Entwicklungen, künftige Ausgestaltung	7,00

	Jahr 2002	€
225	Hans-Wilhelm Windhorst and Aalt A. Dijkhuizen (Editors) Product Safety and Quality Assurance	7,00
227	Franz Ellendorff, Volker Moennig, Jan Ladewig and Lorne Babiuk (Editors) Animal Welfare and Animal Health	7,00
228	Eildert Groeneveld and Peter Glodek (Editors) Animal Breeding and Animal Genetic Resources	7,00
232	Kerstin Panten Ein Beitrag zur Fernerkundung der räumlichen Variabilität von Boden- und Bestandesmerkmalen	7,00
233	Jürgen Krahl Rapsölmethylester in dieselmotorischer Verbrennung – Emissionen, Umwelteffekte, Optimierungspotenziale -	10,00
234	Roger J. Wilkins and Christian Paul (Editors) Legume Silages for Animal Production - LEGSIL	7,00
235	Torsten Hinz, Birgit Rönnpagel and Stefan Linke (Editors) Particulate Matter in and from Agriculture	7,00
236	Mohamed A. Yaseen A Molecular Biological Study of the Preimplantation Expression of Insulin-Like Growth Factor Genes and their Receptors in *In Vitro* Produced Bovine Embryos to Improve *In Vitro* Culture Systems and Embryo Quality	8,00
237	Mohamed Ali Mahmoud Hussein Kandil The effect of fertilizers for conventional and organic farming on yield and oil quality of fennel (*Foeniculum vulgare* Mill.) in Egypt	7,00
238	Mohamed Abd El-Rehim Abd El-Aziz Hassan Environmental studies on coastal zone soils of the north Sinai peninsula (Egypt) using remote sensing techniques	7,00
239	Axel Munack und Jürgen Krahl (Herausgeber) Biodiesel – Potenziale, Umweltwirkungen, Praxiserfahrungen -	7,00
240	Sylvia Kratz Nährstoffbilanzen konventioneller und ökologischer Broilerproduktion unter besonderer Berücksichtigung der Belastung von Böden in Grünausläufen	7,00
241	Ulf Prüße and Klaus-Dieter Vorlop (Editors) Practical Aspects of Encapsulation Technologies	9,00
242	Folkhard Isermeyer (Editor) Milchproduktion 2025	9,00